ISBN 978-82-326-4378-3 (printed version)
ISBN 978-82-326-4379-0 (electronic version)
ISSN 1503-8181

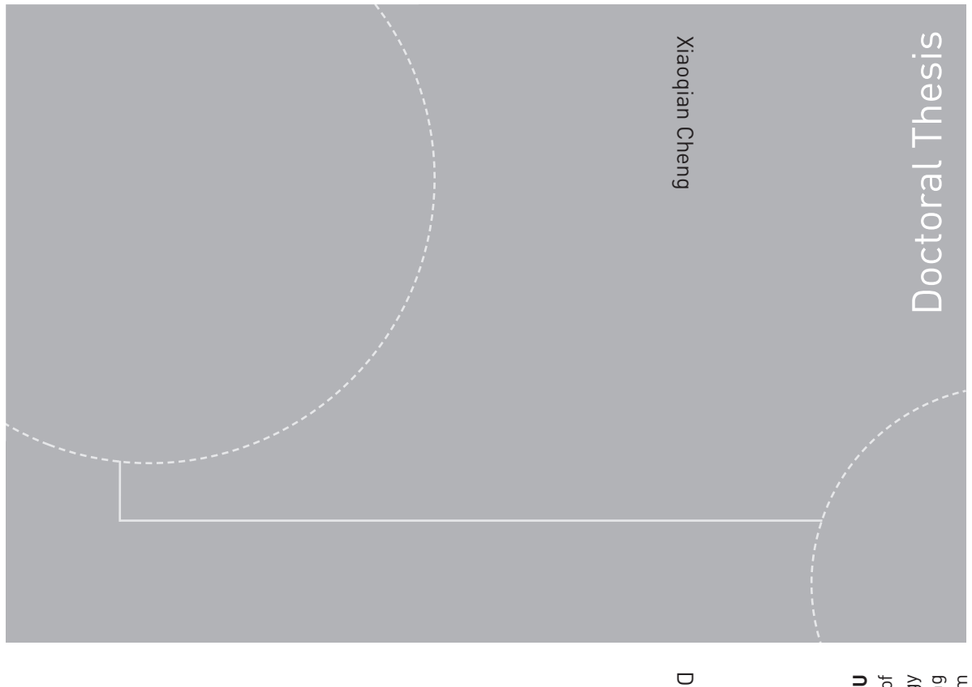

Doctoral theses at NTNU, 2019:387

Xiaoqian Cheng

Surfactant Enhanced Oil Recovery in Fractured Reservoirs

Simulation study of surfactant spontaneous and dynamic imbibition

NTNU
Norwegian University of
Science and Technology
Faculty of Engineering
Department of Geoscience and Petroleum

NTNU
Norwegian University of
Science and Technology

Doctoral theses at NTNU, 2019:387

NTNU

NTNU
Norwegian University of
Science and Technology

Xiaoqian Cheng

Surfactant Enhanced Oil Recovery in Fractured Reservoirs

Simulation study of surfactant spontaneous and dynamic imbibition

Thesis for the degree of Philosophiae Doctor

Trondheim, December 2019

Norwegian University of Science and Technology
Faculty of Engineering
Department of Geoscience and Petroleum

NTNU
Norwegian University of
Science and Technology

NTNU
Norwegian University of Science and Technology

Thesis for the degree of Philosophiae Doctor

Faculty of Engineering
Department of Geoscience and Petroleum

ISBN 978-82-326-4378-3 (printed version)
ISBN 978-82-326-4379-0 (electronic version)
ISSN 1503-8181

Doctoral theses at NTNU, 2019:387

Printed by Skipnes Kommunikasjon as

Abstract

Water flooding has poor performance in fractured reservoirs with mixed- or oil-wet wettability. Surfactant could be used to improve oil recovery by changing wettability to more water-wet or reducing water/oil interfacial tension (IFT). A surfactant spontaneous imbibition model is established using experimental data from literature, and a surfactant dynamic imbibition model is established based on the spontaneous imbibition model. Surfactant mechanisms, matrix properties, surfactant properties, upscaling methods, and surfactant flooding in fractured matrix are studied by simulations with Eclipse 2014.1.

Wettability alteration to more water-wet could enhance oil recovery rate and ultimate oil recovery. If water/oil IFT is reduced by surfactant, ultimate oil recovery is increased when capillary number is larger than the critical capillary number (i.e. 10^{-8}), but oil recovery rate is decreasing with the decrease of IFT. In general, for mixed- or oil-wet systems, wettability alteration is more efficient than IFT reduction to improve oil recovery.

The most frequently used existing upscaling methods are mainly for surfactant imbibition dominated by gravity or capillary pressure. The existing upscaling methods, which consider both wettability alteration and IFT reduction or both gravity and capillary pressure, are not widely used. In this thesis, new upscaling methods are introduced, which include wettability alteration, IFT reduction, gravity and capillary pressure. Therefore, the proposed upscaling methods can be used for surfactant imbibition dominated by gravity or capillary pressure or both gravity and capillary pressure. The proposed upscaling methods are verified by simulation results of surfactant spontaneous imbibition under three different conditions according to the bound number: $N_B \geq 1$, which is for the surfactant imbibition dominated by gravity; $0.1 < N_B < 1$, which is for the surfactant imbibition dominated by both gravity and capillary pressure; $N_B \leq 0.1$, which is for the surfactant imbibition dominated by capillary pressure.

Oil recovery rate and ultimate oil recovery are increasing with the increase of matrix permeability, but surfactant enhanced oil recovery (EOR) is reducing and then increasing with the increase of matrix permeability. The turning point of the trend occurs around the bound number of 1. Matrix porosity has little effect on surfactant imbibition, especially when wettability is changed to strongly water-wet by surfactant. Oil recovery rate is decreasing with the increase of matrix block size both for brine and surfactant imbibition. The increase of matrix block size leads to an increase of ultimate oil recovery, and the increase degree is smaller when

wettability is more water-wet. The proposed upscaling methods are tested and modified based on the simulation results of the effects of matrix permeability, matrix porosity, and matrix block size on surfactant spontaneous imbibition.

The simulation study of the effects of surfactant properties on surfactant spontaneous imbibition shows that viscosity of surfactant solution almost has no effect on surfactant spontaneous imbibition. Surfactant concentration can increase ultimate oil recovery when concentration is lower than critical micelle concentration (CMC). But when concentration is above CMC, ultimate oil recovery does not change with the increase of concentration. Surfactant adsorption could reduce oil recovery rate but has no effect on ultimate oil recovery. Surfactant diffusion could expedite surfactant imbibition into matrix, while it does not affect ultimate oil recovery. Upscaling methods that include the effect of surfactant concentration and adsorption are proposed.

Surfactant injection rate into a fractured matrix could significantly accelerate oil recovery until injection rate reaches 0.0005 PV/h. Using the injection rate of 0.0005 PV/h, the oil recovery after injecting 1 PV surfactant solution is 68% original oil in place (OOIP), which is about 85% of ultimate oil recovery. Surfactant diffusion is very important for surfactant dynamic imbibition since surfactant diffusion is very efficient for surfactant movement into matrix when capillary pressure is very small or negative. The effect of injection rate on surfactant dynamic imbibition is larger when surfactant diffusion is slower, or fracture porosity is smaller. The required injection volume of surfactant solution to obtain ultimate oil recovery is increasing with the increase of pre-water flooding volume. Therefore, surfactant should be applied before water flooding. The surfactant with low diffusion coefficient should not be used in tertiary oil recovery stage. Oil recovery rate is slower, and the required injection volume of surfactant solution is increased when the injected surfactant concentration is smaller. In addition, surfactant solution with lower concentration has lower efficiency because less surfactant could be imbibed into matrix.

Preface

This thesis is submitted to the Norwegian University of Science and Technology (NTNU) for partial fulfilment of the requirements for the degree of Philosophy of doctor.

The work presented in this thesis was conducted at the Department of Geoscience and Petroleum, NTNU, Trondheim, Norway. Professor Jon Kleppe was the main supervisor. Professor Ole Torsæter was the co-supervisor.

Acknowledgements

Thank you to my supervisor, Professor Jon Kleppe, NTNU, for giving me the opportunity to work as a PhD at NTNU. I appreciate it that you gave me great guidance and financial support. It was my great honor to be one of your PhD students. Thank you to my co-supervisor, Professor Ole Torsæter, NTNU, for giving me advice and support. I would not complete my PhD study without you.

Thank you to Dr. Rasoul Khaledialidusti for introducing chemical enhanced oil recovery to me, which introduced the idea of chemical enhanced oil recovery to me. Thank you to Dr. Ying Guo, who was the research director IOR group at International Research in Stavanger (IRIS) then and now is the senior business developer at Norwegian Research Centre (NORCE), for the help during the selection of my PhD topic. During the discussion with you, I got the idea of proposing new upscaling methods of surfactant imbibition. A special thank you to Dr. Dag Chun Standnes, who is a leading researcher at Equinor, for the help with experimental data and the ideas that inspired this research. Thank you to Dr. Per Arne Slotte for the help with simulator Eclipse. Without you I would not solve many questions so fast that I met during the use of Eclipse.

I would like to thank Dr. Nur Suriani Mamat for being a great friend during private life and an awesome colleague during work. It was so fun to have coffee breaks with you. I also thank Dr. Babak Khodabandeloo and Dr. Lucas Cantinelli Sevillano for being such great office mates. It was excellent experience to share the same office with you. And I also would like to thank all the colleagues at the Department of Geoscience and Petroleum who created an excellent working environment. A special thank you to my friends Thomas Øyen, Marie Bjørknes and Jarle Bjørknes for providing support and concern when I was in Stavanger.

I must thank my cousin Dr. Nan Cheng and his family Youlin Yang, Larry Yang Cheng and Julia Yang Cheng, who gave me the warmth of family when I was far from my parents and siblings. Thank you for the support and encouragement. I would never forget the time spending with you. And it was so nice to talk with Youlin all night long every time we met.

Most importantly, millions of thanks to my parents and siblings for being my powerful backing. You have always comforted me and given confidence and courage to me. I would not have been the person that I am now or gotten this far without you.

List of publications

Cheng, X.; Kleppe, J. and Torsæter, O. 2018a. Simulation Study of Surfactant Imbibition Mechanisms in Naturally Fractured Reservoirs. Presented at SPE Norway One Day Seminar, Bergen, 18 April. https://doi.org/10.2118/191309-MS.

Cheng, X.; Kleppe, J. and Torsæter, O. 2018b. Simulation Study of Effects of Surfactant Properties on Surfactant Enhanced Oil Recovery in Fractured Reservoirs. Presented at SPE Kingdom of Saudi Arabia Annual Technical Symposium and Exhibition, Dammam, Saudi Arabia, 23-26 April. https://doi.org/10.2118/192430-MS.

Cheng, X.; Kleppe, J. and Torsæter, O. 2019. Simulation study of surfactant injection in a fractured core. *Journal of Petroleum Exploration and Production Technology* **9** (4): 3079-3090. https://doi.org/10.1007/s13202-019-0705-y.

Cheng X.; Kleppe, J. and Torsæter, O. 2019. Upscaling Method for Surfactant Spontaneous Imbibition. *Journal of Petroleum Science & Engineering*. Under review.

Table of contents

List of figures

List of tables

Abbreviations and nomenclature

	Description	Units
a	Constant	
A	Area of the matrix cross section area	cm^2
A_1	Area under the curve III in USBM method	cm^2
A_2	Area under the curve II in USBM method	cm^2
A_i	Area open to imbibition at the i^{th} direction	cm^2
b	Fracture width	cm
b	Constant in Eqs. 1.43, 1.45, 1.47, 1.48, and 1.49	
BCF	Boundary condition factor	
c	Constant related to rock properties	1/m
cos	Function of mathematics, cosine	
C	Constant	
C_{ads}	Surfactant adsorption concentration on the rock	g/g
C_i	Capillary parameter of phase i	
C_s	Surfactant concentration	g/cm^3
CDC	Capillary desaturation curve	
CMC	Critical micelle concentration	g/cm^3
CT	Computed tomography	
D	Diameter of the core	cm
D_s	Surfactant diffusion coefficient	cm^2/h or m^2/s
E	Adhesion-work-reduction factor	
E_R	Oil recovery	
EOR	Enhanced oil recovery	
$f(\theta)$	Function of contact angle	
$f(N_c)$	Function of the capillary number and corresponds to the capillary desaturation curve	
F	Moore and Slobod dimensionless group	
g	Gravity, g = 9.8	mN/g
$g(S_w)$	Function of water saturation	
GOR	Gas oil ratio	

	Description	Units
H	Height of medium	cm
I	Amott-Harvey index	
IFT	Interfacial tension	mN/m
IFTfactor	Interfacial tension factor	
IOR	Improved oil recovery	
J	Leverett's dimensionless J function	
k_r^*	Reference relative permeability	
k_{re}^*	Pseudo relative permeability	
k_{rw}	Water relative permeability	
k_{ro}	Oil relative permeability	
k_{rw}^0	Endpoint of water relative permeability	
k_{rw}^*	Water relative permeability at S_{wf}	
k_{ro}^0	Endpoint of oil relative permeability	
k_{ro}^*	Oil relative permeability at S_{wf}	
k_w^*	Water effective permeability at S_{wf}	mD
K	Absolute permeability	mD
K^0	Reference matrix permeability	mD
K_f	Fracture absolute permeability	mD
l_{Ai}	Distance from the imbibition face to the no-flow boundary	cm
log, ln	Function of mathematic, logarithm	
L	Length of matrix	cm
L_c	Characteristic dimension of matrix block or sample	cm
$L_{c(field)}$	Characteristic length of the field block	cm
$L_{c(lab)}$	Characteristic length of the laboratory sample	cm
m_{ads}	Adsorption mass of surfactant	g
m_s	Surfactant mass in matrix	g
m_{si}	Initial surfactant mass in matrix	g
m_{sn}	Normalized surfactant mass in matrix	g
m_{smax}	The maximum of surfactant mass in matrix	g
Δm	Mass difference of surfactant between injector and producer	g
n_w	Exponent of the water relative permeability	
n_o	Exponent of the oil relative permeability	

	Description	Units
N_B	Bond number	
N_B^0	Reference Bond number	
N_c	Capillary number	
$(N_c)_c$	Critical capillary number	
N_{ci}	Capillary number of phase i	
$(N_c)_{max}$	Maximum capillary number	
N_{wt}	Water volume imbibed into the matrix	cm^3
OOIP	Original oil in place	cm^3
P_c	Capillary pressure	atm
P_c^*	Effective capillary pressure at S_{wf}	atm
P_c^i	Capillary pressure at the initial condition	atm
P_c^{ww}	Capillary pressure at the strongly water-wet wettability condition	atm
P_c^0	Reference capillary pressure	atm
P_o	Oil pressure	atm
P_w	Water pressure	atm
PV	Pore volume	cm^3
q	Injection rate	PV/h or cm^3/h
q_w	Water imbibition rate	cm^3/s
r	Radius of the tube	cm
r_1, r_2	Radii of curvature of the interface, measured perpendicular to each other	cm
R	Recovery by water imbibition	fraction or %
R^*	Normalized recovery	
R_o	Oil recovery	fraction or %
R_{of}	Ultimate oil recovery	fraction or %
R_{ofs}	Ultimate oil recovery of surfactant imbibition	fraction or %
R_{ofw}	Ultimate oil recovery of brine imbibition	fraction or %
R_{on}	Normalized oil recovery	
$\bar{S}_o$	Average oil saturation	
S_{oi}	Initial oil saturation	fraction or %
S_{or}	Residual oil saturation	fraction or %

	Description	Units
S_{owcr}	Critical oil saturation in water	fraction or %
S_w	Water saturation	fraction or %
S_{wco}	Connate water saturation	fraction or %
S_{wcr}	Critical water saturation	fraction or %
S_{wf}	Average water saturation behind imbibition front	
S_{wi}	Initial water saturation	fraction or %
S_{wmax}	Maximum water saturation	fraction or %
S_{wir}	Irreducible water saturation	fraction or %
t	Time	s
t_c	Simplified existing upscaling group for capillary imbibition	depends on equation
t_{d1}, t_{d2}	Simplified proposed upscaling group	depends on equation
t_{d1}^*, t_{d2}^*	Modified simplified proposed upscaling group	depends on equation
t_{D1}, t_{D2}	Upscaling dimensionless time	
t_{Dc}	Existing upscaling dimensionless time for capillary imbibition	
t_{Dg}	Existing upscaling dimensionless time for gravity imbibition	
$t_{(field)}$	Oil recovery time in the field	s
t_g	Simplified existing upscaling group for graviry imbibition	depends on equation
$t_{(lab)}$	Oil recovery time in the laboratory	s
u	The Darcy flux	cm/s
v	Fluid velocity in porous medium	cm/s
V_b	Bulk volume of the matrix	cm^3
V_f	Fracture volume	cm^3
V_{osp}	Oil volume displaced by spontaneous water imbibition alone	cm^3
V_{ot}	Total oil volume displaced by water imbibition and forced displacement	cm^3
V_p	Pore volume of the matrix	cm^3
V_t	Total injection volume of brine and surfactant	
V_w	Pre-water flooding volume	

	Description	Units
V_{wsp}	Water volume displaced by spontaneous oil imbibition alone	cm^3
V_{wt}	Total water volume displaced by oil imbibition and forced displacement	cm^3
VES	Viscoelastic surfactant	
W_s	Adhesion work of compound system of surfactant/oil/rock	mN/m
W_w	Adhesion work of compound system of water/oil/rock	mN/m
WI	Wettability index of USBM method	
WI_i	USBM wettability index at the initial wettability condition	
WI_{ww}	USBM wettability index at the strongly water-wet wettability	
WLM	Wormlike micelles	
α	Increase factor of matrix size	
β	Increase factor of imbibition time	
γ	Ratio of the flux from the sides to the flux from the core bottom	
δ_o	Displacement-by-oil ratio	
δ_w	Displacement-by-water ratio	
η	Ratio of surfactant adsorption on total surfactant	
θ	Contact angle	degree
θ_i	Contact angle at the initial wettability condition	degree
θ_s	Contact angle of surfactant on rock surface	degree
θ_w	Contact angle of water on rock surface	degree
θ_{ww}	Contact angle at the strongly water-wet wettability condition	degree
λ^*	Reference mobility	mD/cP
λ_e^*	Effective mobility at S_{wf}	mD/cP
λ_j	Mobility of phase j, j = w, o	mD/cP
μ	Viscosity	cP
μ^*	Reference viscosity	cP
μ_e	Effective viscosity of the two phases of oil and water	cP
μ_j	Viscosity of phase j, j = w, o	cP
μ_w	Water viscosity	cP
π	Math constant, 3.1416	
ρ	Density	g/cm^3
ρ_r	Rock density	g/cm^3

	Description	Units
σ	Interfacial tension	mN/m
$\bar{\sigma}$	Average interfacial tension	mN/m
σ_{CMC}	Interfacial tension at CMC	mN/m
σ_i	Initial interfacial tension	mN/m
σ_f	Final interfacial tension	mN/m
σ_{ow}, σ_w	Interfacial tension of oil and water	mN/m
σ_s	Interfacial tension of surfactant and oil	mN/m
σ_{so}	Interfacial tension of solid and oil	mN/m
σ_{sw}	Interfacial tension of solid and water	mN/m
υ	Linear velocity	cm/s
ϕ	Porosity	fraction or %
ϕ^0	Reference porosity	fraction or %
ϕ_f	Fracture porosity	fraction or %
ω	Wettability alteration coefficient	

Superscripts

h	Large capillary number
imm	Immiscible condition
l	Low capillary number
ow	Oil-wet condition
ww	Water-wet condition

Subscripts

j	Phase of j, j = w or o

1 Introduction

1.1 Enhanced oil recovery

Oil recovery process includes three phases, which are primary, secondary, and tertiary phase. Primary recovery phase is oil recovery by natural drive mechanisms, solution gas, water influx, gas cap drive or gravity drainage. Secondary recovery phase includes recovery techniques, which are used to maintain recovery pressure, such as gas or water injection. Tertiary recovery phase includes the technique applied after secondary phase.

Improved oil recovery (IOR) is a general term including any methods that improve oil recovery. However, there is no widely accepted definition of enhanced oil recovery (EOR). Lake et al. (2014) gave a definition of EOR that EOR was oil recovery by injecting materials, which were not normally present in the reservoir, which did not define EOR as a particular phase or exclude waterflooding. However, Green and Willhite (1998) defined EOR as methods used at the tertiary phase. Taber et al. (1997) and Terry (2001) defined EOR as any oil recovery methods excluded the conventional use of reservoir energy and plain water or brine injection. According to Sheng (2011), EOR is any reservoir process that changes the existing rock/oil/brine interactions in reservoirs, such as thermal recovery, miscible flooding, chemical flooding, and microbial. Here chemical injection is considered as an enhanced oil recovery method no matter whether chemical is injected at the secondary phase or the tertiary phase.

Chemical enhanced oil recovery methods include alkaline (A), surfactant (S), polymer (P), any combination of ASP and other chemical EOR, such as emulsion and foam, which are thermodynamically unstable. The key mechanisms of surfactant are to reduce interfacial tension (IFT) between oil and the displacing fluid and change formation wettability to more water-wet. The key mechanism of polymer is to increase aqueous phase viscosity. The alkali can react with acids in crude oil to form in-situ surfactant and it could reduce consumption of polymer and surfactant. This work focuses on surfactant EOR in fractured reservoirs.

1.2 Fractured reservoir

1.2.1 Classification of fractured reservoirs

A reservoir is defined as being 'fractured' only if a continuous network of various degree of fracturing is distributed throughout the reservoir. Such fractures (Fig. 1-1) are formed naturally during the specific geological circumstances of reservoir history.

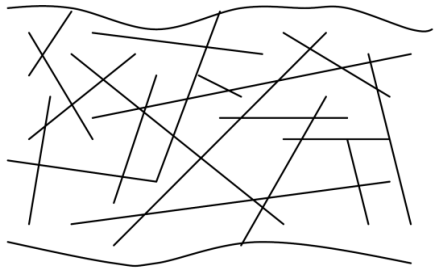

Fig. 1-1—Naturally fractured reservoir (van Golf-Racht 1982).

Firoozabadi (2000) classified fractured reservoirs into three different groups. For group one, reservoirs have little fracture porosity, and the hydrocarbon resides in matrix blocks, like Ekofisk field in the North Sea (Hermansen et al. 1997). For group two, reservoirs have small fracture porosity, which could be as high as 10% to 20%, for example the Asmari limestone reservoir (Saidi 1987). For group three, reservoirs have bigger fracture porosity and smaller matrix porosity. More than half of the hydrocarbon resides in the fracture system, for example, the Keystone (Ellenberger) field in Texas.

Allan and Sun (2003) divided fractured reservoirs into four types. For type I, reservoirs have little matrix porosity and permeability. Fracture system provides both storage capacity and fluid-flow pathway. For type II, reservoirs have low matrix porosity and permeability. Matrix provides some storage capacity and fracture system provides fluid-flow pathway. For type III, (microporous) reservoirs have high matrix porosity and low matrix permeability. Matrix provides storage capacity and fracture system provides fluid-flow pathway. For type IV, (macroporous) reservoirs have high matrix porosity and permeability. Matrix provides both storage capacity and fluid-flow pathway, while fracture system merely enhances permeability.

A significant proportion of world oil reserves, in the order of 20%, is generally assumed to lie in fractured reservoirs (Firoozabadi 2000). The type I, II, III and IV fractured reservoirs have an average ultimate recovery factor of 26%. One third of the fractured oil reservoirs have recovery factors less than 20% (Allan and Sun 2003). Therefore, it is still a big challenge to enhance oil recovery of fractured reservoirs.

1.2.2 Characteristics of fractured reservoirs

Even though fractured reservoirs are divided into three or four groups, people are mostly interested in fractured reservoirs that have low matrix permeability and high matrix porosity. If matrix is water-wet, and enough amount of water is supplied in fracture network, capillary imbibition governs oil recovery process from fractured reservoirs. Rock properties, such as matrix permeability, size and shape, wettability, heterogeneity, and boundary conditions, control the process. The properties of imbibing water, phase viscosity and interfacial tension also play a role on the capillary imbibition recovery. These properties determine recovery rate and ultimate recovery. Reservoirs with unfavorable conditions, such as heavy oil, oil-wet matrix, matrix boundary conditions that limit the dynamics of oil displacement, large matrix size, low matrix permeability and high IFT, require additional effort to enhance oil recovery. In fact, water injection might yield limited recovery when unfavorable conditions exist, and different methods should be applied to overcome these difficulties (Babadagli 2001b).

Since most of fractured reservoirs are oil-wet, in which capillary force tends to retain oil in matrix blocks, water flooding in such reservoirs often results in a poor oil recovery. Because of low permeability of matrix, production kinetics under the effect of gravity force is often very low. Moreover, for a typical fractured reservoir with a well-differentiated and conductive fracture network, fracture flow does not exert a significant viscous drive on matrix oil (Bourbiaux 2009).

The production characteristics of fractured reservoirs differ from those of conventional reservoirs (van Golf-Racht 1982; Allan and Sun 2003).

1. Transition zone is absent in naturally fractured reservoirs (Fig. 1-2) because the high permeability of fracture network provides a mechanism for rapid re-equilibration of fluid contacts.

2. PVT properties may be constant throughout a fractured reservoir if convective circulation occurs. Bubble point pressure and other PVT properties may remain constant with depth (Fig. 1-3).
3. Pressure drop around the production well is very low, and pressure gradients do not play a significant role in production because of the high transmissivity of fracture network (Fig. 1-4).
4. Fracture network gas-cap (Fig. 1-5) is formed because of permeability difference between matrix and fractured network and density differences between gas and fluids.
5. Pressure decline per barrel of oil production is lower in fractured reservoirs than in non-fractured reservoirs (Fig. 1-6), which results from a continuous supply of oil from matrix blocks into fracture network because of fluid expansion, gravity drainage and imbibition during production.
6. Fractured reservoirs usually have lower gas oil ratio (GOR) than non-fractured reservoirs (Fig. 1-7) due to fracture network gas-cap.
7. Water cut is essentially a function of production rate in fractured reservoirs, whereas in non-fractured reservoirs water cut depends on rock characteristics, displacement behavior and production rate (Fig. 1-8).

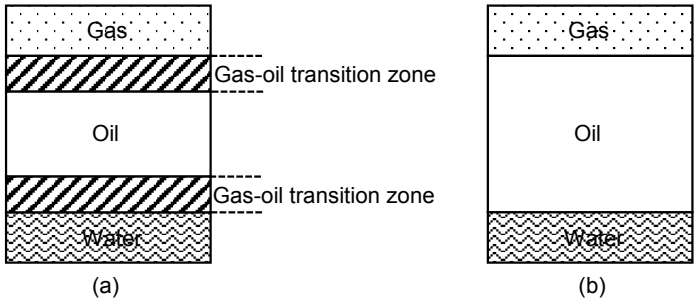

Fig. 1-2—Reservoir transition zone in (a) a non-fractured reservoir and (b) a fractured reservoir (van Golf-Racht 1982).

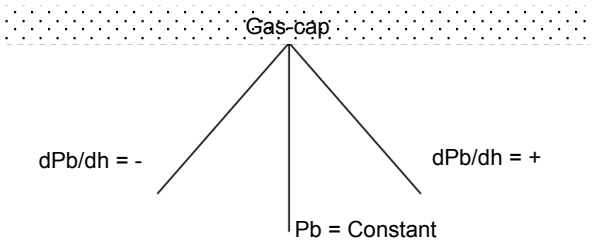

Fig. 1-3—Variation of bubble point pressure (Pb) versus depth (van Golf-Racht 1982).

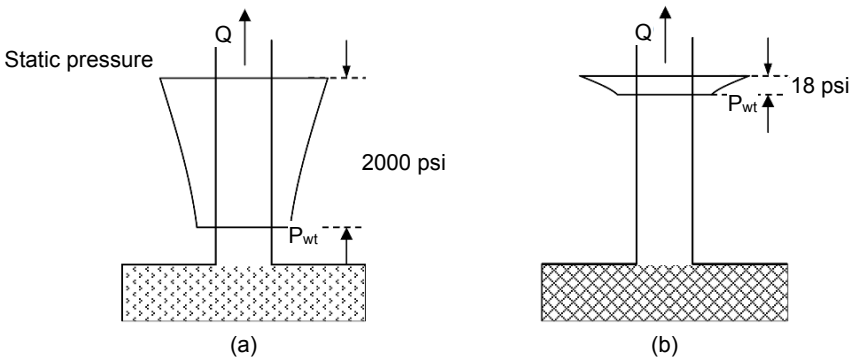

Fig. 1-4—Pressure drop around the production well in (a) a non-fractured reservoir and (b) a fractured reservoir (van Golf-Racht 1982).

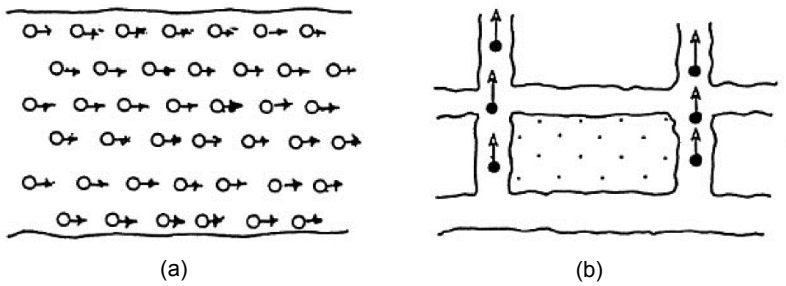

Fig. 1-5—The flow direction of liberated gas in (a) a non-fractured reservoir and (b) a fractured reservoir (van Golf-Racht 1982).

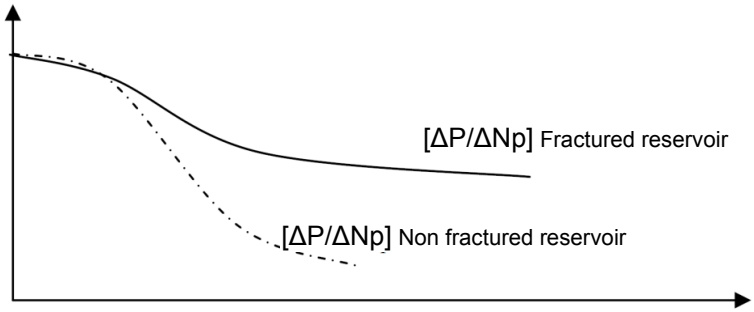

Fig. 1-6—Variation of pressure decline versus recovery (van Golf-Racht 1982).

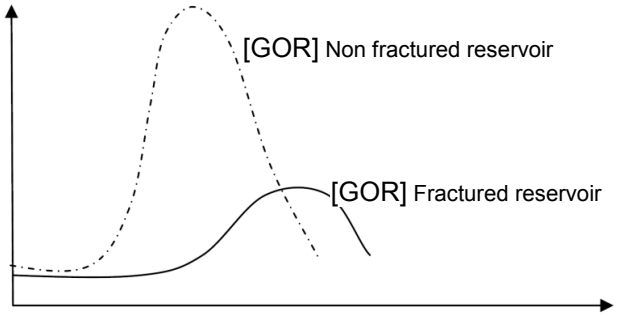

Fig. 1-7—Gas-oil ratio (GOR) versus oil recovery (van Golf-Racht 1982).

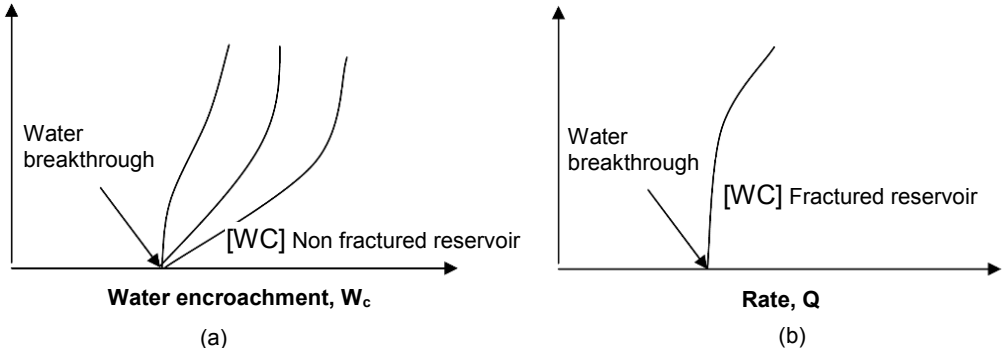

Fig. 1-8—Water cut (WC) in (a) a non-fractured reservoir and (b) a fractured reservoir (van Golf-Racht 1982).

The main challenges for enhancing oil recovery from fractured reservoirs are restoring positive driving capillary forces by changing rock wettability and/or drastically reducing adverse capillary forces to ensure the preponderance of gravity forces over capillary forces. Whereas the former remedial action requires a modification of rock surface from hydrophobic to hydrophilic; the latter remedial action can be obtained through a drastic decrease of water/oil IFT alone. One strategy to meet those purposes consists in adding chemicals to the injected water (Bourbiaux 2009). Chemicals have three primary effects: decreasing water/oil IFT, changing matrix wettability from mixed- or oil-wet to water-wet and increasing viscosity of displacing fluid (Abbasi-Asl et al. 2010).

1.3 Water/oil interfacial tension

1.3.1 Definition

Surface tension is a property of the surface of a liquid that allows it to resist an external force, and liquid surface acts like a thin elastic sheet. When two immiscible liquids, like water and oil, are in contact, there is an interface between them. The acting forces at the interface are called interfacial tension. The cohesive forces among the liquid molecules are responsible for the phenomenon of surface tension. In liquid bulk, the net force on each molecule from neighboring liquid molecules is zero. But the molecules at surface are pulled inwards by unbalanced forces from neighboring liquid molecules because of the lack of liquid molecules from one side, which creates a "surface" with a measurable tension, i.e. surface/interfacial tension (Fig. 1-9).

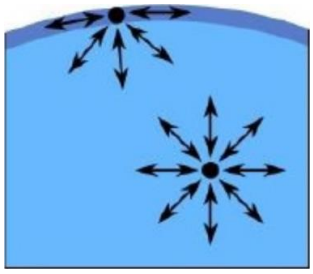

Fig. 1-9—Illustration of surface tension (surface molecules pulled toward liquid causes tension in surface) (Kantzas et al. 2019).

1.3.2 Effects of IFT decrease

Reducing residual oil saturation is closely related to capillary number (Eq. 1.1). According to the concept of capillary number, IFT reduction corresponds to an increase of capillary number, which leads to a decrease of residual oil saturation. As capillary number increases, residual saturations start to decrease at the critical capillary number ($(N_c)_c$), which is the minimum capillary number to mobilize the residual phase but cannot be decreased further at the maximum capillary number ($(N_c)_{max}$), above which the residual saturation would not be further reduced (Sheng 2011). The range between $(N_c)_c$ and $(N_c)_{max}$ is greater for nonwetting phase than for wetting phase. The general relationship between residual saturation of a nonaqueous or aqueous phase and a local capillary number is called capillary desaturation curve (CDC) (Fig. 1-10). The critical capillary number in a normal waterflood is on the order of 10^{-7} (Sheng 2011). For typical sandstone, the critical capillary number is about 5×10^{-6}. The critical capillary number for well sorted sand is about 10^{-4}. However, for carbonates, the critical capillary number is about 10^{-7} (Lake 1984).

$$N_c = \frac{u\mu}{\sigma} \tag{1.1}$$

Where, N_c is capillary number; u is the Darcy flux, cm/s; μ is fluid viscosity, cP; σ is interfacial tension, mN/m.

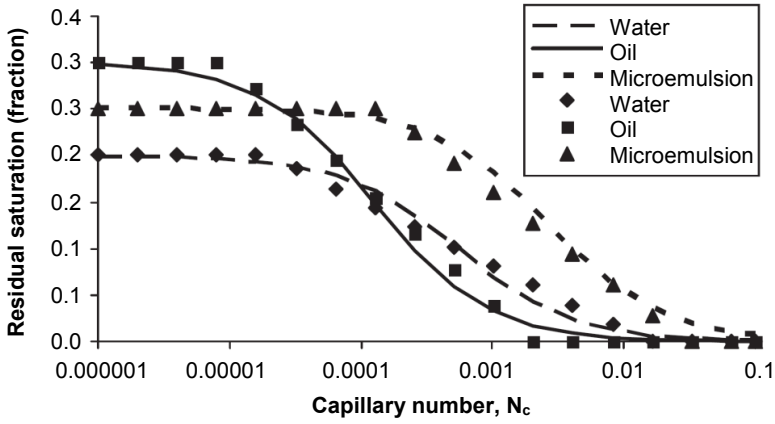

Fig. 1-10—Example of capillary desaturation curve (Sheng 2011).

Abrams (1975) conducted water flooding in short cores of sandstone and limestone to study the influence of interfacial tension, fluid viscosity, and flow velocity on residual oil saturation (S_{or}) of water flooding. For a water-wet rock, the Moore and Slobod dimensionless group (F) (Eq. 1.2) was used to describe residual oil saturation. The results showed that water/oil viscosity ratio had influence on S_{or}. As F increased above 10^{-4}, S_{or} significantly decreased. Since F of normal water flooding is smaller than 10^{-6}, a 100 to 1000 fold increase of F should be yielded to reduce S_{or}. However, the water flooding in carbonate cores conducted by Kamath et al. (2001) showed that the concepts of critical capillary number of residual oil saturation reduction (Abrams 1975) were not valid for those carbonate cores. And the results suggested to increase the pressure gradients through infill drilling or decrease the interfacial tension through low tension flooding to increase oil recovery in those carbonate reservoirs.

$$F = \left(\frac{\upsilon \mu_w}{\sigma_{ow}}\right)\left(\frac{\mu_w}{\mu_o}\right)^{0.4} \tag{1.2}$$

Where, υ is linear velocity, cm/s; μ_j is the viscosity of phase j, j = w or o, cP; σ_{ow} is oil/water interfacial tension, mN/cm.

Water and oil relative permeabilities could be expressed by the following analytical expressions (Eq. 1.3) (Corey 1977), which fit most experimental data. If capillary number is increased, the endpoints and the curvatures are changed and expressed by Eq. 1.4 and Eq. 1.5 (Lake et al. 2014).

$$\begin{aligned} k_{rw} &= k_{rw}^0 \left(\frac{S_w - S_{wr}}{1 - S_{wir} - S_{or}}\right)^{n_w} \\ k_{ro} &= k_{ro}^0 \left(\frac{1 - S_w - S_{or}}{1 - S_{wir} - S_{or}}\right)^{n_o} \end{aligned} \tag{1.3}$$

$$k_{rw}^{0\,h} = k_{rw}^{0\,l} + \left(1 - \frac{S_{or}^{\ h}}{S_{or}^{\ l}}\right)\left(1 - k_{rw}^{0\,l}\right)$$
$$k_{ro}^{0\,h} = k_{ro}^{0\,l} + \frac{S_{wir}^{\ h}}{S_{wir}^{\ l}}\left(1 - k_{ro}^{0\,l}\right) \tag{1.4}$$

$$n_i^{\ h} = n_i^{\ l} + \left(1 - n_i^{\ l}\right)\log\left[\frac{N_c^{\ l}}{(N_c)_c}\right], \quad i = \text{w or o} \tag{1.5}$$

Where, k_{rw}, k_{ro} are water and oil relative permeability, respectively; k_{rw}^0, k_{ro}^0 are the endpoints of water and oil relative permeability, respectively; S_w is water saturation; S_{wir} is irreducible water saturation; S_{or} is residual oil saturation; n_w, n_o are exponents of the water and oil relative permeability, respectively; $(N_c)_c$ is the critical capillary number; the superscripts of h and l means high and low capillary number, respectively.

Experimental and computational observations from Fulcher Jr. et al. (1985) showed that relative permeability of nonwetting (oil) phase was a function of IFT, and relative permeability of wetting (brine) phase was a function of capillary number. Water and oil relative permeabilities increased with the decrease of IFT when IFT was lower than the value of 2 mN/m. At very low IFT values, relative permeability curves straightened out and approached the theoretical X-shape presenting at zero tension. When IFT was lower than 5.5 mN/m, and viscosity was between 2 and 13.6 cP, relative permeability curves were X-shape. As capillary number increased to 0.01, residual oil saturation decreased from approximately 40% to 0. With the increase of capillary number, imbibition-drainage hysteresis was reduced for both k_{ro} and k_{rw}. Results of simulation studies showed that oil recovery increased from 30% to 89% initial oil in place (OOIP) as IFT decreased from 37.9 to 0.0389 mN/m.

Residual saturation is a function of capillary number and can be calculated from an empirical correlation (Eq. 1.6). Endpoint and Corey exponent of relative permeability for each phase can be calculated by linear interpolation of endpoints of relative permeability at high and low capillary number (Eqs. 1.7 and 1.8) (Delshad et al. 1986).

$$S_{ir} = S_{ir}^{\ h} + \frac{S_{ir}^{\ l} - S_{ir}^{\ h}}{1 + C_i N_{ci}} \quad , \qquad i = \text{w or o} \tag{1.6}$$

$$K_{ri}^{0} = K_{ri}^{0l} + \frac{S_{ir}^{\ l} - S_{ir}}{S_{ir}^{\ l} - S_{ir}^{\ h}} \left(K_{ri}^{0h} - K_{ri}^{0l} \right) \quad , \qquad i = \text{w or o} \tag{1.7}$$

$$n_i = n_i^{\ l} + \frac{S_{ir}^{\ l} - S_{ir}}{S_{ir}^{\ l} - S_{ir}^{\ h}} \left(n_i^{\ h} - n_i^{\ l} \right) \quad , \qquad i = \text{w or o} \tag{1.8}$$

Where, S_{ir} is residual saturation of phase i; C_i is capillary parameter of phase i and can be found by curve of CDC; N_{ci} is capillary number of phase i; K_{ri}^0 is endpoint of relative permeability of phase i; n_i is Corey exponent of relative permeability of phase i; superscripts of h and l mean high and low capillary number, respectively.

1.4 Wettability

1.4.1 Definition and test methods

Wettability is the tendency of one fluid to spread on or adhere to a solid surface in the presence of other immiscible fluids (Anderson 1986a). In reservoirs, the liquids could be water, oil or gas, and the solid is rock. The generally used quantitative wettability test methods include contact angle measurement, Amott test, and USBM.

One of the measurement methods of wettability is to measure the contact angle (θ) between two fluids (such as oil and water) which partially wet a solid surface (Fig. 1-11). The experimentally measured contact angle could provide an indication of wettability alteration by some chemicals, like surfactant, even though the wettability indicated by measured contact angle is less oil-wet than the real reservoir wettability because the available adsorption time is much less in the laboratory than that in the reservoir (Treiber and Owens 1972). Contact angle can be calculated from surface tensions considering the equilibrium configuration of two fluid phases on a solid surface. The calculation equation is called Young's equation (Eq. 1.9). However, the values of IFT between solid and oil (σ_{so}) and IFT between solid and water (σ_{sw}) cannot be measured independently in an experiment, and the effects of surface roughness are not considered in this

equation. The range of contact angle is divided into three regions to indicate three different wettability conditions (Table 1-1).

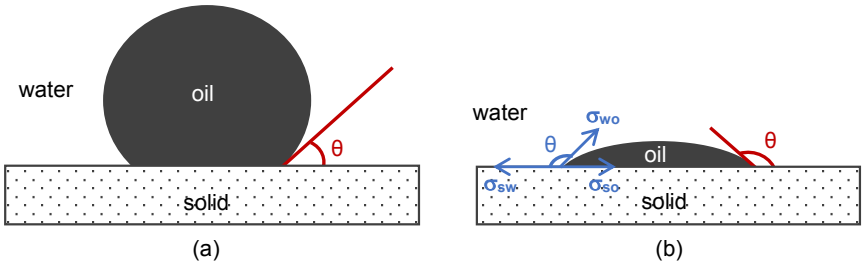

(a) water-wet system; (b) oil-wet system.

Fig. 1-11—The contact angle measured through water.

$$\cos\theta = \frac{\sigma_{so} - \sigma_{sw}}{\sigma_{ow}} \tag{1.9}$$

Where, θ is contact angle, degree; σ_{so} is the interfacial tension of solid and oil, mN/m; σ_{sw} is the interfacial tension of solid and water, mN/m; σ_{ow} is the interfacial tension of oil and water, mN/m.

Table 1-1—The range of contact angle to indicate wettability conditions (Treiber and Owens 1972).

Wettability	Water-wet	Intermediate Wettability	Oil-wet
Contact angle, θ (degree)	0~75°	75~105°	105~180°

Since the roughness, heterogeneity, and complex geometry of reservoir rocks are not taken into account when contact angle is measured, Amott (1959) presented Amott test to avoid the above problem. Amott test includes four displacement operations: (1) spontaneous displacement of water by oil, (2) forced displacement of water by oil in the same system using a centrifuging procedure, (3) spontaneous displacement of oil by water, and (4) forced displacement of oil by water. Ratios of the spontaneous displacement volumes to the total displacement volumes are used as wettability indices (Eq. 1.10 and Eq. 1.11). A modification of Amott index called

Amott-Harvey index is also used (Eq. 1.12), which is varying between -1 and 1. Cuiec (1984) divided the range of Amott-Harvey index into three zones and subdivided the range of intermediate wettability into three parts (Table 1-2). Wettability conditions expressed by the ratios and Amott-Harvey index are shown in Table 1-2. The main problem of Amott and Amott-Harvey methods is that the indexes are insensitive around neutral wettability.

$$\delta_o = \frac{V_{wsp}}{V_{wt}} \tag{1.10}$$

$$\delta_w = \frac{V_{osp}}{V_{ot}} \tag{1.11}$$

$$I = \delta_w - \delta_o \tag{1.12}$$

Where, δ_o is the displacement-by-oil ratio; δ_w is the displacement-by-water ratio; V_{wsp} is the water volume displaced by spontaneous oil imbibition alone; V_{wt} is the total water volume displaced by oil imbibition and forced displacement; V_{osp} is the oil volume displaced by spontaneous water imbibition alone; V_{ot} is the total oil volume displaced by water imbibition and forced displacement; I is Amott-Harvey index.

Table 1-2—Wettability conditions indicated by Amott indexes (Anderson 1986b; Cuiec 1984).

Wettability	Water-wet	Intermediate wettability			Oil-wet
Displacement-by-oil ratio, δ_o	> 0	0			0
Displacement-by-water ratio, δ_w	0	0			> 0
Amott-Harvey index, I	0.3 ~ 1	Slightly water-wet	neutral	Slightly oil -wet	-1 ~ -0.3
		0.1 ~ 0.3	-0.1 ~ 0.1	-0.3 ~ -0.1	

Donaldson et al. (1969) proposed the USBM method based on a correlation between wettability and the areas under capillary pressure curves, which was suggested by Gatenby and Marsden (1957). Fig. 1-12 shows the wettability indexes (WI) of different wettability conditions. A core filled with oil is centrifuged until no more brine is displaced to get the dashed line I. Then the core is placed in a core holder filled with brine and centrifuged to get curve II. Afterwards, the core is placed in a core holder filled with oil and centrifuged to get curve III. A_1 is the area under curve III, and A_2 is the area under curve II. Wettability index is logarithm of the area ratio of A_1 to A_2 (Eq. 1.13). Therefore, when WI is greater than zero, the core is water-wet, and when WI is less than zero, the core is oil-wet. If WI is around zero, the core is intermediate wet (Table 1-3). USBM wettability test overcomes the disadvantage of Amott test, but it cannot determine whether the system is mixed-wet.

$$WI = \log\left(\frac{A_1}{A_2}\right) \tag{1.13}$$

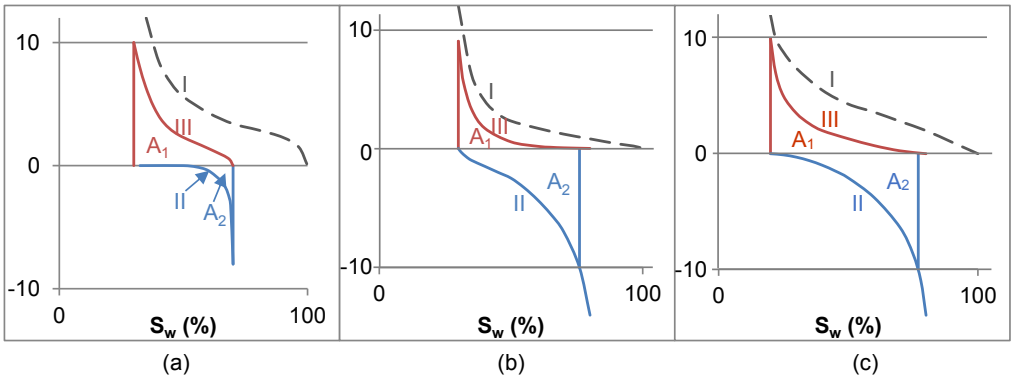

(a) water-wet wettability; (b) oil-wet wettability; (c) neutral wettability.

Fig. 1-12—USBM wettability indexes of different wettability conditions (Donaldson et al. 1969).

Table 1-3—Wettability conditions indicated by USBM wettability indexes (Donaldson et al. 1969).

Wettability	Water-wet	Intermediate wettability	Oil-wet
WI	> 0	0	< 0

1.4.2 Effects of wettability alteration

Some other studies (Richardson et al. 1954; Luffel and Randall 1960; Wissmann 1963) showed that irreducible water saturation decreased as a mixed-wet system became strongly water-wet. But Fatt and Klikoff (1959) and Morrow (1970) gave a conclusion that wettability had little effect on irreducible water saturation at the fractional system, where the strongly water-wet and strongly oil-wet grains distributed randomly. Kennedy et al. (1955) conducted waterflooding in synthetic silica cores by changing wettability while maintaining a constant IFT to study wettability effects on ultimate oil recovery and residual oil saturation. Results showed that the largest ultimate oil recovery happened at a slightly oil-wet condition, but residual oil saturation changed only about 5%. Schwartz (1969) and Lorenz et al. (1974) claimed that when capillary forces dominated oil recovery process, for uniformly wetted cores, both irreducible water saturation and residual oil saturation were minimum at neutral or slightly oil-wet wettability conditions. Jadhunandan and Morrow (1995) conducted slow rate waterflooding experiments in Berea sandstones to study the relationship between wettability and oil recovery, which showed that for crude-oil, brine and rock systems, oil recovery increased, and residual oil saturation decreased with the wettability change from strongly water-wet to nearly neutral wettability. It is believed that the IFTs that disconnect and trap oil are minimized at about neutral wettability condition (Rathmell et al. 1973; Morrow 1979; Wardlaw 1980; Taber 1981; Wardlaw 1982). At strongly water-wet condition, strong IFT will tend to disconnect and snap off some of the oil in matrix, and water tends to move through smaller pores which maybe results in bypassing some of the oil in larger pores. At strongly oil-wet condition, water maybe bypasses some of the oil in small pores by fingering through large pores.

However, Andersen et al. (2015) held a different opinion, which was that water saturation in matrix was smaller when matrix wettability was more oil-wet, because capillary pressure vanished at more oil-wet wettability condition when water saturation was small. They also pointed out that wettability alteration occurred behind water front since components must enter matrix and react, while the frontal water only encountered unaltered areas. Therefore, for fractured matrix, water breakthrough time was not affected by surfactant.

When wettability was more water-wet, water relative permeability decreases and the oil relative permeability increases (Fig. 1-13) (Mungan 1966; Owens and Archer 1971; Donaldson and Thomas 1971; Morrow et al. 1973; McCaffery and Bennion 1974).

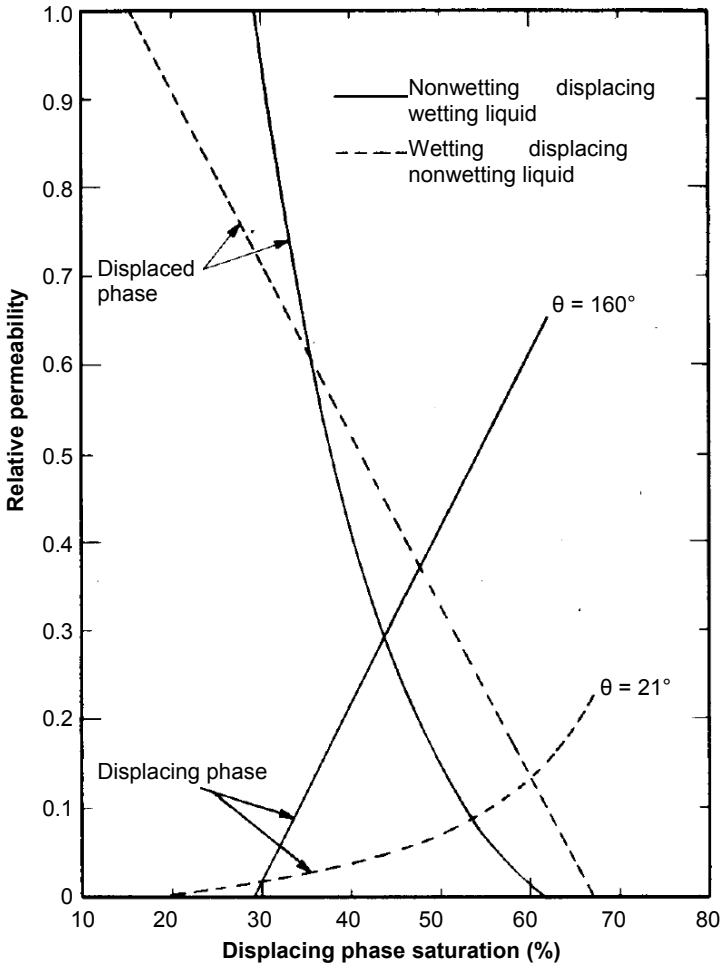

Fig. 1-13—Effect of wettability on relative permeability – sintered Teflon core, refined mineral oil, and water or a sucrose solution. The contact angle (θ) is measured through the displacing phase on a flat Teflon plate (Mungan 1966).

There is no simple relationship between capillary pressure and wettability because the relationship between capillary pressure and saturation is a function of wettability, pore structure, and saturation history. In a uniformly wetted porous medium, the drainage capillary pressure is not affected by contact angle when it is less than 50°, and the spontaneous imbibition capillary pressure is insensitive when the contact angle is less than 22° (Morrow 1975, 1976), which is

because of the simplification of porous medium to be a bundle of capillary tubes, the large number of sharp edges in reservoir rocks, and the rough surfaces of the rocks.

To approximate the relationship between capillary pressure and wettability, the common method is simplifying the porous system as a bundle of capillary tubes. Then Laplace equation (Eq. 1.14) can be rewritten as Eq. 1.15. Therefore, the relationship between capillary pressure and wettability is expressed with Eq. 1.16, which is valid only for capillary tubes and is a poor approximation for porous media (McCaffery and Bennion 1974). Melrose (1965) modified Eq. 1.16 by defining capillary pressure as a function of contact angle (Eq. 1.17). Thus Eq. 1.16 becomes Eq. 1.18 which is valid until contact angle approaches 90° and the application of Eq. 1.18 is limited because of the variation of f(θ) with the type of reservoir rock. Given the assumption that radii are unique function of wetting-phase saturation for a given displacement process (either imbibition or drainage), Laplace equation (Eq. 1.14) can be rewritten as a function of saturation (Eq. 1.19). Then the relationship is expressed with Eq. 1.20 which neglects contact angle and is valid when effective contact angle is zero at the rough surface of porous medium.

$$P_c = P_o - P_w = \sigma\left(\frac{1}{r_1} + \frac{1}{r_2}\right) \tag{1.14}$$

Where, P_c is capillary pressure, atm; P_o is oil pressure, atm; P_w is water pressure, atm; σ is IFT, mN/m; r_1, and r_2 are radii of interface curvature, measured perpendicular to each other, cm.

$$P_c = \frac{2\sigma\cos\theta}{r} \tag{1.15}$$

Where, θ is contact angle through the water in the capillary tube, degree; r is radius of tube, cm.

$$\frac{(P_c/\sigma)_1}{(P_c/\sigma)_2} = \frac{\cos\theta_1}{\cos\theta_2} \tag{1.16}$$

$$P_c = \frac{2\sigma f(\theta)}{r} \tag{1.17}$$

Where, f(θ) is a function of contact angle (θ).

$$\frac{(P_c/\sigma)_1}{(P_c/\sigma)_2} = \frac{f(\theta_1)}{f(\theta_2)} \tag{1.18}$$

$$P_c = \sigma g(S_w) \tag{1.19}$$

Where, g(S_w) is a function of water saturation (S_w).

$$\frac{(P_c)_1}{(P_c)_2} = \frac{\sigma_1}{\sigma_2} \tag{1.20}$$

1.5 Surfactant EOR

1.5.1 Surfactant types

Surfactants are usually organic compounds which are composed of a hydrocarbon chain (hydrophobic group, the "tail") and a polar hydrophilic group (the "head"). Therefore, surfactants are soluble in both organic solvents and water (Fig. 1-14) (Olajire 2014). According to ionic nature of the head group, surfactant can be classified into four groups: anionic, cationic, nonionic, and zwitterionic surfactant (Rosen and Kunjappu 2012). Depending on the formed time, surfactants can be classified into two groups: synthetic surfactant and in-situ surfactant. Surfactant can also be divided into low molecular surfactant and high molecular surfactant according to the weight.

Gao and Sharma (2013) introduced a family of anionic surfactant (Fig. 1-15) synthesized with surfactants with different lengths of hydrophobic tail and linking spacer group. Anionic Gemini surfactants showed a great potential for EOR application at low concentrations and in high-salinity and hard brine conditions. Karasinghe et al. (2016) synthesized new phenol ethoxylate

and IBA ethoxylate co-solvents by adding one PO group between alcohol and EO chain, which remarkably improved the performance of co-solvents and reduced the required co-solvent concentration by as much as one-half. In addition, ultralow IFT, good aqueous stability and low microemulsion viscosity were obtained by the use of ethoxylate and IBA ethoxylate co-solvents. The novel synthesized ultra-short hydrophobe surfactant, 2-ethylhexanol-7PO-sulfate, could further improve oil recovery by reducing the need for nonionic co-solvents in some formulations. The highly branched DIPA ehtoxylate was found to be a good co-solvent by being used to increase pH of formulations in hard brine without conventional alkali with the goal of reducing surfactant retention.

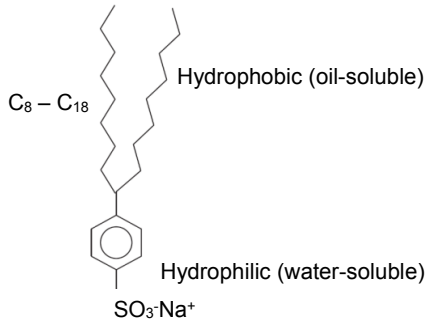

Fig. 1-14—Surfactant molecule (Olajire 2014).

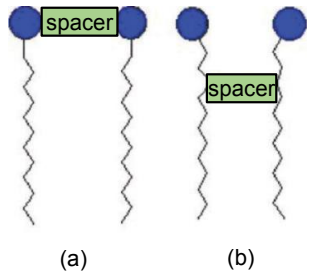

Two possible joint positions: (a) between polar headgroups; (b) close to headgroups.

Fig. 1-15—Schematic of Gemini surfactants (Gao and Sharma 2013).

1.5.2 Surfactant mechanisms

The main mechanisms of surfactant EOR are that surfactant could change matrix wettability and/or reduce water/oil IFT. Surfactant molecules can adsorb on a solid surface to change wettability (Fig. 1-16a) or concentrate at a fluid/fluid interface to change IFT (Fig. 1-16b).

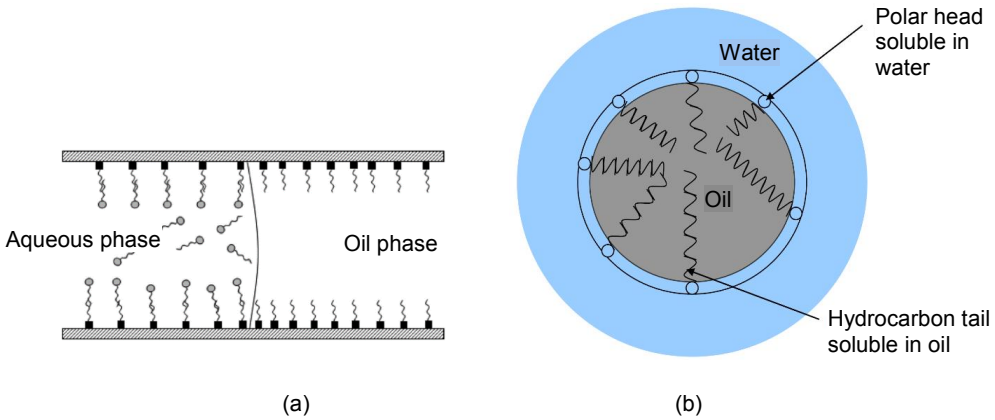

Fig. 1-16—(a) surfactant adsorption on solid surface (Salehi et al. 2008), and (b) surfactant concentration at fluid/fluid interface (Olajire 2014).

The mechanisms of wettability alteration are ion-pair formation and adsorption of surfactant molecules through interactions with the adsorbed crude oil components on rock surface (Standnes and Austad 2000; Salehi et al. 2008). Ion-pair formation is the mechanism of wettability alteration when electrostatic interactions occur. However, in the absence of electrostatic interactions, hydrophobic interaction is the main mechanism. Ion-pair formation is more effective in changing rock wettability, especially the surfactants with higher charge density on the head groups, than the adsorption of surfactant molecules as a monolayer on rock surface. Wettability alteration could be improved by the application of dimeric surfactant, which has two charged head groups and two hydrophobic tails. Gemini surfactants, whose molecules are joined at the head end, are likely to be effective when ion-pair formation is the wettability alteration mechanism, and bolaform surfactants, whose molecules are joined by the hydrophobic tails, should be more effective in the case of surfactant monolayer adsorption.

Surfactant mechanisms are varying with surfactant type and properties, oil, brine, rock, pH, salinity and so on (Babadagli 2003; Babadagli 2003b). Standnes et al. (2002) studied

spontaneous imbibition in oil-wet carbonates using ethoxylated alcohol (EA) (Scamehorn et al. 1982) and cationic surfactant (C12TAB). Results showed that the efficiency of C12TAB was superior to EA, and C12TAB could change wettability to more water-wet than EA. Experiments conducted by Seethepalli et al. (2004) indicated that anionic surfactants (SS-6656, Alfoterra 35, 38, 63, 65, 68) could change the wettability of calcite surface to intermediate/water-wet as well as or better than cationic surfactant DTAB with West Texas crude oil and the presence of Sodium carbonate (Na_2CO_3). Anionic surfactants (5-166, Alfoterra-33, -38, and -68) could lower IFT to a very low value ($< 10^{-2}$ mN/m). Experimental work from Golabi et al. (2012) showed that wettability alteration ability of studied surfactants in limestone rocks was reducing with the sequence of Triton X-100, C_{16}TAB, C_{12}TAB and SDBS.

Tabary et al. (2009) performed both spontaneous and forced imbibition experiments on outcrop carbonate cores using surfactants, alkalis and reactive/non-reactive oils. The experimental results with non-reactive and alkali-reactive oils showed that improved oil recovery was resulted from both rock wettability alteration to more water-wet and water/oil IFT reduction. Na_2CO_3 alone might be sufficient to improve imbibition oil recovery using acidic crude oil, because in-situ surfactants generated from the reaction of sodium carbonate and acidic crude oil could induce a decrease of IFT. For non-reactive oils, alkali could alter wettability of oil-wet cores and make possibility of oil recovery through spontaneous imbibition, and surfactant was playing more as an IFT-reduction agent.

Gao and Sharma (2013) conducted a systematic laboratory testing program on oil/water and solid/water interfacial properties for a family of anionic surfactants. All the anionic Gemini surfactants showed strongly hydrophilic which might be because of the two ionic headgroups and multiple ether groups in the structure. CMC of anionic Gemini surfactants were approximately two to three orders of magnitude lower than those of conventional EOR surfactants. In addition, these surfactants had high tolerance to harsh reservoir conditions (e.g. high temperature, high salinity and/or hardness), and ultralow IFT values were observed toward a higher end of salinity and/or hardness range. Alvarez et al. (2014) evaluated and compared the efficiency of anionic and nonionic surfactants in shale formations by conducting contact angle and IFT measurements, core flooding and computed tomography (CT) scan. Results showed that anionic surfactant had better performance than nonionic surfactant in changing wettability from oil-wet to more water-wet and reducing IFT, thus anionic surfactant could recover more oil than nonionic surfactant. Both anionic and nonionic surfactants could increase the initial and total penetration magnitude.

Experimental study of surfactant imbibition in chalk cores with different wettability (Milter and Austad 1996a, b; Austad et al. 1998; Høgnesen et al. 2006; Austad and Milter 1997) demonstrated that for a water-wet or mixed-wet system with high IFT, fluid flow was countercurrent governed by capillary forces. While in the presence of surfactant, which led to a lower IFT, oil was produced by a slow imbibition process dominated by gravity forces, which was too slow for field application (Fig. 1-17). The dominating displacement forces are changed from capillary forces to gravity forces with IFT reduction. The crossover from countercurrent flow to cocurrent flow happens at an earlier stage for mixed-wet cores than that for water-wet cores.

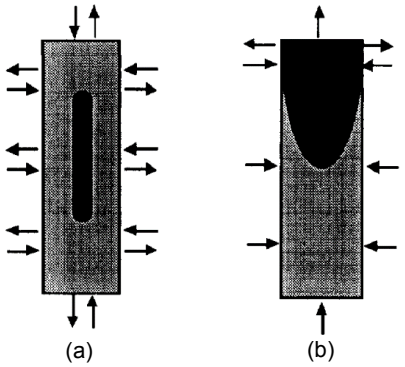

(a) without surfactant, and (b) with anionic surfactant.

Fig. 1-17—Model for experiments of oil production from long water-wet cores (Austad and Milter 1997).

The small-scale simulations conducted by Abbasi-Asl et al. (2010) indicated that lowering the IFT to ultralow and changing the wettability to water-wet at the same time could achieve the largest oil recovery. Chen and Mohanty (2015) studied the effects of synergism between wettability alteration and IFT reduction on surfactant EOR in fractured carbonates by conducting spontaneous imbibition and drainage experiments and numerical simulations. The results showed that divalent ion scavengers could enhance the wettability alteration capability of some sulfonate surfactants in hard brine, which resulted in a higher oil recovery than the sulfonate surfactant only, which could only reduce IFT. They proposed a mechanism that sufficient amount of divalent ion scavengers in anionic surfactant formulation could reduce free divalent cations in hard brine, thus enhance wettability alteration by surfactant adsorption and

promote the release of surfactant monomers from micelles (Fig. 1-18). They concluded that IFT reduction had less effect on imbibition EOR than wettability alteration, but IFT reduction became extremely important when wettability was not changed.

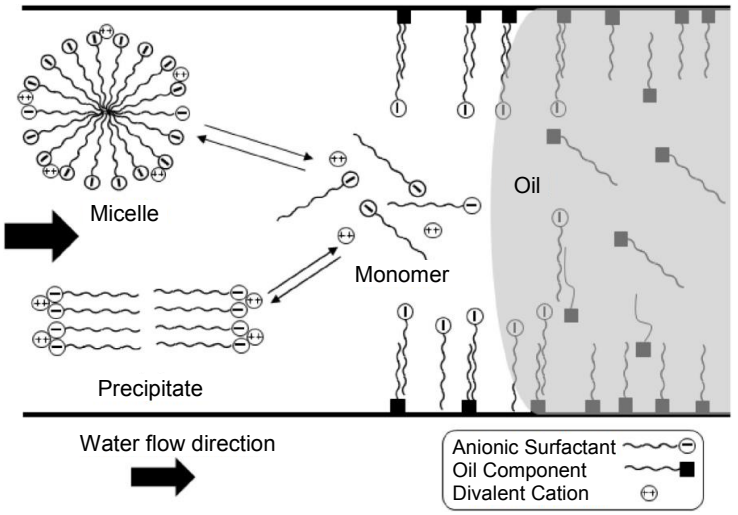

Fig. 1-18—The equilibrium between anionic surfactant micelles, monomers and precipitates and its effects on wettability alteration triggered by surfactant adsorption (Chen and Mohanty 2015).

However, low IFT can lower oil recovery rate especially under unfavorable boundary conditions (Babadagli et al. 1999). In addition, low IFT not always results in incremental recovery (Babadagli 2006). Chabert et al. (2010) studied surfactant effects on wettability and IFT, which showed that the smaller the oil/water IFT, the better the wettability alteration. However, it was proved that it was inefficient to enhance spontaneous water imbibition by using surfactant to lower oil/surfactant solution IFT thus to improve wettability. The best results were obtained through a compromise between good spreading of the water droplet and relatively large IFT ($\sigma > 1$ mN/m). Neog and Schechter (2016) performed spontaneous imbibition experiments and found that surfactant that could significantly alter the wettability but only slightly lower the interfacial tension displaced the most oil because of the creation of strong capillary forces directly responsible for effective spontaneous imbibition. IFT reduction lowered the effectiveness of wettability alteration in improving oil recovery of spontaneous

imbibition. Xie et al. (2018) suggested that during surfactant screening process, the influence of IFT on capillary force should be considered instead of blindly pursuing a lower IFT.

Other experimental studies (Chen et al. 2000; Standnes and Austad 2000; Standnes et al. 2002; Salehi et al. 2008; Golabi et al. 2012; Humphry et al. 2014; Amirpour et al. 2015; Al-Anssari et al. 2017; Delshad et al. 2009) showed that surfactant could enhance oil recovery by changing wettability of sandstones, carbonates, limestones and chalk to more water-wet from mixed- or oil-wet. Wettability alteration depended on oil/brine/rock system, surfactant type and properties, and steric effects close to n-atom (Standnes and Austad 2000; Xu et al. 2005; Alvarez and Schechter 2016; Xie et al. 2018). The extent of wettability alteration increased with the increase of ethoxylation in anionic surfactant. Divalent ions could alter wettability at high temperature (90°C and above). Wettability alteration to more water-wet increased oil recovery rate from fractured carbonates (Gupta and Mohanty 2008). Dynamic phenomena between fracture and matrix played a key role in the efficiency of wettability alteration EOR treatment (Chabert et al. 2010).

1.5.3 Surfactant concentration

Spinler et al. (2000) obtained additional oil recovery from both spontaneous and forced imbibition experiments with low surfactant concentration, but Babadagli (2003) found that the anionic surfactant used in chalks could improve oil recovery only in high surfactant concentration, and surfactant concentration had no effect on nonionic surfactant. Xie et al. (2005) studied surfactant imbibition in carbonate reservoirs, and the results showed that oil recovery of surfactant spontaneous imbibition tended to increase with surfactant concentration, and oil recovery rate was faster with surfactant solution that had higher IFT with crude oil. They believed that the improved recovery was mainly because of wettability alteration rather than buoyancy forces. However, Adibhatla and Mohanty (2008) believed that increasing surfactant concentration did not necessarily enhance oil recovery rate because IFT reduction and wettability alteration were not linearly related to surfactant concentration.

The experiments did by Gupta and Mohanty (2008) indicated that there was an optimal surfactant concentration for varying salinity and an optimal salinity for varying surfactant concentration, at which wettability alteration was the maximum for anionic surfactants. In addition, as reservoir salinity increased, the optimal surfactant concentration decreased. IFT was found to be decreasing or reaching a plateau for increasing surfactant concentration at a

fixed salinity. Karnanda et al. (2013) held the view that IFT reduction had an exponential relationship with the increase of surfactant concentration.

Xie et al. (2018) did spontaneous imbibition experiments using different surfactant concentrations. The results showed that oil recovery was increasing with surfactant concentration and then decreasing when surfactant concentration was above 0.2% (Fig. 1-19). When surfactant concentration was lower than 0.2%, capillary forces dominated the imbibition process, and adhesion-work-reduction factor (Eq. 1.21) and adhesion work on the surface of pore throat decreased with the increase of surfactant concentration. When surfactant concentration was higher than 0.3%, adhesion-work-reduction factor decreased, but surfactant solution had a higher displacement efficiency. When both gravity and capillary forces had effect on imbibition process, the reverse imbibition was restricted, the imbibition strength decreased, and the imbibition recovery decreased.

$$E = \frac{W_s}{W_w} = \frac{\sigma_s \cdot (1 - \cos\theta_s)}{\sigma_w \cdot (1 - \cos\theta_w)} \tag{1.21}$$

where,

$$W_s = \sigma_s \cdot (1 - \cos\theta_s) \tag{1.22}$$

$$W_w = \sigma_w \cdot (1 - \cos\theta_w) \tag{1.23}$$

Where, E is adhesion-work-reduction factor; W_s is the adhesion work of compound system of surfactant/oil/rock, calculated with Eq. 1.22, mN/m; W_w is the adhesion work of compound system of water/oil/rock, calculated with Eq. 1.23, mN/m; σ_s is the surfactant/oil IFT, mN/m; σ_w is the water/oil IFT, mN/m; θ_s is the contact angle of surfactant on rock surface, degree; θ_w is the contact angle of water on rock surface, degree.

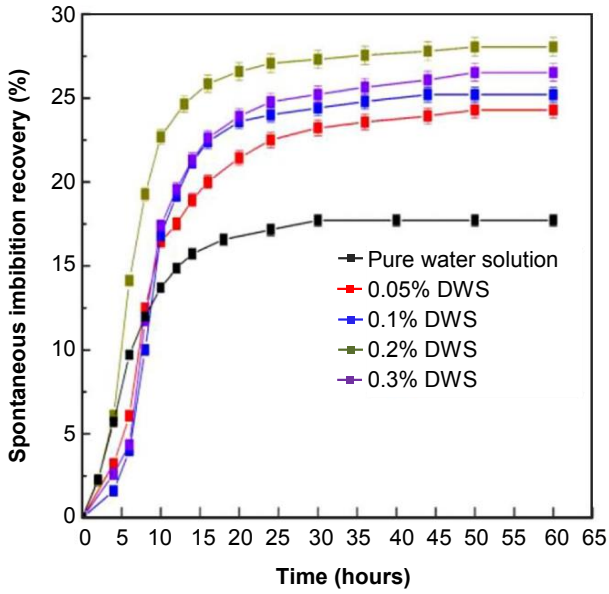

Fig. 1-19—Relationship between spontaneous imbibition recovery and time (Xie et al. 2018).

1.5.4 Surfactant adsorption

The adsorption of three isometrically pure alkylbenzene sulfonates was measured on alumina and kaolinite from very low concentrations to well above CMC (Scamehorn et al. 1982). A typical adsorption isotherm (Fig. 1-20) could be subdivided into four regions. In Region I, the adsorption obeys Henry's Law, which is a linear relationship between surfactant equilibrium concentration and adsorption density. Region II is characterized by a rapid increase in adsorption caused by the formation of local monolayer or bilayer aggregates on solid surface, called hemimicelles or admicelles, respectively. In Region III, surfactant adsorption increases more slowly with concentration than that in Region II. Region IV is the plateau adsorption region and occurs at surfactant concentrations above CMC. The maximum surfactant adsorption occurs at CMC and higher concentrations, but the adsorption levels decrease sharply when surfactant concentration is lower than CMC. Therefore, surfactant adsorption could be reduced to a very low level if surfactant concentration is kept below CMC (Spinler et al. 2000).

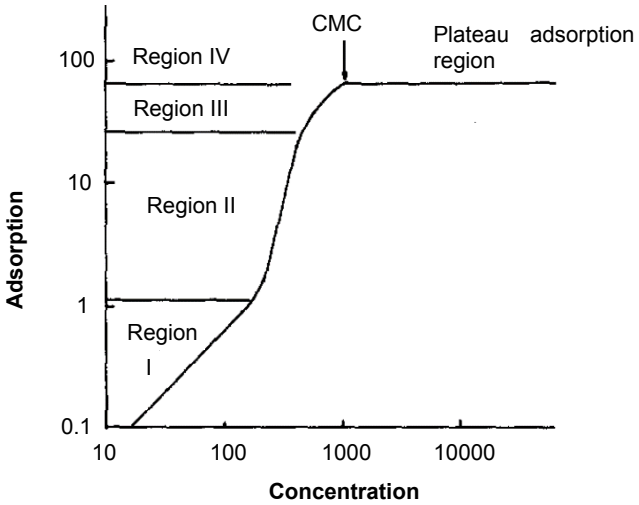

Fig. 1-20—Illustration of adsorption regions for surfactant adsorption on mineral oxide surfaces (Scamehorn et al. 1982).

Figdore (1982) studied the adsorption of anionic ethoxy surfactants on kaolinite at room temperature as a function of pH and electrolyte concentration (NaCl or $CaCl_2$). The results showed that by adding NaCl, surfactant adsorption was increasing with the decrease of pH and increase of NaCl concentration; by adding $CaCl_2$, surfactant adsorption was high at acidic and basic pH's and going through a shallow minimum at approximate pH of 8. In addition, when the concentration of $CaCl_2$ was above a certain minimum concentration, surfactant adsorption was independent on $CaCl_2$, which was interpreted in terms of the ability of Ca^{2+} to form a calcium-surfactant complex, which could adsorb on clay and played a significant role in the adsorption process.

Ahmadall et al. (1993) compared the adsorption of anionic and cationic surfactants on carbonate minerals. The results showed that in the scope of their study, cationic surfactants had significantly lower adsorption concentration than anionic surfactants with similar hydrophobic chain length, especially when the salts of multivalent cations were added. One of the reasons for the decreased adsorption was that the added cations and lattice ions of carbonate minerals could affect mineral surface charge. The other reason was the lowered chemical potential of surfactant in the aggregates resulted from the interaction of multivalent counter-ions and the aggregates of adsorbed anionic surfactants, which counteracted the coulombic repulsions between surfactant head groups. The results suggested that it might be possible to dramatically

reduce surfactant adsorption on carbonates by using a cationic surfactant with an appropriate level of added multivalent electrolyte.

The adsorption of sulphonate surfactants on carbonates can be significantly suppressed by the addition of Na_2CO_3 (Seethepalli et al. 2004). The adsorption of anionic surfactants on calcite decreases with an increase of pH and a decrease of salinity. Surfactant adsorption capacity can be reduced when alkaline is used along with surfactants (Zhang et al. 2016). The temperature effects on anionic surfactant adsorption on calcite depend on whether adsorption is enthalpy-driven or entropy-driven (Adibhatla and Mohanty 2008). Anionic or non-ionic surfactants are adsorbed on oil droplets and rock surfaces, which could increase superficial charge density and electrostatic repulsion between oil droplets and rock surface. Therefore, oil droplets are easily displaced, and sweep efficiency is increased (Xu et al. 2011).

Gao and Sharma (2013) conducted a series of static adsorption tests to study anionic Gemini surfactants adsorption on Berea sand material/water interface. Anionic Gemini surfactant showed a lower plateau adsorption density than conventional surfactants. Decreasing solution salinity could lower surfactant adsorption by prohibiting surface aggregate growth and promoting electrostatic repulsion. However, surfactant adsorption could be promoted by longer alkyl chains and spacer groups because of the reduction of solubility and stronger interactions with solid surface. Garcia-Olvera et al. (2016) estimated chemical static adsorptions on sandstone and carbonate, and results showed that most chemicals adsorbed more on sandstone than on carbonate. They suspected that a bigger size of carbonate fragment led to a smaller surface area, which resulted in a less chemical adsorption on carbonate.

Cui et al. (2014) studied the adsorption of the tertiary amine surfactant Ethomeen C12, which could dissolve in high pressure CO_2 as a nonionic surfactant and equilibrate with brine as a cationic surfactant. The adsorption of C12 was sensitive to equilibrium pH, electrolyte composition of brine, and minerals in carbonate formation materials. Isoelectric divalent-ion concentration ($[Me^{2+}]^*$) was proposed for determining the sign of mineral surface charge. The surface charge was positive if Me^{2+} activity of brine was greater than isoelectric concentration, thus the adsorption of cationic surfactant should be low. If Me^{2+} is less than $[Me^{2+}]^*$, then the adsorption should be high. Cationic surfactant adsorption was high if carbonate formation contained silica or clays because of the negatively charged binding sites on surface. But the increase of divalent ions (Ca^{2+} and Mg^{2+}) and trivalent (Al^{3+}) ions reduced C12 adsorption on silica because of the competition for the negatively charged silica sites between multivalent cations and monovalent cationic surfactant. C12 adsorption was low at low pH. However, the

dissolution of calcite and dolomite might raise pH and thus increase C12 adsorption or even cause surfactant precipitation.

The experimental study of the effect of surfactant adsorption on surfactant imbibition conducted by Qi et al. (2016) showed that the increase of surfactant adsorption improved surfactant imbibition because surfactant adsorption resulted in a decrease of surfactant concentration in microemulsion phase thus reduced IFT. And surfactant adsorption on rock altered the rock wettability to more water-wet which could increase oil recovery. However, Qi et al. (2016) claimed that the balance between surfactant adsorption concentration and EOR efficiency should be considered since excessive surfactant adsorption could lead to an increase of surfactant application cost.

1.5.5 Surfactant diffusion

In the absence of external driving forces and significant spontaneous imbibition, imbibition after wettability modification is limited to the rate of molecular diffusion. In ideally water-wet case, capillary diffusion coefficient is on the order of about 10^{-8} m^2/s. In intermediate-wet case, as established after aging with initial water saturation, diffusion coefficient is on the order of about 10^{-11} m^2/s. This is attributed to a small countercurrent relative permeability to water at low saturations. The time required to achieve full penetration by diffusion increases proportionally with the square of the length scale, $t \propto L^2$. Therefore, it is not economically interesting (Stoll et al. 2008). The small-scale simulations conducted by Abbasi-Asl et al. (2010) indicated that molecular diffusion had an insignificant effect on oil recovery.

1.5.6 Surfactant solution viscosity

The viscosity of surfactant solution can be increased by adding polymer or by changing the salinity of aqueous surfactant solution, which affects the viscosity of in-situ microemulsion (Parra et al. 2016). Transverse pressure gradient induced by microemulsion viscosity can push surfactant farther into matrix and increase sweep efficiency, which is not captured in imbibition cells. And even a small viscous gradient is more effective than diffusion or capillarity (Abbasi-Asl et al. 2010). Parra et al. (2016) conducted a series of low IFT surfactant flooding in Silurian Dolomite and Texas Cream Limestone cores to study the effect of viscous forces on oil recovery of surfactant flooding in fractured oil-wet carbonate cores. Results showed that the increase of

microemulsion viscosity from 0.5 cP to 75 cP by changing salinity of surfactant solution could increase oil recovery by 40% OOIP, which implied that viscous microemulsion had potential to greatly improve oil recovery from fractured oil-wet carbonate reservoirs by being used as mobility control agents.

Another way to increase the viscosity of surfactant solution is to use viscoelastic surfactant (VES), which is self-assembling surfactant that contributes to displacement and sweet efficiency through the formation of wormlike micelles (WLM) that can generate higher viscosity especially at harsh conditions (Fig. 1-21) (Azad and Sultan 2014).

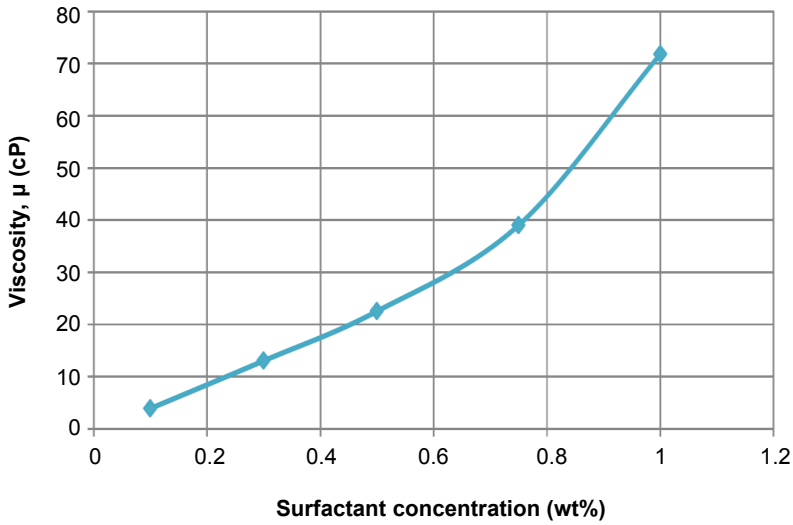

Fig. 1-21—Viscosity of surfactant solution vs. surfactant concentration for viscoelastic surfactant system at 70 °C (Azad and Sultan 2014).

1.5.7 Matrix properties

Qi et al. (2016) did spontaneous imbibition experiments and claimed that brine imbibition recovery decreased with the increase of matrix permeability and initial water saturation. Some surfactant imbibition experiments (Adibhatla and Mohanty 2008; Delshad et al. 2009; Qi et al. 2016; Xie et al. 2018) showed that surfactant enhanced oil recovery increased with the increase of matrix permeability and the decrease of initial water saturation. Chen et al. (2000) claimed that high porosity and homogeneous formations were essential for achieving effective gravity segregation, thus more oil could be recovered. Temperature and pressure have different effects

on wettability and IFT depending on the properties of rock and fluid, and surfactant type (Rao 1999; Strand et al. 2003; Xu et al. 2005; Karnanda et al. 2013). Cuiec et al. (1994) conducted surfactant spontaneous imbibition experiments in cores with different sizes. The study showed that ultimate oil recovery did not change much with core length, but imbibition rate was strongly affected by core length (Fig. 1-22a). However, the surfactant spontaneous imbibition experiments in chalk cores (Milter and Austad 1996a) showed that oil recovery from the small core was larger than that from the long core (Fig. 1-22b). Simulation studies of surfactant imbibition in oil-wet fractured blocks did by Adibhatia et al. (2005) indicated that as the increase of matrix height or wettability alteration to a lesser degree or the decrease of permeability, oil production rate decreased.

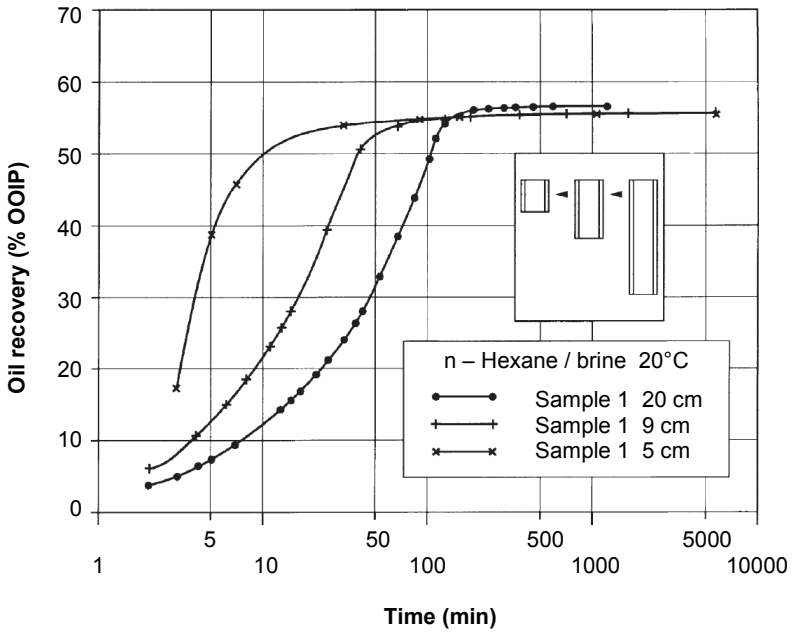

(a)

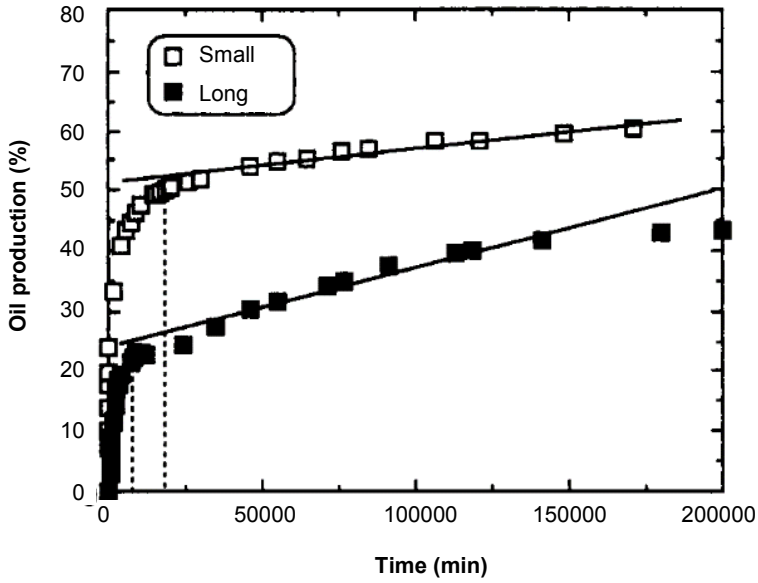

(b)

(a) Cuiec, Louis et al. (1994), and (b) Milter and Austad (1996a).

Fig. 1-22—Length influence on imbibition in chalk cores.

1.5.8 Tertiary surfactant EOR

Experiments of surfactant spontaneous imbibition in oil-wet and water-wet chalk cores (Austad et al. 1998) showed that in tertiary spontaneous imbibition stage, surfactant could recover some oil from oil- and mixed-wet cores, but there was no extra oil was recovered from water-wet cores. It is believed that the extra oil obtained from oil-wet and mixed-wet cores results from wettability alteration to more water-wet during imbibition process. When surfactant is used in the secondary spontaneous imbibition stage, the displacement process gradually changes from countercurrent flow governed by capillary forces to cocurrent flow governed by gravity forces. Babadagli et al. (2005) conducted surfactant flooding and capillary imbibition experiments. If surfactant solution was used in secondary recovery phase, surfactant flooding did not recover more oil than waterflooding at the untouched un-fractured portions of reservoir. For the untouched fractured zones of chalk reservoir, starting the project with surfactant injection is more effective than waterflooding. Sweep efficiency was more important than IFT reduction. When surfactant is used in tertiary recovery phase, different recovery trends were observed. Earlier water breakthrough was observed in some cases. Some other cases exhibited high

waterflooding oil recovery. Whereas some cases exhibited low waterflooding oil recovery but high surfactant oil recovery. Surfactant concentration and type and IFT are important factors. Oil recovery from a fractured formation is a function of both capillary imbibition rate and injection rate. As the flow rate increases, the contact time between matrix and fluid in the fracture decreases, which reduces the effect of capillary pressure, chemical transport, diffusion, etc. (Abbasi-Asl et al. 2010).

The application of low IFT surfactants at tertiary recovery phase could significantly increase the oil recovery by mobilizing residual oil over that of water flooding in originally oil-wet low permeability carbonate rocks (Karnanda et al. 2013; Bennetzen et al. 2014; Garcia-Olvera et al. 2016). The ultimate oil recovery is high, but the recovery occurs at a very low rate.

The static imbibition and forced imbibition experiments (Dong and Al Yafei 2015; Parra et al. 2016) showed that the IFT reduction had more effect on static imbibition than the wettability alteration, but the wettability alteration was more efficient than the IFT reduction to recover oil by forced imbibition process. However, the IFT reduction increased the static imbibition time required to reach the equilibrium. Therefore, the balance between gravity and capillary drainage must be taken into account to choose the best tertiary recovery solution.

Xie et al. (2018) did dynamic imbibition experiments to study the influence of the flow speed of the imbibition solution flowing in the fracture on the surfactant EOR in fractured reservoirs. The results showed that the flow speed had obvious influence on surfactant dynamic imbibition. They suggested that in a practical field application, in order to obtain a higher imbibition recovery, a suitable injection velocity should be chosen to take full advantage of the adsorbing water and discharging oil function of the capillary force, the displacement function of the viscous force, and wettability alteration.

1.6 Upscaling of surfactant EOR

1.6.1 Upscaling methods for capillary dominating imbibition

Mattax and Kyte (1962) introduced a dimensionless parameter (Eq. 1.24) used to scale up the imbibition oil recovery behavior for a given rock type and oil/water viscosity ratio. Assumptions made in development of the method are as follows: (a) the volume of oil contained in fractures is negligible compared with the volume of oil in matrix blocks; (b) there is no

resistance to fluid flow in fractures; (c) the effect of gravity on fluid flow in matrix blocks is ignored; and (d) water in fractures rises uniformly in a horizontal plane throughout the reservoir.

$$t_{Dc} = \sqrt{\frac{K}{\phi}} \frac{\sigma}{\mu_w L^2} t \tag{1.24}$$

Where, t_{Dc} is upscaling dimensionless time for capillary dominating imbibition; K is absolute permeability, mD; ϕ is porosity; σ is interfacial tension, mN/m; μ_w is water viscosity, cP; L is characteristic linear dimension of matrix block or sample, cm; t is time, s.

To account for the effect of viscosity ratio, sample shape and boundary conditions, water viscosity is displaced by geometric mean of water and oil viscosities. So the dimensionless scaling parameter is modified as Eq. 1.25 (Ma et al. 1999).

$$t_{Dc} = \sqrt{\frac{K}{\phi}} \frac{\sigma}{\sqrt{\mu_w \mu_o} L_c^2} t \tag{1.25}$$

where,

$$L_c = \sqrt{\frac{V_b}{\sum_{i=1}^{n} \frac{A_i}{l_{Ai}}}} \tag{1.26}$$

Where, μ_o is oil viscosity, cP; L_c is a characteristic length; V_b is bulk volume of the matrix, cm^3; A_i is the area open to imbibition at the i^{th} direction, cm^2; l_{Ai} is the distance from the imbibition face to the no-flow boundary, which is illustrated in Fig. 1-23 (Babadagli 2001a), cm.

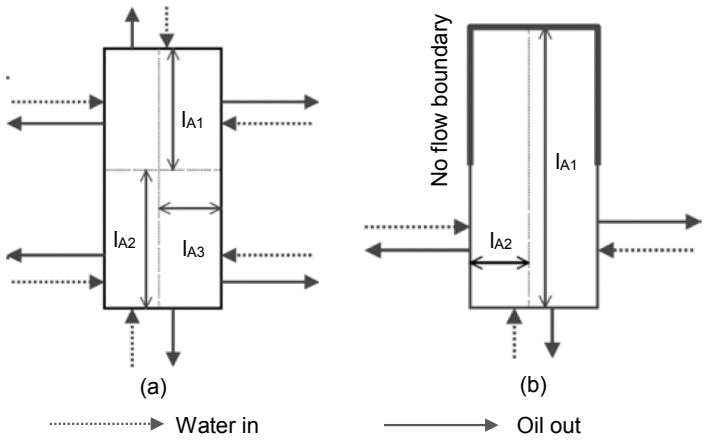

Fig. 1-23—Determination of characteristic length L_c for different types of matrix boundary conditions (Babadagli 2001a).

Wang et al. (2016) conducted spontaneous imbibition experiments and modified the upscaling group proposed by Ma et al. (1999) (Eq. 1.25). They used a similar equation (Eq. 1.27) for the field scale as the equation for laboratory samples (Eq. 1.25). It was assumed that t_{Dc50} was the t_{Dc} value, at which half of the oil had been displaced from rock. Therefore, t_{Dc} had the same value in a laboratory core as in a field for the proper conditions. They assumed that porosity, permeability and viscosity of water and oil were similar between laboratory and field, then they developed Eq. 1.28.

$$t_{Dc} = \sqrt{\frac{K}{\phi}} \frac{\sigma}{\sqrt{\mu_o \mu_w}} \frac{1}{L^2_{c(field)}} t_{(field)} \tag{1.27}$$

$$t_{(field)} = \frac{L^2_{c(field)}}{L^2_{c(lab)}} t_{(lab)} \tag{1.28}$$

Where, $t_{(field)}$ is field scale time, s; $L_{c(field)}$ is field scale characteristic length, cm; $t_{(lab)}$ is laboratory scale time, s; $L_{c(lab)}$ is laboratory scale characteristic length, cm.

Schechter et al. (1994) defined an inverse Bond number (N_B^{-1}) (Eq. 1.29) and then proposed a time scale (Eq. 1.30) for capillary dominating imbibition when the inverse Bond numer is big ($N_B^{-1} >> 1$):

$$N_B^{-1} = C\frac{\sigma}{\Delta\rho g H}\sqrt{\frac{\phi}{K}} \tag{1.29}$$

$$t_c^* = \frac{\phi}{C\sigma\lambda^*}\frac{H^2}{R^2}\sqrt{\frac{K}{\phi}} \tag{1.30}$$

where,

$$\lambda^* = \frac{Kk_r^*}{\mu^*} \tag{1.31}$$

Where, N_B is Bond number; C = 0.4 for the capillary tube model; σ is interfacial tension, mN/m; ϕ is porosity; K is absolute permeability, mD; Δρ is density difference between water and oil, g/cm^3; g is earth gravity, cm/s^2; H is core length, cm; t_c^* is time scale for capillary imbibition, s/cm^2; λ^* is reference mobility, mD/cP; R is core radius, cm; k_r^* is reference relative permeability; μ^* is reference viscosity, cP.

1.6.2 Upscaling methods for gravity dominating imbibition

For gravity driven flow, when the inverse Bond number is small ($N_B^{-1} << 1$), Schechter et al. (1994) proposed a time scale (Eq. 1.32):

$$t_g^* = \frac{\phi H}{\lambda^*\Delta\rho g} \tag{1.32}$$

Where, t_g^* is time scale for gravity imbibition; λ^* is a reference mobility, mD/cP; ϕ is porosity; $\Delta\rho$ is density difference between water and oil, g/cm^3; g is earth gravity, cm/s^2; H is core length, cm.

Mirzaei et al. (2016) modified Eq. 1.32 using experimental and numerical results to include both core length and core diameter (Eq. 1.33).

$$t_{Dg} = \frac{\lambda^* \Delta\rho g}{\phi}\left(\frac{1}{H} + \frac{8\gamma}{\pi D}\right)t \tag{1.33}$$

Where, t_{Dg} is upscaling dimensionless time for gravity dominating imbibition; π is circular constant, 3.14; γ is the ratio of the flux from the sides to the flux from the core bottom; D is core diameter, cm.

Cuiec et al. (1994) proposed a dimensionless upscaling group (Eq. 1.34) for matrix-fracture interaction dominated by gravity force due to greater matrix size, less water-wet or lower IFT.

$$t_{Dg} = \frac{K\Delta\rho}{\phi\mu_o L}t \tag{1.34}$$

Boundary conditions affect the mechanisms of gravity dominating imbibition. Babadagli (2001) took this effect into consideration by multiplying the group by a boundary condition factor (BCF) (Eq. 1.35). And Babadagli (2003a) modified Eq. 1.34 by using water viscosity (μ_w) to replace oil viscosity (μ_o) (Eq. 1.36).

$$t_{Dg} = t\frac{K\Delta\rho}{\phi\mu_o L}BCF \tag{1.35}$$

$$t_{Dg} = \frac{K\Delta\rho}{\phi\mu_w L}t \tag{1.36}$$

1.6.3 Upscaling methods for imbibition dominated by both capillarity and gravity

During upscaling, the effects of gravity, buoyancy and a viscous pressure differential relative to capillary pressure must be accounted for cautiously (Stoll et al. 2008). Simulation studies of surfactant imbibition in initially oil-wet fractured blocks conducted by Adibhatia et al. (2005) indicated that capillary pressure was the dominating force in the early stage, and gravity dominated the process in the later stage. Therefore, both capillarity and gravity helped to improve oil recovery.

Babadagli (1996) conducted capillary imbibition experiments on Berea Sandstone cores, which had the same rock properties, such as permeability, porosity and size, and he modified a dimensionless time for capillary imbibition (Eq. 1.24) by accounting for the effect of wettability (Eq. 1.37).

$$t_{Dc} = ct\frac{\sigma f(\theta)}{\mu_o} \tag{1.37}$$

Where, f(θ) is a certain function of rock wettability, dimensionless; c is a constant related to rock properties, 1/m.

Goudarzi et al. (2012) conducted imbibition experiments using cores with different sizes to study the impact of matrix size and fracture spacing on oil recovery. They modified published gravity-based dimensionless time (Eqs. 1.38 and 1.39) (Hagoort 1980) by including the effect of IFT on both large and small cores (Eqs. 1.40 ~ 1.42), and the upscaling results showed that the increase of matrix height resulted in a decrease of oil recovery and a linear increase of imbibition time.

$$t_{Dg} = \frac{Kk_{ro}^{0}\Delta\rho g}{(S_{oi} - S_{or})\phi\mu_o L}t \tag{1.38}$$

$$E_R = \frac{(S_{oi} - \overline{S_o})}{(S_{oi} - S_{or})} \tag{1.39}$$

$$t_D = t\frac{Kk_{ro}^{0}\Delta\rho g}{(S_{oi} - S_{or})\phi\mu_o L}IFTfactor \tag{1.40}$$

$$E_R = \frac{(S_{oi} - \overline{S_o})}{(S_{oi} - S_{or})}IFTfactor \tag{1.41}$$

where,

$$IFTfactor = \frac{\sigma_i - \overline{\sigma}}{\sigma_i - \sigma_f} \tag{1.42}$$

Where, t_D is dimensionless time; k_{ro}^0 is endpoint of oil relative permeability; E_R is oil recovery; S_{oi} is initial oil saturation; S_{or} is residual oil saturation; $\overline{S}_o$ is average oil saturation; IFTfactor is interfacial tension factor; $\overline{\sigma}$ is average interfacial tension, mN/m; σ_i is initial interfacial tension, mN/m; σ_f is final interfacial tension, mN/m.

Li and Horne (2001) derived a function (Eq. 1.43) for charactering the water imbibition into gas-saturated rocks with the assumptions that: (1) Darcy's Law was applicable during the process of water spontaneous imbibition: (2) gas mobility was infinite; (3) water imbibition was a piston-like flow process; and (4) initial water saturation in the porous medium was homogeneous, which revealed that the rate of the water spontaneous imbibition had a linear relationship with the reciprocal of gas recovery. In addition, based on Eqs. 1.44 and 1.45, the effective capillary pressure and effective water permeability at S_{wf} could be calculated with Eqs. 1.47 and 1.48.

$$q_w = a\frac{1}{R} - b \tag{1.43}$$

where,

$$a = \frac{Ak_w^*\left(S_{wf} - S_{wi}\right)}{\mu_w L} P_c^* \tag{1.44}$$

$$b = \frac{Ak_w^*}{\mu_w}\Delta\rho g \tag{1.45}$$

$$R = \frac{N_{wt}}{V_p} \tag{1.46}$$

$$P_c^* = \frac{\Delta\rho g L}{\left(S_{wf} - S_{wi}\right)}\frac{a}{b} \tag{1.47}$$

$$k_w^* = \frac{\mu_w}{A\Delta\rho g} b \tag{1.48}$$

Where, q_w is water imbibition rate, cm^3/s; a and b are constants related to matrix size, water saturation, water relative permeability, water viscosity, capillary pressure, and gravity; A is cross-section area of the matrix, cm^2; S_{wf} is the average water saturation behind imbibition front; S_{wi} is initial water saturation; μ_w is water viscosity, cP; L is matrix length, cm; k_w^* is the effective water permeability at S_{wf}, mD; P_c^* is the effective capillary pressure at S_{wf}, atm; $\Delta\rho$ is density difference between gas and water, g/cm^3; g is gravity constant, mN/g; R is recovery by water imbibition; N_{wt} is water volume imbibed into the matrix, cm^3; V_p is pore volume of the matrix, cm^3.

Then Li and Horne (2004) defined the ratio of b/a (Eq. 1.49), the normalized recovery (R^*) (Eq. 1.50) and the dimensionless time (Eq. 1.51) to obtain the relationship between recovery and imbibition time in gas/water/rock systems. So, when $0 \leq R^* < 1$, the relationship was expressed by Eq. 1.52 or 1.53. In this model, gravity and capillary forces, effective water permeability, water saturation, water viscosity, matrix size, wettability, and matrix porosity are considered.

$$N_B = \frac{b}{a} = \frac{\Delta\rho g L}{\left(S_{wf} - S_{wi}\right) P_c^*} \tag{1.49}$$

$$R^* = N_B R \tag{1.50}$$

$$t_{D1} = N_B^2 \frac{k_w^* P_c^* \left(S_{wf} - S_{wi}\right)}{\phi \mu_w L_c^2} t \tag{1.51}$$

$$\ln\left(1 - R^*\right) + R^* = -t_{D1} \tag{1.52}$$

$$\left(1 - R^*\right) e^{R^*} = e^{-t_{D1}} \tag{1.53}$$

Where, N_B is the ratio of gravity force to capillary force; R^* is normalized recovery; t_{D1} is dimensionless time, which includes both gravity and capillary forces.

Because gas mobility is assumed infinite, Eq. 1.51 cannot be applied to other systems such as oil/water/rock systems. To consider the mobility of water in oil/water/rock systems, Li and Horne (2002) developed another scaling method (Eq. 1.54).

$$t_{D2} = \frac{K k_{re}^* P_c^* \left(S_{wf} - S_{wi}\right)}{\phi \mu_e L_c^2} t \tag{1.54}$$

where,

$$\lambda_e^* = \frac{Kk_{re}^*}{\mu_e} \tag{1.55}$$

Where, t_{D2} is dimensionless time; k_{re}^* is the pseudo relative permeability; ϕ is porous medium porosity; μ_e is effective viscosity of the two phases, cP; λ_e^* is the effective mobility at S_{wf}, mD/cP.

For cocurrent and countercurrent spontaneous imbibition, the effective mobility was expressed as Eq. 1.56 and Eq. 1.57, respectively.

$$\lambda_e^* = \frac{Kk_{re}^*}{\mu_e} = \frac{\lambda_o^* \lambda_w^*}{\lambda_o^* - \lambda_w^*} = K \frac{\frac{k_{ro}^*}{\mu_o} - \frac{k_{rw}^*}{\mu_w}}{\frac{k_{ro}^*}{\mu_o} - \frac{k_{rw}^*}{\mu_w}} \tag{1.56}$$

$$\lambda_e^* = \frac{Kk_{re}^*}{\mu_e} = \frac{\lambda_o^* \lambda_w^*}{\lambda_o^* + \lambda_w^*} = K \frac{\frac{k_{ro}^*}{\mu_o} - \frac{k_{rw}^*}{\mu_w}}{\frac{k_{ro}^*}{\mu_o} + \frac{k_{rw}^*}{\mu_w}} \tag{1.57}$$

Where, λ_o^* and λ_w^* are the oil and water mobility at S_{wf}, respectively, mD/cP; μ_o and μ_w are oil and water phase viscosity, respectively, cP; k_{ro}^* and k_{rw}^* are the oil and water phase relative permeability at S_{wf}, respectively.

However, gravity was neglected in the above method (Eq. 1.54), therefore, Li and Horne (2006) proposed a general scaling approach for spontaneous imbibition which included both gravity and capillarity. The dimensionless time was expressed as Eq. 1.58.

$$t_D = N_B^2 \frac{Kk_{re}^* P_c^* \left(S_{wf} - S_{wi}\right)}{\phi \mu_e L_c^2} t \tag{1.58}$$

1.7 Simulation study of surfactant EOR

1.7.1 Fractured reservoir model

To model fractured reservoirs, Warren and Root (1963) introduced the concept of dual porosity (Fig. 1-24). They presented an analytical solution for single-phase, unsteady-state flow in a naturally fractured reservoir.

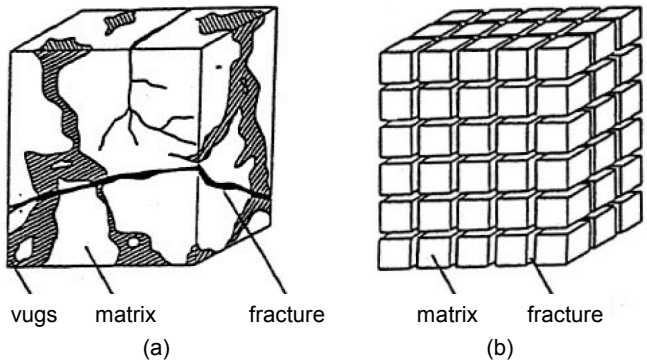

Fig. 1-24—(a) fractured reservoir and (b) dual porosity model (Warren and Root 1963).

Some improvements were made to make the original dual porosity model more realistic. Reiss (1980) discussed the effect of gravity on fluid transfer between matrix and fracture. Thomas et al. (1983) developed a 3D, three-phase, finite difference dual porosity model for simulating naturally fractured reservoirs. They assumed that the reservoir comprised continuous fracture system and discontinuous matrix blocks. Primary flow in reservoir occurred within fractures with local exchange of fluids between fracture system and matrix blocks. Each block had known properties and geometric shape, and all blocks within a given grid block were identical. In order to account for gravity effects, they introduced pseudo capillary pressure for matrix. Dean and Lo (1988) proposed that the effect of gravity segregation could be included in pseudo capillary pressure terms for both matrix and fracture. Shirdel et al. (2011) introduced a new method to

derive pseudo capillary pressures that preserved gravity effects for both water/oil and gas/oil systems under various conditions.

1.7.2 Surfactant EOR simulation

The mostly used simulators of surfactant EOR include Eclipse, UTCHEM, and CMG-STAR. Here only the simulator Eclipse is introduced, which is the simulator used for the simulation studies in this thesis.

To simulate wettability alteration, immiscible oil-wet and water-wet saturation tables are used in the programming. Wettability alteration is described as a function of surfactant adsorption concentration. The extent of wettability alteration is expressed by the parameter of ω. If the value of ω is 1, wettability is not changed; if the value of ω is 0, the purely water-wet saturation table is used, which means that wettability is changed to the largest extent. To simulate IFT decrease, a miscible saturation table is used. IFT decrease is described by a function of surfactant concentration in brine. The functions used to simulate wettability alteration and IFT reduction in Eclipse are Eqs. 1.59~1.64. Immiscible saturation end-points are interpolated between immiscible oil-wet and water-wet saturation end-points (Eq. 1.59). The final saturation end-points are interpolated between immiscible and miscible saturation end-points (Eq. 1.60).

$$\begin{aligned} S_{wco}^{imm} &= \omega S_{wco}^{ow} + (1-\omega) S_{wco}^{ww} \\ S_{wcr}^{imm} &= \omega S_{wcr}^{ow} + (1-\omega) S_{wcr}^{ww} \\ S_{w\max}^{imm} &= \omega S_{w\max}^{ow} + (1-\omega) S_{w\max}^{ww} \\ S_{owcr}^{imm} &= \omega S_{owcr}^{ow} + (1-\omega) S_{owcr}^{ww} \end{aligned} \tag{1.59}$$

Where, ω is wettability alteration coefficient; S_{wco} is connate water saturation; S_{wcr} is critical water saturation; S_{wmax} is the maximum water saturation; S_{owcr} is the critical oil saturation in water; the superscript of imm denotes immiscible condition; ow denotes oil-wet condition; ww denotes water-wet condition.

$$
\begin{aligned}
S_{wco} &= f\left(N_c\right)S_{wco}^{mis} + \left(1 - f\left(N_c\right)\right)S_{wco}^{imm} \\
S_{wcr} &= f\left(N_c\right)S_{wcr}^{mis} + \left(1 - f\left(N_c\right)\right)S_{wcr}^{imm} \\
S_{w\max} &= f\left(N_c\right)S_{w\max}^{mis} + \left(1 - f\left(N_c\right)\right)S_{w\max}^{imm} \\
S_{owcr} &= f\left(N_c\right)S_{owcr}^{mis} + \left(1 - f\left(N_c\right)\right)S_{owcr}^{imm}
\end{aligned}
\tag{1.60}
$$

Where, $f(N_c)$ is a function of the capillary number and corresponds to the capillary desaturation curve.

Immiscible oil-wet and water-wet capillary pressures and relative permeabilities are looked up in the immiscible oil-wet and water-wet saturation tables by applying two-point saturation (horizontal) end-point scaling using the interpolated saturation end-points. Miscible relative permeabilities are looked up in the miscible table by applying two-point saturation (horizontal) end-point scaling using the interpolated saturation end-points. Immiscible capillary pressure and relative permeabilities are interpolated between immiscible oil-wet and water-wet capillary pressure and relative permeabilities (Eq. 1.61). The relative permeabilities at current surfactant concentration are interpolated between immiscible and miscible relative permeabilities (Eq. 1.62).

$$
\begin{aligned}
P_c^{imm} &= \omega P_c^{ow} + \left(1 - \omega\right)P_c^{ww} \\
k_{rw}^{imm} &= \omega k_{rw}^{ow} + \left(1 - \omega\right)k_{rw}^{ww} \\
k_{ro}^{imm} &= \omega k_{ro}^{ow} + \left(1 - \omega\right)k_{ro}^{ww}
\end{aligned}
\tag{1.61}
$$

$$
\begin{aligned}
k_{rw} &= f\left(N_c\right)k_{rw}^{mis} + \left(1 - f\left(N_c\right)\right)k_{rw}^{imm} \\
k_{ro} &= f\left(N_c\right)k_{ro}^{mis} + \left(1 - f\left(N_c\right)\right)k_{ro}^{imm}
\end{aligned}
\tag{1.62}
$$

Oil/water capillary pressure is only interpolated between immiscible oil-wet and water-wet values. When surfactant is applied, capillary pressure is calculated with the interpolated immiscible capillary pressure and surfactant concentration (Eq. 1.63). IFT reduction leads to the transition from immiscible conditions to miscible conditions which is described as a function of capillary number (Eq. 1.64).

$$P_c = \frac{\sigma_{ow}(C_{surf})}{\sigma_{ow}(0)} P_{\mathrm{c}}^{imm} \tag{1.63}$$

$$N_c = \frac{C_N}{C_D} \frac{\left\| T \cdot \Delta P_o \right\|}{A} \frac{1}{\sigma_{ow}} = C_N \frac{\left\| K \cdot \nabla P_o \right\|}{\sigma_{ow}} \tag{1.64}$$

Where, N_c is capillary number; C_N is the conversion factor depending on the units used; C_D is the Darcy constant; T is the transmissibility number; P_o is the potential, atm; A is the flow cross-sectional area, cm^2.

1.8 Introduction of thesis

1.8.1 Motivation

Many carbonate reservoirs are mixed-wet or oil-wet and naturally fractured with high matrix and fractured permeability contrast (i.e. high permeability fractures and low permeability matrix), which often results in poor waterflooding efficiency in these reservoirs (Chilingar and Yen 1983; Akbar et al. 2000; Roehl and Choquette 2012; Skjæveland et al. 2019). The current main drive mechanisms of the fields on the Norwegian Continental Shelf (NCS) are water injection and reservoir compaction (Barkved et al. 2019). The Norwegian Petroleum Directorate (2014) estimated that about 50% of the oil on the Norwegian Continental Shelf (NCS) remained in reservoirs with current production methods in 2014. Thus, more efficient recovery methods, like surfactant injection, should be studied and applied to extend the production life of existing reservoirs.

The main mechanisms of surfactant EOR are that surfactant could change matrix wettability to more water-wet and/or reduce water/oil IFT, thus change capillary pressure, residual oil saturation, relative permeability, etc. Therefore, surfactant could be used to improve oil recovery in fractured reservoirs. However, the interactions between surfactant mechanisms, surfactant dynamic imbibition in a fractured matrix, and the upscaling methods, which include wettability alteration, IFT reduction, gravity and capillary pressure, need further study. The objectives of this thesis are as follows.

- The main objective is to establish upscaling methods considering wettability alteration, IFT reduction, gravity and capillary pressure. Because the most used existing upscaling methods are only for capillary dominating imbibition or gravity dominating imbibition, and the existing upscaling methods which include both gravity and capillarity are not widely used.
- Another objective is to improve the understanding of surfactant EOR mechanisms, the effects of matrix properties and surfactant properties.
- The third objective is to study the application of surfactant in fractured matrix and the effects of matrix properties and surfactant properties on surfactant dynamic imbibition.

1.8.2 Contributions

The primary contributions of this thesis are as follows:

- New upscaling methods are proposed, which include the effect of wettability alteration, IFT reduction, gravity and capillary pressure.
- New calculation expressions of capillary pressure and bond number are established.
- Two upscaling groups for the effect of surfactant concentration and surfactant adsorption separately are proposed.
- The individual and combined effect of wettability alteration and IFT reduction are studied, which clarifies the importance of these two surfactant mechanisms at different conditions.
- The effects of matrix properties and surfactant properties on surfactant spontaneous imbibition are further studied and the mechanisms are explained with simulation results.
- The study of injection rate, injection timing, and surfactant slug size of surfactant flooding in fractured matrix provides a reference for surfactant application into fractured reservoirs.

1.8.3 Thesis structure

First of all, the background of surfactant EOR and fractured reservoirs and the introduction of thesis, which includes motivation, contributions and thesis structure, are presented in Chapter

1. In Chapter 2, a spontaneous imbibition model is established based on experimental data from literature. Then the mechanisms of surfactant imbibition are studied, and the relative importance of mechanisms are analyzed. In addition, new upscaling methods, which include wettability alteration, IFT reduction, gravity and capillary pressure, are proposed and verified by simulation results. In Chapter 3, the effects of matrix properties on surfactant spontaneous imbibition are studied. The existing upscaling methods for capillary imbibition and gravity imbibition are tested. And the proposed upscaling methods are verified and slightly modified according to simulation results. In Chapter 4, the effects of surfactant properties on surfactant spontaneous imbibition are studied, and two upscaling methods are proposed considering surfactant concentration and surfactant adsorption, respectively. In Chapter 5, a surfactant dynamic imbibition model is created based on the surfactant spontaneous imbibition model. With the dynamic imbibition model, the effects of surfactant injection rate, injection timing, and surfactant slug size on surfactant dynamic imbibition are studied. At the same time, the sensitivity of surfactant diffusion, concentration, adsorption, and fracture permeability and porosity are analyzed. The main conclusions and some recommendations for future work are listed in Chapter 6.

2 Surfactant imbibition mechanisms

The main mechanisms of surfactant enhanced oil recovery (EOR) are wettability alteration and water/oil interfacial tension (IFT) reduction. In this chapter, those mechanisms are studied with simulation in a model, which is established based on experiments performed by Standnes and Austad (2000) and verified by history matching. Both the individual effect and combined effect of wettability alteration and IFT reduction are studied. New upscaling methods are proposed and tested by simulation results, which include both IFT reduction and wettability alteration and consider both gravity and capillary force. The proposed upscaling methods are compared with the most frequently used existing dimensionless upscaling methods for gravity dominating imbibition process and capillary dominating imbibition process.

2.1 Experiments from literature

The experimental data of Test 31 from one paper by Standnes and Austad (2000) is used. The core was an outcrop rock from the Stevns Klint near Copenhagen, Denmark. The oil was an acidic crude oil from the North Sea diluted with n-heptane by 40 vol.%. Cationic surfactant n-C_{12}-$N(CH_3)_3Br$ (C12TAB) was used to do the spontaneous imbibition. Assume that the surfactant has no effect on brine density, i.e. the density of surfactant solution is 1.031 g/cm^3. Then the CMC is about 0.004 g/cm^3. The imbibition experiment was conducted at 70 °C in an Amott cell filled with 350 cm^3 surfactant solution with concentration of 1 wt.% (Fig. 2-1a). The core and fluid properties are listed in Table 2-1 ~ Table 2-4.

Table 2-1—Properties of core (Test 31) (Standnes and Austad 2000).

Core diameter, D (cm)	Core height, H (cm)	Porosity, ϕ (%)	Absolute permeability, K (mD)	Initial water saturation, S_{wi} (%)	Density*, ρ (g/cm^3)
3.83	4.61	44.3	2-7	27.7	2.7

*Density, the value refers to the paper of Hjuler and Fabricius (2009).

Table 2-2—Properties of brine 1 (Standnes and Austad 2000).

Brine	pH (21°C)	Density, ρ_w (21°C, g/cm^3)	Viscosity, μ_w (cP)	Brine/oil IFT, σ (mN/m)	Compositions	
1	8	1.031	0.8	15.4	Na^+	12.14
					K^+	0.25
					Ca^{2+}	3.43
					Mg^{2+}	0.93
					Cl^-	26.54
					SO_4^{2-}	1.56
					HCO_3^-	0.09
					Total	44.49

Table 2-3—Properties of oil A (Standnes and Austad 2000).

Oil	Density, ρ (20°C, g/cm^3)	Viscosity, μ_o (cP)	AN (mg KOH/g oil)	BN (mg KOH/g oil)	Wax-formation temp. (°C)	Asphaltenes (wt.%)
A	0.816	1.446	1.73	Trace	25-30	0.23

Table 2-4—Properties of the cationic surfactant C12TAB (Standnes and Austad 2000).

Surfactant	CMC (25°C, wt.%; g/cm^3*)	Experimental conc. (wt.%; g/cm^3*)	Conc. (wt.%; g/cm^3*)	IFT, σ (mN/m)	Contact angle, θ (± 3°)
C12TAB	0.43; 0.004	1; 0.01	0; 0	15.4	70
			0.1; 0.001	-	28
			1; 0.01	0.81	12
			5; 0.048	0.76	-

*g/cm^3, calculated with the assumption that surfactant solution has the same density as brine, 1.031 g/cm^3.

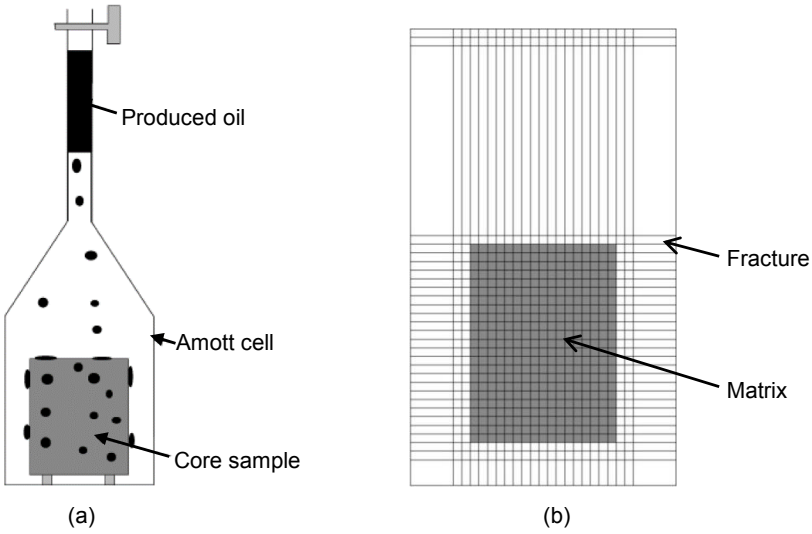

Fig. 2-1—(a) experimental setup (Shuler and Tang 2010) and (b) simulation model.

2.2 Simulation model

A Cartesian model (Fig. 2-1b) is established according to the experimental setup. The core and Amott cell in the experiments are simulated as the matrix and fracture in the model, respectively. The basic size of the simulation grid is 23 × 23 × 30, and the matrix is represented by a 17 × 17 × 23 grid.

2.2.1 Model description

In order to have the same volume in the model as in the experiment, the matrix length in the model is calculated with Eq. 2.1. The simulation data used in the model based on the experimental data of Test 31 is listed in Table 2-5. The water and oil relative permeability curves in fracture are X shape (Fig. 2-2). The water/oil relative permeability in matrix can be calculated with Eq. 2.2 (Corey 1977) and then shown in Fig. 2-3. The key parameters are listed in Table 2-6. Capillary pressure curves at oil-wet and strongly water-wet conditions are shown in Fig. 2-4. The adsorption curve shown in Fig. 2-5 is created based on the surfactant adsorption theory (Scamehorn et al. 1982) in section 1.5.4. Surfactant adsorption occurs when surfactant concentration in solution is higher than 0.001 g/cm^3. Surfactant adsorption rate is slow when

surfactant concentration is between 0.001 and 0.003 g/cm^3. Afterwards, surfactant adsorption rate is sharply increased between the surfactant concentration of 0.003 and 0.004 g/cm^3. When surfactant concentration in solution is higher than 0.005 g/cm^3, surfactant adsorption is plateau, and the value is 0.2 mg/g. Water/oil IFT is decreasing with the increase of surfactant concentration in solution, but when the concentration is above critical micellar concentration (CMC), water/oil IFT keeps constant, which is 0.8 mN/m (Fig. 2-6). The water/oil IFT at CMC is expressed with σ_{CMC}. With the decrease of IFT, capillary number is increasing, and residual oil saturation is decreasing. When capillary number is 10^{-8}, residual oil saturation starts to decrease. When capillary number is larger than 10^{-3}, residual oil saturation is decreased to minimum, which is zero in this case. Therefore, in this thesis, the critical capillary number ($(N_c)_c$) is 10^{-8}, and the maximum capillary number ($(N_c)_{max}$) is 10^{-3}. The capillary desaturation curve of residual oil saturation is shown in Fig. 2-7. When water/oil IFT is reduced to ultralow, which results in a capillary number larger than 10^{-3}, the water phase and oil phase are miscible, and the relative permeability curves are like X shape (Fig. 2-8). According to section 1.5.6, surfactant diffusion coefficient is on the order of about 10^{-8} m^2/s or 10^{-11} m^2/s when the wettability is intermediate wet or water-wet. Therefore, in the model, the surfactant diffusion coefficient is set as 5×10^{-4} cm^2/h (i.e. 1.4×10^{-11} m^2/s). In the model, the effects of temperature, brine salinity and heterogeneity on surfactant mechanisms are not considered.

$$L = \sqrt{\frac{\pi D^2}{4}} \tag{2.1}$$

Where, L is the matrix length in the model, cm; π is math constant, 3.1416; D is core diameter in experiments, cm.

$$\begin{aligned} k_{rw} &= k_{rw}^0 \left(\frac{S_w - S_{wir}}{1 - S_{wir} - S_{or}} \right)^{n_w} \\ k_{ro} &= k_{ro}^0 \left(\frac{1 - S_w - S_{or}}{1 - S_{wir} - S_{or}} \right)^{n_o} \end{aligned} \tag{2.2}$$

Where, k_{rw} and k_{ro} are water and oil relative permeability; k_{rw}^0 and k_{ro}^0 are the endpoints of water and oil relative permeability; S_w is water saturation; S_{wir} is the irreducible water saturation; S_{or} is the residual oil saturation; n_w and n_o are exponents of the water and oil relative permeability.

Table 2-5—Simulation data of matrix and fracture in the model.

Properties	Length, L (cm)	Height, H (cm)	Porosity, ϕ	Absolute permeability, K (mD)	Initial water saturation, S_{wi}
Matrix	3.4	4.6	0.443	3	0.277
Fracture	6.2	10.6	0.999	10^7	1

Table 2-6—Key parameters for water and oil relative permeability.

Case	Irreducible water saturation, S_{wir}	Residual oil saturation, S_{or}	Water relative permeability		Oil relative permeability	
			Endpoint, k_{rw}^0	Exponent, n_w	Endpoint, k_{ro}^0	Exponent, n_o
Original	0.277	0.15	0.4	2.5	0.7	4
Strongly water-wet	0.277	0.15	0.2	4	1	2
$(N_c)_{max}$	0	0	1	1	1	1

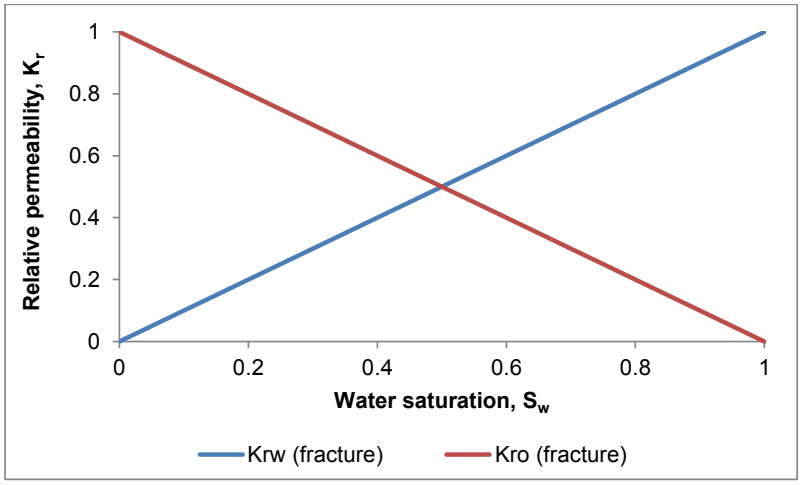

Fig. 2-2—Water and oil relative permeability curves in fracture.

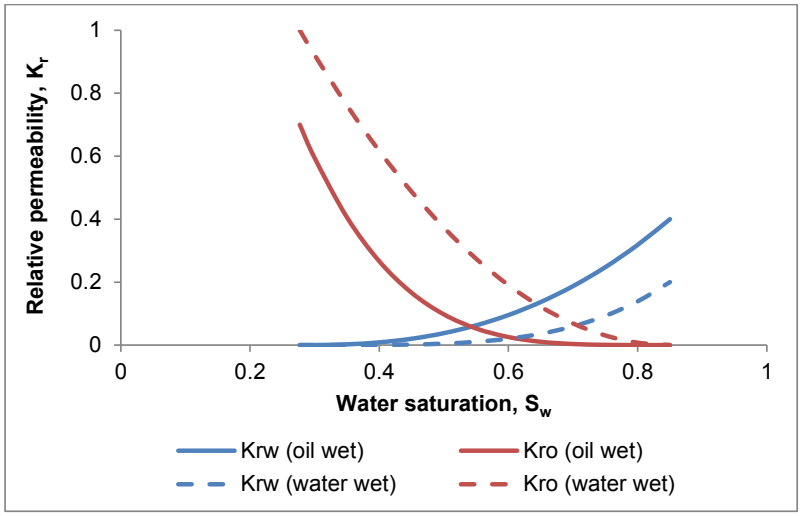

Fig. 2-3—Water and oil relative permeability curves in matrix at oil-wet and water-wet conditions.

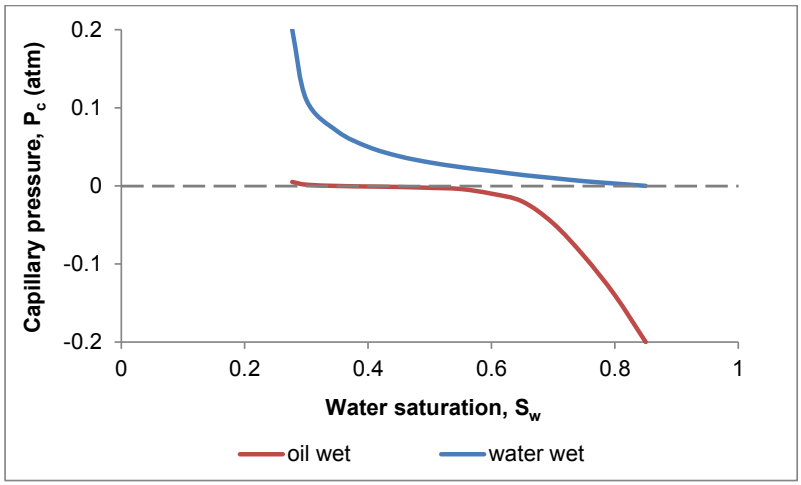

Fig. 2-4—Matrix capillary pressure at oil-wet and water-wet conditions.

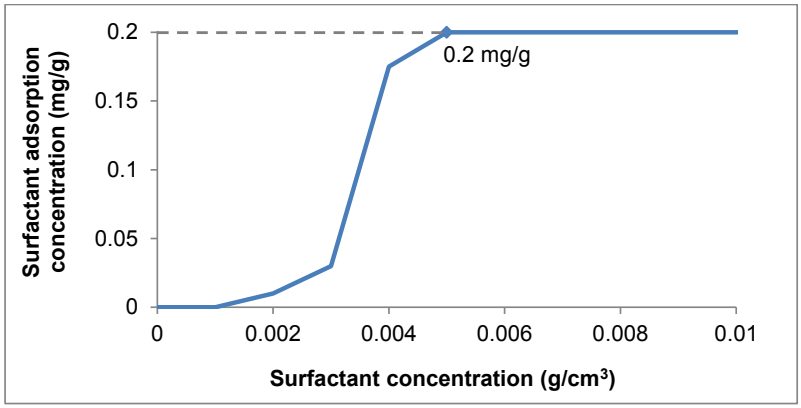

Fig. 2-5—Surfactant adsorption vs. surfactant concentration in solution.

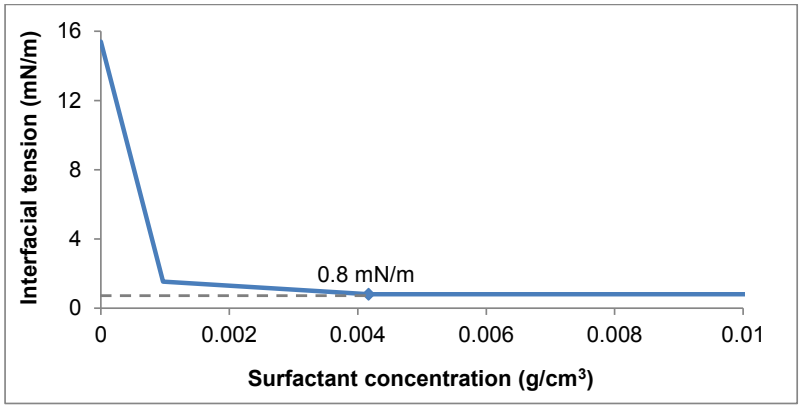

Fig. 2-6—Effect of surfactant concentration in solution on water/oil IFT.

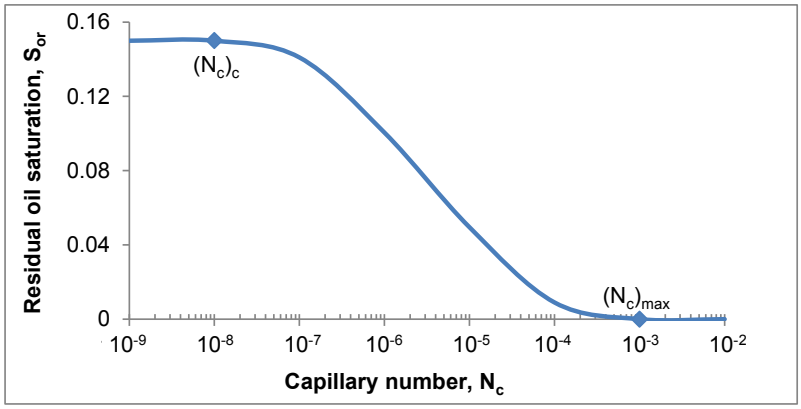

Fig. 2-7—Capillary desaturation curve.

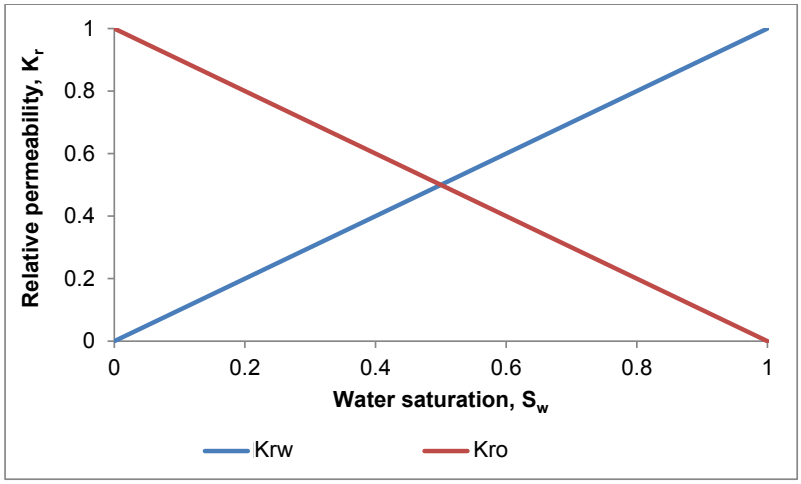

Fig. 2-8—Water and oil relative permeability curves when the capillary number is larger than 10^{-3}.

2.2.2 Model verification

The established model in section 2.2.1 is used for the simulations of brine spontaneous imbibition and surfactant spontaneous imbibition. Oil recovery is calculated with Eq. 2.3. The experiment of brine spontaneous imbibition showed that the oil recovery reached a plateau after 42 days, which was about 15% of OOIP. The simulation of brine spontaneous imbibition gives the same result, which is about 15% OOIP after 42 days (Fig. 2-9). The simulation result of surfactant spontaneous imbibition can well match the experimental result in test 31 (Standnes and Austad 2000) (Fig. 2-10). Therefore, the model is verified and can be used to do simulation studies in this thesis.

$$R_o = \frac{S_w - S_{wi}}{1 - S_{wi}} \tag{2.3}$$

Where, R_o is oil recovery; S_w is water saturation; S_{wi} is initial water saturation.

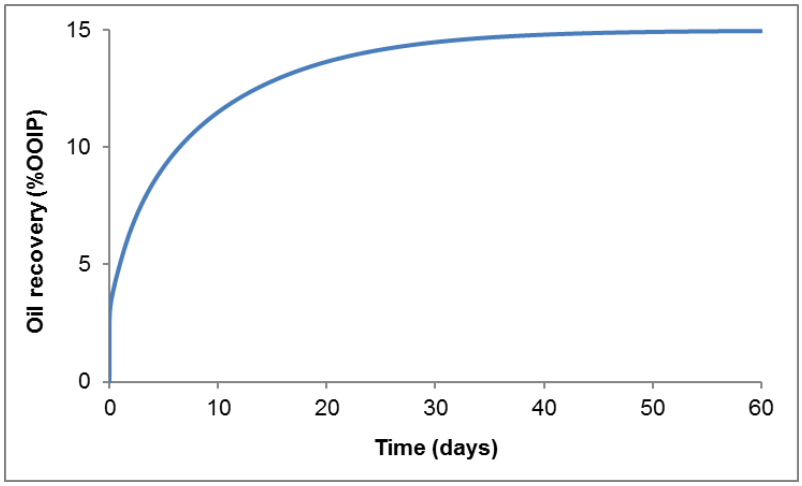

Fig. 2-9—Simulation result of brine spontaneous imbibition in the model.

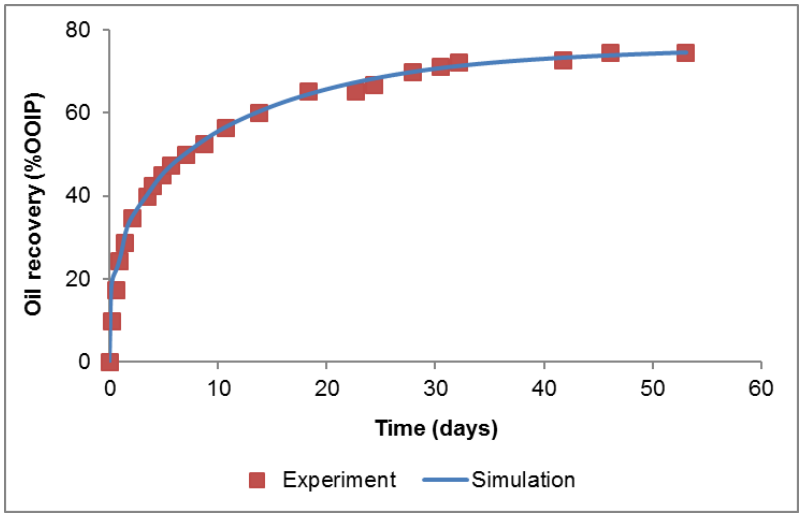

Fig. 2-10—History matching of experimental (test 31) and simulation oil recovery.

2.3 Study on surfactant EOR mechanisms

The established model is used to study the main surfactant EOR mechanisms that surfactant could change the matrix wettability or/and reduce the water/oil IFT. Simulations of surfactant

spontaneous imbibition are performed with simulator Eclipse 2014.1. The simulation code of surfactant spontaneous imbibition is in Appendix A.

2.3.1 Individual effect of wettability alteration

Surfactant effects on water/oil IFT and wettability depends on the type of surfactant, brine, oil, rock, temperature et al. Wettability alteration by surfactant is studied in this section.

To study the effect of wettability alteration, it assumes that surfactant has no effect on water/oil IFT, which means water/oil IFT always equals to 15.4 mN/m, and the effects of surfactant on other properties are the same. The wettability is changed by different extent from original wettability (i.e. mixed-wet) to strongly water-wet, which is expressed by the wettability alteration coefficient (ω) calculated with Eq. 2.4 or Eq. 2.5.

$$\omega = \frac{\cos\theta_{ww} - \cos\theta}{\cos\theta_{ww} - \cos\theta_i} \tag{2.4}$$

Where, ω is wettability alteration coefficient, $\omega \in [0,1]$; θ is the contact angle at the current situation, degree; θ_i is the contact angle at the initial wettability condition, degree; θ_{ww} is the contact angle when the wettability is changed to strongly water-wet, degree.

$$\omega = \frac{WI_{ww} - WI}{WI_{ww} - WI_i} \tag{2.5}$$

Where, WI is the USBM wettability index (Gatenby and Marsden 1957) at the current situation; WI_i is the USBM wettability index at the initial wettability condition; WI_{ww} is the USBM wettability index when the wettability is changed to strongly water-wet.

When ω is 1, the wettability is the original wettability (i.e. oil-wet), and when ω is 0, the wettability is strongly water-wet. Surfactant concentration in solution is 0.01 g/cm^3, which is higher than CMC (i.e. 0.004 g/cm^3) and also higher than the required surfactant concentration (about 0.005 g/cm^3) to change the wettability to strongly water-wet.

Capillary pressure is changing with wettability alteration and IFT reduction and calculated with Eq. 2.6. Bond number is the ratio of gravity force on capillary force, thus it can be calculated with Eq. 2.7 with the assumptions that: (1) wettability alteration and IFT reduction are completed immediately when surfactant contacts with rock and water/oil phase; and (2) water saturation is still the initial water saturation. Eq. 2.7 is different from the expression (Eq. 1.29) given by Schechter et al. (1994). The effect of surfactant on wettability and water/oil IFT can be explicitly reflected in Eqs. 2.6 and 2.7. In this thesis, $\sigma = \sigma_{CMC} = 0.8$ mN/m when surfactant concentration is higher than 0.004 g/cm^3.

$$P_c = \left[P_c^{ww} - \omega\left(P_c^{ww} - P_c^{i} \right) \right] \frac{\sigma}{\sigma_i} \tag{2.6}$$

Where, P_c^i is the initial water/oil capillary force, atm; P_c^{ww} is the water/oil capillary force when the wettability is changed to strongly water-wet by surfactant, atm; ω is the wettability alteration coefficient; σ_i is initial water/oil IFT, mN/m; σ is the lowest IFT at the current surfactant concentration, mN/m.

$$N_B = \frac{\Delta\rho g H}{P_c} = \frac{\Delta\rho g H}{P_c^{ww} - \omega\left(P_c^{ww} - P_c^{i} \right)} \frac{\sigma_i}{\sigma} \tag{2.7}$$

Where, N_B is Bond number; $\Delta\rho$ is the density difference between water and oil phases, g/cm^3; g is gravity, 9.8, mN/g; H is the height of matrix, cm.

When surfactant changes the matrix wettability to strongly water-wet, the ultimate oil recovery is about 0.79 OOIP, and the enhanced oil recovery is about 0.64 OOIP (Table 2-7). So, wettability alteration is a highly efficient enhanced oil recovery method for the oil-wet matrix. Fig. 2-11 shows that oil recovery is increasing with the increase of wettability alteration extent to more water-wet. Oil recovery is normalized with Eq. 2.8 and plotted in Fig. 2-12, which tells that the oil recovery rate however is similar for all the wettability conditions when IFT keeps the same. In this case, since the water/oil IFT is not changed, capillary force is the largest at the strongly water-wet condition. At the same time, the critical water saturation, where the capillary

force is zero, is increasing with the change of wettability to more water-wet, therefore, the ultimate oil recovery is increased. The critical water saturation depends on the curvature of the capillary pressure curve. Fig. 2-4 shows that when matrix wettability is oil-wet (ω = 1) and strongly water-wet (ω = 0), the capillary force is dramatically changed around the residual oil saturation and irreducible water saturation separately, so the critical water saturation is increased faster when the wettability is slightly changed or when the wettability is approaching to strongly water-wet, thus the ultimate oil recovery is increasing faster when the wettability alteration coefficient is about 0 and 1 (Fig. 2-13). If the capillary pressure curves at the initial wettability condition and the strongly water-wet wettability condition are measured, then for a certain wettability condition, the critical water saturation is calculated and as a result the ultimate oil recovery could be estimated. The Bond number is becoming smaller when the wettability is changing to more water-wet. The ultimate oil recovery has a power function relation with Bond number (Fig. 2-14).

$$R_{on} = \frac{R_o}{R_{of}} \tag{2.8}$$

Where, R_{on} is normalized oil recovery; R_o is oil recovery; R_{of} is ultimate oil recovery.

Table 2-7—Summary of Bond number, ultimate oil recovery and enhanced oil recovery for different wettability conditions and constant water/oil IFT.

Wettability alteration coefficient, ω	Bond number, N_B	Ultimate oil recovery, R_{of} (1/OOIP)	Enhanced oil recovery*, EOR (1/OOIP)
0	0.0048	0.792	0.642
0.2	0.0059	0.577	0.427
0.4	0.0078	0.521	0.371
0.6	0.012	0.466	0.316
0.8	0.022	0.404	0.254
1	0.19	0.15	0

*EOR = ultimate oil recovery of surfactant imbibition (R_{ofs}) – ultimate oil recovery of brine imbibition (R_{ofw}).

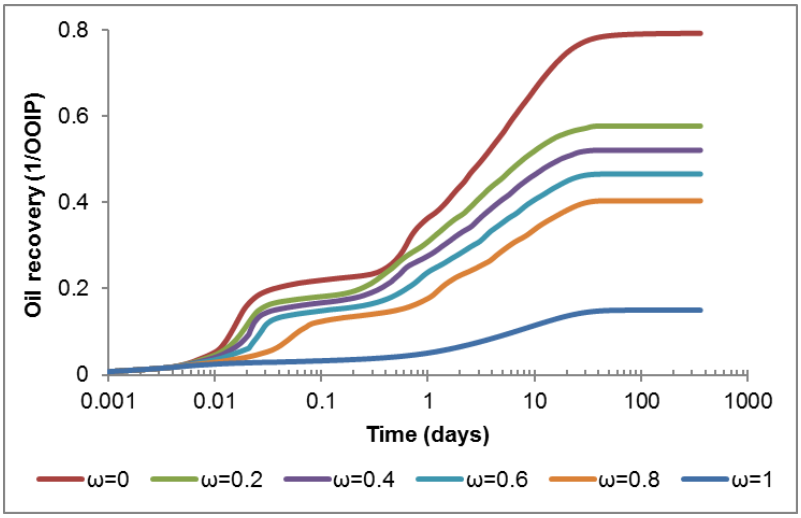

Fig. 2-11—Oil recovery of surfactant spontaneous imbibition when the wettability is changing from oil-wet to strongly water-wet.

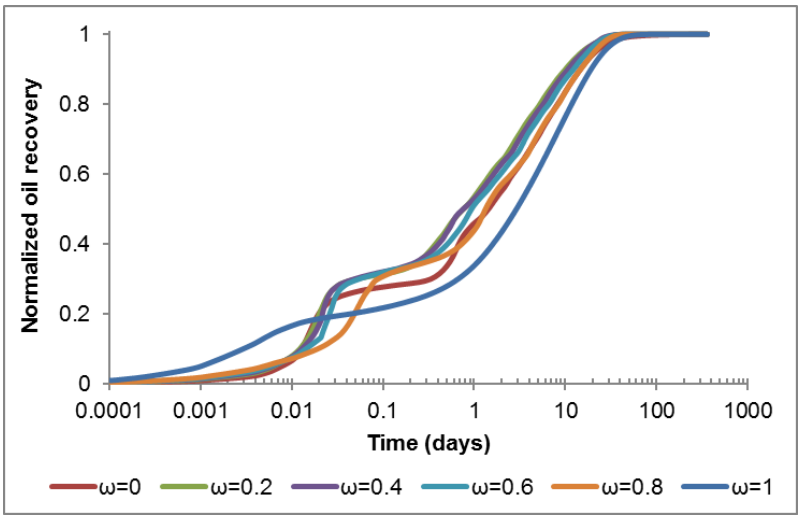

Fig. 2-12—Normalized oil recovery of surfactant spontaneous imbibition when the wettability is changing from oil-wet to strongly water-wet.

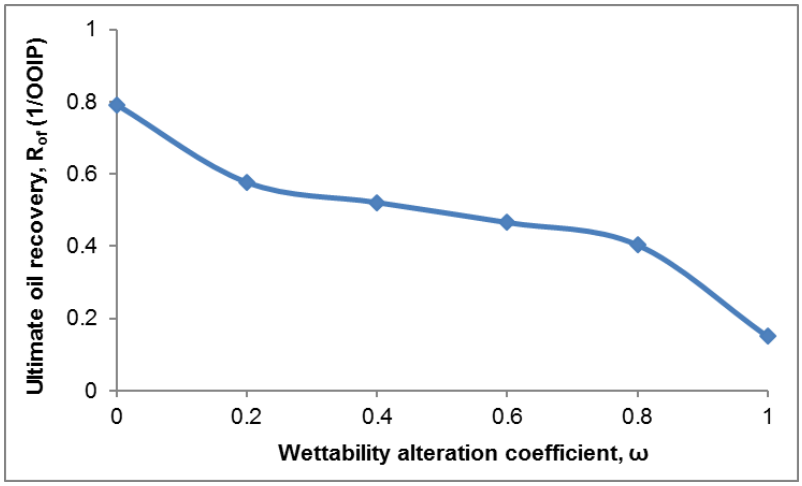

Fig. 2-13—The relationship between wettability alteration coefficient (ω) and ultimate oil recovery (R_{of}) of surfactant spontaneous imbibition.

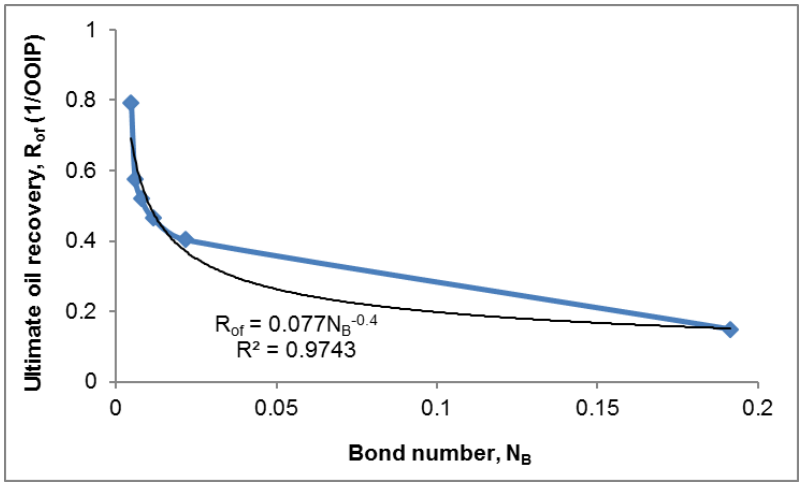

Fig. 2-14—The relationship between Bond number (N_B) and ultimate oil recovery (R_{of}) of surfactant spontaneous imbibition.

2.3.2 Individual effect of IFT reduction

To study the effect of IFT reduction on surfactant spontaneous imbibition, it is assumed that surfactant has no effect on matrix wettability (i.e. ω = 1), while the surfactant can reduce the water/oil IFT by different extent from the initial water/oil IFT (i.e. 15.4 mN/m), to the ultralow

IFT (i.e. 0.000154 mN/m) (Fig. 2-15). In addition, the effects of surfactant on other properties, for example solution viscosity, are the same.

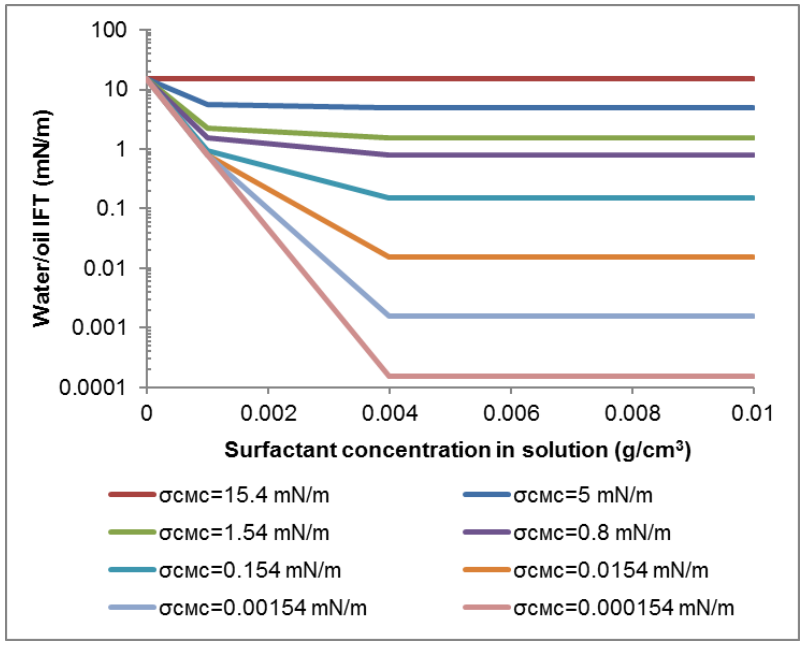

Fig. 2-15—The water/oil IFT is decreased by surfactant.

Bond number and oil recovery are increasing with the decrease of IFT (Table 2-8 and Fig. 2-16). When the IFT is 0.000154 mN/m at CMC, the ultimate oil recovery is 0.97 OOIP, which means nearly all the oil is recovered and the capillary number is almost 10^{-3}. Comparing with the case with strongly water-wet wettability and a constant IFT, the enhanced oil recovery is higher when the IFT at CMC is lower than 0.0154 mN/m, which means the IFT is reduced by at least 1000 times. The normalized oil recovery curves (Fig. 2-17) tell that with the decrease of IFT at CMC, oil recovery rate is reducing. But when IFT at CMC is smaller than 0.154 mN/m, the final oil recovery time starts to decrease. When IFT at CMC is higher than 0.154 mN/m, the imbibition process is dominated by capillary force, so with the decrease of IFT, the dominating force is reducing, thus the oil recovery is slower. However, the dominating force is changing from capillary force to gravity force with the decrease of IFT. When IFT at CMC is lower than 0.154 mN/m, the dominating force is becoming gravity force. Oil is recovered from the top side of matrix. Capillary force could be a resistance of oil recovery. Therefore, when IFT at CMC

is lower than 0.154 mN/m, the final oil recovery time is becoming shorter with the decrease of IFT at CMC. But when IFT at CMC is smaller than 0.00154 mN/m, capillary pressure is very small, thus oil is slowly recovered by gravity force only.

Table 2-8—Bond number and ultimate oil recovery for different IFT reduction.

IFT at CMC, σ_{CMC} (mN/m)	Bond number, N_B	Ultimate oil recovery, R_{of} (1/OOIP)	Enhanced oil recovery, EOR (1/OOIP)
15.4	0.19	0.15	0
5	0.59	0.249	0.099
1.54	1.91	0.369	0.219
0.8	3.68	0.431	0.281
0.154	19.13	0.592	0.442
0.0154	191.32	0.832	0.682
0.00154	1913.24	0.912	0.762
0.000154	19132.4	0.971	0.821

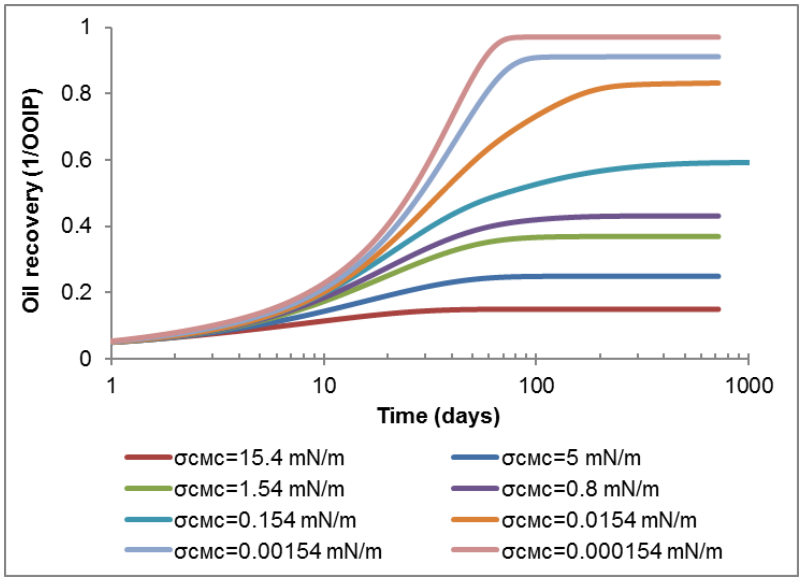

Fig. 2-16—Oil recovery of surfactant spontaneous imbibition when the water/oil IFT is reduced.

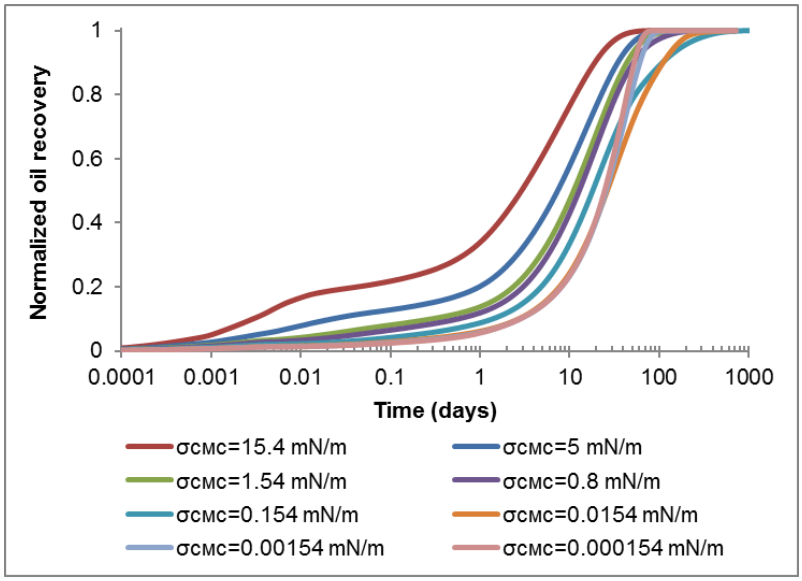

Fig. 2-17—Normalized oil recovery of surfactant spontaneous imbibition when the water/oil IFT is reduced.

With the reduction of IFT from 15.4 mN/m to the ultralow value of 0.000154 mN/m, Bond number is increasing from 0.2 to 2×10^4. Therefore, the imbibition dominating force is transiting from capillary force to gravity force. Fig. 2-18 shows that when Bond number is about 0.2 which means capillary force is larger than gravity force, the spontaneous imbibition process is counter-current, and oil is recovered from all the sides of matrix (Fig. 2-18a); when Bond number is 191 which means gravity force is larger than capillary force, the cocurrent flow occurs, so oil is mainly recovered from the top side of matrix (Fig. 2-18b). IFT reduction results in an increase of capillary number and leads to a decrease of residual oil saturation when capillary number is between 10^{-8} and 10^{-3} (Fig. 2-7). Therefore, the ultimate oil recovery depends on capillary number when wettability is not changed by surfactant. However, for spontaneous imbibition, it is very difficult to calculate or measure the fluid flow velocity in the matrix, so the capillary number is hard to obtain. Fig. 2-19 shows that the ultimate oil recovery has a logarithmic relation with IFT at CMC. But the increase of ultimate oil recovery is becoming slower when IFT at CMC is smaller than 0.0154 mN/m, which could be explained by the capillary desaturation curve (Fig. 2-7). When capillary number is larger than 10^{-4}, the capillary desaturation curve is changing slower and then keeping plateau when the capillary

number is larger than 10^{-3}. When IFT at CMC is smaller than 0.0154 mN/m, capillary number is larger than 10^{-4}, so the increase of ultimate oil recovery is slower.

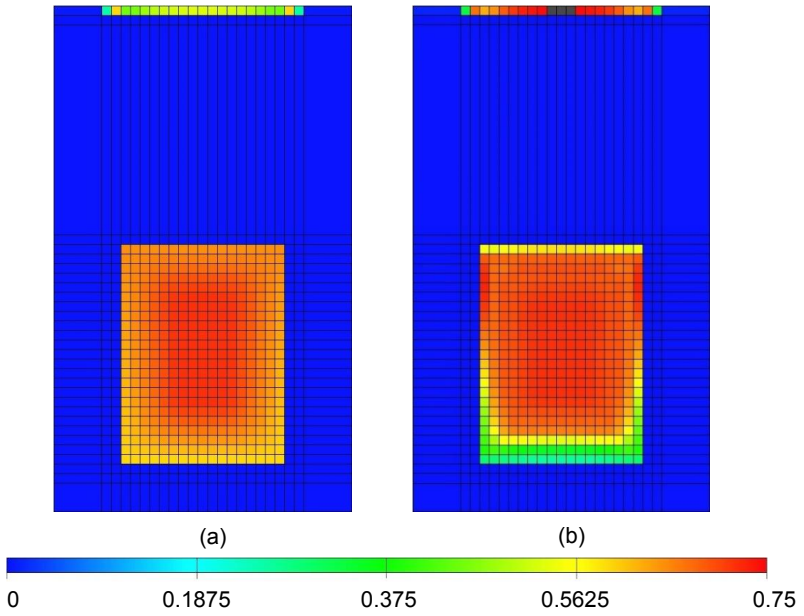

(a) σ_{CMC} = 15.4 mN/m, ω = 1, N_B = 0.19; (b) σ_{CMC} = 0.0154 mN/m, ω = 1, N_B = 191.

Fig. 2-18—Oil saturation distribution in matrix after spontaneous imbibition for 5 days.

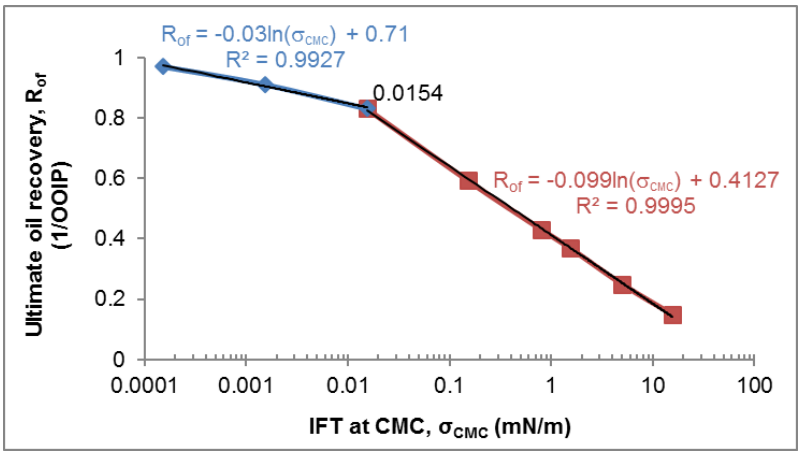

Fig. 2-19—The relationship between ultimate oil recovery and IFT at CMC.

2.3.3 Combined effect of wettability alteration and IFT reduction

To study the effect of surfactant on oil recovery when surfactant can change both wettability and IFT at the same time, the simulations in Table 2-9 are performed. Fig. 2-20 and Fig. 2-21 show that ultimate oil recovery is increasing with the decrease of IFT. For the strongly water-wet condition (Fig. 2-21), ultimate oil recovery has an obvious increase only when IFT at CMC is lower than 0.154 mN/m. That is because capillary pressure is always positive when wettability is strongly water-wet, ultimate oil recovery is the same until capillary number exceeds 10^{-8} caused by the reduction of IFT. The normalized oil recovery curves of the cases with wettability alteration coefficient of 0.5 and 0 are plotted in Fig. 2-22 and Fig. 2-23, respectively, which tell that in general, with the decrease of IFT at CMC, oil recovery rate is decreasing, and final imbibition time is increasing. However, when $\sigma_{CMC} \geq 0.0154$ mN/m, final imbibition time is decreasing with the decrease of IFT at CMC.

Table 2-9—Ultimate oil recovery for different wettability alteration and IFT reduction conditions.

Wettability alteration coefficient, ω	IFT at CMC, σ_{CMC} (mN/m)	Bond number, N_B	Ultimate oil recovery, R_{of} (1/OOIP)	Enhanced oil recovery, EOR (1/OOIP)
0.5	15.4	0.009	0.494	0.344
	1.54	0.09	0.527	0.377
	0.8	0.18	0.551	0.401
	0.154	0.93	0.697	0.547
	0.0154	9.22	0.844	0.694
	0.00154	93.33	0.91	0.76
	0.000154	933.3	0.971	0.821
0	15.4	0.005	0.792	0.642
	1.54	0.05	0.793	0.643
	0.8	0.09	0.793	0.643
	0.154	0.48	0.801	0.651
	0.0154	4.78	0.844	0.694
	0.00154	47.83	0.91	0.76
	0.000154	478.3	0.97	0.82

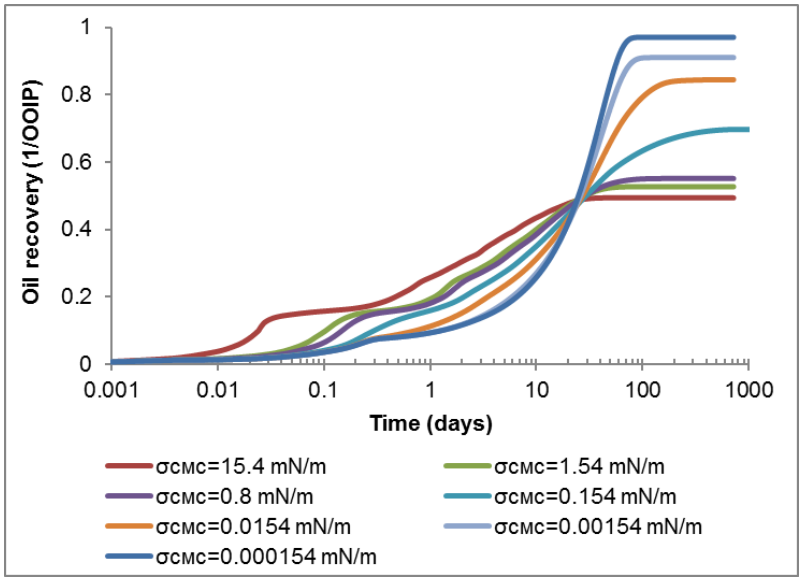

Fig. 2-20—Oil recovery of surfactant spontaneous imbibition for different IFT at CMC when ω = 0.5.

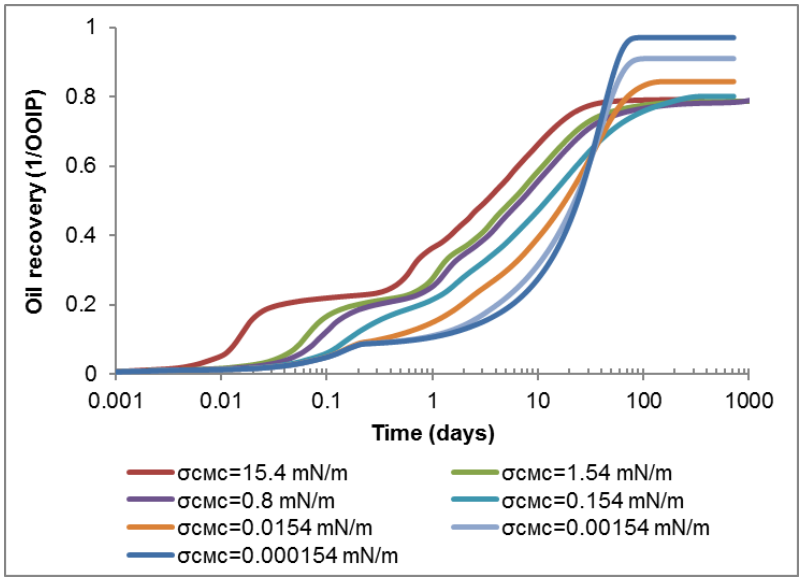

Fig. 2-21—Oil recovery of surfactant spontaneous imbibition for different IFT at CMC when ω = 0.

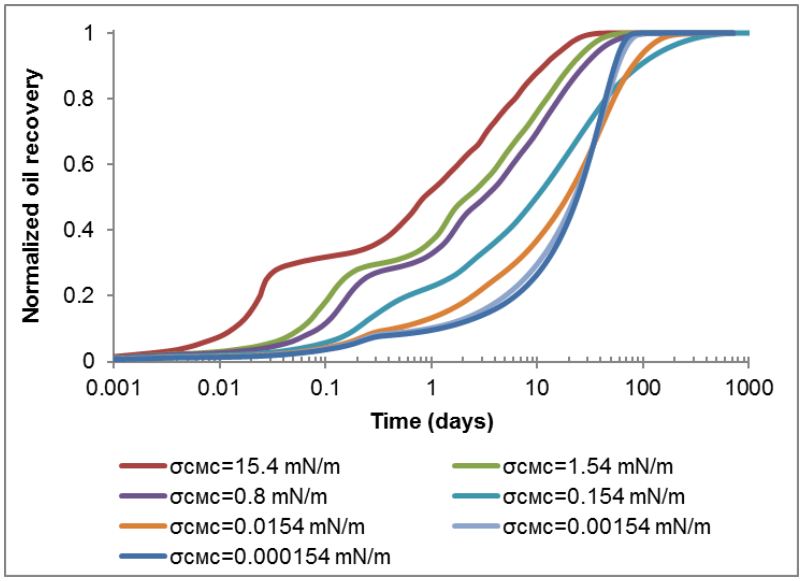

Fig. 2-22—Normalized oil recovery of surfactant spontaneous imbibition for different IFT at CMC when ω = 0.5.

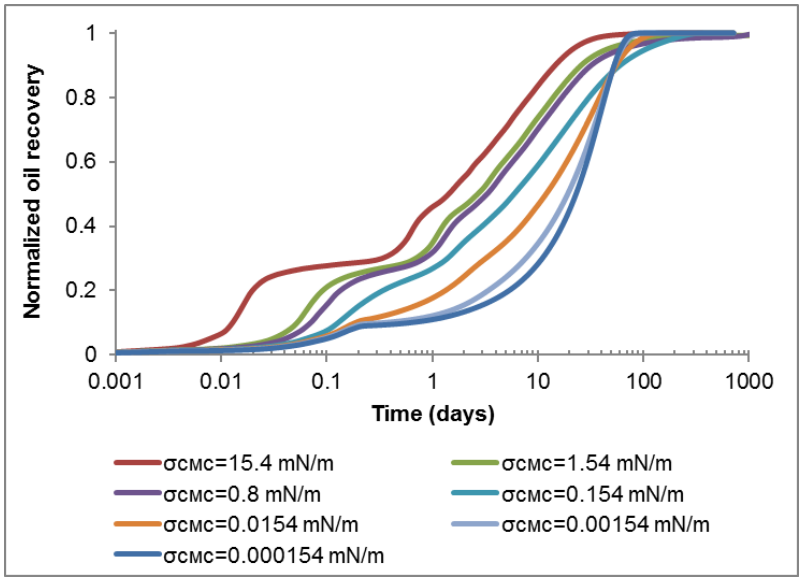

Fig. 2-23—Normalized oil recovery of surfactant spontaneous imbibition for different IFT at CMC when ω = 0.

Comparing the ultimate oil recovery of cases with different IFT reduction and wettability alteration conditions (Fig. 2-24), it can be seen that in general the ultimate oil recovery is increasing with the reduction of IFT and the wettability alteration to more water-wet. The effect of IFT reduction has a larger effect on a less water-wet system, and the wettability alteration has a larger effect on a system with higher water/oil IFT. When $\sigma_{CMC} \leq 0.0154$ mN/m, wettability alteration has no effect on ultimate oil recovery, which means when IFT at CMC is lower than a certain value, all the wettability conditions have the same ultimate oil recovery. One of the reasons is when IFT at CMC is ultralow, the decrease of residual oil saturation is very small because of the large capillary number. Another reason is the imbibition process is dominated by gravity force, which is constant.

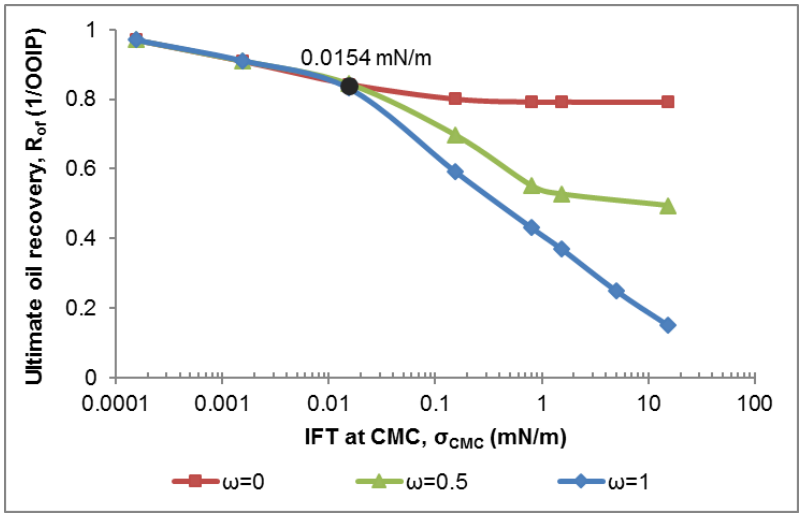

Fig. 2-24—The ultimate oil recovery for different IFT reduction and wettability alteration conditions.

2.4 Upscaling methods of surfactant imbibition

The existing upscaling methods are mainly divided into three groups: one is for the imbibition process dominated by gravity force; the second is for the imbibition process dominated by capillary force; and the last is for the imbibition process affected by both capillary and gravity forces. However, the existing scaling methods that include both capillary pressure and gravity are not widely used. The most used upscaling method for gravity dominating imbibition process

is the dimensionless upscaling time introduced by Cuiec et al. (1994) (Eq. 1.34). The most frequently used upscaling method for capillary dominating process is the dimensionless upscaling time proposed by Ma et al. (1999) (Eq. 1.25). Neither of those equations includes the effect of wettability alteration. The dominating force of imbibition process could be changed from capillary force to gravity force by reducing water/oil IFT or changed from gravity force to capillary force by changing wettability to more water-wet. So, both IFT reduction and wettability alteration are very important and should be considered in upscaling methods. In this section, upscaling methods are proposed, which include both IFT reduction and wettability alteration.

$$t_{Dg} = \frac{K\Delta\rho}{\phi\mu_o L} t \tag{1.34}$$

$$t_{Dc} = t\sqrt{\frac{K}{\phi}}\frac{\sigma}{\sqrt{\mu_w\mu_o}L_c^2} \tag{1.25}$$

Where, t_{Dg} is the dimensionless upscaling time for gravity dominating imbibition process; t_{Dc} is the dimensionless upscaling time for capillary dominating imbibition process; K is matrix absolute permeability, mD; σ is water/oil IFT, mN/m; $\Delta\rho$ is the density difference of displacing fluid and displaced fluid g/cm^3; ϕ is matrix porosity; μ_o is oil viscosity, cP; μ_w is water viscosity, cP; L is matrix length, cm; L_c is a characteristic length, cm; t is imbibition time, s.

Water/oil IFT is reduced by different extent from the initial value of 15.4 mN/m (i.e. σ_i = 15.4 mN/m) to an ultralow value of 0.000154 mN/m at CMC (i.e. σ_{CMC} = 0.000154 mN/m), and wettability is changing from oil-wet (i.e. ω = 1) to strongly water-wet (i.e. ω = 0). Bond numbers calculated with Eq. 2.7 are shown in Table 2-10 and Fig. 2-25. When IFT at CMC is smaller than 0.07 mN/m, Bond number is always bigger than 1. When IFT at CMC is larger than 3 mN/m, Bond number is always smaller than 1. While when IFT at CMC is between 0.07 and 3 mN/m, Bond number is reducing from the value bigger than 1 to the value smaller than 1 with the wettability alteration from oil-wet to water-wet.

Table 2-10—Summary of Bond number for different IFT reduction and wettability alteration conditions.

Wettability alteration coefficient, ω	IFT at CMC, σ_{CMC} (mN/m)								
	0.000154	0.00154	0.0154	0.07	0.154	0.8	1.54	3	15.4
1	19132	1913	191	42.1	19.1	3.68	1.91	0.98	0.19
0.8	2174	217	21.7	4.78	2.17	0.42	0.22	0.11	0.02
0.6	1152	115	11.5	2.54	1.15	0.22	0.12	0.06	0.01
0.4	784	78.4	7.84	1.73	0.78	0.15	0.08	0.04	0.008
0.2	594	59.4	5.94	1.31	0.59	0.11	0.06	0.03	0.006
0	478	47.8	4.78	1.05	0.48	0.09	0.05	0.02	0.005

The values in the grey cells are calculated Bond number.

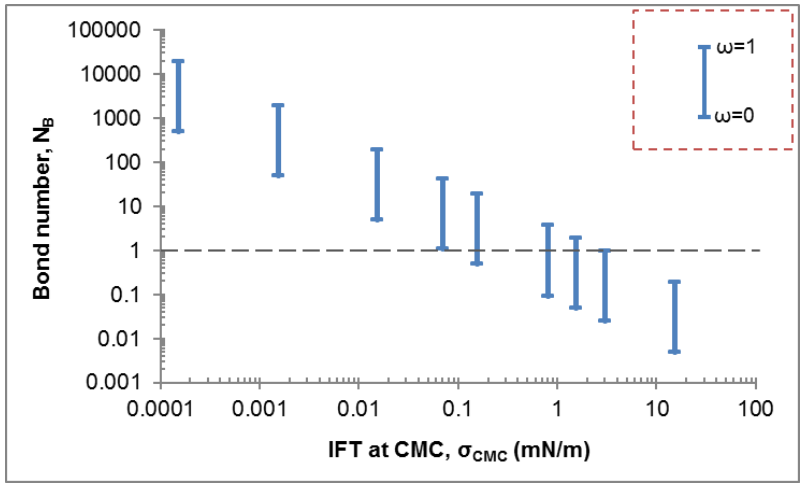

The red box in the figure shows that the blue bar means the wettability alteration coefficient is changing from 1 to 0 from the top to the bottom.

Fig. 2-25—Bond number for cases with different IFT reduction and wettability alteration conditions.

Since Bond number is the ratio of gravity to capillary pressure, capillary pressure could be expressed with Bond number and gravity (Eq. 2.9). Assume that the Darcy's law is applicable in surfactant spontaneous imbibition. And the Darcy flux is calculated with Eq. 2.10. The fluid velocity in porous medium related to the Darcy flux by the porosity can be expressed with Eq. 2.11, in which the characteristic length (L_c) (Eq. 1.26) is used. Insert Eq. 2.9 into Eq. 2.11, then the fluid velocity is expressed with Eq. 2.12. An upscaling dimensionless time expressed as Eq.

2.13 is proposed. With the assumption in Eclipse that surfactant only exists in water phase, the fluid viscosity (μ) is water viscosity (Eq. 2.14). In reality, surfactant could exist in both water and oil phases, thus the fluid viscosity is calculated with Eq. 2.15.

$$P_c = N_B^{-1}\Delta\rho g H \tag{2.9}$$

$$u = \frac{Kk_r}{\mu L}\left(P_c + \Delta\rho g H\right) \tag{2.10}$$

$$v = \frac{Kk_r}{\phi\mu L_c}\left(P_c + \Delta\rho g H\right) \tag{2.11}$$

$$v = \frac{Kk_r}{\phi\mu L_c}\left(N_B^{-1} + 1\right)\Delta\rho g H \tag{2.12}$$

$$t_{D1} = t\frac{K\Delta\rho g H}{\phi\mu L_c^2}\left(N_B^{-1} + 1\right) \tag{2.13}$$

where,

$$\mu = \mu_w \tag{2.14}$$

or

$$\mu = \sqrt{\mu_o \mu_w} \tag{2.15}$$

Where, u is the Darcy flux, cm/s; v is fluid velocity, cm/s; K is absolute permeability, mD; k_r is relative permeability; ϕ is porosity; μ is fluid viscosity, cP; μ_o is oil viscosity, cP; μ_w is water viscosity, cP; P_c is capillary pressure, atm; Δρ is density difference of water and oil, g/cm^3; g is gravity, 9.8 mN/g; H is matrix height, cm; N_B is Bond number; t_{D1} is dimensionless upscaling time; t is time, s; L_c is characteristic length, cm.

Wettability alteration to more water-wet can increase capillary pressure, thus enhance the effect of capillary force. However, capillary pressure is dramatically decreasing with the increase of water saturation in matrix and water/oil IFT reduction, so gravity effect will become larger with the proceeding of imbibition. In addition, when capillary force is reduced to negative, it becomes the resistance of surfactant imbibition. Therefore, gravity may be important for capillary dominating imbibition. When gravity effect is significant for capillary imbibition, Eq. 2.13 is slightly modified into Eq. 2.16 by displacing N_B^{-1} with $N_B^{-0.5}$.

$$t_{D2} = t\frac{K\Delta\rho gH}{\phi\mu L_c^2}\left(N_B^{-0.5}+1\right) \tag{2.16}$$

Bond number is calculated based on the assumptions that: (1) wettability alteration and IFT reduction are completed immediately when surfactant contacts with rock and water/oil phase; and (2) water saturation is still the initial water saturation. However, in reality, the reactions between surfactant and rock/oil/water take time. So, when wettability alteration and IFT reduction are completed, water saturation in matrix is higher than initial water saturation, and capillary force is smaller because of the increase of water saturation. Therefore, the calculated Bond number is larger than the real Bond number. To verify the proposed upscaling methods (Eqs. 2.13 and 2.16) and compare them with the existing upscaling methods for gravity or capillary dominating imbibition (Eqs. 1.34 and 1.25), the simulation results are divided into three groups: $N_B \geq 1$, $0.1 < N_B < 1$ and $N_B \leq 0.1$. When Bond number is bigger than 1, gravity force is larger than capillary force. When Bond number is smaller than 1, capillary force is larger than gravity force. But when Bond number is between 0.1 and 1, the dominating force is greatly affected by wettability alteration and IFT reduction, thus, the case of $N_B < 1$ is subdivided into $0.1 < N_B < 1$ and $N_B \leq 0.1$.

2.4.1 $N_B \geq 1$

When Bond number is bigger than 1, gravity force is larger than capillary force. The main results are shown in Table 2-11. The relationship between ultimate oil recovery of surfactant spontaneous imbibition and Bond number plotted in Fig. 2-26 shows that from a general view,

ultimate oil recovery is larger when Bond number is bigger. The relationship between ultimate oil recovery and IFT at CMC (Fig. 2-27) tells that on one hand, ultimate oil recovery is increasing with the decrease of IFT at CMC, which is because with the decrease of IFT at CMC, absolute value of negative capillary pressure is decreasing, thus more oil could be recovered at the end of imbibition when the total force of capillary and gravity forces is zero. In addition, the decrease of IFT at CMC leads to an increase of capillary number, which results in a decrease of residual oil saturation when capillary number is bigger than 10^{-8}, thus ultimate oil recovery increases. When IFT at CMC results in a capillary number larger than 10^{-3}, residual oil saturation is 0 and ultimate oil recovery reaches to 100% OOIP (Fig. 2-7). On the other hand, for a certain IFT at CMC, e.g. σ_{CMC} = 0.0154 mN/m, ultimate oil recovery is almost the same for all the wettability conditions, which implies that wettability alteration has no effect on ultimate oil recovery when IFT at CMC is ultralow, because the dominating force is gravity force, which is not affected by the change of wettability.

The oil recovery curves for the cases in Table 2-11 are shown in Fig. 2-28. Oil recovery is normalized with Eq. 2.8 and plotted in Fig. 2-29. It can be seen that the normalized oil recovery curves are well converged, which means the existing upscaling method for gravity imbibition in Eq. 1.34 can be used as upscaling method when $N_B \geq 1$ for the upscaling of normalized oil recovery. The proposed upscaling methods (Eqs. 2.13 and 2.16) are simplified into Eqs. 2.17 and 2.18 for the change of wettability and IFT. The upscaling results of normalized oil recovery using Eqs. 2.17 and 2.18 are shown in Fig. 2-30 and Fig. 2-31, respectively, which prove that the proposed upscaling methods could be used when $N_B \geq 1$.

$$t_{d1} = t\left(N_B^{-1} + 1\right) \tag{2.17}$$

$$t_{d2} = t\left(N_B^{-0.5} + 1\right) \tag{2.18}$$

Where, t_{d1} is simplified proposed upscaling group from t_{D1} (Eq. 2.13), s; t_{d2} is simplified proposed upscaling group from t_{D2} (Eq. 2.16), s; t is imbibition time, s; N_B is Bond number.

Table 2-11—Summary of ultimate oil recovery for the cases with $N_B \geq 1$.

Bond number, N_B	IFT at CMC, σ_{CMC} (mN/m)	Wettability alteration coefficient, ω	Ultimate oil recovery, R_{of} (1/OOIP)
19132	0.000154	1	0.971
1913	0.00154	1	0.912
478	0.000154	0	0.97
191	0.0154	1	0.832
48	0.00154	0	0.91
19	0.154	1	0.592
12	0.0154	0.6	0.842
6	0.0154	0.2	0.847
4	0.8	1	0.432
2	1.54	1	0.369

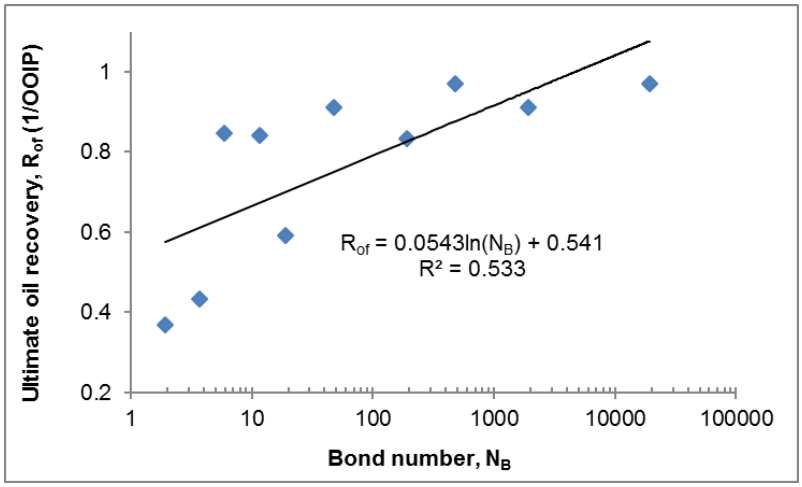

Fig. 2-26—The relationship between ultimate oil recovery of surfactant spontaneous imbibition and Bond number when $N_B \geq 1$.

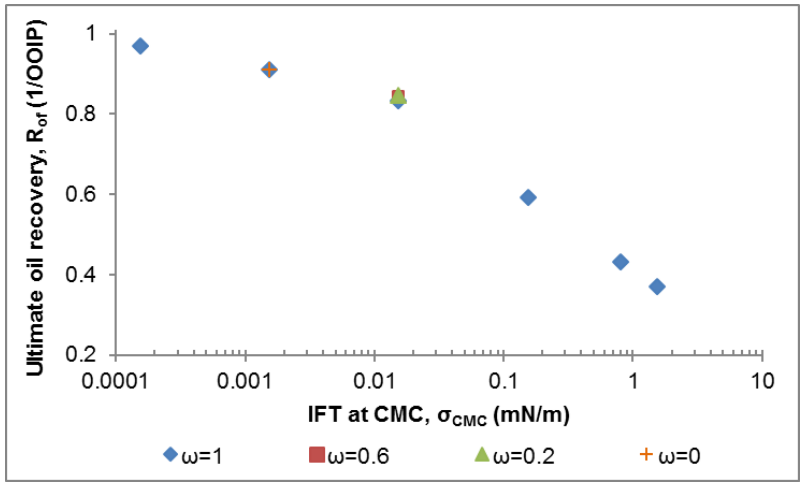

Fig. 2-27—The relationship between ultimate oil recovery of surfactant spontaneous imbibition and IFT at CMC when $N_B \geq 1$.

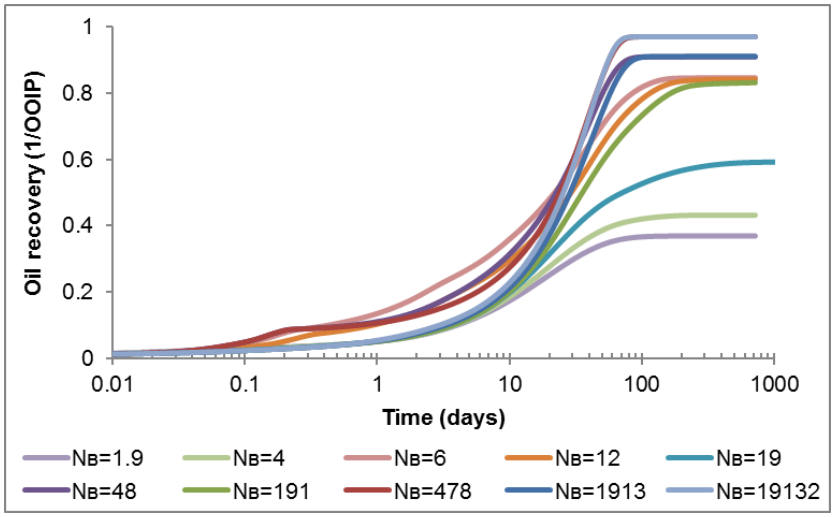

Fig. 2-28—Oil recovery of surfactant spontaneous imbibition vs. imbibition time when $N_B \geq 1$.

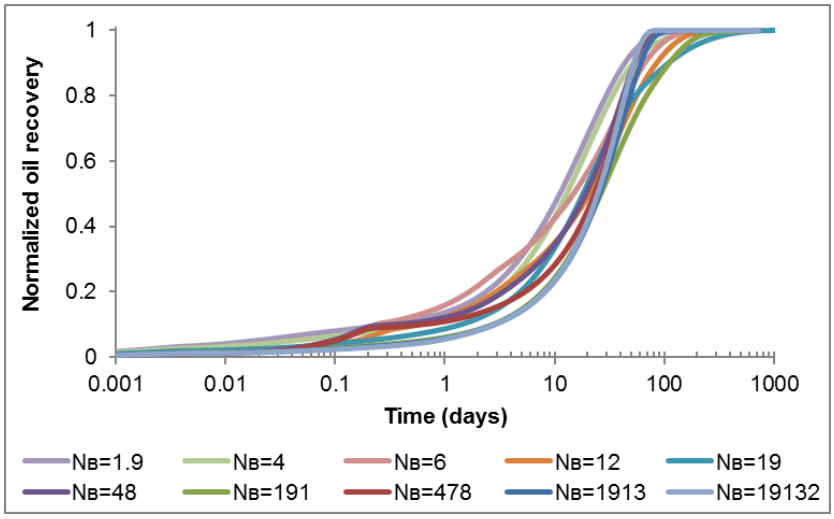

Fig. 2-29—Normalized oil recovery of surfactant spontaneous imbibition vs. imbibition time when $N_B \geq 1$.

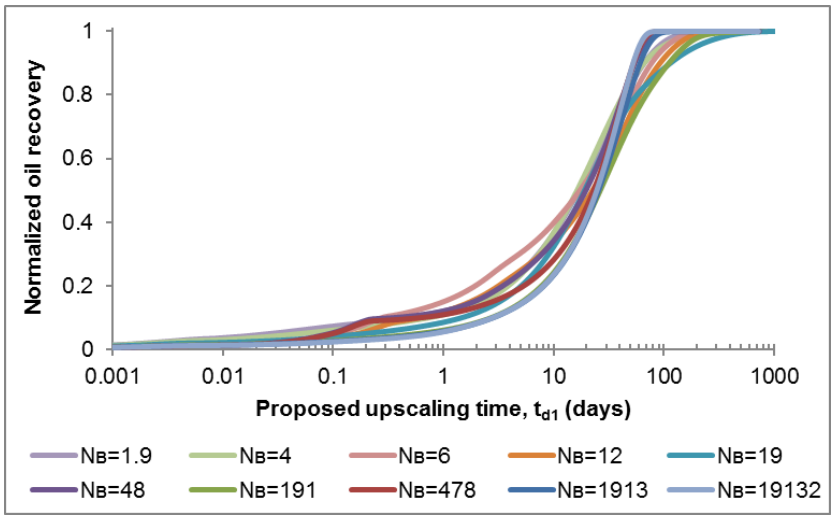

Fig. 2-30—Normalized oil recovery of surfactant spontaneous imbibition vs. simplified proposed upscaling group (t_{d1}) when $N_B \geq 1$.

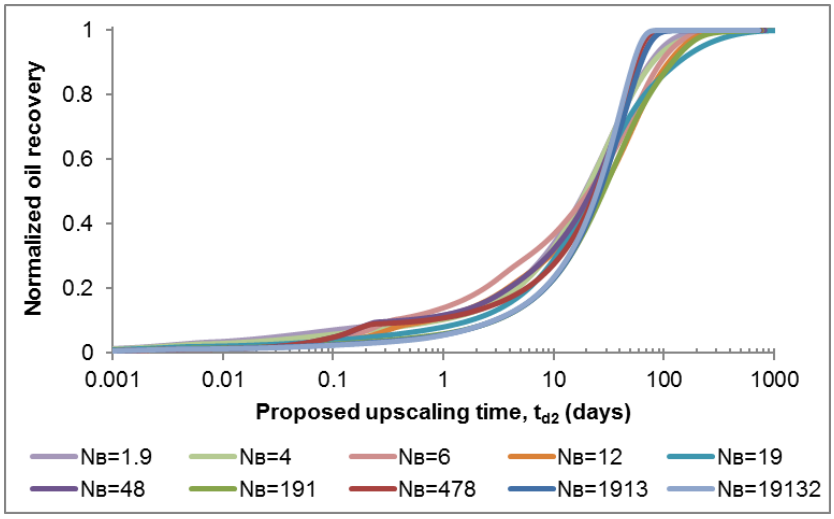

Fig. 2-31—Normalized oil recovery of surfactant spontaneous imbibition vs. simplified proposed upscaling group (t_{d2}) when $N_B \geq 1$.

2.4.2 $0.1 < N_B < 1$

Different combinations of IFT reduction and wettability alteration are chosen, so that both IFT and wettability are varying. The summary of the main results is in Table 2-12. When Bond number is between 0.1 and 1, both capillary force and gravity force are important for the whole imbibition process. The relationship between Bond number and ultimate oil recovery (Fig. 2-32) indicates that ultimate oil recovery cannot be predicted based on Bond number.

Table 2-12—Summary of ultimate oil recovery for the cases with $0.1 < N_B < 1$.

Bond number, N_B	IFT at CMC, σ_{CMC} (mN/m)	Wettability alteration coefficient, ω	Ultimate oil recovery, R_{of} (1/OOIP)
0.9	0.154	0.5	0.697
0.6	5	1	0.249
0.5	0.154	0	0.801
0.4	0.8	0.8	0.491
0.2	0.8	0.4	0.574
0.1	1.54	0.6	0.506

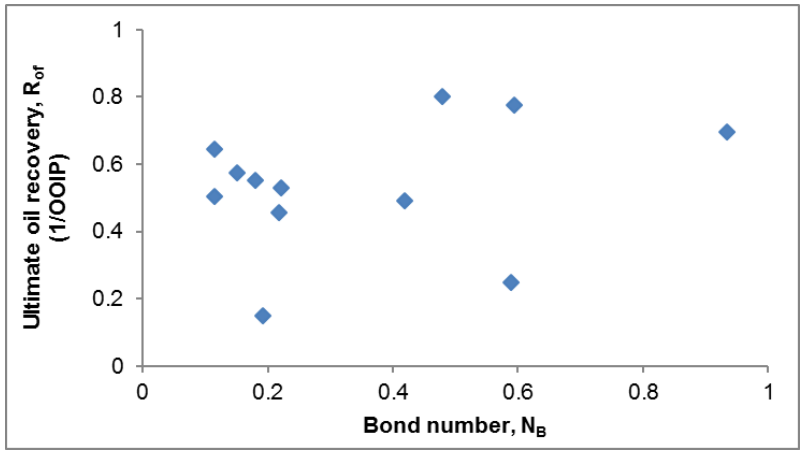

Fig. 2-32—The relationship between Bond number and ultimate oil recovery when $0.1 < N_B < 1$.

The curves of oil recovery and normalized oil recovery are plotted in Fig. 2-33 and Fig. 2-34, respectively. The curves of normalized oil recovery are not well converged. So, the upscaling method for surfactant imbibition dominated by gravity force cannot be used when $0.1 < N_B < 1$. Only wettability and IFT can be changed, so the upscaling dimensionless time for capillary imbibition in Eq. 1.25 is simplified into Eq. 2.19 by removing the constants. But the upscaling results of oil recovery (Fig. 2-35) and normalized oil recovery (Fig. 2-36) using Eq. 2.19 are not satisfied. So, the existing upscaling method for capillary imbibition is not applicable when the imbibition is dominated by both gravity and capillary pressure. Then use the simplified proposed upscaling group of t_{d1} (Eq. 2.17) to upscale the oil recovery and normalized oil recovery. The upscaling curves of oil recovery (Fig. 2-37) are not well converged, but the upscaling result of normalized oi recovery (Fig. 2-38) is very good. The proposed upscaling group of t_{d2} (Eq. 2.18) gives a similar upscaling result of normalized oil recovery (Fig. 2-39). Therefore, the proposed upscaling groups are valid for the upscaling of normalized oil recovery when $0.1 < N_B < 1$.

$$t_c = t\sigma \tag{2.19}$$

Where, t_c is simplified existing upscaling group for capillary imbibition, mN/m·s; t is imbibition time, s; σ is water/oil IFT, mN/m.

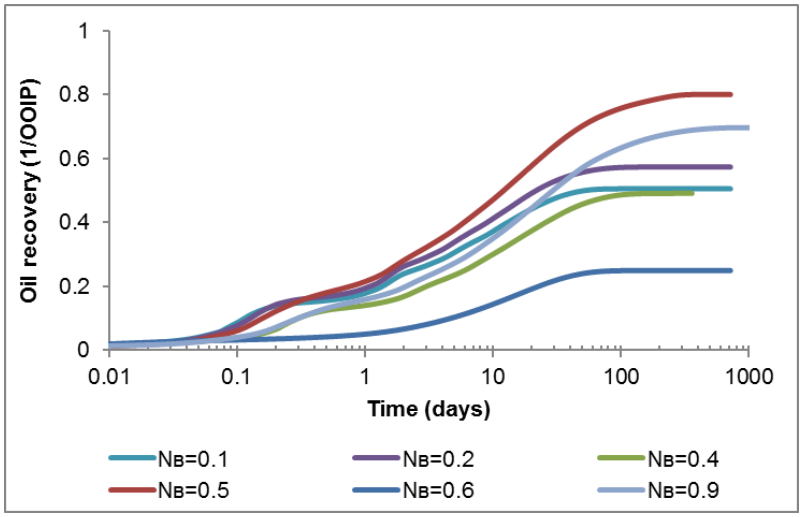

Fig. 2-33—Oil recovery of surfactant spontaneous imbibition vs. imbibition time when $0.1 < N_B < 1$.

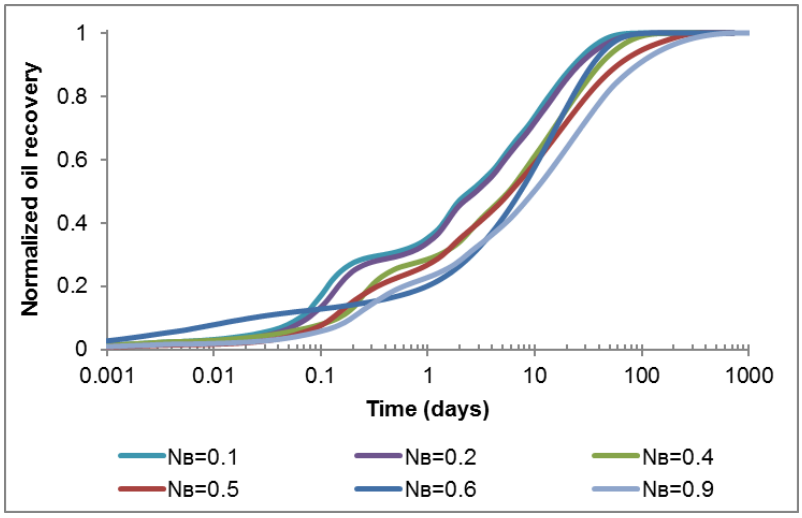

Fig. 2-34—Normalized oil recovery of surfactant spontaneous imbibition vs. imbibition time when $0.1 < N_B < 1$.

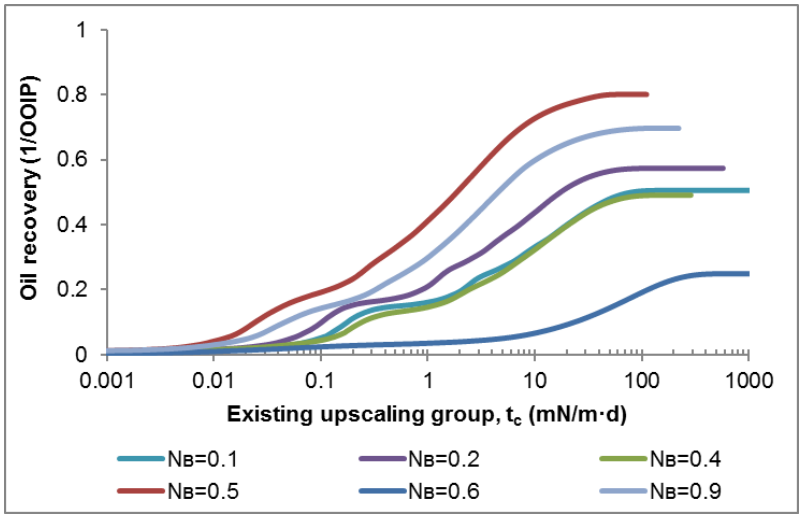

Fig. 2-35—Oil recovery of surfactant spontaneous imbibition vs. simplified existing upscaling group for capillary imbibition (t_c) when $0.1 < N_B < 1$.

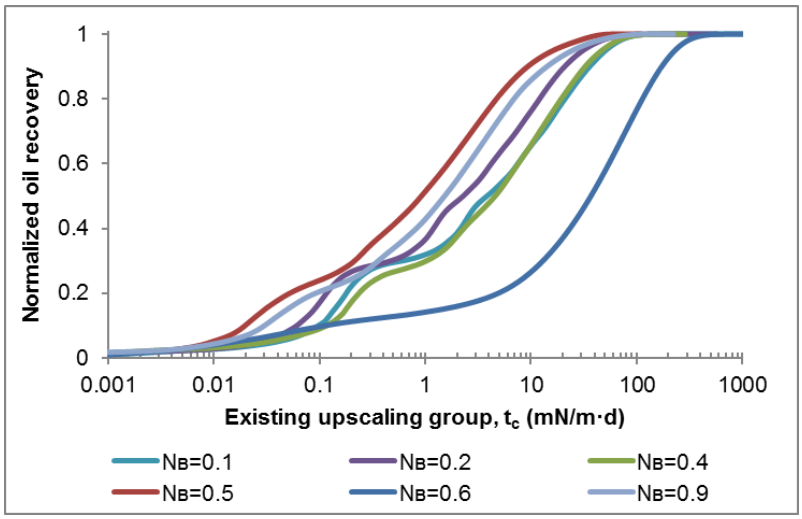

Fig. 2-36—Normalized oil recovery of surfactant spontaneous imbibition vs. simplified existing upscaling group for capillary imbibition (t_c) when $0.1 < N_B < 1$.

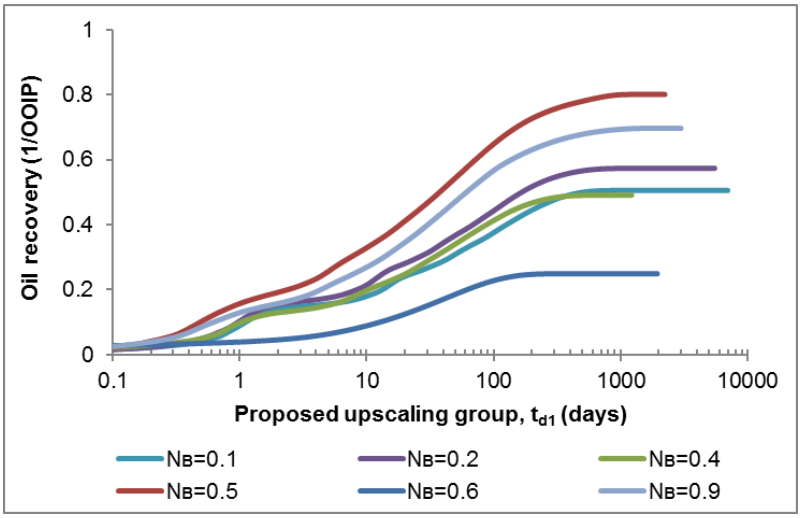

Fig. 2-37—Oil recovery of surfactant spontaneous imbibition vs. simplified proposed upscaling group (t_{d1}) when $0.1 < N_B < 1$.

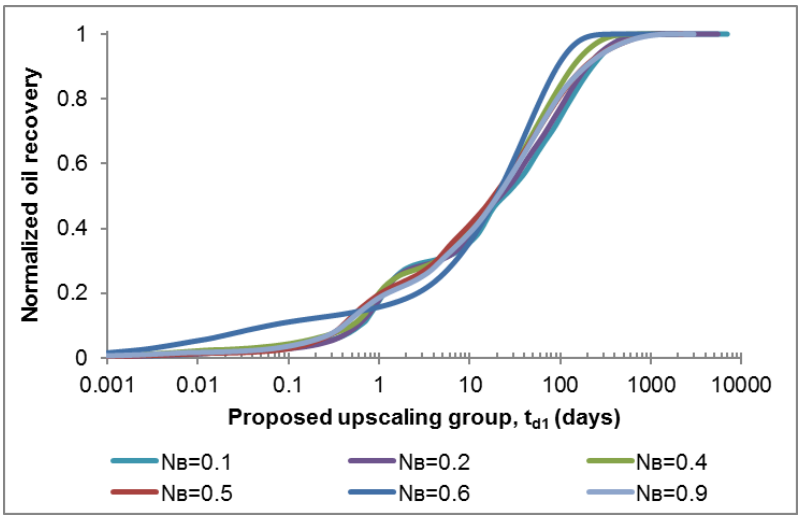

Fig. 2-38—Normalized oil recovery of surfactant spontaneous imbibition vs. simplified proposed upscaling group (t_{d1}) when $0.1 < N_B < 1$.

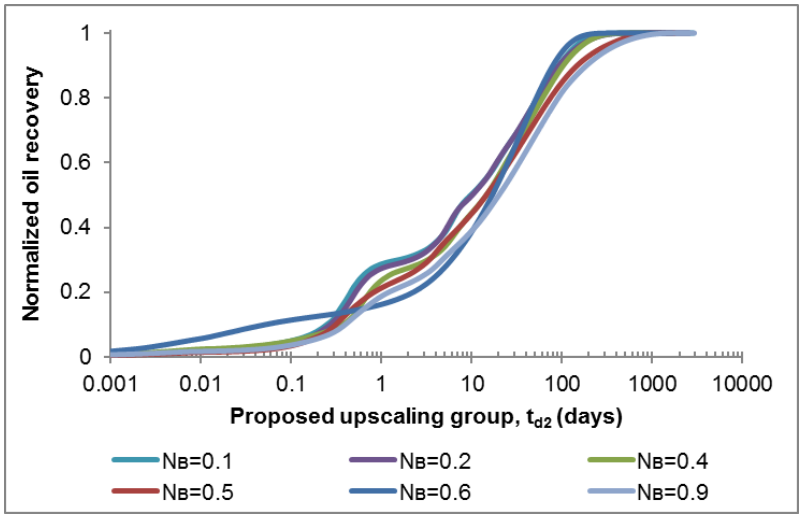

Fig. 2-39—Normalized oil recovery of surfactant spontaneous imbibition vs. simplified proposed upscaling group (t_{d2}) when $0.1 < N_B < 1$.

2.4.3 $N_B \leq 0.1$

In this section, the cases with Bond number smaller than 0.1 are studied. The main results are shown in Table 2-13. The relationship between ultimate oil recovery and Bond number is plotted in Fig. 2-40, which tells that it hardly estimates ultimate oil recovery based on Bond number only. However, ultimate oil recovery has a power function relation with wettability alteration coefficient (Fig. 2-41), which implies that ultimate oil recovery is increasing with the decreasing of wettability alteration coefficient. So, the more water-wet the matrix is changed to, the more oil can be recovered when capillary force dominates the imbibition process. Capillary pressure is dramatically increasing when wettability is changing to more water-wet (Fig. 2-4), thus oil recovery is enhanced. Therefore, wettability alteration is a key parameter for surfactant EOR in mixed- or oil-wet reservoirs.

Table 2-13—Summary of the ultimate oil recovery for the cases with $N_B \leq 0.1$.

Bond number, N_B	Wettability alteration coefficient, ω	IFT at CMC, σ_{CMC} (mN/m)	Ultimate oil recovery, R_{of} (1/OOIP)
0.09	0	0.8	0.793
0.08	0.4	1.54	0.548

Bond number, N_B	Wettability alteration coefficient, ω	IFT at CMC, σ_{CMC} (mN/m)	Ultimate oil recovery, R_{of} (1/OOIP)
0.05	0	1.54	0.793
0.03	0.5	5	0.505
0.02	0.8	15.4	0.404
0.009	0.2	10	0.58

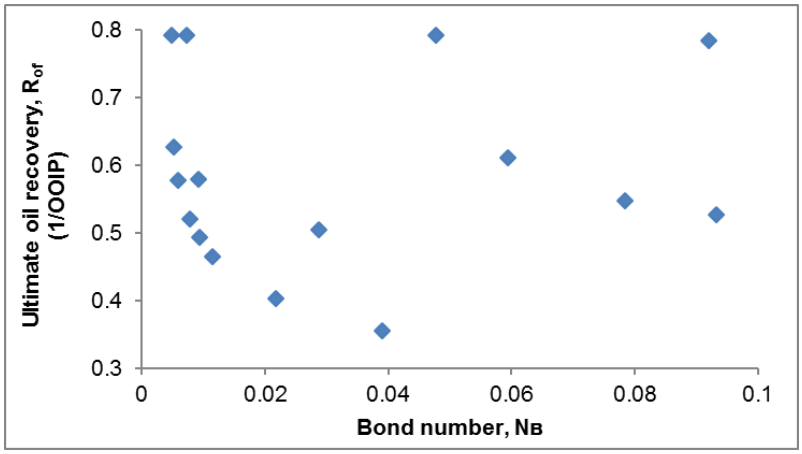

Fig. 2-40—The relationship between ultimate oil recovery of surfactant spontaneous imbibition and Bond number when $N_B \leq 0.1$.

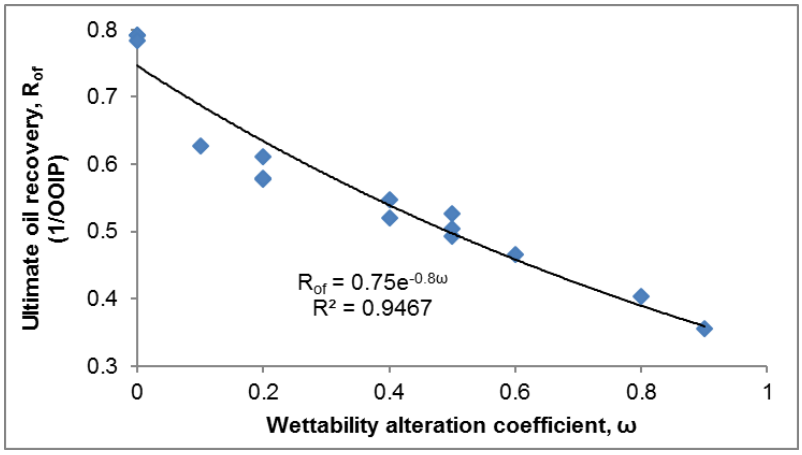

Fig. 2-41—The relationship between ultimate oil recovery of surfactant spontaneous imbibition and wettability alteration coefficient when $N_B \leq 0.1$.

Oil recovery and normalized oil recovery are plotted in Fig. 2-42 and Fig. 2-43, respectively. Since the dominating force is capillary force, based on the literature, oil recovery could be upscaled with the upscaling method for capillary imbibition (Eq. 1.25). The upscaling results of oil recovery and normalized oil recovery using the simplified existing upscaling group for capillary imbibition (Eq. 2.19) are shown in Fig. 2-44 and Fig. 2-45, respectively. But neither the oil recovery nor the normalized oil recovery has satisfactory upscaling result, which can be explained by that the wettability alteration effect is not included in Eq. 2.19. So, the simplified proposed upscaling groups (t_{d1} and t_{d2}) in Eqs. 2.17 and 2.18 are applied. The upscaling results of oil recovery are not improved (Fig. 2-46 and Fig. 2-48). The proposed upscaling group of t_{d1} does not give a satisfactory upscaling result of normalized oil recovery (Fig. 2-47). But the proposed upscaling group of t_{d2} results in a significant improvement of the upscaling result of normalized oil recovery (Fig. 2-49).

In conclusion, when both wettability and IFT are changing and the other properties are constant, the existing upscaling method for gravity imbibition can be used when $N_B \geq 1$, but the existing upscaling group for capillary imbibition (Eq. 1.25) is not valid when $N_B < 1$. The proposed upscaling method of t_{d1} (Eq. 2.17) can be used when $N_B > 0.1$, and the proposed upscaling method of t_{d2} (Eq. 2.18) is valid for all the cases. The proposed upscaling methods are used for the upscaling of normalized oil recovery.

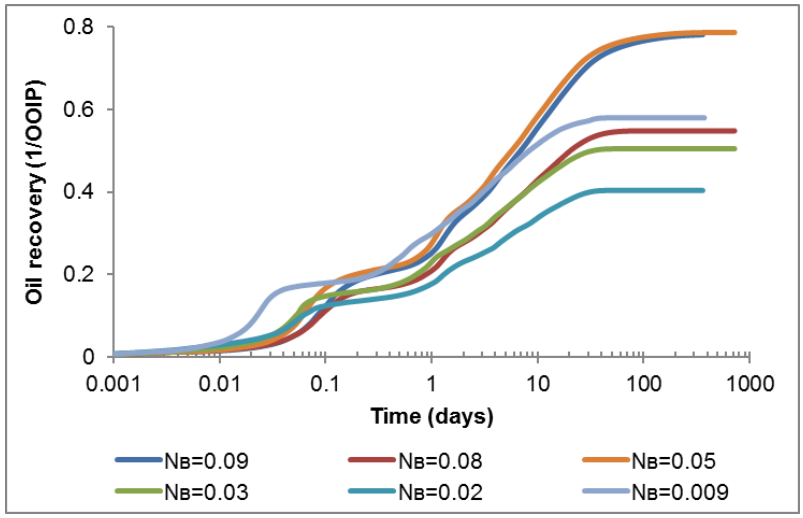

Fig. 2-42—Oil recovery of surfactant spontaneous imbibition vs. imbibition time when $N_B \leq 0.1$.

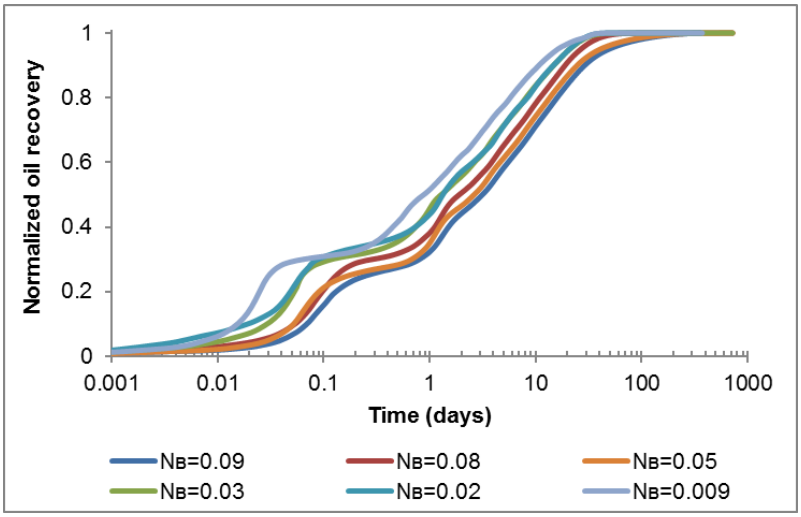

Fig. 2-43—Normalized oil recovery of surfactant spontaneous imbibition vs. imbibition time when $N_B \leq 0.1$.

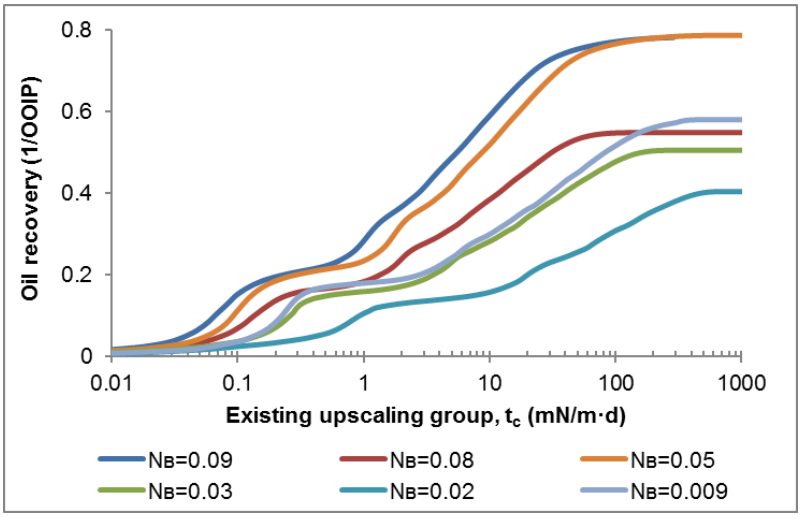

Fig. 2-44—Oil recovery of surfactant spontaneous imbibition vs. simplified existing upscaling group for capillary imbibition (t_c) when $N_B \leq 0.1$.

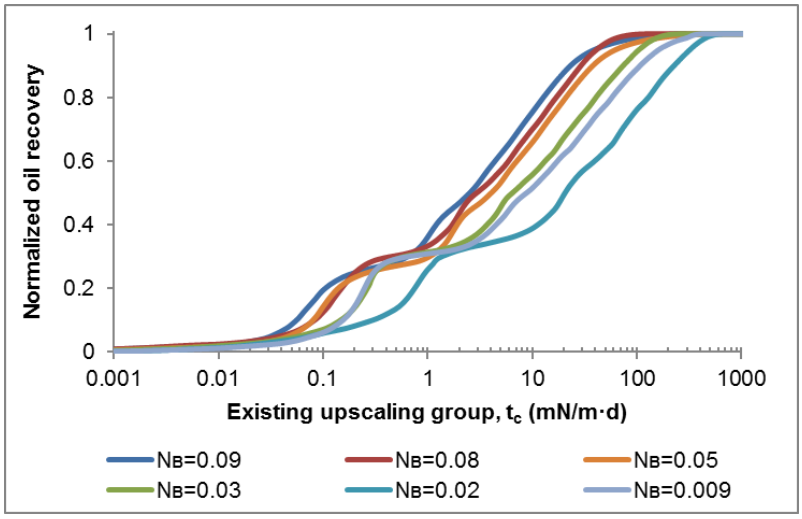

Fig. 2-45—Normalized oil recovery of surfactant spontaneous imbibition vs. simplified existing upscaling group for capillary imbibition (t_c) when $N_B \leq 0.1$.

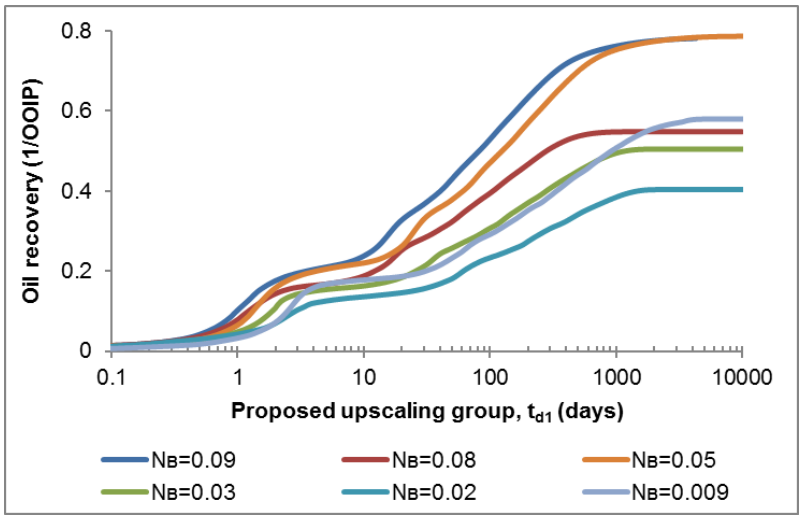

Fig. 2-46—Oil recovery of surfactant spontaneous imbibition vs. simplified proposed upscaling group when (t_{d1}) $N_B \leq 0.1$.

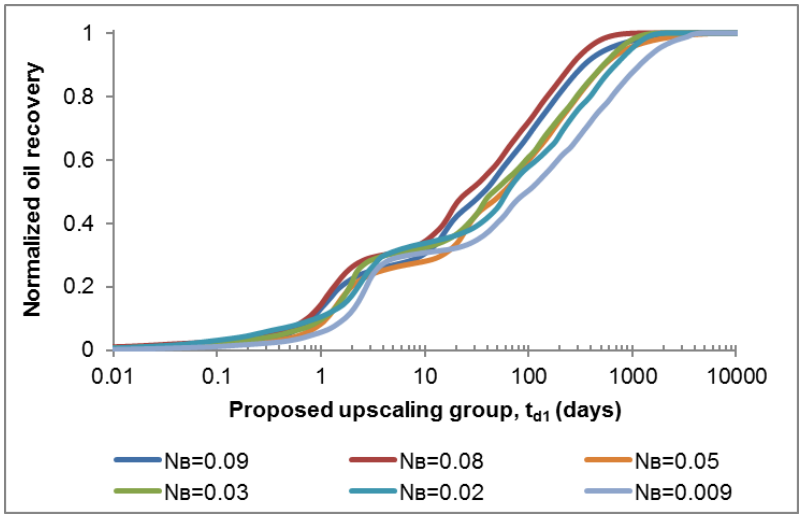

Fig. 2-47—Normalized oil recovery of surfactant spontaneous imbibition vs. simplified proposed upscaling group (t_{d1}) when $N_B \leq 0.1$.

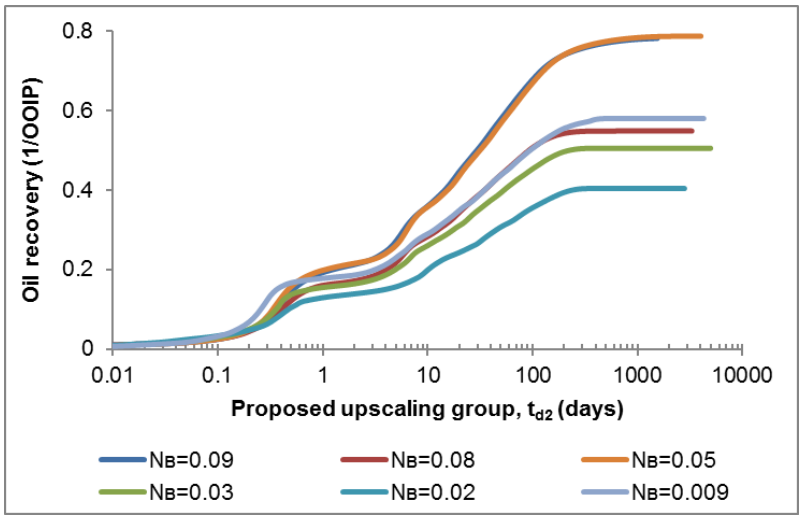

Fig. 2-48—Oil recovery of surfactant spontaneous imbibition vs. simplified proposed upscaling group when (t_{d2}) $N_B \leq 0.1$.

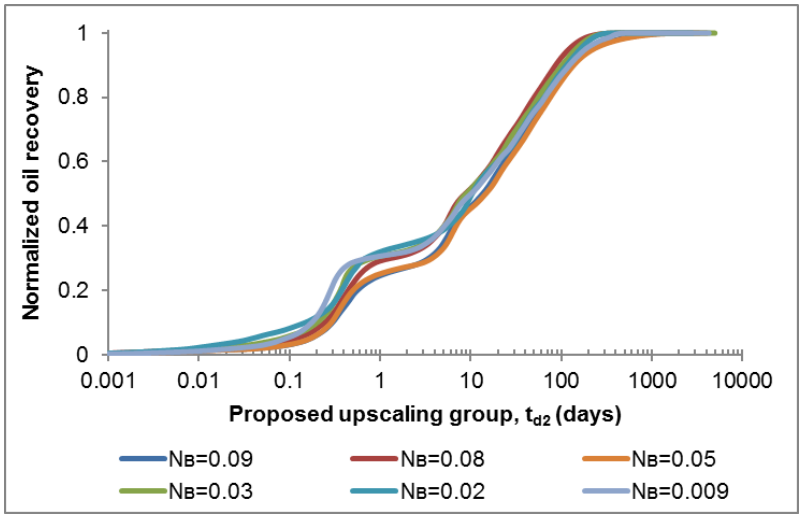

Fig. 2-49—Normalized oil recovery of surfactant spontaneous imbibition vs. simplified proposed upscaling group (t_{d2}) when $N_B \leq 0.1$.

2.5 Summary

In this chapter, a model of surfactant spontaneous imbibition is established based on the experimental data from literature (Standnes and Austad 2000) and verified by history matching of oil recovery of experiment and simulation. The main surfactant EOR mechanisms, wettability alteration and IFT reduction, are studied. New upscaling methods are proposed and verified by simulation results. The main conclusions are as follows.

1. The capillary pressure and Bond number calculation equations include both wettability alteration and IFT reduction.
2. Two proposed upscaling methods, which include the effect of wettability alteration, IFT reduction, gravity and capillary pressure, are proposed by combining equations of capillary pressure, Bond number and Darcy's law.
3. The validity of proposed upscaling groups and the existing upscaling group for gravity dominating imbibition are proved with simulation results when $N_B \geq 1$. The existing upscaling method for capillary dominating imbibition cannot be used when $N_B < 1$ because the method ignores wettability alteration.

4. The proposed upscaling method of t_{D1} could improve the upscaling result of normalized oil recovery when $N_B > 0.1$. The proposed upscaling method of t_{D2} is applicable for the upscaling of normalized oil recovery for all the cases, especially when $N_B \leq 0.1$.
5. When only wettability is changed, Bond number is always smaller than 1 in the model. Ultimate oil recovery has a power function relation with Bond number.
6. Wettability alteration is a highly efficient EOR method for mixed- or oil-wet matrix. The ultimate oil recovery is about 0.79 OOIP, and the enhanced oil recovery is about 0.64 OOIP when matrix wettability is altered to strongly water-wet even though the water/oil IFT is not changed.
7. Ultimate oil recovery is enhanced by reducing IFT when wettability is not changed. Ultimate oil recovery has a logarithmic function relation with IFT at CMC (σ_{CMC}). When $\sigma_{CMC} \leq 0.0154$ mN/m, the increase of ultimate oil recovery with the reduction of σ_{CMC} is slower.
8. Wettability alteration efficiency could be a more important factor for surfactant screening for mixed- or oil-wet reservoirs when IFT is larger than 0.0154 mN/m at CMC. But if IFT is reduced to 0.0154 mN/m or lower at CMC, wettability alteration has no effect on ultimate oil recovery.

3 Effect of matrix properties on surfactant spontaneous imbibition

The effect of surfactant on oil recovery is varying with the properties of matrix, for example permeability, porosity and matrix size. The effect of permeability and porosity on capillary pressure could be calculated with Leverett's dimensionless J function (Eq. 3.1). The properties of rock and fluids used in the spontaneous imbibition model in chapter 2 are regarded as the reference parameters in this chapter. The main parameters of the base case are in Table 3-1.

$$J\left(S_w\right)=\frac{P_c\left(S_w\right)}{\sigma\cos\theta}\sqrt{\frac{K}{\phi}} \tag{3.1}$$

Where, S_w is water saturation; P_c is capillary pressure, atm; σ is interfacial tension, mN/m; θ is contact angle, degree; K is matrix absolute permeability, mD; ϕ is matrix porosity.

Table 3-1—The main parameters used in the base case.

Matrix size (cm)	Length, L	3.4
	Height, H	4.6
Matrix absolute permeability, K (mD)		3
Matrix porosity, ϕ (fraction)		0.443
Initial water saturation, S_{wi} (fraction)		0.277
Endpoint of positive capillary pressure (atm)	Oil-wet, P_c^i	0.005
	Water-wet, P_c^{ww}	0.2
Water/oil IFT (mN/m)	Initial, σ_i	15.4
	At CMC, σ_{CMC}	0.8

3.1 Matrix permeability

The effect of matrix permeability on oil recovery is studied with the assumptions: (1) there is no relationship between permeability and porosity, which means the porosity is the same for all the cases with varying permeability; (2) the porous matrix can be modelled as a bundle of non-connecting capillary tubes; (3) the rock properties except permeability are the same; the properties of brine, oil, and surfactant are the same; (4) the matrix is homogeneous. The matrix permeability in the base case is 3 mD. In order to study the effect of matrix permeability, there are seven comparative simulations with the matrix permeability of 1.5, 6, 30, 60, 150, 300 and 600 mD separately. According to Eq. 3.1, capillary pressure is changing with matrix permeability, and since the properties except matrix permeability keep constant, capillary pressure can be expressed by the known capillary pressures in base case (Eq. 3.2). Thus, Bond number can be calculated with Eq. 3.3. In addition, fluid mobility is changing with matrix permeability (Eq. 3.4). With the increase of matrix permeability, capillary pressure is decreasing, Bond number is increasing, and fluid mobility is increasing.

$$P_c = P_c^0 \sqrt{\frac{K^0}{K}} \tag{3.2}$$

$$N_B = \frac{\Delta\rho g H}{P_c} = \frac{\Delta\rho g H}{P_c^0}\sqrt{\frac{K}{K^0}} = N_B^0\sqrt{\frac{K}{K^0}} \tag{3.3}$$

$$\lambda_j = \frac{K k_{rj}}{\mu_j} \tag{3.4}$$

Where, K^0 is the reference matrix permeability, mD; K is matrix permeability, mD; P_c is capillary pressure for matrix permeability K, atm; P_c^0 is the reference capillary pressure, atm; $\Delta\rho$ is density difference of water and oil, g/cm^3; g is gravity, 9.8 mN/g; H is matrix height, cm; N_B^0 is the reference Bond number; N_B is Bond number for matrix permeability K; λ_j is mobility of phase j, mD/cP; k_{rj} is relative permeability of phase j; μ_j is viscosity of phase j, cP; j means phase oil or water, j = o or w.

3.1.1 Brine spontaneous imbibition

The summary of brine spontaneous imbibition is in Table 3-2. Bond number is changing between 0.1 and 3 with matrix permeability, which means with the increase of permeability the dominating force is transferring from capillary force to gravity force. The oil saturation distribution in the middle of the matrix after a certain time of imbibition before it stops is shown in Fig. 3-1. For the matrix with permeability of 3 mD, after 12 days of spontaneous imbibition the oil saturation is the highest in the middle of the matrix (Fig. 3-1a), which means capillary force is the dominating force for the imbibition. For the matrix with permeability of 300 mD, the oil saturation in the upper part of the matrix is much higher than the lower part (Fig. 3-1b), which implies that gravity force is the dominating force.

Ultimate oil recovery is increasing with the increase of matrix permeability (Fig. 3-2). Oil recovery rate is higher in the matrix with smaller permeability at the beginning of the imbibition, but with the proceeding of surfactant imbibition, oil recovery rate is becoming lower in the matrix with smaller permeability (Fig. 3-3). Since the original wettability of matrix is oil-wet, the largest positive capillary pressure is very small (i.e. 0.005 atm), and the capillary pressure reduces to negative when the water saturation is higher than 35%, the capillary imbibition stops in a short time and the imbibition stops when the total pressure of capillary pressure and gravity is zero.

Base on Eq. 3.2, in the matrix with smaller permeability, capillary pressure is larger, so oil recovery rate is higher at the beginning of imbibition. When capillary pressure is reduced to negative with the increase of water saturation in matrix, the absolute value of negative capillary pressure is bigger, and water and oil move slower, so that oil recovery is slower. For the matrix with higher permeability, the total force is zero at a higher water saturation, thus the ultimate oil recovery is larger. And ultimate oil recovery has a positive logarithmic function relation with matrix permeability (Fig. 3-4).

Table 3-2—Summary of brine spontaneous imbibition in matrices with permeability between 1.5 and 600 mD.

Matrix permeability, K (mD)	Bond number, N_B	Ultimate oil recovery, R_{ofw} (1/OOIP)
1.5	0.14	0.132
3	0.19	0.15
6	0.27	0.176
30	0.61	0.253
60	0.86	0.292
150	1.35	0.337
300	1.91	0.37
600	2.71	0.403

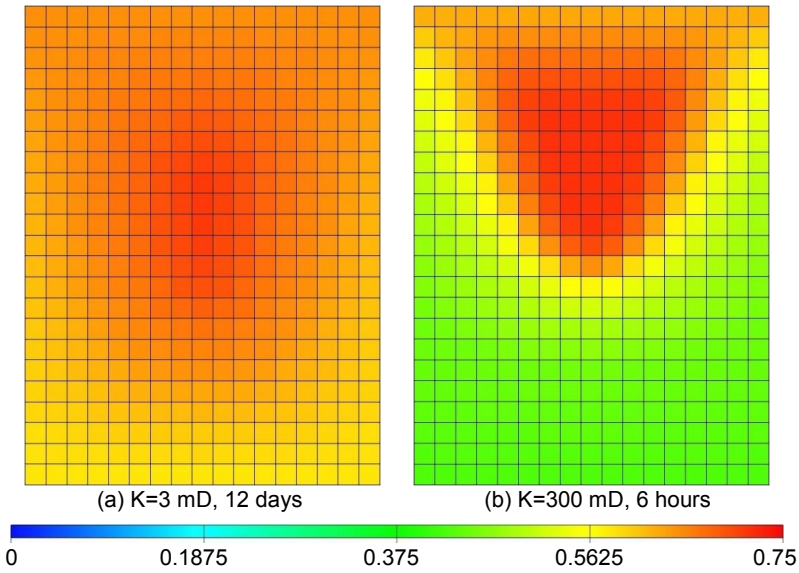

(a) matrix permeability is 3 mD, and the imbibition time is 12 days; (b) matrix permeability is 300 mD, and the imbibition time is 6 hours.

Fig. 3-1—Oil saturation distribution in the middle of matrix.

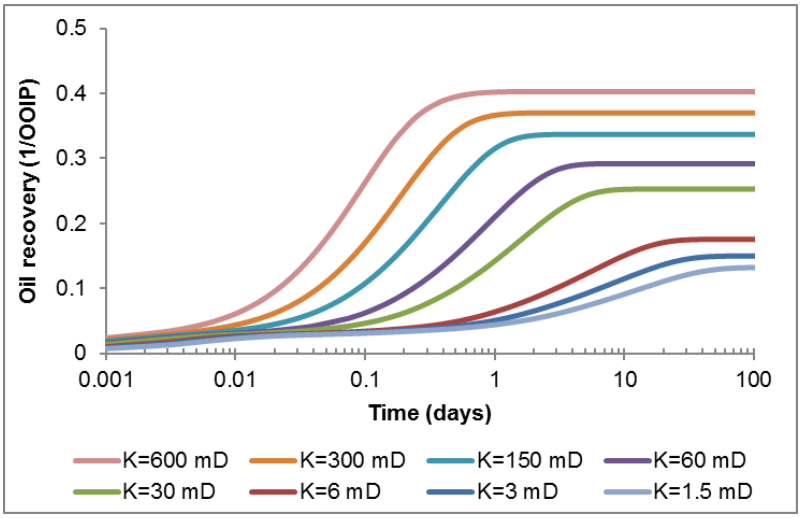

Fig. 3-2—Oil recovery of brine spontaneous imbibition in matrices with permeability between 1.5 and 600 mD.

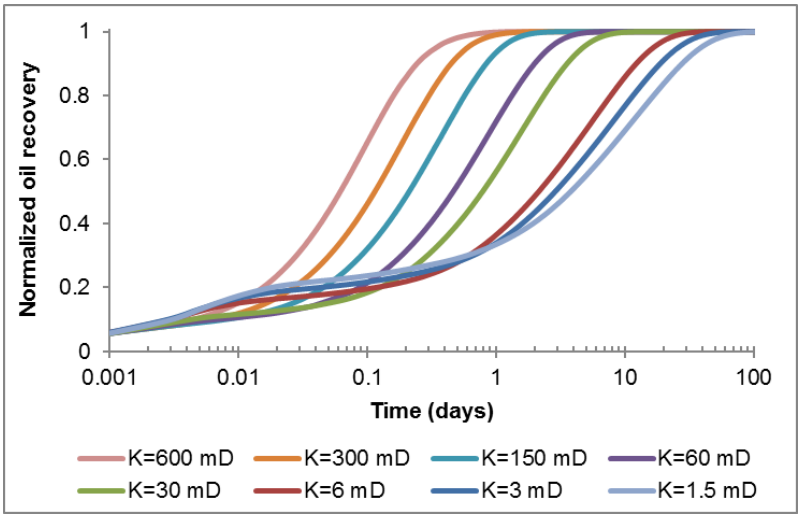

Fig. 3-3—Normalized oil recovery of brine spontaneous imbibition in matrices with permeability between 1.5 and 600 mD.

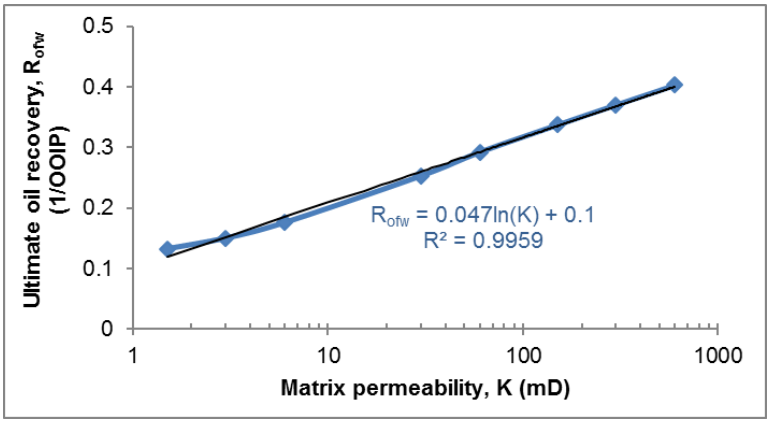

Fig. 3-4—The relationship between matrix permeability and ultimate oil recovery of brine spontaneous imbibition in matrices with permeability between 1.5 and 600 mD.

3.1.2 Surfactant spontaneous imbibition

In the base case of surfactant spontaneous imbibition, the wettability alteration coefficient is 0 (i.e. $\omega = 0$), and the IFT at CMC is 0.8 mN/m (i.e. $\sigma_{CMC} = 0.8$ mN/m). Bond number is between 0.05 and 1.5 in matrices with permeability between 1.5 and 600 mD. The summary of surfactant spontaneous imbibition is in Table 3-3.

Table 3-3—Summary of surfactant spontaneous imbibition under the conditions of $\omega = 0$ and $\sigma_{CMC} = 0.8$ mN/m.

Matrix permeability, K (mD)	Bond number, N_B	Ultimate oil recovery, R_{ofs} (1/OOIP)		Enhanced oil recovery, EOR (1/OOIP)
		Surfactant imbibition	Brine imbibition	
1.5	0.07	0.784	0.132	0.652
3	0.09	0.784	0.15	0.634
6	0.13	0.796	0.176	0.62
30	0.29	0.808	0.253	0.555
60	0.41	0.829	0.292	0.537
150	0.65	0.857	0.337	0.52
300	0.92	0.877	0.37	0.507
600	1.3	0.898	0.403	0.496

Fig. 3-5 shows that the effect of matrix permeability on surfactant imbibition is very small when surfactant changes the wettability to strongly water-wet and reduces IFT to 0.8 mN/m at CMC. The ultimate oil recovery does not have obvious increase when the matrix permeability is smaller than 30 mD. And the oil recovery is only increased by 0.114 OOIP when the permeability is increased to 600 mD from 3 mD. With the increase of permeability, capillary pressure is decreasing, thus the water saturation, where the total force is zero, is increasing. Therefore, more oil could be recovered with the increase of matrix permeability. The decrease of capillary pressure because of the increase of matrix permeability leads to an increase of capillary number. When capillary number exceeds 10^{-8}, the residual oil saturation starts to decrease, so ultimate oil recovery starts to increase.

Fig. 3-6 tells that oil recovery is faster in the matrix with higher matrix permeability, which is due to the increase of fluid mobility with the increase of matrix permeability. The increase of fluid velocity in matrix also can increase the capillary number, thus enhance the ultimate oil recovery.

Fig. 3-7 shows that the ultimate oil recovery has a strongly positive linear function relation with ln(K), but it is increasing faster when the permeability is larger than 30 mD. However, surfactant EOR is decreasing with the increase of matrix permeability, and it has a negative power function relation with matrix permeability (Fig. 3-8). In conclusion, the ultimate oil recovery of surfactant spontaneous imbibition is higher in the matrix with larger permeability, but the surfactant EOR is lower in the matrix with smaller permeability.

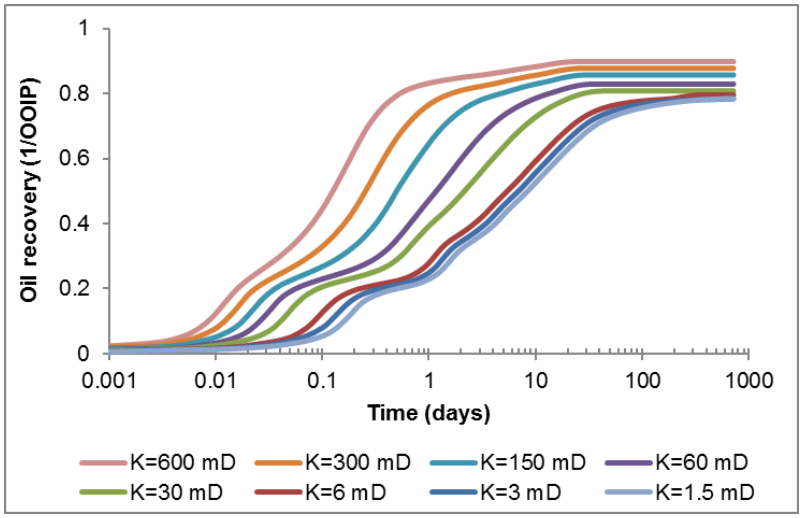

Fig. 3-5—Oil recovery of surfactant spontaneous imbibition in matrices with permeability between 1.5 and 600 mD under the conditions of ω = 0 and σ_{CMC} = 0.8 mN/m.

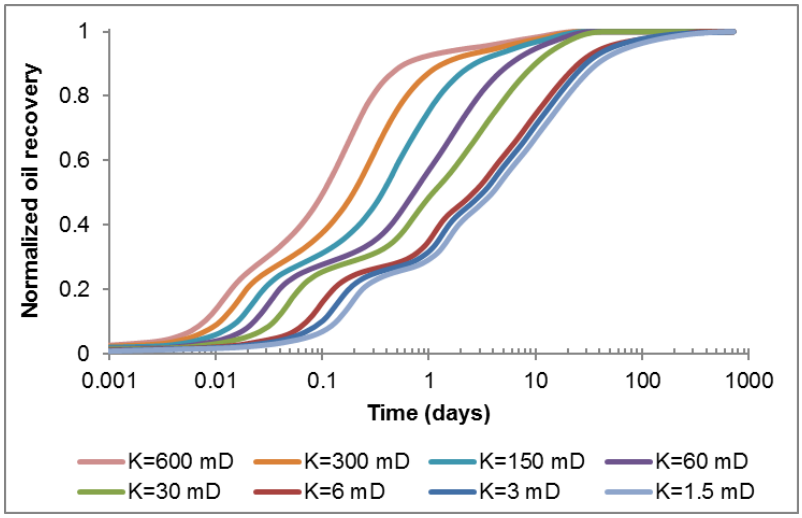

Fig. 3-6—Normalized oil recovery of surfactant spontaneous imbibition in matrices with permeability between 1.5 and 600 mD under the conditions of ω = 0 and σ_{CMC} = 0.8 mN/m.

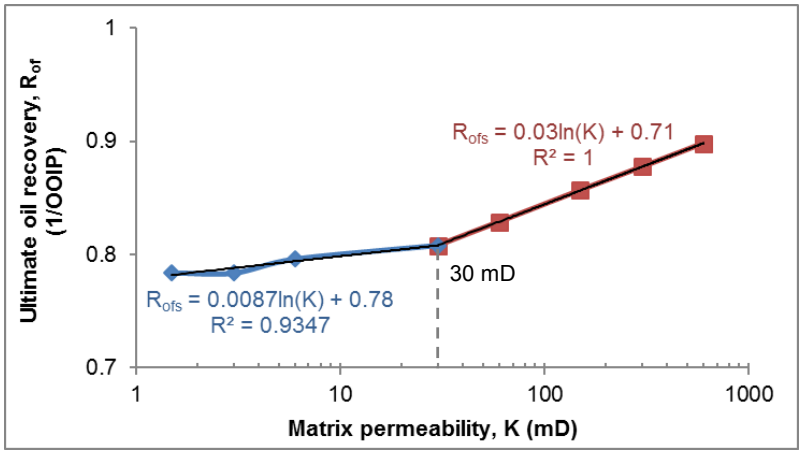

Fig. 3-7—The relationship between matrix permeability and ultimate oil recovery of surfactant spontaneous imbibition under the conditions of ω = 0 and σ_{CMC} = 0.8 mN/m.

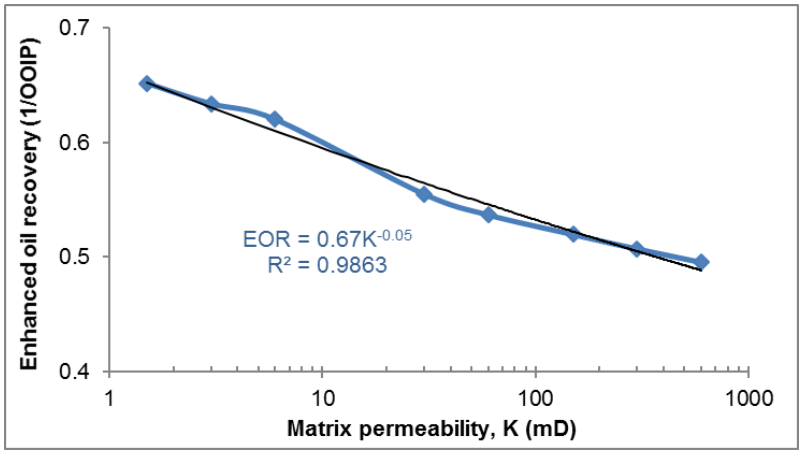

Fig. 3-8—The relationship between matrix permeability and surfactant enhanced oil recovery under the conditions of ω = 0 and σ_{CMC} = 0.8 mN/m.

3.1.3 Matrix permeability effect on upscaling methods of surfactant imbibition

Bond number is changing with IFT reduction, wettability alteration and matrix permeability. The summary of surfactant spontaneous imbibition in matrices with varying permeability is

shown in Table 3-4. The relationship between Bond number and ultimate oil recovery of surfactant imbibition (Fig. 3-9) tells that in general, ultimate oil recovery is increasing with the increase of matrix permeability under the same conditions of IFT reduction and wettability alteration. But when wettability is changed to strongly water-wet (i.e. $\omega = 0$), ultimate oil recovery does not have significant increase with matrix permeability. The relationship between Bond number and surfactant enhanced oil recovery is shown in Fig. 3-10. With the increase of Bond number, surfactant EOR is reducing and then start to increase around the Bond number of 1. To study the effect of matrix permeability on upscaling methods of surfactant imbibition, it is divided into three groups according to Bond number: $N_B \geq 1$, $0.1 < N_B < 1$, and $N_B \leq 0.1$.

Table 3-4—Summary of surfactant spontaneous imbibition in matrices with permeability between 1.5 and 600 mD under different IFT and wettability conditions.

Case	Matrix permeability, K (mD)	Bond number, N_B	Ultimate oil recovery of surfactant imbibition, R_{ofs} (1/OOIP)	Surfactant EOR (1/OOIP)
$\omega = 0$; $\sigma_{CMC} = 10$ mN/m; $N_B \leq 0.1$	1.5	0.005	0.792	0.66
	3	0.007	0.792	0.642
	6	0.01	0.791	0.616
	30	0.02	0.793	0.54
	60	0.03	0.795	0.503
	150	0.05	0.803	0.466
	300	0.07	0.817	0.447
	600	0.1	0.835	0.432
$\omega = 0$; $\sigma_{CMC} = 0.8$ mN/m; $0.05 < N_B < 2$	1.5	0.07	0.784	0.652
	3	0.09	0.784	0.634
	6	0.13	0.796	0.62
	30	0.3	0.808	0.555
	60	0.4	0.829	0.537
	150	0.65	0.857	0.52
	300	0.9	0.877	0.507
	600	1.3	0.898	0.496

Case	Matrix permeability, K (mD)	Bond number, N_B	Ultimate oil recovery of surfactant imbibition, R_{ofs} (1/OOIP)	Surfactant EOR (1/OOIP)
$\omega = 0.5$; $\sigma_{CMC} = 0.8$ mN/m; $0.1 \leq N_B < 3$	1.5	0.1	0.537	0.404
	3	0.2	0.552	0.402
	6	0.3	0.57	0.395
	30	0.6	0.639	0.387
	60	0.8	0.685	0.394
	150	1.3	0.757	0.421
	300	1.8	0.807	0.437
	600	2.5	0.848	0.446
$\omega = 0.8$; $\sigma_{CMC} = 0.8$ mN/m; $0.3 \leq N_B \leq 6$	1.5	0.3	0.473	0.34
	3	0.4	0.491	0.341
	6	0.6	0.512	0.337
	30	1.3	0.576	0.323
	60	2	0.613	0.321
	150	3	0.679	0.342
	300	4	0.745	0.375
	600	6	0.803	0.401
$\omega = 1$; $\sigma_{CMC} = 0.8$ mN/m; $2 < N_B \leq 60$	1.5	3	0.398	0.266
	3	4	0.432	0.282
	6	5	0.465	0.289
	30	12	0.54	0.287
	60	16	0.579	0.287
	150	26	0.64	0.303
	300	37	0.704	0.334
	600	52	0.772	0.369
$\omega = 1$; $\sigma_{CMC} = 0.154$ mN/m; $10 < N_B < 300$	1.5	14	0.554	0.421
	3	19	0.592	0.442
	6	27	0.638	0.463
	30	61	0.766	0.513
	60	86	0.812	0.52
	150	135	0.866	0.529
	300	191	0.9	0.53
	600	271	0.928	0.526

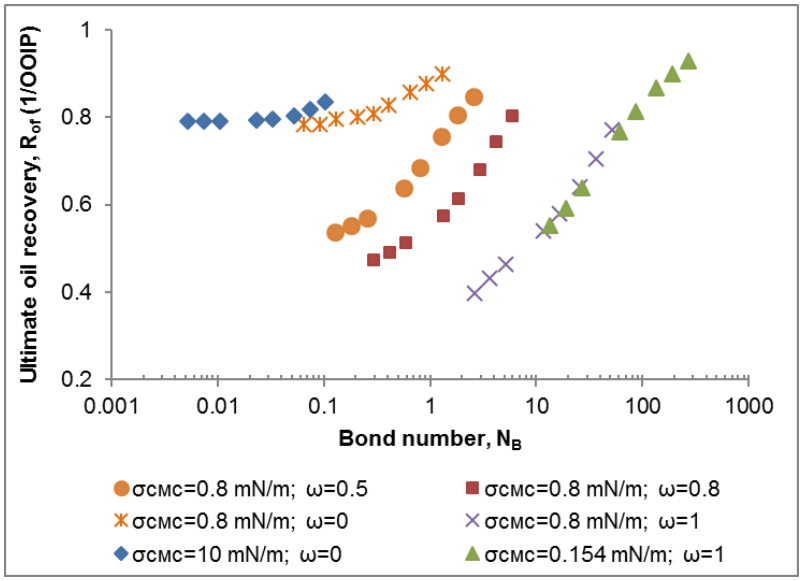

Dots with the same color mean matrix permeability varying between 1.5 and 600 mD.

Fig. 3-9—The relationship between ultimate oil recovery of surfactant imbibition and Bond number.

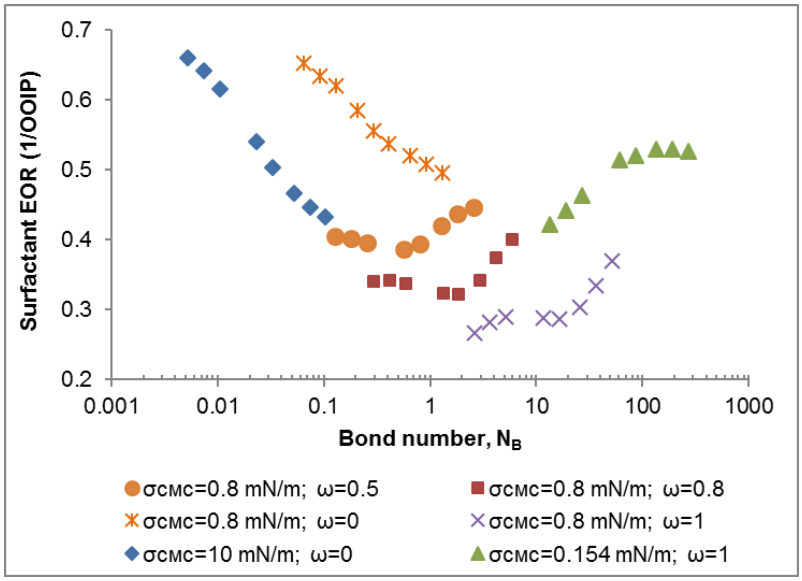

Dots with the same color mean matrix permeability varying between 1.5 and 600 mD.

Fig. 3-10—The relationship between surfactant enhanced oil recovery and Bond number.

3.1.3.1 $N_B \geq 1$

When IFT is reduced to 0.8 mN/m at CMC (i.e. σ_{CMC} = 0.8 mN/m) and wettability keeps oil-wet (i.e. ω = 1), Bond number is larger than 1 in the matrix with permeability bigger than 1.5 mD. The oil recovery and normalized oi recovery shown in Fig. 3-11 and Fig. 3-12 imply that both ultimate oil recovery and oil recovery rate can be enhanced by the increase of matrix permeability.

The existing upscaling method for gravity imbibition in Eq. 1.34 is simplified into Eq. 3.5 by removing the constant parameters. Then Eq. 3.5 is applied to upscaling of oil recovery and normalized oil recovery. Fig. 3-13 and Fig. 3-14 show that the oil recovery and normalized oil recovery are well converged, which implies that the existing upscaling group for gravity imbibition (Eq. 1.34) could be used when $N_B \geq 1$. The proposed upscaling methods (Eqs. 2.13 and 2.16) are simplified into Eqs. 3.6 and 3.7, and then used to upscale the normalized oil recovery. The excellent upscaling results shown in Fig. 3-15 and Fig. 3-16 prove that the proposed upscaling methods could be used when $N_B \geq 1$.

$$t_g = tK \tag{3.5}$$

$$t_{d1} = tK\left(N_B^{-1} + 1\right) \tag{3.6}$$

$$t_{d2} = tK\left(N_B^{-0.5} + 1\right) \tag{3.7}$$

Where, t_g is simplified existing upscaling group for gravity imbibition, mD·s; t_{d1} and t_{d2} are simplified proposed upscaling groups, mD·s; t is imbibition time, s; K is matrix permeability, mD; N_B is Bond number.

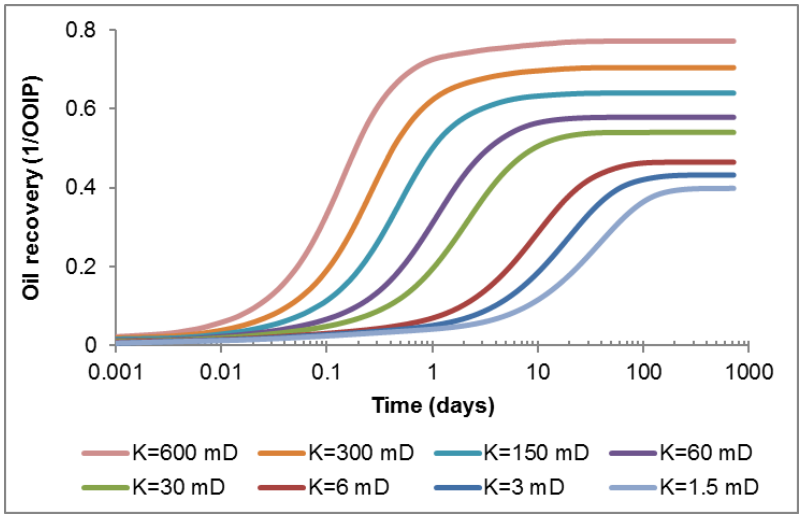

Fig. 3-11—Oil recovery of surfactant spontaneous imbibition vs. imbibition time in matrices with permeability between 1.5 and 600 mD when $N_B \geq 1$.

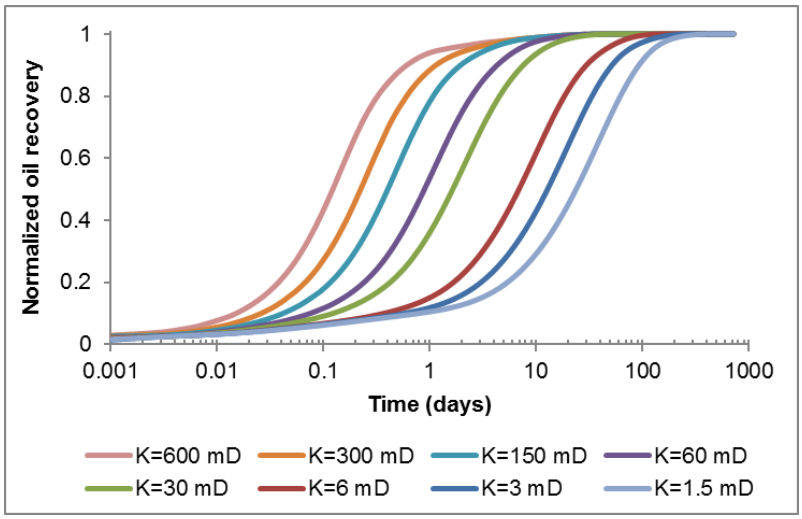

Fig. 3-12—Normalized oil recovery of surfactant spontaneous imbibition vs. imbibition time in matrices with permeability between 1.5 and 600 mD when $N_B \geq 1$.

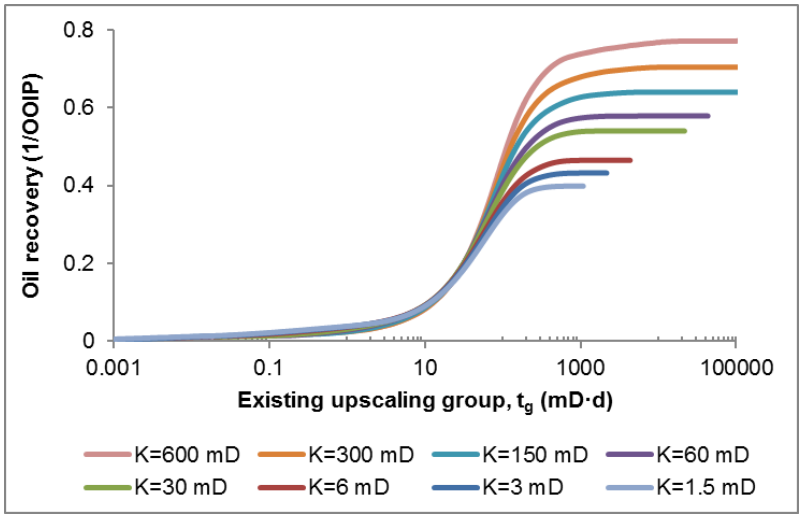

Fig. 3-13—Oil recovery of surfactant spontaneous imbibition vs. simplified existing upscaling group for gravity imbibition (t_g) in matrices with permeability between 1.5 and 600 mD when $N_B \geq 1$.

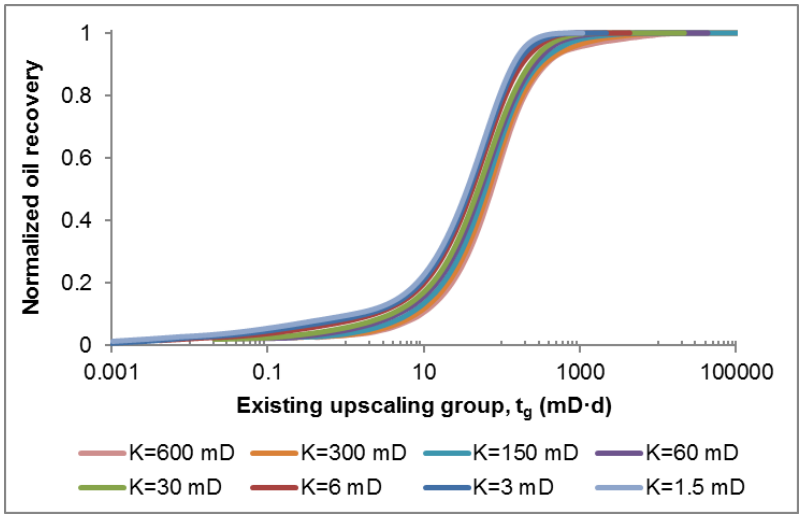

Fig. 3-14—Normalized oil recovery of surfactant spontaneous imbibition vs. simplified existing upscaling group for gravity imbibition (t_g) in matrices with permeability between 1.5 and 600 mD when $N_B \geq 1$.

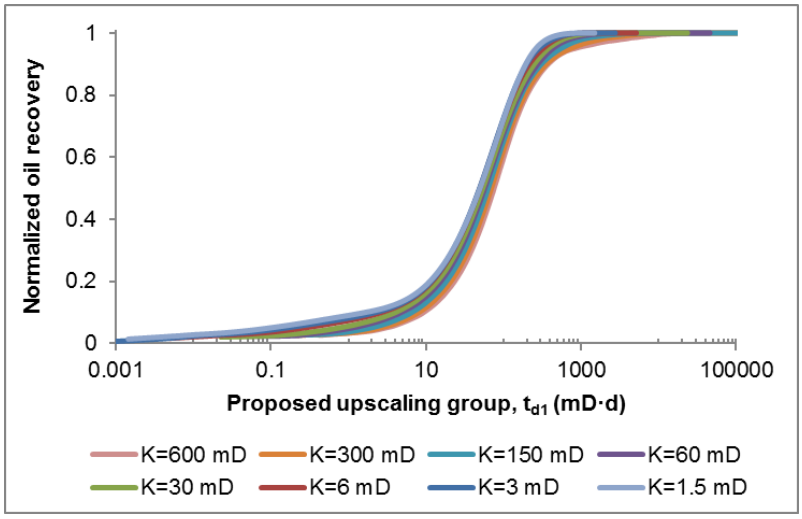

Fig. 3-15—Normalized oil recovery of surfactant spontaneous imbibition vs. simplified proposed upscaling group (t_{d1}) in matrices with permeability between 1.5 and 600 mD when $N_B \geq 1$.

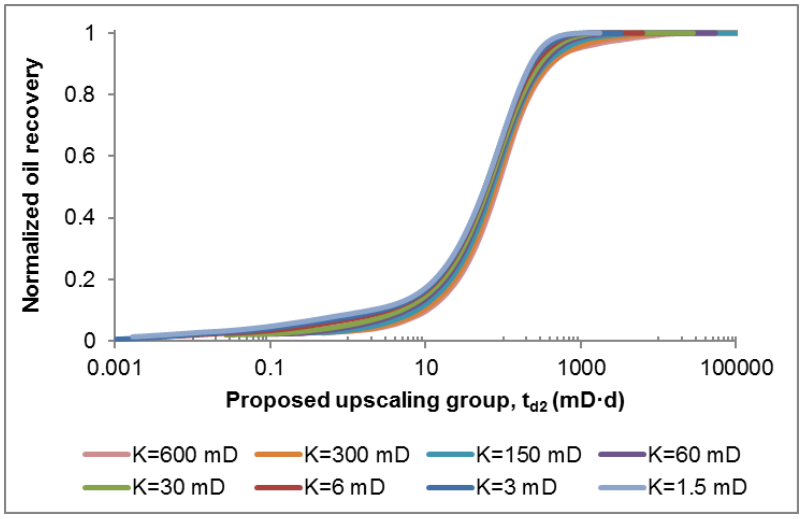

Fig. 3-16—Normalized oil recovery of surfactant spontaneous imbibition vs. simplified proposed upscaling group (t_{d2}) in matrices with permeability between 1.5 and 600 mD when $N_B \geq 1$.

3.1.3.2 0.1 < N_B < 1

When IFT is reduced to 0.8 mN/m at CMC (i.e. σ_{CMC} = 0.8 mN/m) and the wettability is altered to strongly water-wet (i.e. ω = 0), Bond number is between 0.1 and 1 when matrix permeability is changing between 3 and 300 mD. The existing dimensionless upscaling time for capillary imbibition (Eq. 1.25) can be simplified into Eq. 3.8 by removing the constants. The upscaled normalized oil recovery by Eq. 3.8 are shown in Fig. 3-17. The normalized oil recovery curves are well converged except the curves in matrix with permeability of 150 mD and 300 mD. The simplified proposed upscaling group of t_{d1} (Eq. 3.6) leads to a good upscaling result of normalized oil recovery (Fig. 3-18). Therefore, the proposed upscaling method of t_{d1} is valid when $0.1 < N_B < 1$.

$$t_c = t\sqrt{K} \tag{3.8}$$

Where, t_c is simplified existing upscaling group for capillary imbibition, $mD^{0.5}\cdot s$; t is imbibition time, s; K is matrix permeability, mD.

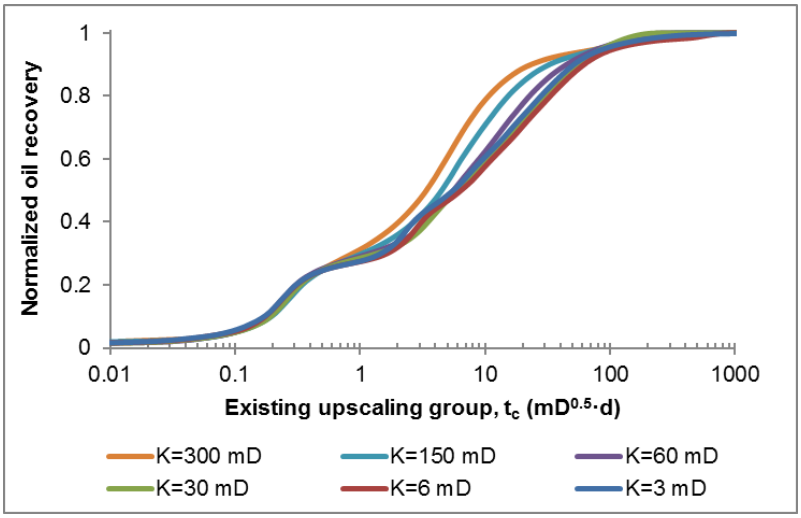

Fig. 3-17—Normalized oil recovery of surfactant spontaneous imbibition vs. simplified existing upscaling group for capillary imbibition (t_c) in matrices with permeability between 3 and 300 mD when $0.1 < N_B < 1$.

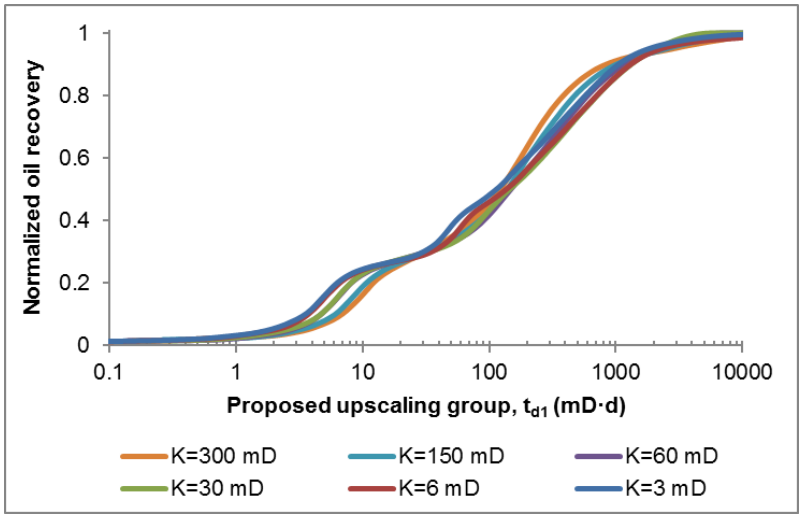

Fig. 3-18—Normalized oil recovery of surfactant spontaneous imbibition vs. simplified proposed upscaling group (t_{d1}) in matrices with permeability between 1.5 and 600 mD when $0.1 < N_B < 1$.

3.1.3.3 $N_B \leq 0.1$

When IFT is reduced to 10 mN/m at CMC (i.e. σ_{CMC} = 10 mN/m) and wettability is changed to strongly water-wet (i.e. $\omega = 0$), Bond number is smaller than 0.1 when matrix permeability is smaller than 600 mD. Fig. 3-19 and Fig. 3-20 illustrate that with the increase of matrix permeability, oil recovery rate increases, but ultimate oil recovery does not have significant increase.

Fig. 3-21 and Fig. 3-22 tell that the oil recovery and normalized oil recovery could be roughly upscaled with the existing upscaling group for capillary imbibition (Eq. 3.8). The proposed upscaling group of t_{d2} (Eq. 3.7) does not improve the upscaling results. But the proposed upscaling group of t_{d1} (Eq. 3.6) gives a similar upscaling result of normalized oil recovery (Fig. 3-23) as the existing upscaling group for capillary imbibition (Eq. 3.8), which demonstrates the validity of t_{d1}. Therefore, both the existing upscaling method for capillary imbibition and the proposed upscaling method of t_{d1} could be used to upscale the normalized oil recovery in matrix with varying permeability when $N_B \leq 0.1$.

In conclusion, when surfactant is used in a reservoir with varying permeability, the existing upscaling method for gravity imbibition could be used when $N_B \geq 1$, and the existing upscaling

method for capillary imbibition could be used when $N_B \leq 0.1$ but cannot be used when $0.1 < N_B < 1$. However, the proposed upscaling method of t_{d1} could be used for all the cases.

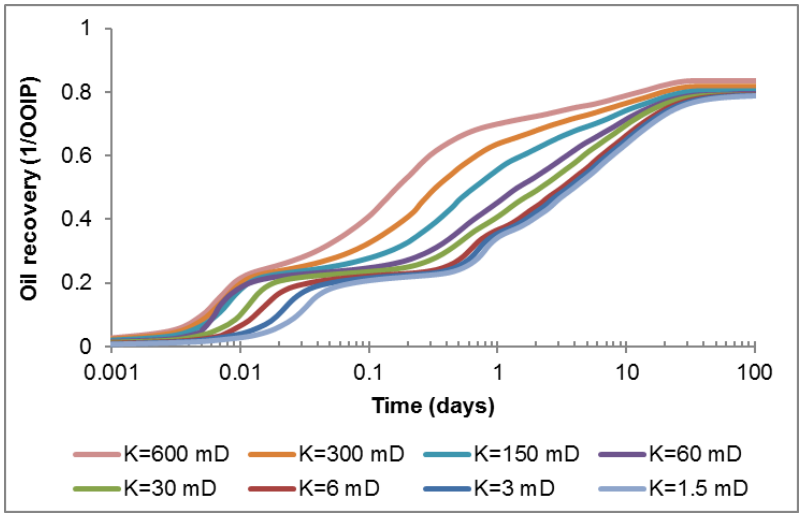

Fig. 3-19—Oil recovery of surfactant spontaneous imbibition vs. imbibition time in matrices with permeability between 1.5 and 600 mD when $N_B \leq 0.1$.

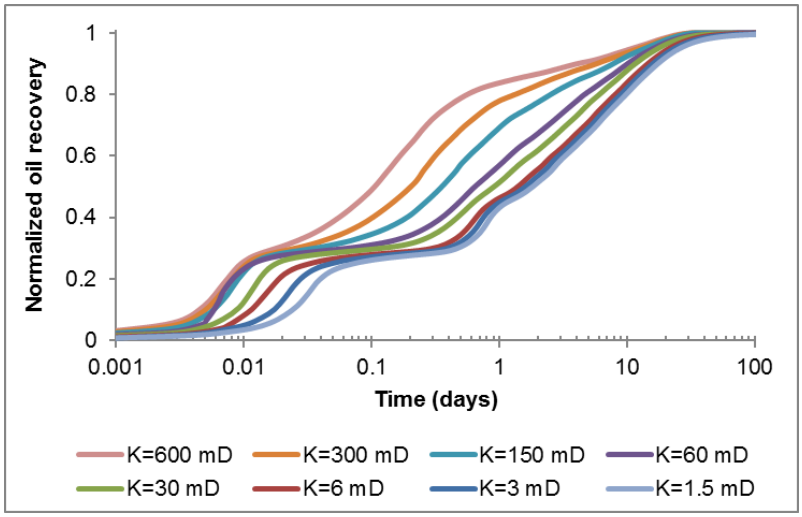

Fig. 3-20—Normalized oil recovery of surfactant spontaneous imbibition vs. imbibition time in matrices with permeability between 1.5 and 600 mD when $N_B \leq 0.1$.

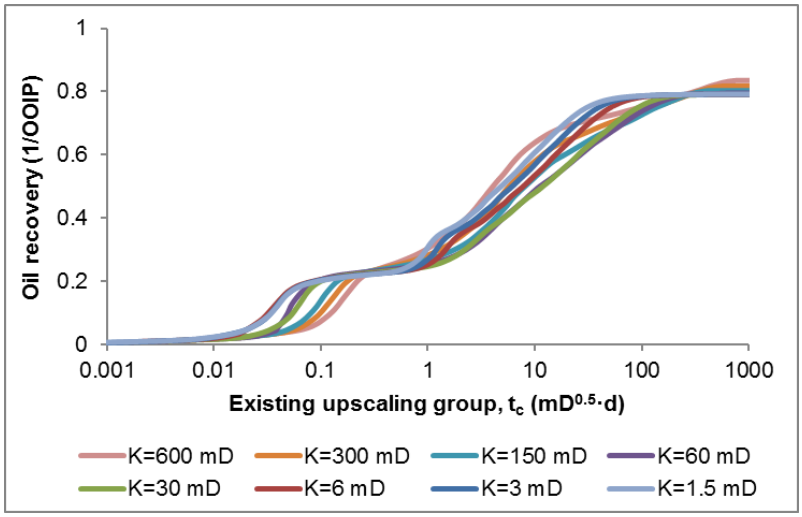

Fig. 3-21—Oil recovery of surfactant spontaneous imbibition vs. simplified existing upscaling group for capillary imbibition (t_c) in matrices with permeability between 1.5 and 600 mD when $N_B \leq 0.1$.

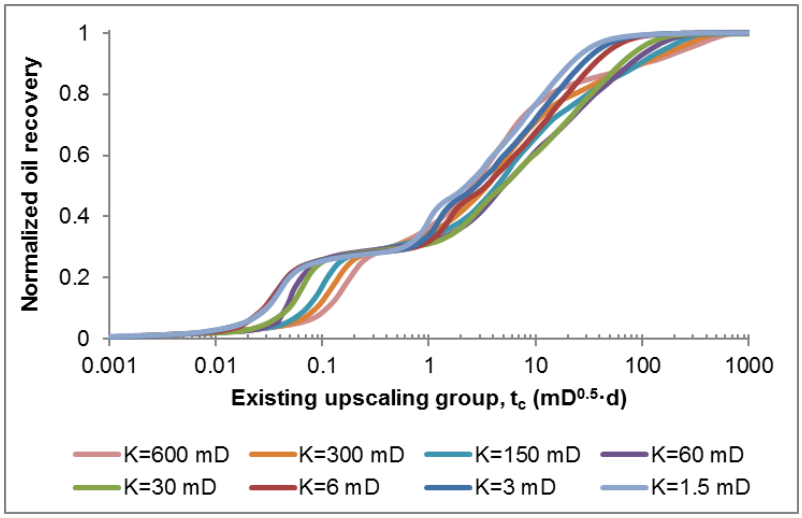

Fig. 3-22—Normalized oil recovery of surfactant spontaneous imbibition vs. simplified existing upscaling group for capillary imbibition (t_c) in matrices with permeability between 1.5 and 600 mD when $N_B \leq 0.1$.

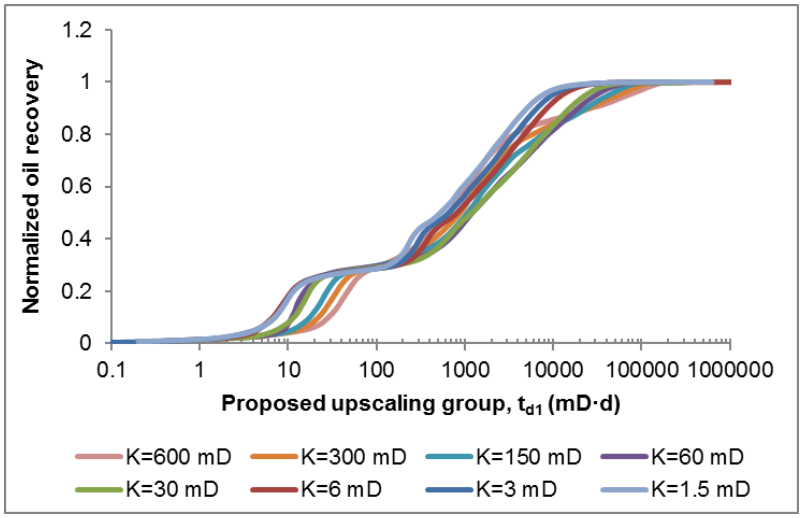

Fig. 3-23—Normalized oil recovery of surfactant spontaneous imbibition vs. simplified proposed upscaling group (t_{d1}) in matrices with permeability between 1.5 and 600 mD when $N_B \leq 0.1$.

3.2 Matrix porosity

To study the effect of matrix porosity on surfactant spontaneous imbibition, I assume that: (1) there is no relationship between permeability and porosity, which means the permeability is the same for all the cases with varying porosity; (2) the porous matrix can be modelled as a bundle of non-connecting capillary tubes; (3) the rock properties except porosity are the same; the properties of brine, oil, and surfactant are the same; (4) the matrix is homogeneous. The matrix porosity is 0.443 in the base case. In order to study the sensitivity of matrix porosity, the porosity of 0.6, which is maybe not reality, is included in the simulation study. There are five comparative simulations with matrix porosity of 0.2, 0.3, 0.4, 0.5, and 0.6 separately.

According to Leverett's dimensionless J function (Eq. 3.1), capillary pressure is changing with matrix porosity. Since the properties, except matrix porosity, keep constant, capillary pressure can be expressed by the known capillary pressure and porosity in the base case (Eq. 3.9), which is used as the reference capillary pressure and porosity. Thus, Bond number can be calculated with Eq. 3.10. With the increase of matrix porosity, capillary pressure is increasing, and Bond number is reducing.

$$P_c = P_c^0 \sqrt{\frac{\phi}{\phi^0}} \tag{3.9}$$

$$N_B = N_B^0 \sqrt{\frac{\phi^0}{\phi}} \tag{3.10}$$

Where, ϕ^0 is the reference matrix porosity; ϕ is matrix porosity; P_c^0 is the reference capillary pressure, atm; P_c is capillary pressure for matrix porosity ϕ, atm; N_B^0 is the reference Bond number; N_B is Bond number for matrix porosity ϕ.

3.2.1 Brine spontaneous imbibition

The summary of brine imbibition is in Table 3-5. Because the changing range of matrix porosity is small, Bond number slightly changes with matrix porosity. And the ultimate oil recovery increase is only 0.039 OOIP when the porosity decreases from 0.6 to 0.2. Fig. 3-24 and Fig. 3-25 show that ultimate oil recovery and oil recovery rate are decreasing with the increase of matrix porosity, which is because the increase of porosity leads to an increase of capillary pressure. The detailed explanation refers to section 3.1.1. The ultimate oil recovery of brine spontaneous imbibition has a negative power function relation with matrix porosity (Fig. 3-26).

Table 3-5—Summary of brine spontaneous imbibition in matrices with porosity between 0.2 and 0.6.

Matrix porosity, ϕ	Bond number, N_B	Ultimate oil recovery, R_{ofw} (1/OOIP)
0.2	0.28	0.18
0.3	0.23	0.164
0.4	0.2	0.153
0.443	0.19	0.15
0.5	0.18	0.146
0.6	0.16	0.141

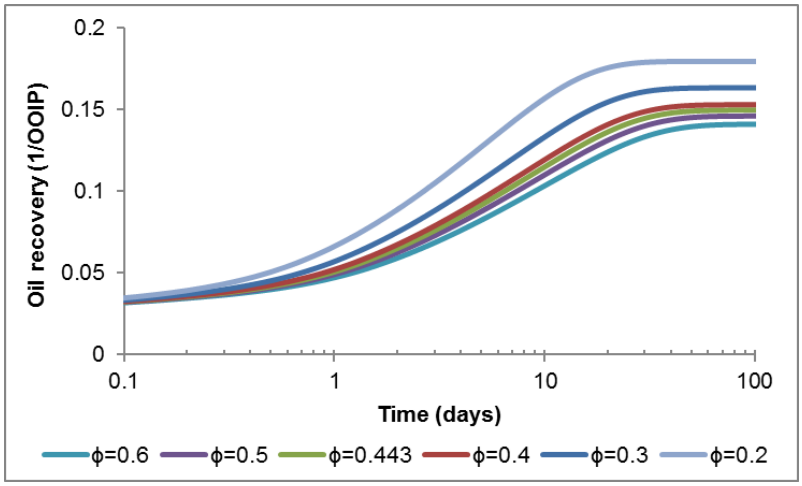

Fig. 3-24—Oil recovery of brine spontaneous imbibition in matrices with porosity between 0.2 and 0.6.

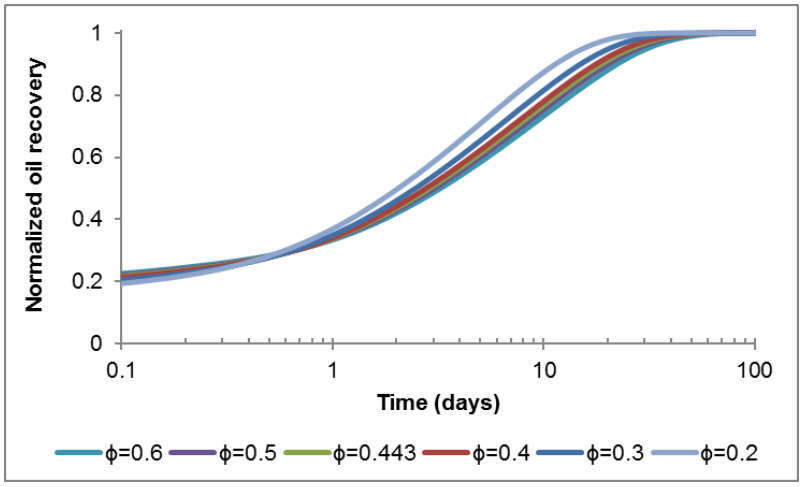

Fig. 3-25—Normalized oil recovery of brine spontaneous imbibition in matrices with porosity between 0.2 and 0.6.

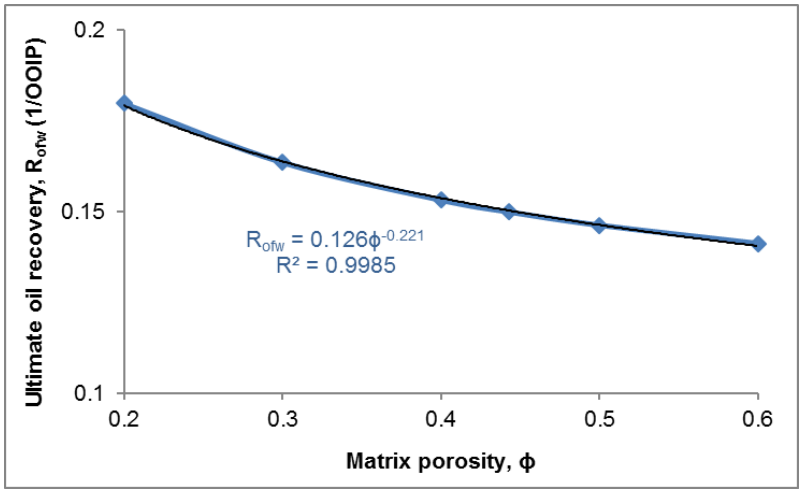

Fig. 3-26—The relationship between matrix porosity and ultimate oil recovery of brine spontaneous imbibition in matrices with porosity between 0.2 and 0.6.

3.2.2 Surfactant spontaneous imbibition

In the base case of surfactant imbibition, water/oil IFT is reduced to 0.8 mN/m at CMC (i.e. σ_{CMC} =0.8 mN/m) and matrix wettability is changed to strongly water-wet (i.e. $\omega = 0$). So that the capillary pressure is positive until the residual oil saturation. Because of the small effect of porosity on capillary pressure, Bond number is changing from 0.14 to 0.08 with the increase of porosity from 0.2 to 0.6. So, capillary force is larger than gravity force. The summary of surfactant imbibition is in Table 3-6. Fig. 3-27 shows that oil recovery is almost the same for all the cases with different porosity, which is because of the strongly water-wet wettability. Since porosity has small effect on capillary pressure (Fig. 3-28), oil recovery rate does not change much with matrix porosity.

Table 3-6—Summary of surfactant spontaneous imbibition in matrices with porosity between 0.2 and 0.6.

Matrix porosity, ϕ	Bond number, N_B	Ultimate oil recovery, R_{ofs} (1/OOIP)	Enhanced oil recovery, EOR (1/OOIP)
0.2	0.14	0.793	0.613
0.3	0.11	0.793	0.629
0.4	0.1	0.787	0.634

Matrix porosity, ϕ	Bond number, N_B	Ultimate oil recovery, R_{ofs} (1/OOIP)	Enhanced oil recovery, EOR (1/OOIP)
0.443	0.09	0.784	0.634
0.5	0.09	0.783	0.637
0.6	0.08	0.783	0.642

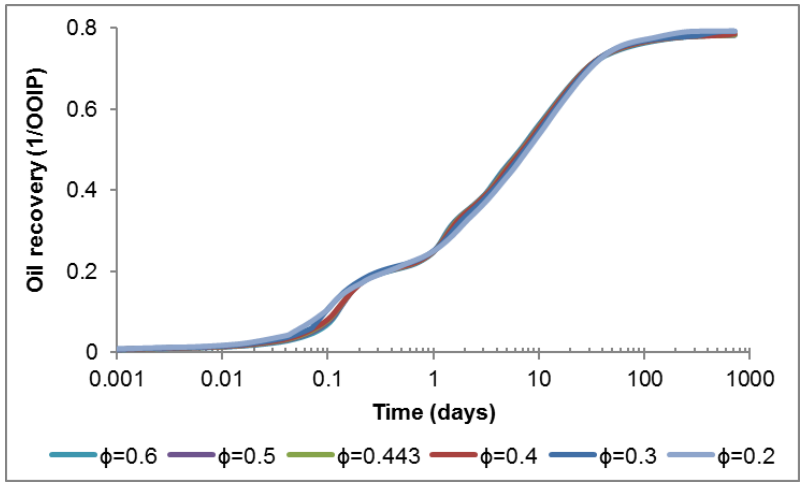

Fig. 3-27—Oil recovery of surfactant spontaneous imbibition vs. imbibition time in matrices with porosity between 0.2 and 0.6 under the conditions of σ_{CMC} = 0.8 mN/m and ω = 0.

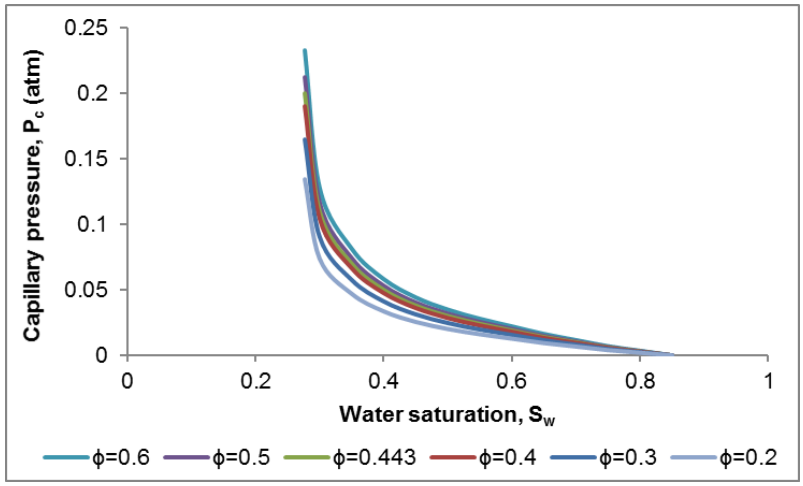

Fig. 3-28—Capillary pressure curves in matrices with porosity between 0.2 and 0.6 when the wettability is changed to strongly water-wet by surfactant.

3.2.3 Matrix porosity effect on upscaling methods of surfactant imbibition

The relationship between ultimate oil recovery of surfactant spontaneous imbibition and Bond number (Fig. 3-29) shows that ultimate oil recovery is increasing with the increase of Bond number, and the increase of ultimate oil recovery is slower when the wettability is more water-wet. Surfactant EOR decreases with the increase of matrix porosity and then increases (Fig. 3-30). The trend of surfactant EOR is changing around the Bond number of 1. The study on matrix porosity is divided into three groups based on Bond number: $N_B \geq 1$, $0.1 < N_B < 1$, and $N_B \leq 0.1$.

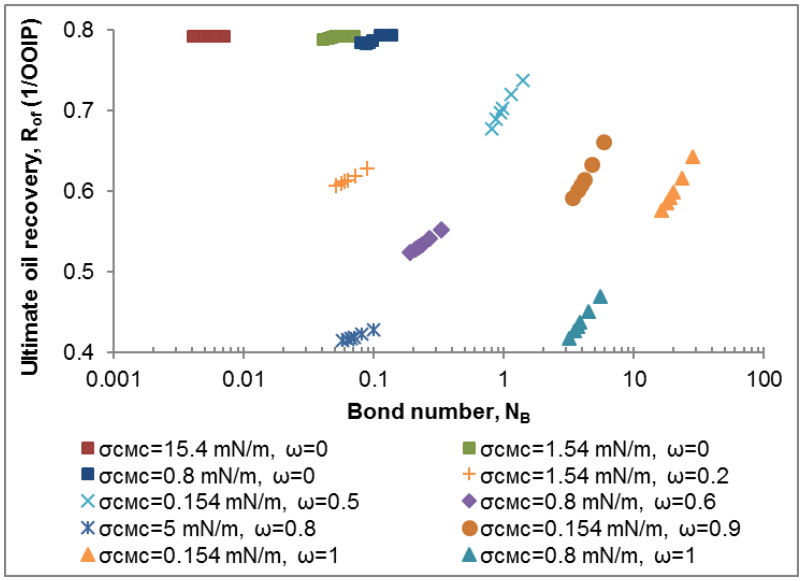

Dots with the same color mean matrix porosity varying between 0.2 and 0.6.

Fig. 3-29—The relationship between ultimate oil recovery of surfactant imbibition and Bond number in matrices with porosity between 0.2 and 0.6.

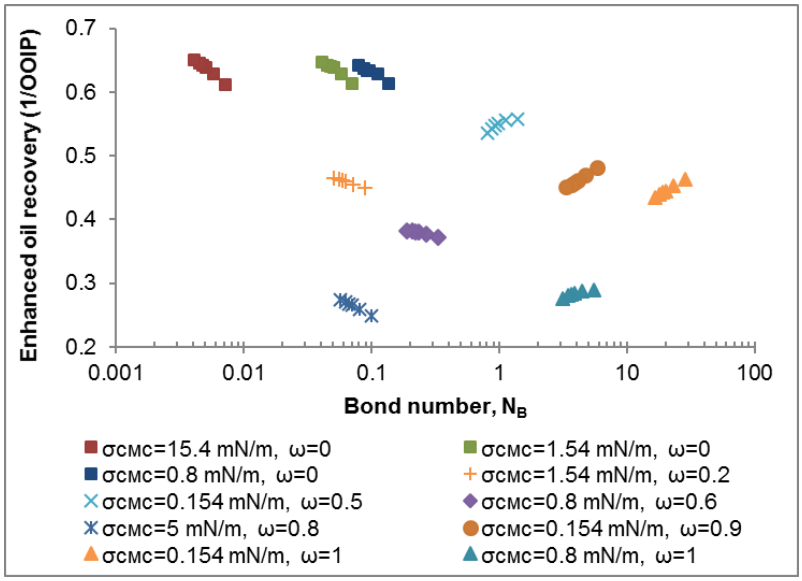

Dots with the same color mean matrix porosity varying between 0.2 and 0.6.

Fig. 3-30—The relationship between enhanced oil recovery of surfactant imbibition and Bond number in matrices with porosity between 0.2 and 0.6.

3.2.3.1 $N_B \geq 1$

When IFT is reduced to 0.154 mN/m at CMC (i.e. σ_{CMC} = 0.154 mN/m), and wettability is kept oil-wet (i.e. ω = 1), Bond number is decreasing from 28 to 16 with the change of porosity from 0.2 to 0.6. The ultimate oil recovery is increased by 6.7% OOIP with the decrease of matrix porosity from 0.6 to 0.2. When IFT is reduced to 0.8 mN/m at CMC (i.e. σ_{CMC} = 0.8 mN/m), and wettability is kept oil-wet (i.e. ω = 1), Bond number is decreasing from 5.5 to 3.2 with the increase of porosity from 0.2 to 0.6. The ultimate oil recovery is increased by 5.2% OOIP with the decrease of matrix porosity from 0.6 to 0.2. The summary of the results is shown in Table 3-7.

Table 3-7—Summary of surfactant spontaneous imbibition in matrices with porosity between 0.2 and 0.6 when $N_B \geq 1$.

Cases	Matrix porosity, ϕ	Bond number, N_B	Ultimate oil recovery, R_{of} (1/OOIP)	Enhanced oil recovery (1/OOIP)
$\sigma_{CMC} = 0.154$ mN/m; $\omega = 1$; $N_B \geq 10$	0.2	28	0.643	0.463
	0.3	23	0.616	0.452
	0.4	20	0.598	0.445
	0.443	19	0.592	0.443
	0.5	18	0.585	0.439
	0.6	16	0.575	0.434
$\sigma_{CMC} = 0.8$ mN/m; $\omega = 1$; $1 \leq N_B < 10$	0.2	5.5	0.469	0.290
	0.3	4.5	0.451	0.287
	0.4	3.9	0.437	0.284
	0.443	3.7	0.432	0.282
	0.5	3.5	0.426	0.280
	0.6	3.2	0.417	0.276

$N_B \geq 10$. Fig. 3-31 and Fig. 3-32 show that both ultimate oil recovery and oil recovery rate increase with the reduction of matrix porosity. Since the wettability is oil-wet, capillary pressure is reduced to negative at a relatively low water saturation. The absolute value of negative capillary pressure is lower in the matrix with smaller porosity. Therefore, gravity is more efficient in the matrix with lower porosity, which can explain the increase of oil recovery rate with the decrease of porosity. In addition, the final water saturation in matrix, where spontaneous imbibition stops, is increasing with the decrease of capillary pressure, which results in an increase of ultimate oil recovery with the decrease of matrix porosity.

The existing dimensionless upscaling time for gravity imbibition (Eq. 1.34) is simplified into Eq. 3.11 by removing the constants, and then applied to upscale the oil recovery and normalized oil recovery, which gives good upscaling results (Fig. 3-33 and Fig. 3-34). The proposed upscaling method of t_{D1} (Eq. 2.13) can be simplified into Eq. 3.12, which leads to similar upscaling results of oil recovery (Fig. 3-35) and normalized oil recovery (Fig. 3-36). The proposed upscaling method of t_{D2} (Eq. 2.16) can be simplified into Eq. 3.13 and results into the same upscaling oil recovery and normalized oil recovery. So, the existing upscaling method for gravity imbibition and the proposed upscaling methods are proved can be used when $N_B \geq 10$.

$$t_g = \frac{t}{\phi} \tag{3.11}$$

$$t_{d1} = \frac{t}{\phi}\left(N_B^{-1} + 1\right) \tag{3.12}$$

$$t_{d2} = \frac{t}{\phi}\left(N_B^{-0.5} + 1\right) \tag{3.13}$$

Where, t_g is simplified existing upscaling group for gravity imbibition, s; t_{d1} and t_{d2} are simplified proposed upscaling groups, s; t is imbibition time, s; ϕ is matrix porosity; N_B is Bond number.

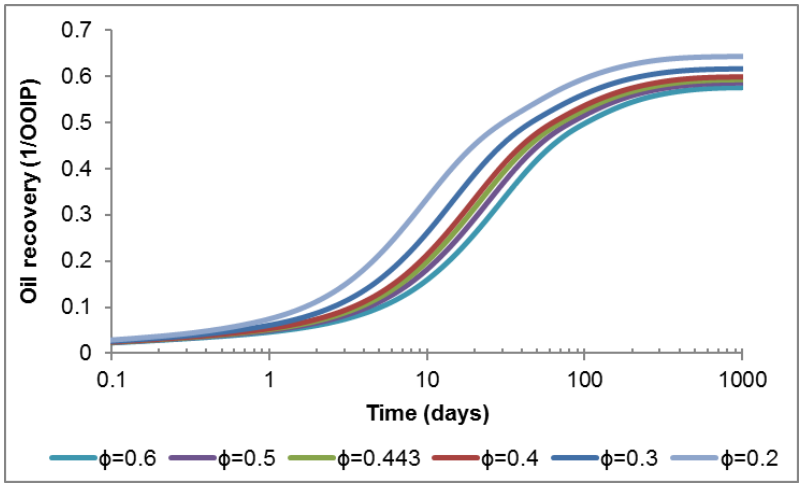

Fig. 3-31—Oil recovery of surfactant spontaneous imbibition vs. imbibition time in matrices with porosity between 0.2 and 0.6 when $N_B \geq 10$.

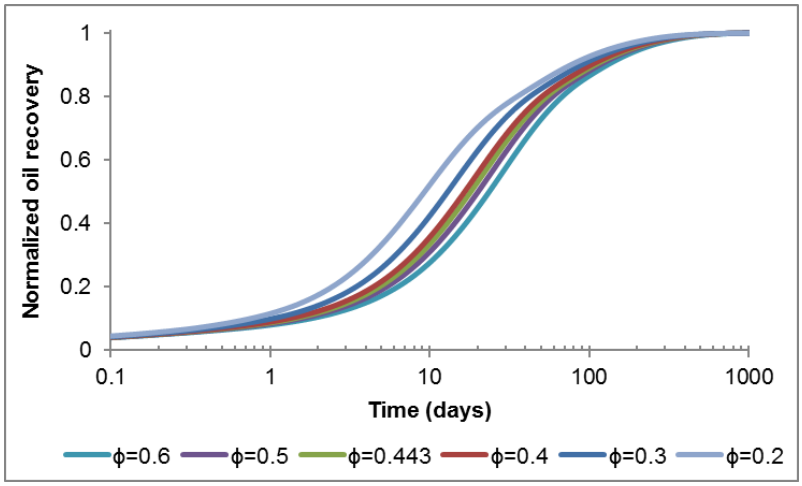

Fig. 3-32—Normalized oil recovery of surfactant spontaneous imbibition vs. imbibition time in matrices with porosity between 0.2 and 0.6 when $N_B \geq 10$.

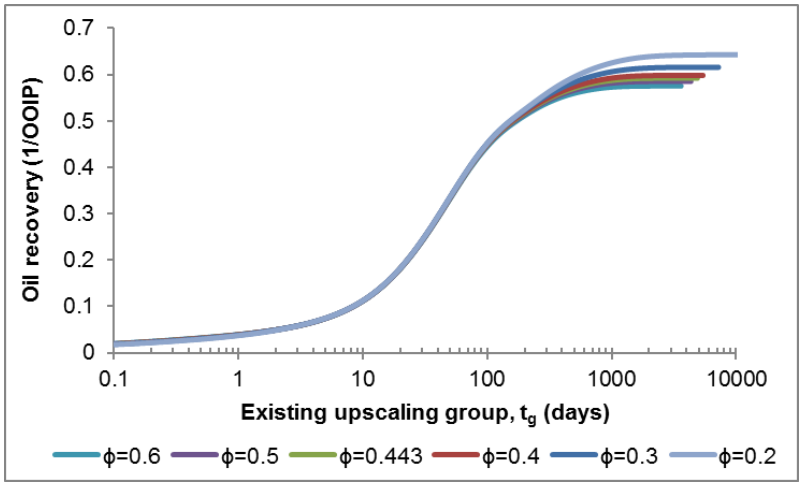

Fig. 3-33—Oil recovery of surfactant spontaneous imbibition vs. simplified existing upscaling group for gravity imbibition (t_g) in matrices with porosity between 0.2 and 0.6 when $N_B \geq 10$.

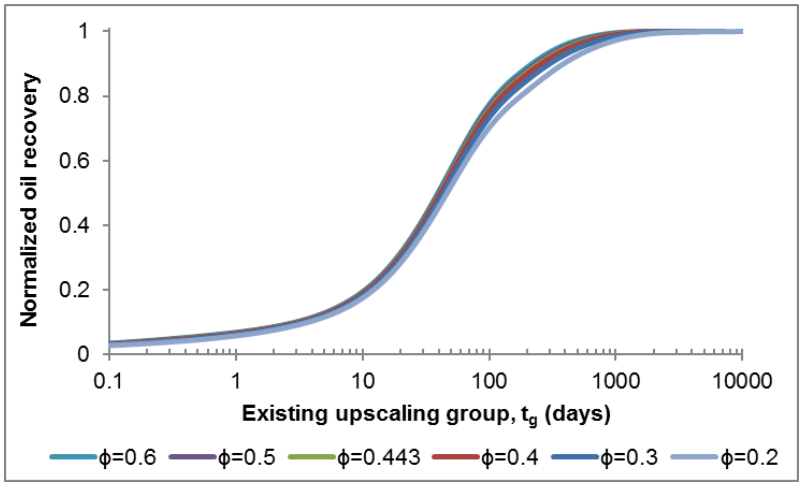

Fig. 3-34—Normalized oil recovery of spontaneous surfactant imbibition vs. simplified existing upscaling group for gravity imbibition (t_g) in matrices with porosity between 0.2 and 0.6 when $N_B \geq 10$.

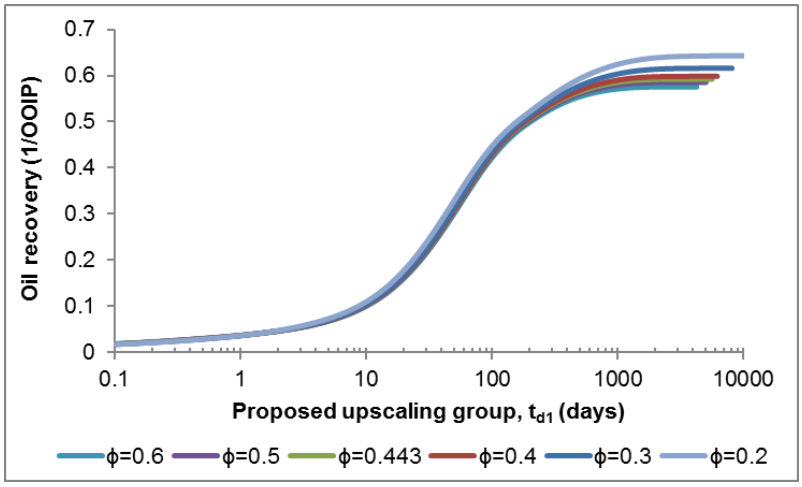

Fig. 3-35—Oil recovery of surfactant spontaneous imbibition vs. simplified proposed upscaling group (t_{d1}) in matrices with porosity between 0.2 and 0.6 when $N_B \geq 10$.

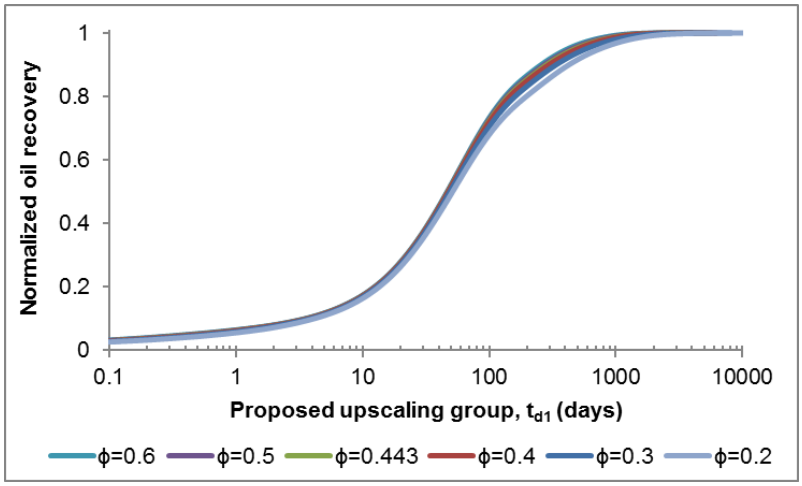

Fig. 3-36—Normalized oil recovery of surfactant spontaneous imbibition vs. simplified proposed upscaling group (t_{d1}) in matrices with porosity between 0.2 and 0.6 when $N_B \geq 10$.

$1 \leq N_B < 10$. The oil recovery and normalized oil recovery of surfactant spontaneous imbibition are shown in Fig. 3-37 and Fig. 3-38, respectively. Ultimate oil recovery and oil recovery rate are increasing with the decrease of matrix porosity. The simplified existing upscaling group for gravity imbibition (Eq. 3.11) is used to upscale the oil recovery and normalized oil recovery. The upscaling results (Fig. 3-39 and Fig. 3-40) demonstrate that the existing upscaling method for gravity imbibition can be used when $1 \leq N_B < 10$. The upscaling results of oil recovery (Fig. 3-41) and normalized oil recovery (Fig. 3-42) using the proposed upscaling group of t_{d1} (Eq. 3.12) attest that the proposed upscaling method can be used when $1 \leq N_B < 10$. The proposed upscaling group of t_{d2} gives the same upscaling results as the proposed upscaling group of t_{d1}. In conclusion, both the existing upscaling method for gravity imbibition and the proposed upscaling methods can be used when $N_B \geq 1$.

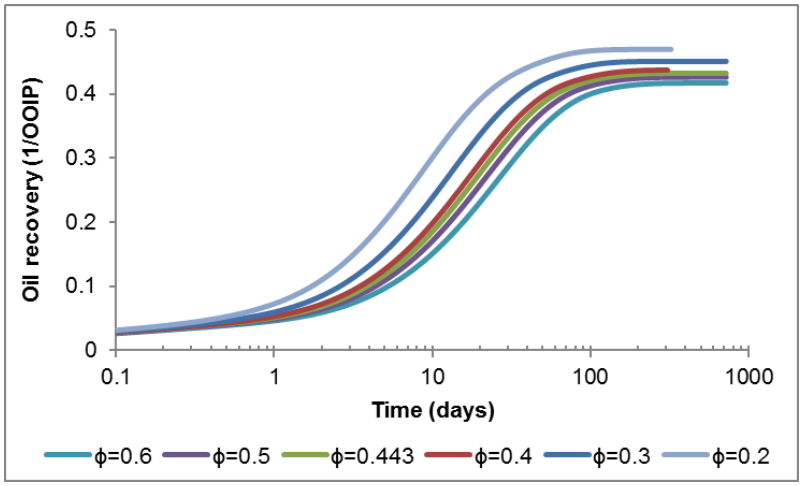

Fig. 3-37—Oil recovery of surfactant spontaneous imbibition vs. imbibition time in matrices with porosity between 0.2 and 0.6 when $1 \leq N_B < 10$.

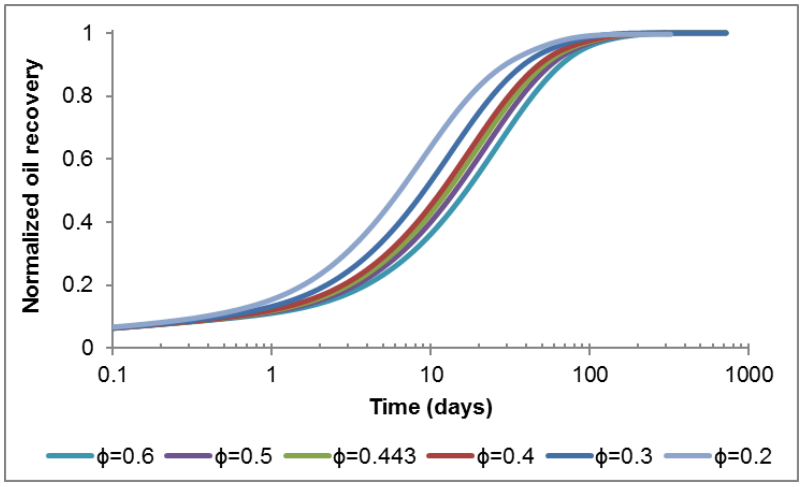

Fig. 3-38—Normalized oil recovery of surfactant spontaneous imbibition vs. imbibition time in matrices with porosity between 0.2 and 0.6 when $1 \leq N_B < 10$.

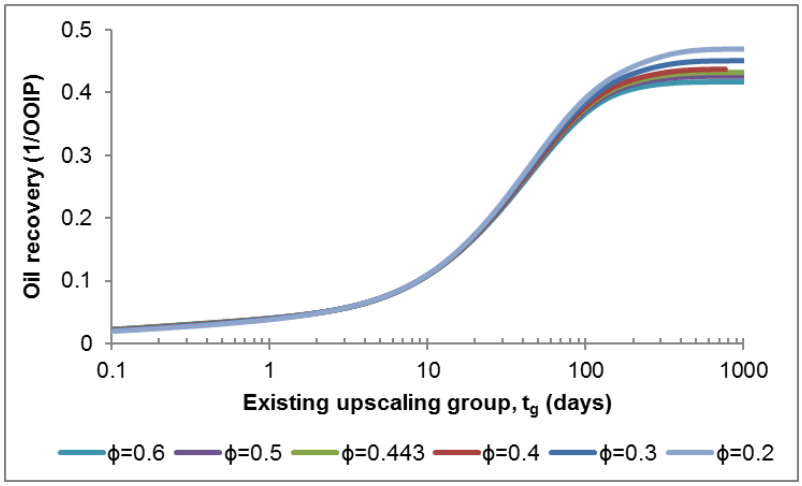

Fig. 3-39—Oil recovery of surfactant spontaneous imbibition vs. simplified existing upscaling group for gravity imbibition (t_g) in matrices with porosity between 0.2 and 0.6 when $1 \leq N_B < 10$.

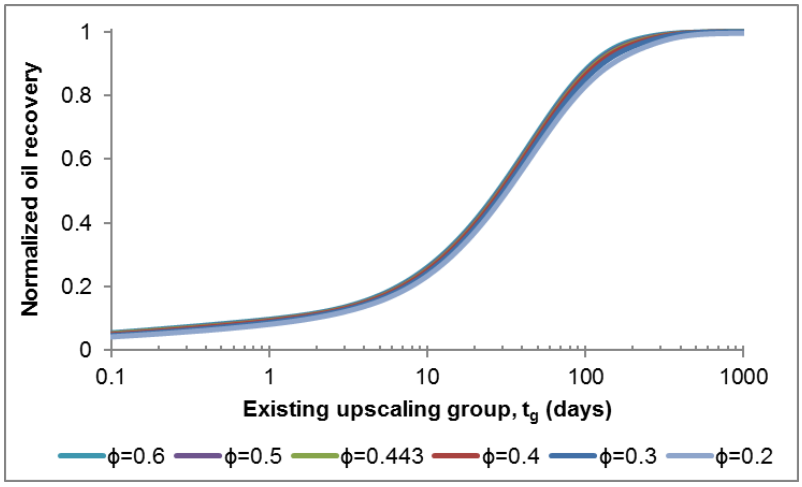

Fig. 3-40—Normalized oil recovery of surfactant spontaneous imbibition vs. simplified existing upscaling group for gravity imbibition (t_g) in matrices with porosity between 0.2 and 0.6 when $1 \leq N_B < 10$.

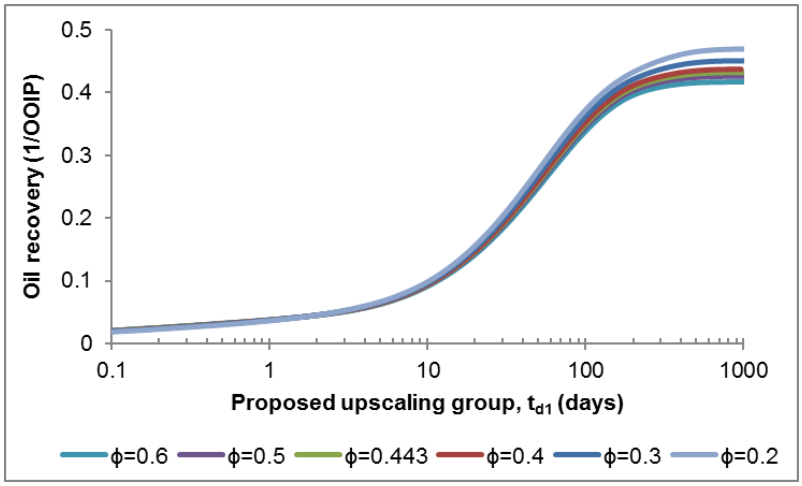

Fig. 3-41—Oil recovery of surfactant spontaneous imbibition vs. simplified proposed upscaling group (t_{d1}) in matrices with porosity between 0.2 and 0.6 when $1 \leq N_B < 10$.

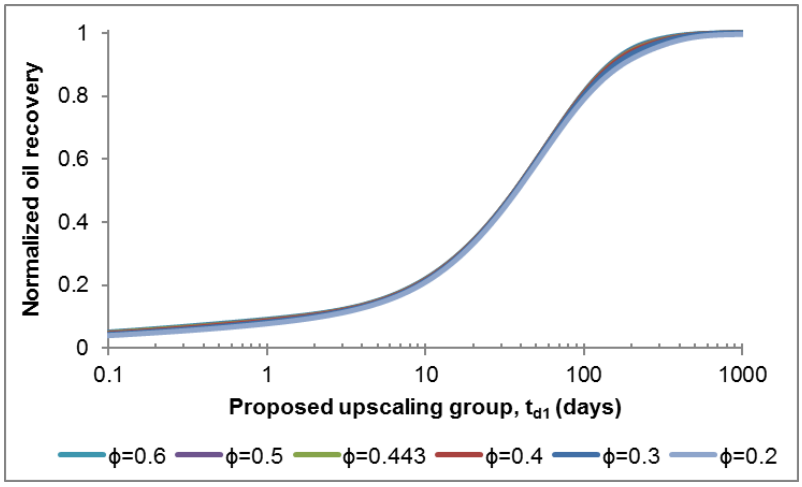

Fig. 3-42—Normalized oil recovery of surfactant spontaneous imbibition vs. simplified proposed upscaling group (t_{d1}) in matrices with porosity between 0.2 and 0.6 when $1 \leq N_B < 10$.

3.2.3.2 0.1 < N_B < 1

When IFT is reduced to 0.8 mN/m at CMC (i.e. σ_{CMC} = 0.8 mN/m) and wettability alteration coefficient is 0.6 (i.e. ω = 0.6), Bond number is between 0.1 and 1. The summary of oil recovery is listed in Table 3-8.

Table 3-8—Summary of surfactant spontaneous imbibition in matrices with porosity between 0.2 and 0.6 when 0.1 < N_B < 1.

Matrix porosity, ϕ	Bond number, N_B	Ultimate oil recovery, R_{of} (1/OOIP)	Enhanced oil recovery, EOR (1/OOIP)
0.2	0.33	0.552	0.373
0.3	0.27	0.541	0.377
0.4	0.23	0.533	0.38
0.443	0.22	0.531	0.381
0.5	0.21	0.528	0.382
0.6	0.19	0.524	0.383

The oil recovery and normalized oil recovery are shown in Fig. 3-43 and Fig. 3-44, respectively. Ultimate oil recovery is slightly increasing with the decrease of matrix porosity, but oil recovery rate is the same. To keep or improve the convergence of normalized oil recovery curves, the proposed upscaling group of t_{d1} (Eq. 3.12) is modified as Eq. 3.14 by replacing porosity (ϕ) with square root of porosity ($\phi^{0.5}$). The upscaling result of normalized oil recovery using Eq. 3.14 (Fig. 3-45) demonstrates the validity of the modified proposed upscaling group. Since Bond number is smaller than 1, which means capillary pressure is larger than gravity, the existing upscaling method for capillary imbibition (Eq. 1.25) is simplified into Eq. 3.15 and used to upscale the normalized oil recovery. The upscaling result (Fig. 3-46) shows that the existing upscaling method for capillary imbibition is not valid when 0.1 < N_B < 1.

$$t_{d1}^{*} = \frac{t}{\sqrt{\phi}}\left(N_B^{-1} + 1\right) \tag{3.14}$$

$$t_c = \frac{t}{\sqrt{\phi}} \tag{3.15}$$

Where, t_{dl}^* is simplified modified proposed upscaling group, s; t_c is simplified existing upscaling group for capillary imbibition, s; t is imbibition time, s; ϕ is matrix porosity; N_B is Bond number.

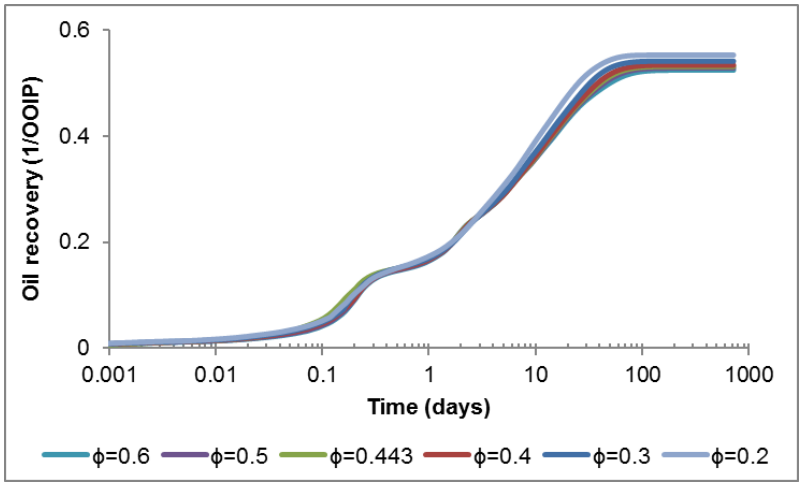

Fig. 3-43—Oil recovery of surfactant spontaneous imbibition vs. imbibition time in matrices with porosity between 0.2 and 0.6 when $0.1 < N_B < 1$.

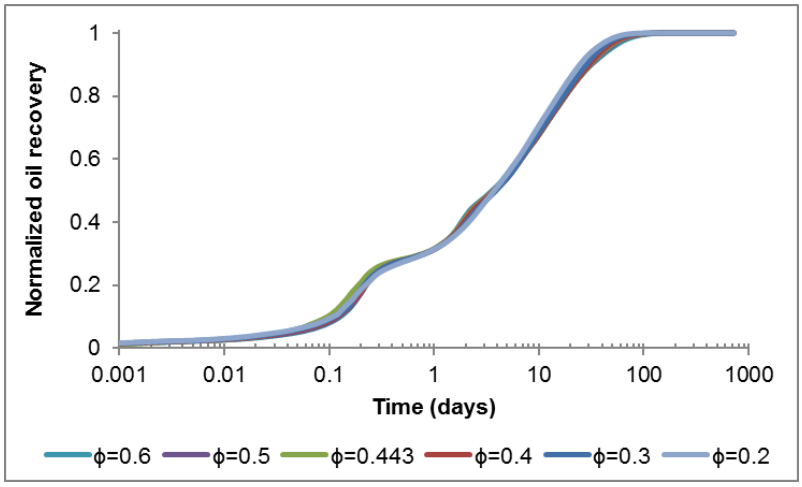

Fig. 3-44—Normalized oil recovery of surfactant spontaneous imbibition vs. imbibition time in matrices with porosity between 0.2 and 0.6 when $0.1 < N_B < 1$.

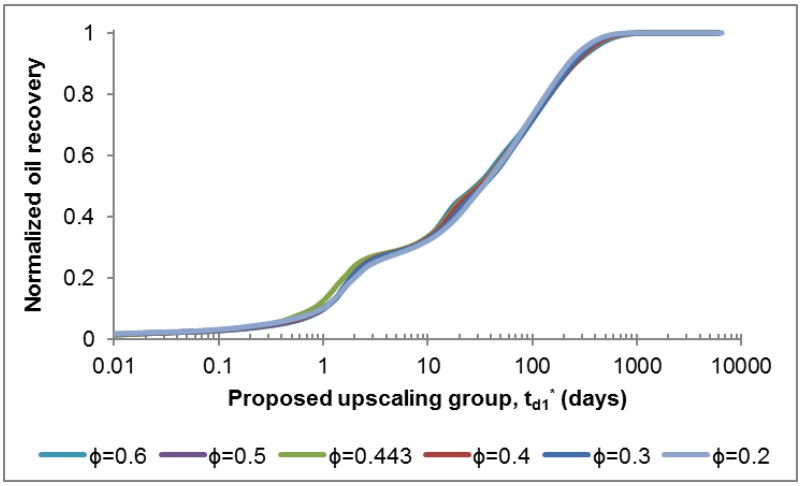

Fig. 3-45—Normalized oil recovery of surfactant spontaneous imbibition vs. simplified modified proposed upscaling group (t_{d1}^*) in matrices with porosity between 0.2 and 0.6 when $0.1 < N_B < 1$.

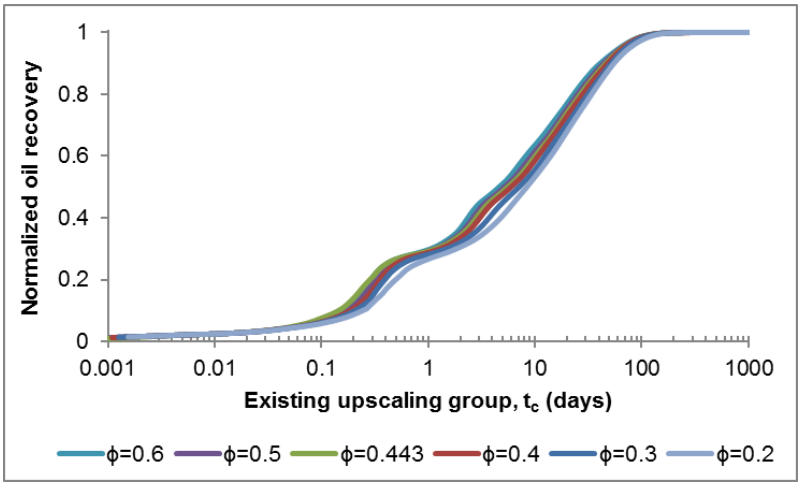

Fig. 3-46—Normalized oil recovery of surfactant spontaneous imbibition vs. simplified existing upscaling group for capillary imbibition(t_c) in matrices with porosity between 0.2 and 0.6 when $0.1 < N_B < 1$.

3.2.3.3 $N_B \leq 0.1$

When IFT is reduced to 5 mN/m at CMC (i.e. σ_{CMC} = 5 mN/m) and wettability alteration coefficient is 0.8 (i.e. ω = 0.8), Bond number is between 0.05 and 0.1 when matrix porosity is in the range of 0.2 to 0.6. The summary of the results is in Table 3-9.

Table 3-9—Summary of surfactant spontaneous imbibition in matrices with porosity between 0.2 and 0.6 when $N_B \leq 0.1$.

Matrix porosity, ϕ	Bond number, N_B	Ultimate oil recovery, R_{of} (1/OOIP)	Enhanced oil recovery, EOR (1/OOIP)
0.2	0.1	0.428	0.248
0.3	0.081	0.423	0.259
0.4	0.07	0.419	0.266
0.443	0.067	0.418	0.268
0.5	0.063	0.417	0.27
0.6	0.058	0.415	0.274

Fig. 3-47 and Fig. 3-48 show that the oil recovery and normalized oil recovery are almost the same for all the cases with different matrix porosity. So the simplified proposed upscaling method of t_{d2} is modified as Eq. 3.16 by removing porosity (ϕ) and then used as the upscaling group. The upscaling result of normalized oil recovery (Fig. 3-49) demonstrates the validity of the modified proposed upscaling group (Eq. 3.16). However, the upscaling result of normalized oil recovery using the simplified upscaling group for capillary imbibition (Eq. 3.15) (Fig. 3-50) tells that the existing upscaling method for capillary imbibition cannot be used when $N_B \leq 0.1$.

$$t_{d2}^{*} = t\left(N_B^{-0.5} + 1\right) \tag{3.16}$$

Where, t_{d2}^{*} is simplified modified proposed upscaling group, s; t is time, s; N_B is Bond number.

In conclusion, when only matrix porosity is varying, the existing upscaling group for gravity imbibition can be used for the cases with $N_B \geq 1$. The modified proposed upscaling group of

t_{d1}^* is valid when $0.1 < N_B < 1$. And the modified proposed upscaling group of t_{d2}^* is the upscaling group for the cases with $N_B \leq 0.1$.

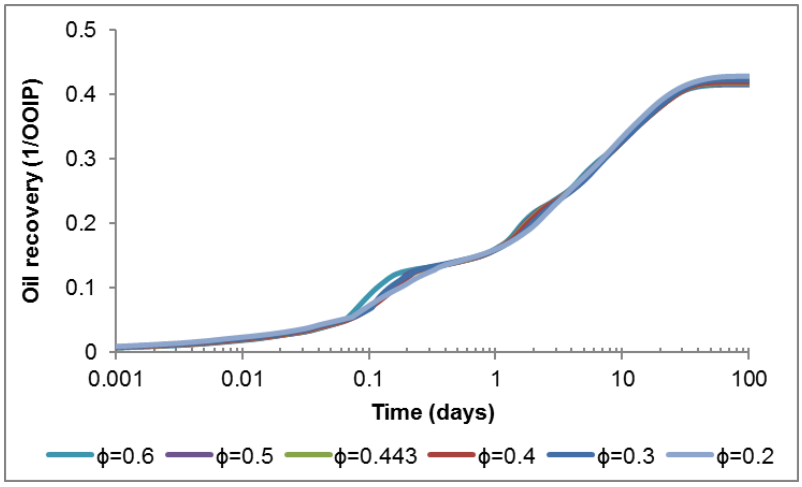

Fig. 3-47—Oil recovery of surfactant spontaneous imbibition vs. imbibition time in matrices with porosity between 0.2 and 0.6 when $N_B \leq 0.1$.

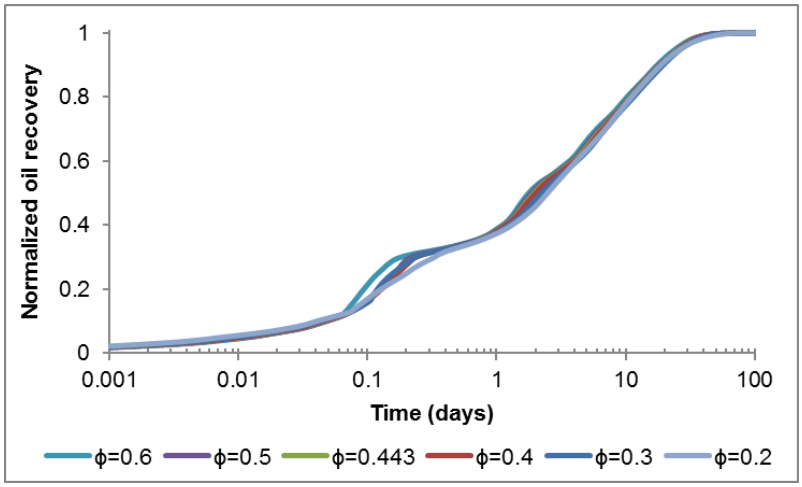

Fig. 3-48—Normalized oil recovery of surfactant spontaneous imbibition vs. imbibition time in matrices with porosity between 0.2 and 0.6 when $N_B \leq 0.1$.

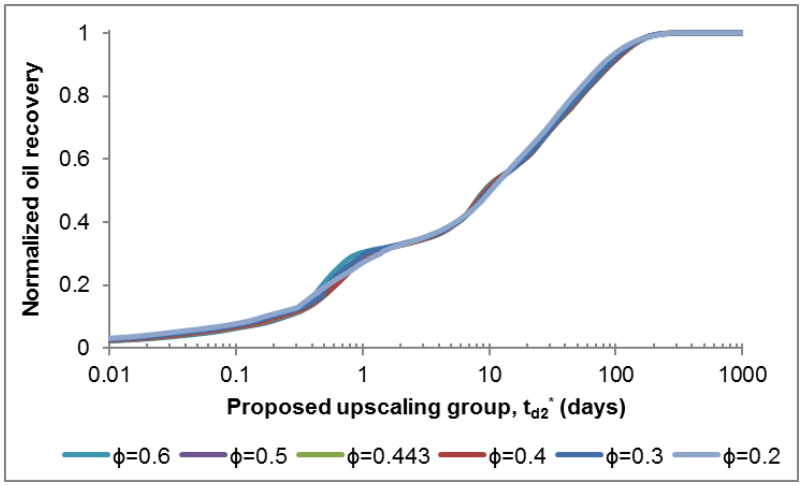

Fig. 3-49—Normalized oil recovery of surfactant spontaneous imbibition vs. simplified modified proposed upscaling group (t_{d2}^*) in matrices with porosity between 0.2 and 0.6 when $N_B \leq 0.1$.

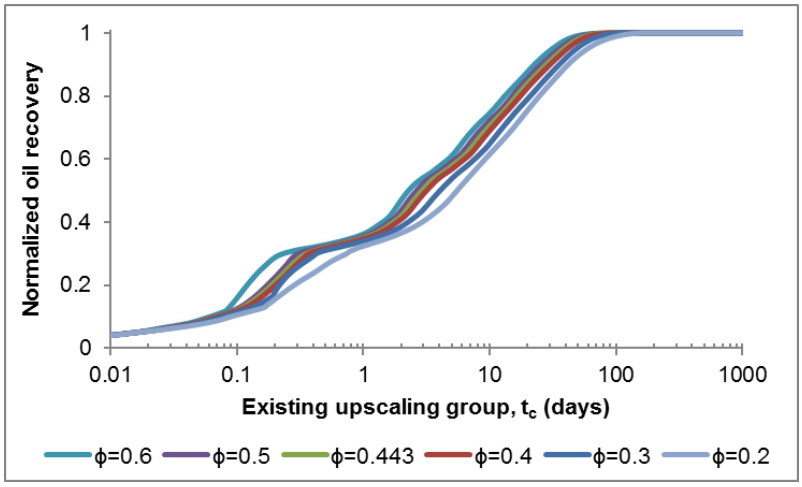

Fig. 3-50—Normalized oil recovery of surfactant spontaneous imbibition vs. simplified existing upscaling group for capillary imbibition (t_c) in matrices with porosity between 0.2 and 0.6 when $N_B \leq 0.1$.

3.3 Matrix block size

Matrix block size has effect on gravity force, thus affects the imbibition process. In the base case, the length of the matrix is 3.4 cm, and the height is 4.6 cm. The matrix is put in a container filled with brine or surfactant solution with concentration of 0.01 g/cm^3. To study the effect of matrix block size, the length and height of the matrix is multiplied by an increase factors (α) of 0.5, 2, 5, and 10 separately, so that the matrix length is varying from 1.7 to 34 cm, and the matrix height is varying from 2.3 to 46 cm. The increase of matrix height leads to an increase of gravity force. Thus Bond number (Eq. 3.17) is increasing with the increase of the matrix height.

$$N_B = \frac{\Delta\rho g H}{P_c^{ww} - \omega\left(P_c^{ww} - P_c^i\right)}\frac{\sigma_i}{\sigma_{CMC}} = \frac{\alpha\Delta\rho g H^0}{P_c^{ww} - \omega\left(P_c^{ww} - P_c^i\right)}\frac{\sigma_i}{\sigma_{CMC}} = \alpha N_B^0 \qquad (3.17)$$

Where, N_B is Bond number; N_B^0 is the reference Bond number; α is matrix block size increase factor; Δρ is density difference, g/cm^3; g is gravity, 9.8 mN/g; H is matrix length, cm; H^0 is the reference matrix length, cm; P_c^{ww} is capillary pressure when the wettability is changed to strongly water-wet, atm; P_c^i is the initial capillary pressure, atm; ω is wettability alteration coefficient; σ_i is the initial water/oil IFT, mN/m; σ_{CMC} is water/oil IFT at CMC, mN/m.

The relationship between increase factor of matrix block size and the ultimate oil recovery of surfactant imbibition is plotted in Fig. 3-51, and it shows that ultimate oil recovery does not change with matrix block size when the wettability is strongly water-wet (i.e. ω = 0). For the case under the conditions of ω = 1 and σ_{CMC} = 0.154 mN/m, the ultimate oil recovery from the matrix with height of 46 cm is about 32% OOIP more than the ultimate oil recovery from the matrix with height of 2.3 cm. Fig. 3-51 implies that matrix block size has more significant effect on surfactant imbibition when matrix wettability is less water-wet.

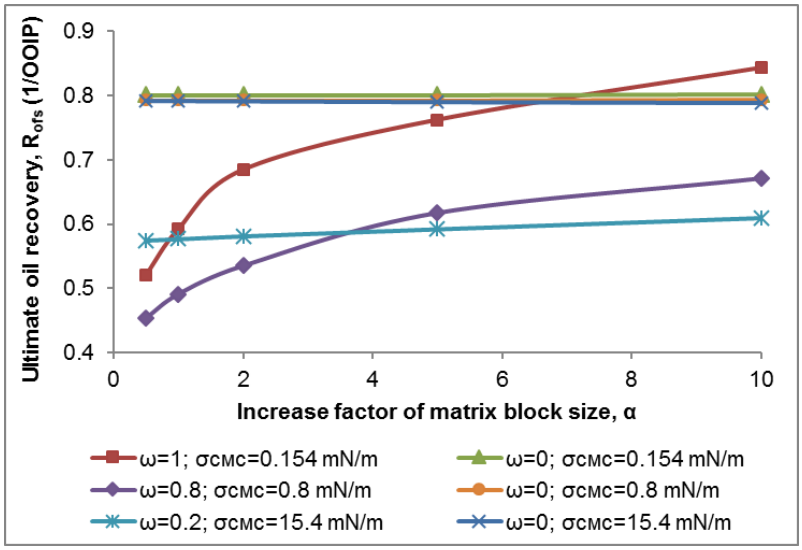

Fig. 3-51—The relationship between increase factor of matrix block size and ultimate oil recovery of surfactant spontaneous imbibition.

3.3.1 Brine spontaneous imbibition

The summary of the brine spontaneous imbibition is listed in Table 3-10. The required imbibition time to recover the same amount of normalized oil recovery is increasing with the increase of matrix block size. The oil recovery of brine imbibition (Fig. 3-52) shows that with the increase of matrix block size, ultimate oil recovery has a dramatic increase, which is because when the total force of gravity force and capillary force is zero, the water saturation in matrix is higher in the larger matrix. But the oil recovery rate (Fig. 3-53) is decreasing with the increase of matrix block size because it takes more time for the oil and water to move through the matrix. The ultimate oil recovery has a power function relation with the increase factor of matrix block size (Fig. 3-54). Assume that when the oil recovery is 95% of ultimate oil recovery (i.e. R_{on} = 0.95), the imbibition process should be ended considering the economics. Then the required time to recover 95% of ultimate oil recovery is regarded as the final imbibition time. Fig. 3-55 tells that the increase factor of final imbibition time (β) (Eq. 3.18) has a power function relation with the increase factor of matrix block size (α), which implies that the final imbibition time is increasing as a power function of the increase of the matrix block size.

$$\beta = \frac{t(\alpha)}{t(1)} \tag{3.18}$$

Where, β is the increase factor of imbibition time, fraction; t(α) is imbibition time when the matrix block size of the base case is increased by α times, s. t(1) is imbibition time at the base case (α = 1), s.

Table 3-10—Summary of brine spontaneous imbibition in matrices with different sizes.

Increase factor, α	Height, H (cm)	Bond number, N_B	Ultimate oil recovery of brine imbibition, R_{ofw} (1/OOIP)	Time (days)	
				50% R_{ofw}	95% R_{ofw}
0.5	2.3	0.1	0.12	0.7	7.6
1	4.6	0.2	0.15	3	26.4
2	9.2	0.4	0.206	11.7	78.3
5	23	1	0.303	48	261
10	46	2	0.37	113.8	583

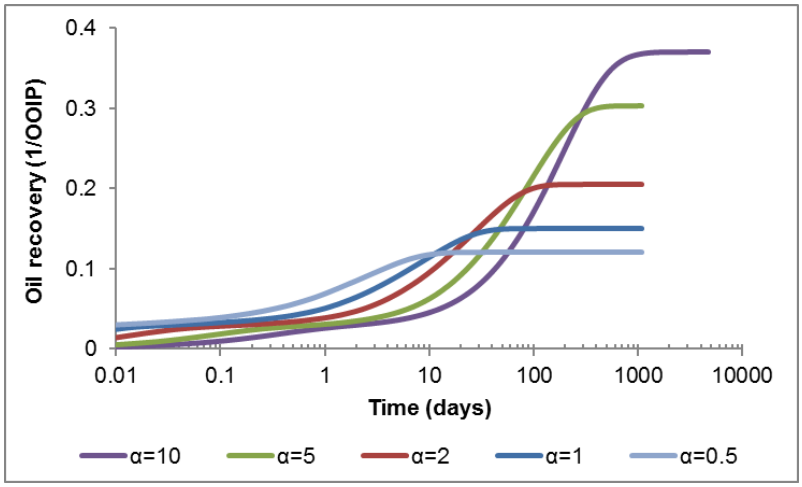

Fig. 3-52—Oil recovery of brine spontaneous imbibition from matrices with different sizes.

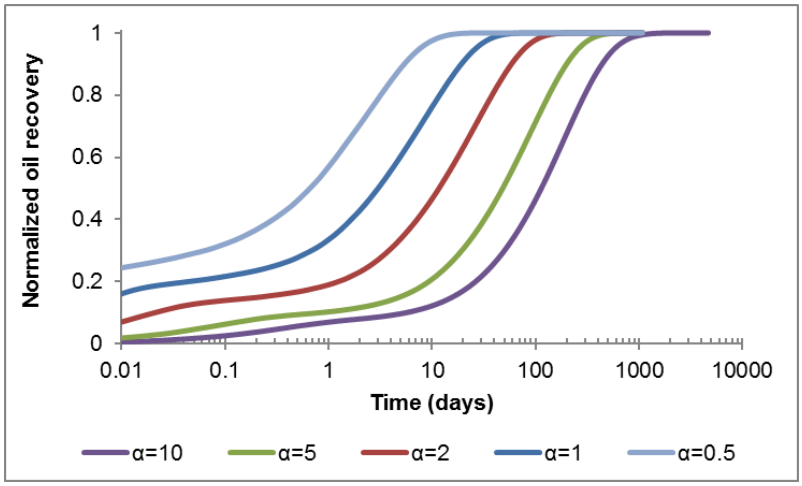

Fig. 3-53—Normalized oil recovery of brine spontaneous imbibition from matrices with different sizes.

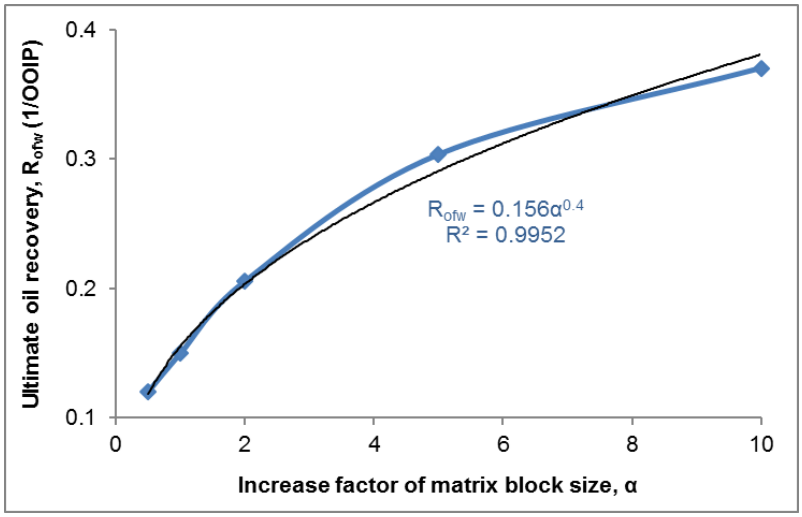

Fig. 3-54—The relationship between increase factor of matrix block size and ultimate oil recovery of brine spontaneous imbibition.

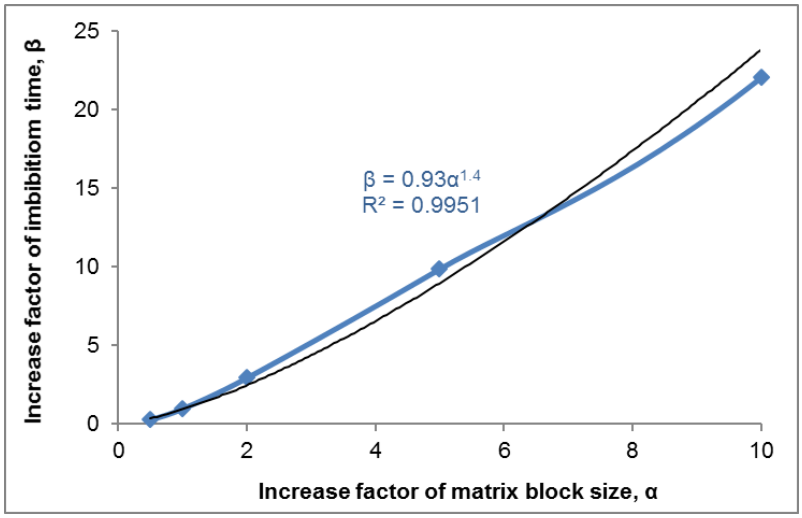

Fig. 3-55—The relationship between increase factor of matrix block size and increase factor of required imbibition time of brine spontaneous imbibition.

3.3.2 Surfactant spontaneous imbibition

In the base case of surfactant imbibition, water/oil IFT is reduced to 0.8 mN/m at CMC (i.e. σ_{CMC} = 0.8 mN/m) and wettability is altered to strongly water-wet (i.e. ω = 0). Bond number is changing from 0.05 to 0.9 with the increase of matrix block size by factors from 0.5 to 10. The summary of surfactant spontaneous imbibition is listed in Table 3-11. It shows that when the wettability is strongly water-wet, ultimate oil recovery is the same for all the cases, the reason is when wettability is changed to strongly water-wet, capillary pressure is positive until the residual oil saturation. But surfactant enhanced oil recovery is decreasing the increase of matrix block size. Fig. 3-56 shows that oil recovery rate is slower in a larger matrix. The increase of final imbibition time has a positive power function relation with the increase of matrix block size (Fig. 3-57).

Table 3-11—Summary of surfactant spontaneous imbibition in matrices with different block sizes under the conditions of σ_{CMC} = 0.8 mN/m and ω = 0.

Increase factor, α	Height, H (cm)	Bond number, N_B	Ultimate oil recovery, R_{ofs} (1/OOIP)	Enhanced oil recovery, EOR (1/OOIP)
0.5	2.3	0.05	0.793	0.672

Increase factor, α	Height, H (cm)	Bond number, N_B	Ultimate oil recovery, R_{ofs} (1/OOIP)	Enhanced oil recovery, EOR (1/OOIP)
1	4.6	0.09	0.793	0.643
2	9.2	0.2	0.793	0.587
5	23	0.5	0.793	0.489
10	46	0.9	0.793	0.423

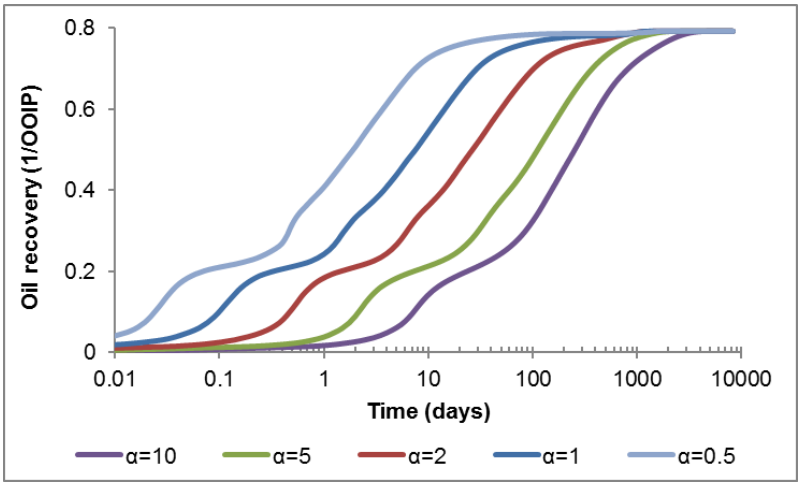

Fig. 3-56—Oil recovery of surfactant spontaneous imbibition vs. imbibition time in matrices with different block sizes in the base case.

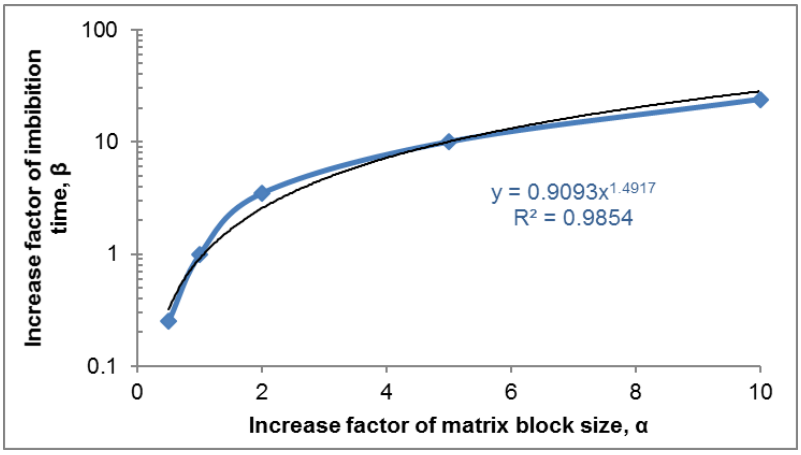

Fig. 3-57—The relationship between increase factor of matrix block size and increase factor of final imbibition time in the base case.

3.3.3 Matrix block size effect on upscaling methods of surfactant imbibition

When IFT is reduced to 0.8 mN/m at CMC (i.e. σ_{CMC} = 0.8 mN/m) and wettability is kept oil-wet (i.e. ω = 1), Bond number is bigger than 1 for the matrix with height between 2.3 and 46 cm (Table 3-12). When IFT is reduced to 0.8 mN/m at CMC (i.e. σ_{CMC} = 0.8 mN/m) and wettability is changed to strongly water-wet (i.e. ω = 0), Bond number is between 0.1 and 1 for the matrix with height between 4.6 and 46 cm (Table 3-11). When IFT is kept constant (i.e. σ_{CMC} = 15.4 mN/m) and wettability is altered with the coefficient of 0.5 (i.e. ω = 0.5), Bond number is smaller than 0.1 for the matrix with height between 2.3 and 46 cm (Table 3-12). The existing and proposed upscaling methods of surfactant imbibition are studied in these cases.

Table 3-12—Summary of surfactant spontaneous imbibition in matrices with different sizes.

Cases	Increase factor, α	Bond number, N_B	Ultimate oil recovery, R_{ofs} (1/OOIP)	Enhanced oil recovery, EOR (1/OOIP)
ω = 1; σ_{CMC} = 0.8 mN/m; $N_B \geq 1$	0.5	1.8	0.365	0.245
	1	4	0.432	0.282
	2	7	0.496	0.29
	5	18	0.585	0.281
	10	37	0.68*	0.31
ω = 0.5; σ_{CMC} = 15.4 mN/m; $N_B \leq 0.1$	0.5	0.005	0.521	0.4
	1	0.009	0.592	0.442
	2	0.02	0.685	0.479
	5	0.05	0.762	0.456
	10	0.09	0.843*	0.483

*the value is calculated based on the known ultimate oil recovery.

3.3.3.1 $N_B \geq 1$

When IFT is reduced to 0.8 mN/m at CMC (i.e. σ_{CMC} = 0.8 mN/m), and the wettability is oil-wet (i.e. ω = 1), Bond number is larger than 1. Oil recovery and normalized oil recovery of surfactant spontaneous imbibition are shown in Fig. 3-58 and Fig. 3-59, respectively, which tell

that ultimate oil recovery is higher in a bigger matrix, but oil is recovered faster in a smaller matrix.

Since gravity force is larger than capillary force, the existing upscaling method for gravity imbibition (Eq. 1.34) is tested. The simplified upscaling group for gravity imbibition (Eq. 3.19) is obtained by removing the constants in Eq. 1.34. Both oil recovery and normalized oil recovery are well upscaled with the simplified upscaling group for gravity imbibition (Fig. 3-60 and Fig. 3-61). Therefore, the existing upscaling group for gravity imbibition is applicable when $N_B \geq 1$. The proposed upscaling method of t_{D1} (Eq. 2.13) can be simplified into Eq. 3.20. Since all the faces of the matrix are open to surfactant solution, characteristic length (L_c) is calculated with Eq. 3.21. The upscaling result of normalized oil recovery using Eq. 3.20 is shown in Fig. 3-62, which proves that the proposed upscaling method of t_{D1} can be used when $N_B \geq 1$.

$$t_g = \frac{t}{H} \tag{3.19}$$

$$t_{d1} = t\frac{H}{L_c^2}\left(N_B^{-1} + 1\right) \tag{3.20}$$

$$L_c = \frac{LH}{\sqrt{4L^2 + 8H^2}} \tag{3.21}$$

Where, t_g is simplified existing upscaling group for gravity imbibition, s/cm; t_{d1} is simplified proposed upscaling group, s/cm; t is imbibition time, s; H is matrix height, cm; L_c is characteristic length, cm; N_B is Bond number; L is matrix length, cm.

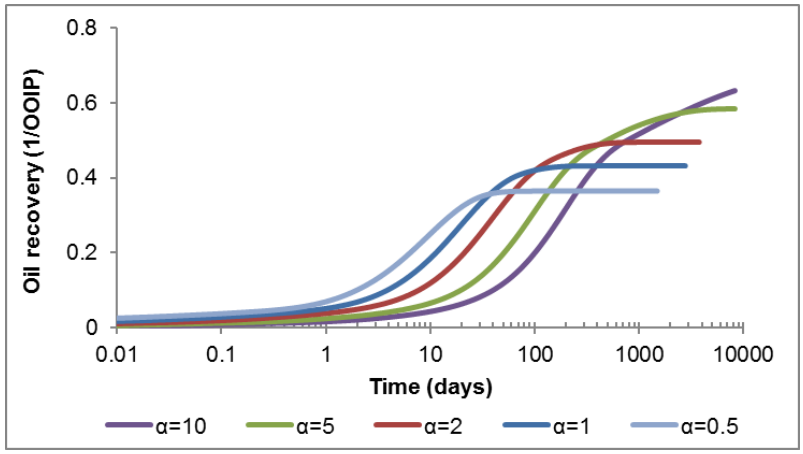

Fig. 3-58—Oil recovery of surfactant spontaneous imbibition vs. imbibition time in matrices with different block sizes when $N_B \geq 1$.

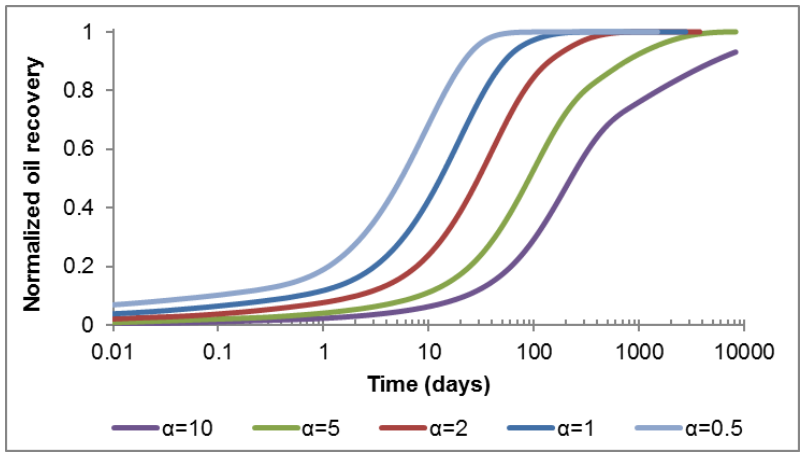

Fig. 3-59—Normalized oil recovery of surfactant spontaneous imbibition vs. imbibition time in matrices with different block sizes when $N_B \geq 1$.

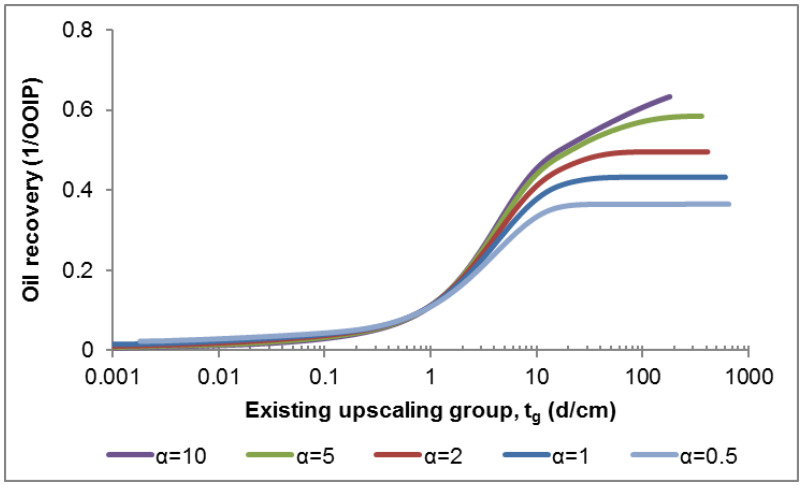

Fig. 3-60—Oil recovery of surfactant spontaneous imbibition vs. simplified existing upscaling group for gravity imbibition (t_g) in matrices with different block sizes when $N_B \geq 1$.

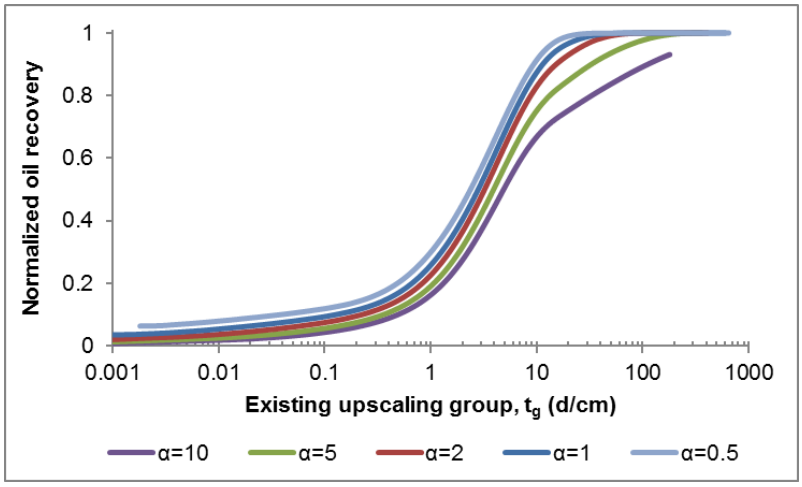

Fig. 3-61—Normalized oil recovery of surfactant spontaneous imbibition vs. simplified existing upscaling group for gravity imbibition (t_g) in matrices with different block sizes when $N_B \geq 1$.

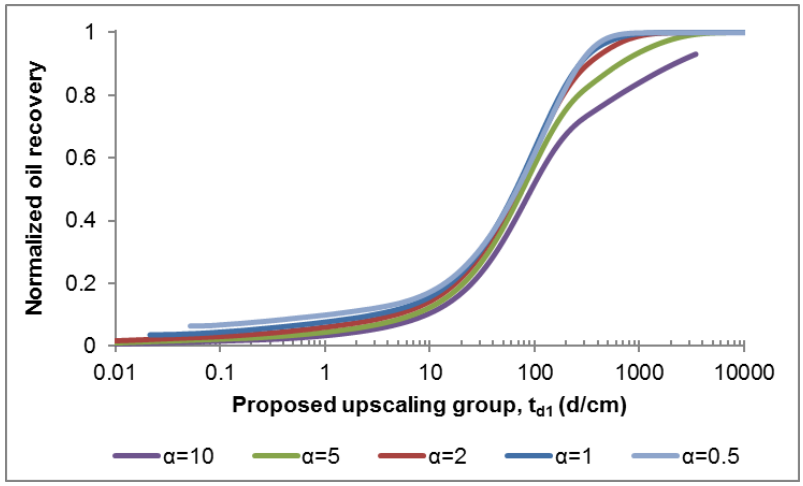

Fig. 3-62—Normalized oil recovery of surfactant spontaneous imbibition vs. simplified proposed upscaling group (t_{d1}) in matrices with different block sizes when $N_B \geq 1$.

3.3.3.2 $0.1 < N_B < 1$

In section 3.3.2, Bond number is between 0.1 and 1 when matrix height is changing between 4.6 and 46 cm (i.e. $1 \leq \alpha \leq 10$). Since the ultimate oil recovery is the same for all the matrix block sizes, oil recovery is not normalized, and the upscaling groups are used for upscaling of oil recovery. Capillary force is larger than gravity force, so the existing upscaling method for capillary imbibition is simplified into Eq. 3.22 and used to upscale the oil recovery. However, the upscaling result (Fig. 3-63) is not satisfactory. The simplified proposed upscaling group of t_{d1} (Eq. 3.20) could improve the upscaling of oil recovery (Fig. 3-64). So, the validity of the proposed upscaling group of t_{d1} for the case with $0.1 < N_B < 1$ is confirmed.

$$t_c = \frac{t}{L_c^2} \tag{3.22}$$

Where, t_c is simplified existing upscaling group for capillary imbibition, s/cm^2; t is imbibition time, s; L_c is characteristic length, cm.

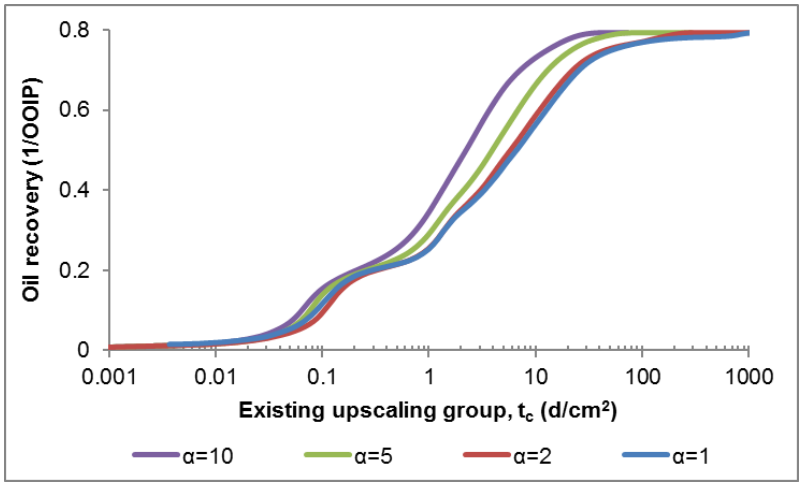

Fig. 3-63—Oil recovery of surfactant spontaneous imbibition vs. simplified existing upscaling group for capillary imbibition (t_c) in matrices with different block sizes when $0.1 < N_B < 1$.

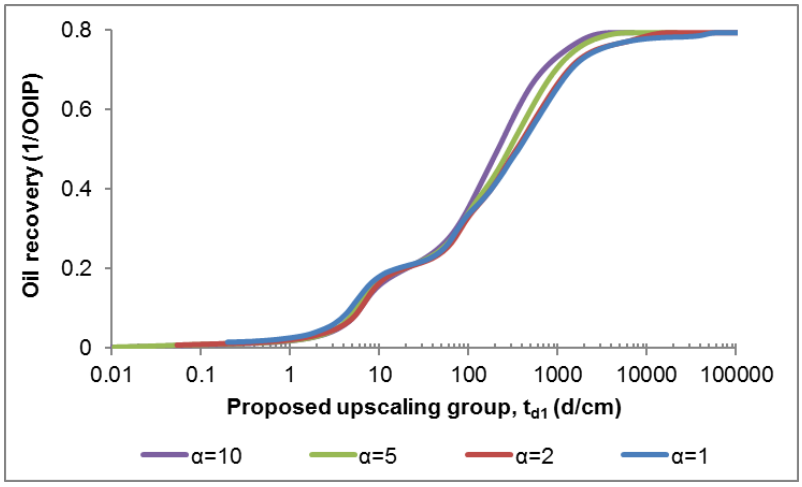

Fig. 3-64—Oil recovery of surfactant spontaneous imbibition vs. simplified proposed upscaling group (t_{d1}) in matrices with different block sizes when $0.1 < N_B < 1$.

3.3.3.3 $N_B \leq 0.1$

In this section, IFT at CMC is 15.4 mN/m at CMC (i.e. σ_{CMC} = 15.4 mN/m), and wettability alteration coefficient is 0.5 (i.e. ω = 0.5). Bond number is smaller than 0.1, so the dominating force is capillary force. The oil recovery and normalized oil recovery are shown in Fig. 3-65 and Fig. 3-66, respectively, which tell that ultimate oil recovery is slightly increasing with the increase of matrix block size, and oil recovery rate is increasing with the decrease of matrix block size.

The simplified existing upscaling group for capillary imbibition (Eq. 3.22) is applied to upscale the normalized oil recovery, which gives a good result (Fig. 3-67). The simplified proposed upscaling group of t_{dl} (Eq. 3.20) leads to a similar result (Fig. 3-68). So both the existing upscaling method for capillary imbibition of t_{Dc} (Eq. 1.25) and the proposed upscaling method of t_{D1} (Eq. 2.13) could be used when $N_B \leq 0.1$.

In conclusion, the existing upscaling method for gravity imbibition could be used when $N_B \geq 1$, and the existing upscaling method for capillary imbibition can be used when $N_B \leq 0.1$, but it does not give a satisfactory upscaling result when $0.1 < N_B < 1$. The proposed upscaling method of t_{D1} could be used for all the cases.

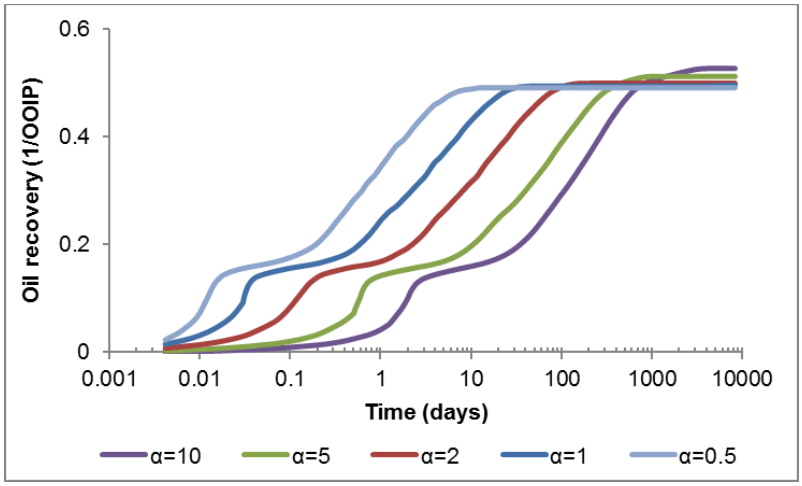

Fig. 3-65—Oil recovery of surfactant spontaneous imbibition vs. imbibition time in matrices with different block sizes when $N_B \leq 0.1$.

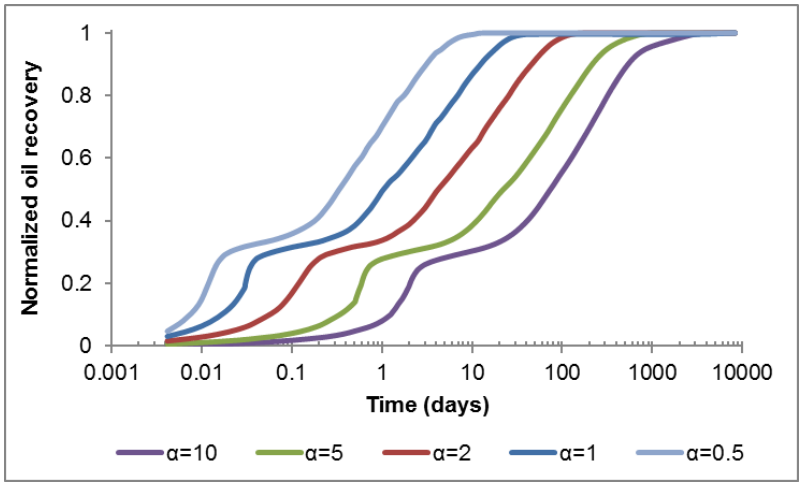

Fig. 3-66—Normalized oil recovery of surfactant spontaneous imbibition vs. imbibition time in matrices with different block sizes when $N_B \leq 0.1$.

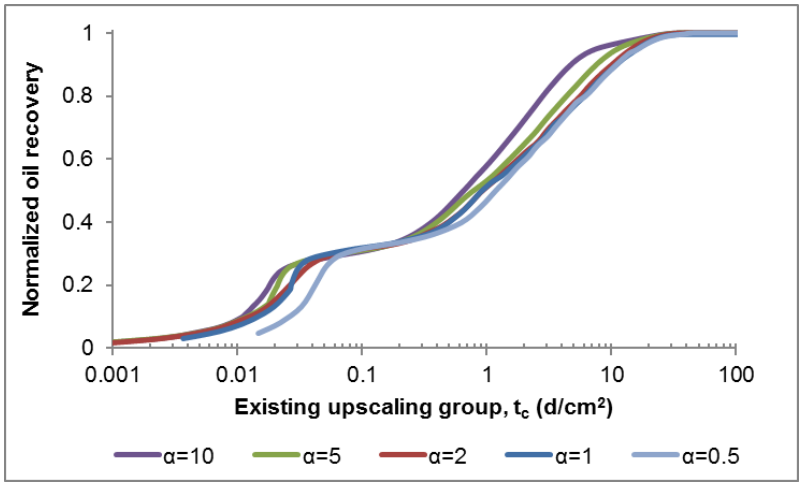

Fig. 3-67—Normalized oil recovery of surfactant spontaneous imbibition vs. simplified existing upscaling group for capillary imbibition (t_c) in matrices with different block sizes when $N_B \leq 0.1$.

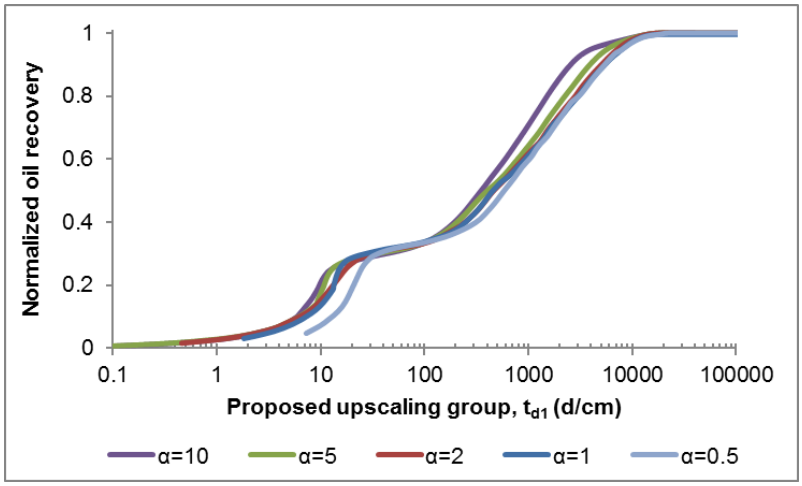

Fig. 3-68—Normalized oil recovery of surfactant spontaneous imbibition vs. simplified proposed upscaling group (t_{d1}) in matrices with different block sizes when $N_B \leq 0.1$.

3.4 Summary

1. When only matrix permeability is varying, the oil recovery rate and ultimate oil recovery of brine and surfactant spontaneous imbibition are increasing with the increase of matrix permeability.
2. When only matrix permeability is varying, Bond number is increasing with the increase of permeability. When only matrix porosity is varying, Bond number is decreasing with the increase of porosity.
3. When only matrix permeability or porosity is varying, with the increase of Bond number, ultimate oil recovery of surfactant spontaneous imbibition is generally increasing, and the increase of ultimate oil recovery is larger when Bond number is bigger. But when wettability is changed to strongly water-wet (i.e. $\omega = 0$), ultimate oil recovery does not have significant increase.
4. When only the matrix permeability or porosity is varying, with the increase of Bond number, surfactant EOR is reducing and then increasing. The turning point of the trend occurs around the Bond number of 1.

5. The oil recovery rate is decreasing with the increase of matrix block size both for brine spontaneous imbibition and surfactant spontaneous imbibition. When matrix wettability is changed to strongly water-wet (i.e. ω = 0), the ultimate oil recovery is the same (i.e. about 80% OOIP) for all the matrices with different sizes. But when wettability alteration coefficient is bigger than 0, the increase of matrix block size results in an increase of ultimate oil recovery.
6. The upscaling methods used for the cases with varying permeability, porosity or matrix block size are shown in Table 3-13.
7. The existing upscaling methods for capillary imbibition and gravity imbibition, and the proposed upscaling methods are expressed in Eq. 1.25, Eq. 1.34, Eq. 2.13 and Eq. 2.16, respectively.

$$t_{Dc} = t\sqrt{\frac{K}{\phi}}\frac{\sigma}{\sqrt{\mu_w \mu_o}\,L_c^2} \tag{1.25}$$

$$t_{Dg} = \frac{K\Delta\rho}{\phi\mu_o L}t \tag{1.34}$$

$$t_{D1} = t\frac{K\Delta\rho g H}{\phi\mu L_c^2}\left(N_B^{-1}+1\right) \tag{2.13}$$

$$t_{D2} = t\frac{K\Delta\rho g H}{\phi\mu L_c^2}\left(N_B^{-0.5}+1\right) \tag{2.16}$$

Table 3-13—Summary of upscaling groups of surfactant spontaneous imbibition and the application conditions.

Matrix property	Conditions	Equations
1.5 ≤ K ≤ 600 mD	$N_B \geq 1$	Eq. 1.34, Eq. 2.13, and Eq. 2.16
	$0.1 < N_B < 1$	Eq. 2.13
	$N_B \leq 0.1$	Eq. 1.25, and Eq. 2.13

Matrix property	Conditions	Equations
$0.2 \le \phi \le 0.6$	$N_B \ge 1$	Eq. 1.34, Eq. 2.13, and Eq. 2.16
	$0.1 < N_B < 1$	$t_{d1}^{*} = \frac{t}{\sqrt{\phi}}\left(N_B^{-1} + 1\right)$ (Eq. 3.14)
	$N_B \le 0.1$	$t_{d2}^{*} = t\left(N_B^{-0.5} + 1\right)$ (Eq. 3.16)
$0.5 \le \alpha \le 10$	$N_B \ge 1$	Eq. 1.34, Eq. 2.13, and Eq. 2.16
	$N_B < 1$	Eq. 2.13

4 Effect of surfactant properties on surfactant spontaneous imbibition

Surfactant imbibition is affected by viscosity of surfactant solution, surfactant concentration in the solution, surfactant adsorption concentration on the rock, and surfactant diffusion. In this chapter, the effect of these surfactant properties on surfactant spontaneous imbibition is analyzed, and upscaling methods for some of these properties are given.

4.1 Viscosity of surfactant solution

The application of surfactant may increase brine viscosity. If use polymer at the same time or change the salinity of surfactant solution, the viscosity of surfactant solution could be higher. In the base case, brine viscosity is 0.8 cP, and the surfactant concentration is 0.01 g/cm^3 in the surfactant solution. IFT at CMC is 0.8 mN/m (i.e. σ_{CMC} = 0.8 mN/m) and wettability can be changed to strongly water-wet (i.e. $\omega = 0$). To study the effect of viscosity of surfactant solution on surfactant spontaneous imbibition, I assume that the surfactant solution with surfactant concentration of 0.01 g/cm^3 may be 0.8 cP, 1.6 cP, 4 cP and 8 cP. And it is assumed in Eclipse that surfactant only exists in water phase.

Fig. 4-1 shows that the viscosity of surfactant solution almost has no effect on oil recovery of surfactant spontaneous imbibition. The ultimate oil recovery is the same for all the cases with different viscosity since the ultimate oil recovery depends on the wettability alteration and IFT reduction if the surfactant could sweep the whole matrix. The oil recovery rate slightly reduces when the viscosity is increased, which is because that brine with higher viscosity moves slower in matrix. In conclusion, viscosity of surfactant solution does not have important effect on surfactant spontaneous imbibition, so that the water viscosity which is affected by the surfactant can be ignored in the upscaling methods for surfactant spontaneous imbibition.

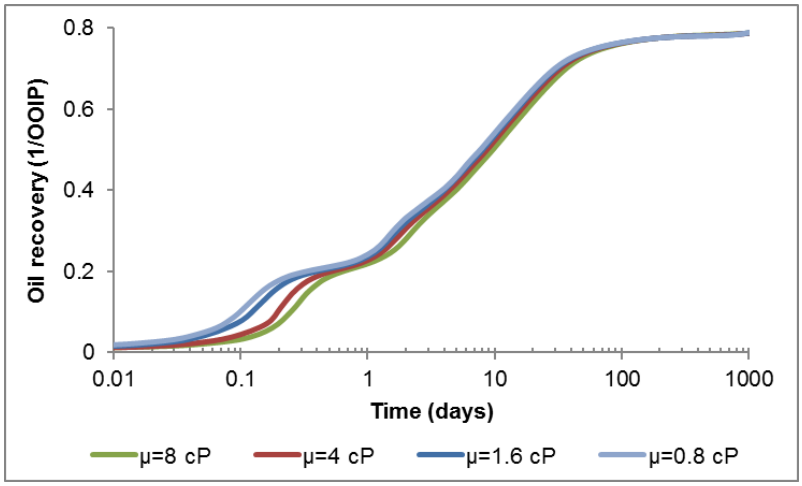

Fig. 4-1—Oil recovery of surfactant spontaneous imbibition using surfactant solution with different viscosity.

4.2 Surfactant concentration

Surfactant concentration has effect on wettability alteration and IFT reduction. To study the effect, surfactant solutions with surfactant concentration of 0.001, 0.002, 0.004, 0.005, 0.007, and 0.01 g/cm^3 are used to do spontaneous imbibition. Fig. 2-5 and Fig. 2-6 tells that when surfactant concentration is 0.001 g/cm^3, surfactant could reduce water/oil IFT to 1.54 mN/m but cannot change the wettability. When surfactant concentration is 0.002 g/cm^3, surfactant could change matrix wettability to slightly more water-wet, and the wettability alteration coefficient is 0.95, at the same time, surfactant could reduce IFT to 1.29 mN/m. When surfactant concentration is 0.004 g/cm^3, which is the critical micelle concentration (CMC), IFT is changed to the lowest value, which is 0.8 mN/m. When surfactant concentration is 0.005 g/cm^3, wettability is altered to strongly water-wet (i.e. $\omega = 0$). In the base case, the surfactant concentration is 0.01 g/cm^3. The surfactant concentration of 0.007 g/cm^3 is between two important surfactant concentrations that 0.005 g/cm^3 and 0.01 g/cm^3. The summary of surfactant spontaneous imbibition with different surfactant concentration is in Table 4-1.

Table 4-1—Summary of surfactant spontaneous imbibition with different surfactant concentrations.

Surfactant concentration, C_s (g/cm^3)	IFT at CMC, σ_{CMC} (mN/m)	Wettability alteration coefficient, ω	Bond number, N_B	Ultimate oil recovery, R_{of} (1/OOIP)
0.001	1.54	1	1.9	0.353
0.002	1.29	0.95	0.77	0.416
0.004	0.8	0.125	0.10	0.636
0.005	0.8	0	0.09	0.792
0.007	0.8	0	0.09	0.793
0.01	0.8	0	0.09	0.793

Fig. 4-2 shows that oil recovery rate is increasing with the increase of the surfactant concentration in solution, and recovery time is shorter for imbibition with higher surfactant concentration, which are the same as the observation by Andersen et al. (2015). But when surfactant concentration is 0.005, 0.007, and 0.01 g/cm^3, the ultimate oil recovery is the same, which is because that when surfactant concentration is higher than CMC, the wettability alteration and IFT reduction are not changing with surfactant concentration. So, the ultimate oil recovery reaches the maximum when IFT is reduced to the lowest value and the wettability is altered to strongly water-wet. Since the effect of water viscosity on surfactant spontaneous imbibition can be neglected in the simulation, the proposed upscaling method of t_{D2} (Eq. 2.16) is simplified into the upscaling group of t_{d2} (Eq. 4.1), and then modified into Eq. 4.2 by adding the effect of surfactant concentration. Eq. 4.2 is used to upscale oil recovery of surfactant imbibition, and its validity is proved by the upscaling result of oil recovery (Fig. 4-3).

$$t_{d2} = t\left(N_B^{-0.5} + 1\right) \tag{4.1}$$

$$t_{d2}^{*} = t\frac{C_s}{CMC}\left(N_B^{-0.5} + 1\right) \tag{4.2}$$

Where, t_{d2} is simplified proposed upscaling group, s; t_{d2}^{*} is modified simplified proposed upscaling group including the effect of surfactant concentration, s; t is imbibition time, s; N_B is

Bond number; C_s is surfactant concentration in solution, g/cm^3; CMC is critical micelle concentration, g/cm^3.

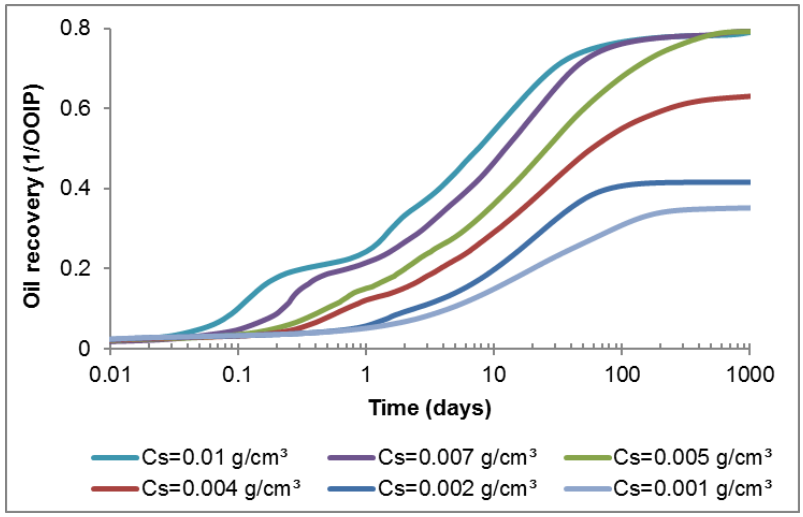

Fig. 4-2—Oil recovery of surfactant spontaneous imbibition vs. imbibition time using different surfactant concentrations.

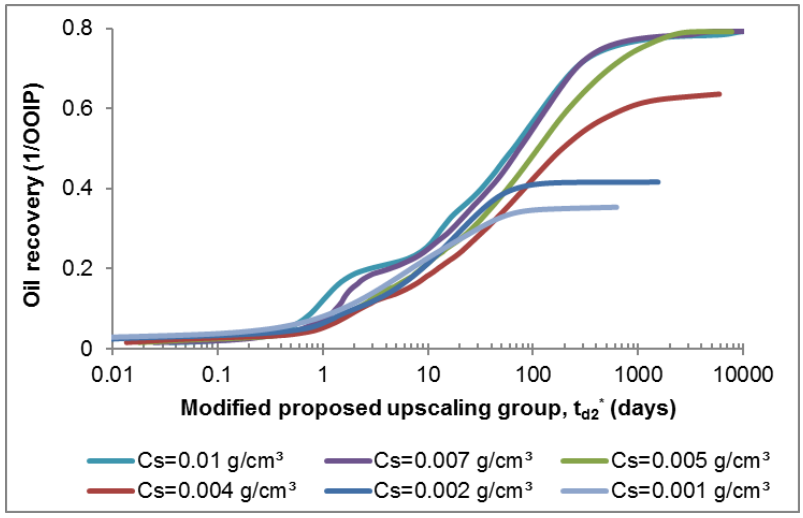

Fig. 4-3—Oil recovery of surfactant spontaneous imbibition vs. modified simplified proposed upscaling group (t_{d2}^*) using different surfactant concentrations.

4.3 Surfactant adsorption

Surfactant adsorption on matrix could change matrix wettability, at the same time, it can reduce surfactant concentration in solution in matrix, thus affects surfactant efficiency. The maximum surfactant mass in matrix is calculated with Eq. 4.3, and the maximum surfactant adsorption mass on rock is calculated with Eq. 4.4. The ratio of adsorbed surfactant mass on total surfactant mass is calculated with Eq. 4.5. In simulation studies, matrix wettability is changed to strongly water-wet at the maximum surfactant adsorption concentration, which happens when the surfactant concentration is above 0.005 g/cm^3. So, matrix wettability alteration depends on the ratio of adsorbed surfactant mass on the maximum mass of surfactant adsorption. Surfactant adsorption could slower water/oil IFT reduction by reducing surfactant concentration in solution in the matrix.

$$m_s = V_b \phi C_s \tag{4.3}$$

$$m_{ads} = V_b (1-\phi) \rho_r C_{ads} \tag{4.4}$$

$$\eta = \frac{m_{ads}}{m_s} \tag{4.5}$$

Where, m_s is the total mass of surfactant, g; V_b is the bulk volume of matrix, cm^3; ϕ is matrix porosity; C_s is surfactant concentration, g/cm^3; m_{ads} is adsorption mass of surfactant, g; ρ_r is rock density, g/cm^3; C_{ads} is surfactant adsorption concentration on the rock, g/g; η is the mass ratio of surfactant adsorption on total surfactant.

In the base case, the surfactant concentration is 0.01 g/cm^3, so the total surfactant mass is 0.234 g. The adsorption concentration is 0.0002 g/g, so the adsorption percentage is 6.87%. To study the effect of surfactant adsorption, five comparative simulations with different surfactant adsorption concentrations are performed. The summary of the results is listed in Table 4-2. Oil recovery curves (Fig. 4-4) show that ultimate oil recovery does not change with adsorption

concentration, which is because the injected surfactant concentration is higher than CMC which results in the same IFT reduction and the same wettability condition (i.e. strongly water-wet), while these two factors decide the ultimate oil recovery. However, oil recovery rate is reducing with the increase of surfactant adsorption concentration, which is the same observation as Andersen et al. (2015). Surfactant concentration in solution in matrix is reduced by surfactant adsorption on rock and can be diluted by brine in the matrix, thus surfactant concentration is smaller and smaller with the imbibition into matrix. A high surfactant adsorption concentration can accelerate the decrease of surfactant concentration in solution, and then reduce the surfactant sweep efficiency. Therefore, oil recovery is slower when surfactant adsorption concentration is higher. An upscaling method (Eq. 4.6), which includes surfactant adsorption ratio, is proposed and used to upscale oil recovery of surfactant spontaneous imbibition. The upscaling result of oil recovery is shown in Fig. 4-5.

$$t^* = \frac{t}{\sqrt{\eta}} \tag{4.6}$$

Where, t^* is proposed upscaling group, s; t is imbibition time, s; η is the mass ratio of surfactant adsorption on total surfactant.

Table 4-2—Summary of surfactant adsorption mass and adsorption ratio (in percentage) for different cases.

Cases	Surfactant adsorption mass, m_{ads} (g)	Surfactant adsorption percentage, η (%)
base case	0.016	6.87
comparative 1	0.008	3.44
comparative 2	0.032	13.75
comparative 3	0.064	27.49
comparative 4	0.096	41.24
comparative 5	0.225	96.22

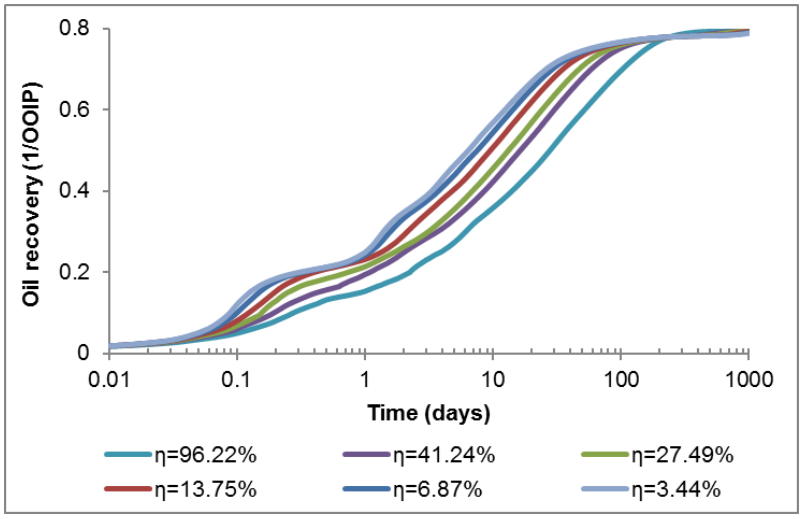

Fig. 4-4—Oil recovery of surfactant spontaneous imbibition vs. imbibition time for cases with different surfactant adsorption ratios (in percentage).

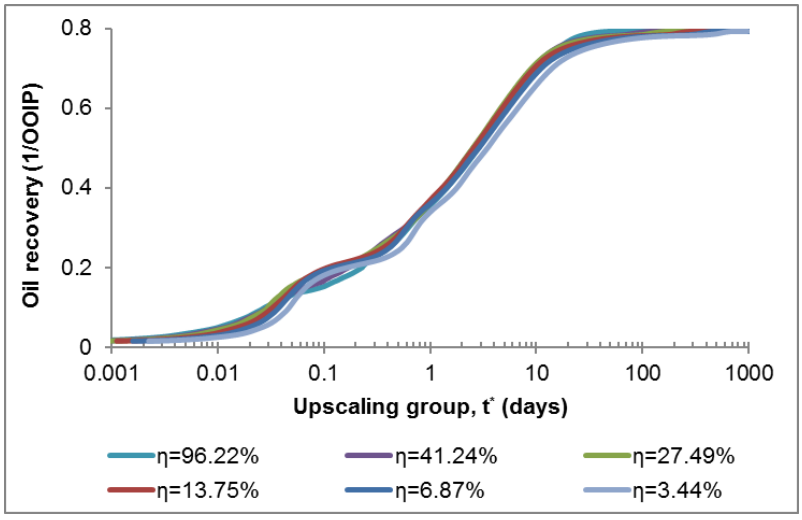

Fig. 4-5—Oil recovery of surfactant spontaneous imbibition vs. proposed upscaling group (t^*) for cases with different surfactant adsorption ratios (in percentage).

4.4 Surfactant diffusion

Since surfactant efficiency is decreasing with the imbibition into matrix, which results from the reduction of surfactant concentration in solution due to adsorption and dilution in matrix, surfactant diffusion will be very important for surfactant spontaneous imbibition to compensate the reduction of surfactant spontaneous imbibition rate. The capillary diffusion coefficient is on the order about 10^{-8} m^2/s and 10^{-11} m^2/s in the ideally water-wet case and the intermediate wet case, respectively (Stoll et al. 2008). In the base case in this study, the surfactant diffusion coefficient is 5×10^{-4} cm^2/h (i.e. 1.4×10^{-11} m^2/s). To study the effect of surfactant diffusion on surfactant spontaneous imbibition, three comparative cases with surfactant diffusion coefficients of 5×10^{-1}, 5×10^{-3}, and 5×10^{-6} cm^2/h separately are used. Table 4-3 is the imbibition time to recover 95% of ultimate oil recovery (i.e. $R_{on} = 0.95$) for all the cases.

Table 4-3—Imbibition time to recover 95% of ultimate oil recovery of surfactant spontaneous imbibition using surfactant with different diffusion coefficient.

Surfactant diffusion coefficient, D_s		Imbibition time when $R_{on} = 0.95$ (days)
cm^2/h	m^2/s	
5×10^{-1}	1.4×10^{-8}	51.5
5×10^{-3}	1.4×10^{-10}	52
5×10^{-4}	1.4×10^{-11}	65
5×10^{-6}	1.4×10^{-13}	1228

Fig. 4-6 gives the same conclusion as Andersen et al. (2015) that the oil recovery rate decreases with the decrease of surfactant diffusion coefficient, which is because if the surfactant diffuses faster, it can sweep the whole matrix faster. However, Andersen et al. (2015) claimed that at early time, the higher recovery happened at the cases with lower diffusion coefficient, which is different from my result. The study in section 4.2 tells that surfactant concentration can accelerate surfactant spontaneous imbibition. Surfactant diffusion can increase the surfactant concentration in the front of surfactant solution in matrix, thus the increase of surfactant diffusion coefficient enhances the recovery. Comparing the oil recovery curves with diffusion coefficient of 5×10^{-1} and 5×10^{-3} cm^2/h, the oil recovery rate is faster for the case with diffusion coefficient of 5×10^{-1} cm^2/h in 3 days, but after 3 days the oil recovery rate for both cases are

almost the same. The oil recovery curves with diffusion coefficient of 5×10^{-4} and 5×10^{-6} cm^2/h are almost the same before 1 day, afterwards, the oil recovery rate is much faster for the case with diffusion coefficient of 5×10^{-4} cm^2/h. So, the conclusion is that higher surfactant diffusion has larger effect at the early recovery time, while lower surfactant diffusion has larger effect at later recovery time.

Water saturation and surfactant mass in matrix are normalized with Eq. 4.7 and Eq. 4.8, respectively, and then plotted in Fig. 4-7. It shows that when surfactant diffusion coefficient is 5×10^{-1} cm^2/h, surfactant mass increases faster than water saturation in matrix, which means that surfactant diffusion is faster than imbibition. When surfactant diffusion coefficient is 5×10^{-3} cm^2/h, the curves of normalized water saturation and normalized surfactant mass in matrix coincide, which implies that surfactant diffusion rate is the same as imbibition rate. When surfactant diffusion coefficient is 5×10^{-4} or 5×10^{-6} cm^2/h, the normalized water saturation curve is above the normalized surfactant mass curve, which implies that surfactant diffusion is behind water imbibition. Therefore, when surfactant coefficient is high, the increase of surfactant concentration in matrix can even be faster than the increase of water saturation in matrix. Surfactant can sweep the whole matrix in a relatively short time. When surfactant diffusion coefficient is low, the increase of surfactant concentration is slower than the increase of water saturation in matrix. When water sweeps the whole matrix, capillary pressure is zero, so the capillary imbibition stops. Afterwards, surfactant moves into matrix based on diffusion.

$$S_{wn} = \frac{S_w - S_{wi}}{S_{w\max} - S_{wi}} \tag{4.7}$$

Where, S_{wn} is the normalized water saturation in matrix; S_w is water saturation in matrix; S_{wi} is initial water saturation in matrix; S_{wmax} is the maximum water saturation in matrix.

$$m_{sn} = \frac{m_s - m_{si}}{m_{s\max} - m_{si}} \tag{4.8}$$

Where, m_{sn} is the normalized surfactant mass in matrix; m_s is surfactant mass in matrix, g; m_{si} is initial surfactant mass in matrix, g; m_{smax} is the maximum surfactant mass in matrix, g.

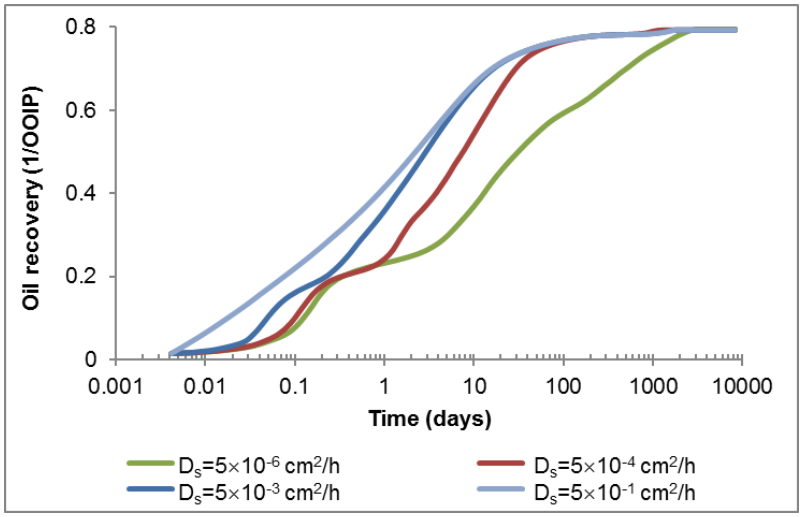

Fig. 4-6—Oil recovery of surfactant spontaneous imbibition vs. imbibition time using surfactant with different diffusion coefficients.

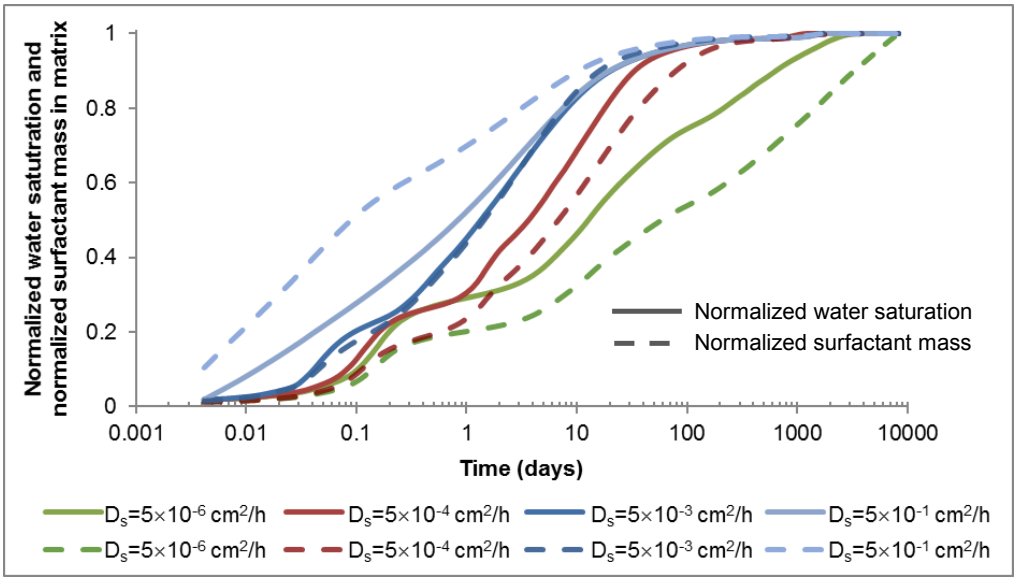

The solid lines represent the curves of normalized water saturation, and the dashed lines represent the curves of normalized surfactant mass in matrix.

Fig. 4-7—The normalized water saturation and surfactant mass in matrix for cases with different surfactant diffusion coefficients.

4.5 Summary

1. Two upscaling groups are proposed for the effects of surfactant concentration and adsorption separately.
2. Viscosity of surfactant solution almost has no effect on surfactant spontaneous imbibition. Thus, water viscosity affected by surfactant can be ignored in upscaling methods for surfactant spontaneous imbibition.
3. Oil recovery rate is faster when surfactant concentration is higher. With the increase of surfactant concentration, ultimate oil recovery is increasing when surfactant concentration is smaller than CMC. When surfactant concentration is higher than CMC, ultimate oil recovery does not change with surfactant concentration.
4. Surfactant adsorption could reduce oil recovery rate but has no effect on ultimate oil recovery.
5. Oil recovery rate decreases with the decrease of surfactant diffusion coefficient, and surfactant diffusion does not affect ultimate oil recovery of surfactant spontaneous imbibition.

5 Surfactant flooding in fractured matrix

The performance of water flooding in mixed- or oil-wet fractured reservoirs can be very unsatisfactory. The complicated matrix/fracture system may lead to a low water sweep efficiency, and the oil-wet wettability can result in a low oil recovery in the water swept area. Therefore, surfactant application may improve the oil recovery due to the mechanisms of wettability alteration and IFT reduction. In this chapter, a model of fractured matrix is established, and the injection rate, injection timing and the surfactant slug size are studied.

5.1 Model description

The matrix used in the study of surfactant spontaneous imbibition is cut into two parts in the middle to create a vertical fracture in the matrix and used as the model in the simulation study of surfactant flooding (Fig. 5-1). Matrix and fracture are simulated as separate regions with different absolute permeability, relative permeability, porosity, capillary pressure, and flow properties. The capillary pressure in the fracture is zero. Brine/surfactant solution is injected from the horizontal injector at the bottom of the fracture, and fluids are produced from the horizontal producer at the top of the fracture. The original pressure is 270 atm which is about the same as Ekofisk field. Surfactant concentration is 0.01 g/cm^3, which is the same as the concentration in the base case of surfactant spontaneous imbibition. The main properties of the matrix and fracture in the model of fractured matrix are listed in Table 5-1. The fracture width is 0.017 cm, so that the fracture porosity is 0.5% (Eq. 5.1) based on the definition that fracture porosity is the ratio of fracture volume on total volume. The fracture absolute permeability is calculated with Eq. 5.2 (van Golf-Racht 1982). The simulation code of the base case of surfactant flooding in the fractured matrix is attached in Appendix B.

$$\phi_f = \frac{V_f}{V_b} \tag{5.1}$$

Where, ϕ_f is fracture porosity; V_f is fracture volume, cm^3; V_b is bulk volume, cm^3.

$$K_f = C\frac{b^2}{12} \tag{5.2}$$

Where, K_f is absolute permeability of fracture, mD; b is fracture width, cm; C is unit conversion constant, 10^{11}.

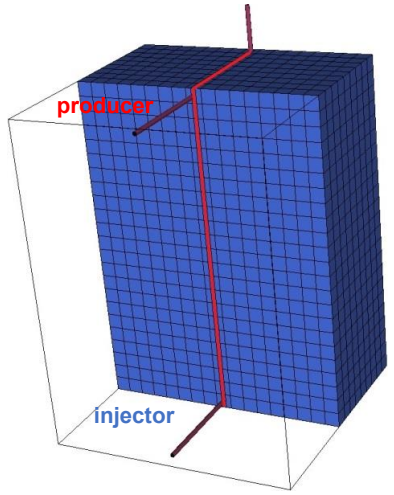

The blue part is matrix and the red part is fracture. There is a horizontal injector at the bottom of the fracture and a horizontal producer at the top of the fracture.

Fig. 5-1—The model of surfactant flooding in a fractured matrix.

Table 5-1—Properties of the matrix and fracture in the model of fractured matrix.

Properties	Length, L (cm)	Width, b (cm)	Height, H (cm)	Volume, V (cm^3)	Porosity, ϕ	Permeability, K (mD)	Initial water saturation, S_{wi}
Matrix	3.4	3.4	4.6	53.176	0.443	3	0.277
Fracture	3.4	0.017	4.6	0.266	0.005	2.4×10^6	0

5.2 Injection rate

Surfactant solution with concentration of 0.01 g/cm^3 is injected into the fracture, and oil and surfactant solution are produced at the same rate as injection rate from the top of the fracture. The injection rates are listed in Table 5-2. The pressure drop between the injector and producer is increasing with the increase of injection rate. But because the matrix block size is small, the pressure drop is only 0.33 atm even when the injection rate is 0.1 PV/h.

Table 5-2— Summary of surfactant flooding with different injection rates.

Injection rate, q		Pressure drop (atm)	Oil recovery, R_o (1/OOIP)		Ultimate oil recovery, R_{of} (1/OOIP)
PV/h	cm^3/h		Injection volume is 1 PV	Injection volume is 10 PV	
0.00005	0.0012	0.0046	0.791	-	
0.0001	0.0024	0.0048	0.781	-	
0.0005	0.012	0.0061	0.677	0.793	
0.001	0.024	0.0077	0.526	0.784	0.796
0.01	0.24	0.037	0.187	0.563	
0.1	2.38	0.33	0.066	0.191	
1	23.8	3.23	0.03	0.066	

Fig. 5-2 shows that oil recovery has a linear relation with time before water breakthrough, which is the same conclusion as Andersen et al. (2015). Furthermore, water breakthrough happens earlier when the injection rate is higher. Fig. 5-3 tells that all the injection rates lead to the same ultimate oil recovery, which is around 80% OOIP, and that oil recovery rate is dramatically increasing with the increase of injection rate when injection rate is smaller than 0.0005 PV/h (i.e. 0.012 cm^3/h). For injection rates which are higher than 0.0005 PV/h, the oil recovery curves are not changing much. When the injection rate is 0.0005 PV/h, oil recovery is about 67% OOIP after 80 days of surfactant injection, which is about 85% of ultimate oil recovery. And oil recovery rate is slower afterwards. Oil recovery reaches 95% of ultimate oil recovery after 180 days of surfactant flooding. Fig. 5-4 shows that a higher injection rate results in a smaller oil recovery after injecting a certain amount of surfactant solution. Because of the small size of the matrix, most the injected fluid could be produced directly without any contribution to oil recovery when the injection rate is high. When the injection volume is 1 PV, surfactant flooding time is about 83 days, and oil recovery is about 70% OOIP with injection rate of 0.0005 PV/h.

Fig. 5-5 shows that ultimate oil recovery increases slower when injection rate is slower than 0.0005 PV/h, and ultimate oil recovery has a power function relation with injection rate when injection rate is faster than 0.0005 PV/h.

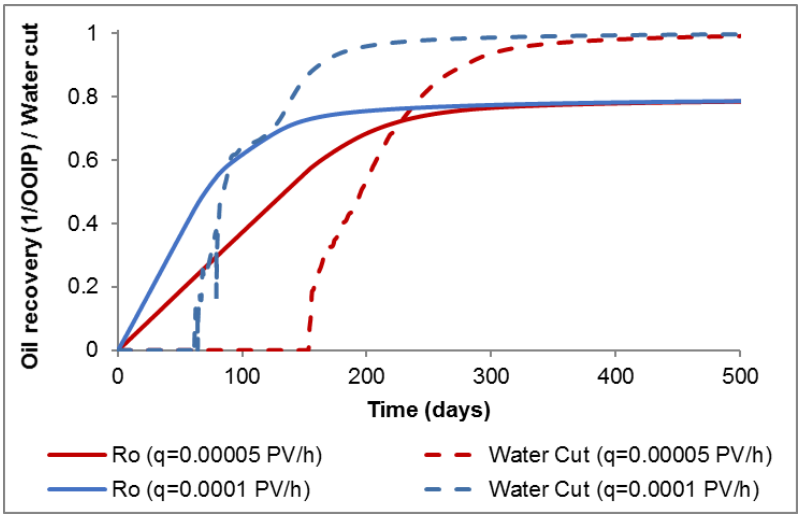

Fig. 5-2—Oil recovery and water cut vs. time using different injection rates.

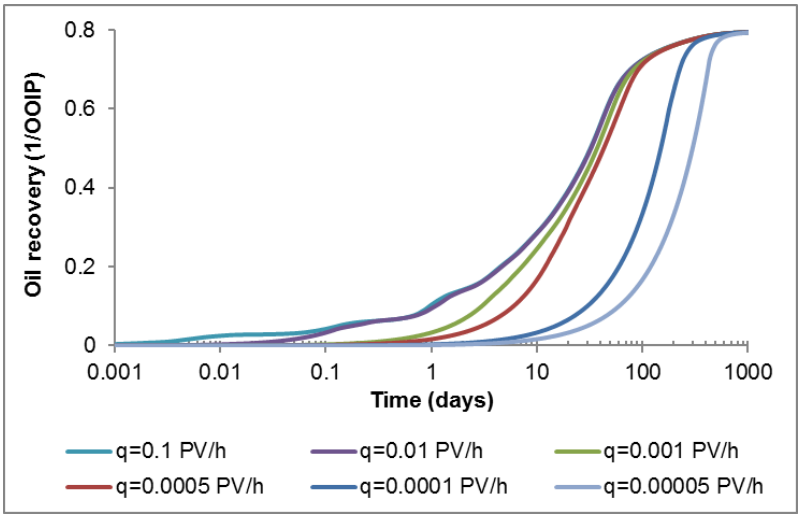

Fig. 5-3—Oil recovery of surfactant flooding in a fractured matrix vs. time using different injection rates.

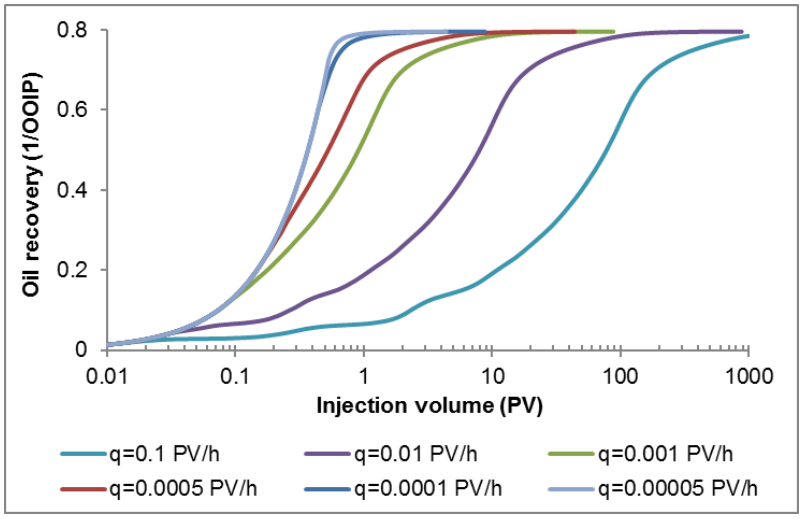

Fig. 5-4—Oil recovery of surfactant flooding in a fractured matrix vs. injection volume using different injection rates.

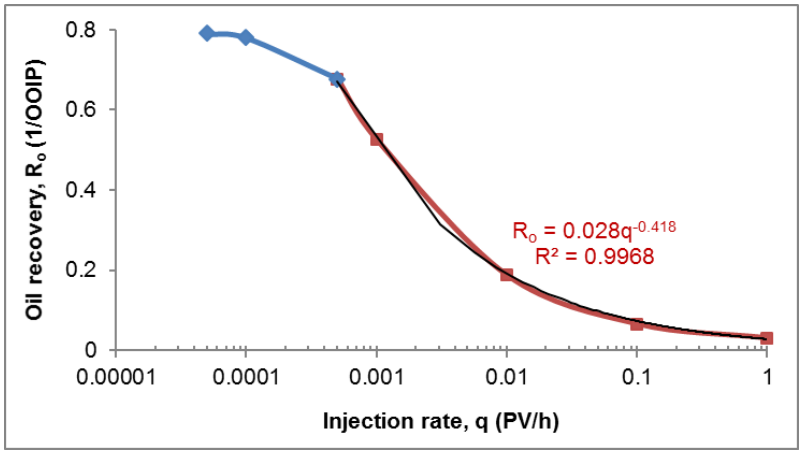

Fig. 5-5—The relationship between oil recovery and the injection rate after injecting 1 PV surfactant solution.

When oil recovery reaches 95% of ultimate oil recovery, oil recovery rate becomes very slow, so the further oil recovery has no economic benefit. Thus, I assume that the oil recovery is finished when the normalized oil recovery is 0.95. It can be seen from Fig. 5-6 that the final oil recovery time is about 175 days when injection rate is faster than 0.0005 PV/h, then the final

oil recovery time is dramatically increasing with the decrease of injection rate. However, injection volume of surfactant solution rapidly increases with the increase of injection rate when injection rate is higher than 0.0005 PV/h. Considering surfactant flooding time, injection volume, the oil recovery, the proper injection rate for the model is 0.0005 PV/h.

Even though pressure drop increases with the increase of injection rate, oil recovery does not change with the increase of injection rate when the rate is higher than 0.0005 PV/h, which implies that pressure drop does not have significant effect on oil recovery. When injection rate is lower than 0.0005 PV/h, the injection rate is smaller than the imbibition rate, so the oil recovery rate is decided by the injection rate. But when injection rate is higher than 0.0005 PV/h, the injection rate is larger than the imbibition rate, thus the oil recovery rate depends on the imbibition rate. Surfactant imbibition into matrix could be affected by surfactant diffusion and fracture properties. Therefore, some contrastive simulations are did to study these parameters.

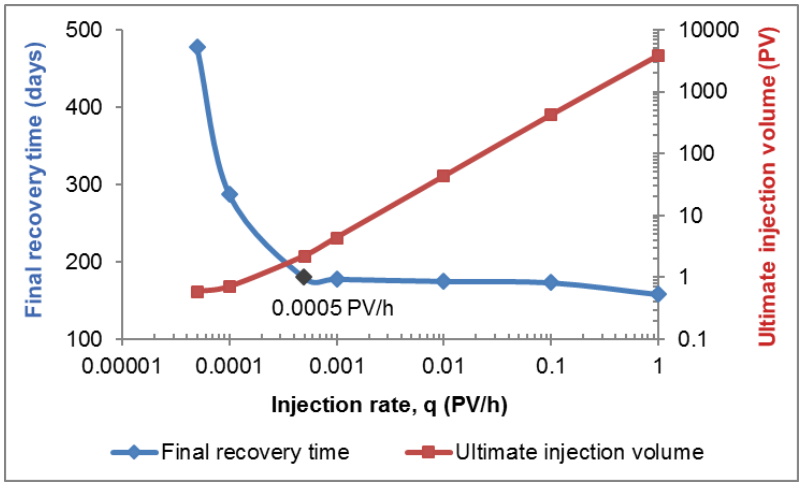

Fig. 5-6—The final oil recovery time and ultimate injection volume of surfactant flooding with different injection rates when oil recovery reaches 95% of ultimate oil recovery.

5.2.1 Effect of surfactant diffusion

In the base case, the surfactant diffusion coefficient is 5×10^{-4} cm^2/h. In order to study the effect of surfactant diffusion on surfactant dynamic imbibition, the surfactant diffusion is set to zero

in the contrastive simulation, so that surfactant only flows with brine. The summary of the simulation results is listed in Table 5-3. Oil recovery obviously decreases faster with the increase of injection rate when the injection rate is higher than 0.0005 PV/h.

Table 5-3—Summary of the surfactant flooding with different injection rate when the surfactant diffusion is zero.

Injection Rate, q		Pressure drop (atm)	Oil recovery, R_o (1/OOIP)	
PV/h	cm^3/h		Injection volume is 1 PV	Injection volume is 10 PV
0.00005	0.0012	0.0046	0.466	-
0.0001	0.0024	0.0048	0.47	-
0.0005	0.012	0.0061	0.416	0.485
0.001	0.024	0.0077	0.339	0.474
0.01	0.24	0.037	0.114	0.341
0.1	2.38	0.33	0.041	0.11
1	23.8	3.23	0.03	0.044

Fig. 5-7 shows that injection rate has a larger effect on ultimate oil recovery when surfactant diffusion coefficient is zero. When surfactant diffusion coefficient is 5×10^{-4} cm^2/h, all the injection rates lead to the same ultimate oil recovery. But when the coefficient is 0, the ultimate oil recovery is much smaller at lower injection rate. And when the injection rate is 1 PV/h, the ultimate oil recovery is increased to 0.8 OOIP. When surfactant diffusion is ignored, surfactant is imbibed into matrix by capillary pressure, gravity and the pressure difference between fracture and matrix. But capillary force is decreasing with the increase of water saturation in matrix, and in this matrix the gravity force is very small (about 0.001 atm), in addition, surfactant concentration will be diluted by the water in matrix and decreased by the adsorption on rock. So, surfactant efficiency is reducing with the imbibition distance into matrix. When the total force of gravity and capillary forces is decreased to zero, surfactant imbibition will only depend on the pressure difference between fracture and matrix, which is increasing with the increase of the injection rate. But the increase is very small at low injection rate, so that ultimate oil recovery is not enhanced at low injection rate.

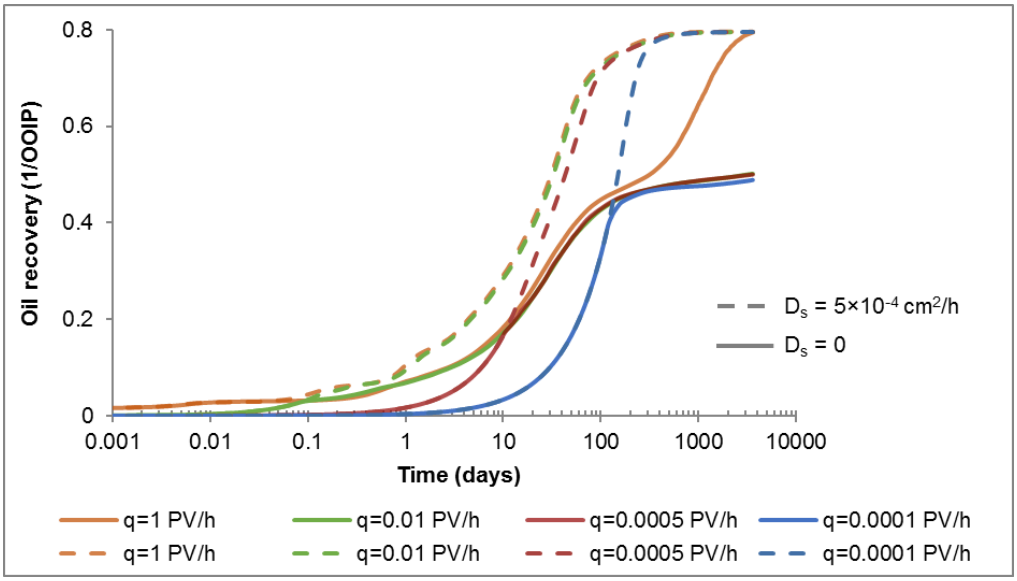

Dashed curves are oil recovery with surfactant diffusion of 5×10^{-4} cm^2/h; solid curves are oil recovery without surfactant diffusion.

Fig. 5-7—Oil recovery vs. time of the base case ($D_s = 5\times10^{-4}$ cm^2/h) and the contrastive case ($D_s = 0$).

Comparing the oil recovery between the base case and the contrastive case (Fig. 5-8), it is obvious that surfactant diffusion could significantly increase oil recovery. One reason could be that the surfactant could diffuse into the whole matrix in a relatively short time due to the small size of matrix. Another reason is that the matrix is homogeneous, so the water sweep efficiency is not improved by the pressure difference, and fluid could be easily flow through the fracture system which makes it difficult to result in a large pressure drop between injector and producer. In reality, reservoir conditions are very complicated, so the injection rate may lead to a big pressure difference between the fracture and matrix, thus improve surfactant sweep efficiency. Since surfactant imbibition rate depends on brine imbibition rate, surfactant adsorption, and surfactant diffusion, the large size of the matrix in reservoir could decrease the relative efficiency of surfactant diffusion when the diffusion rate is slower than brine imbibition rate.

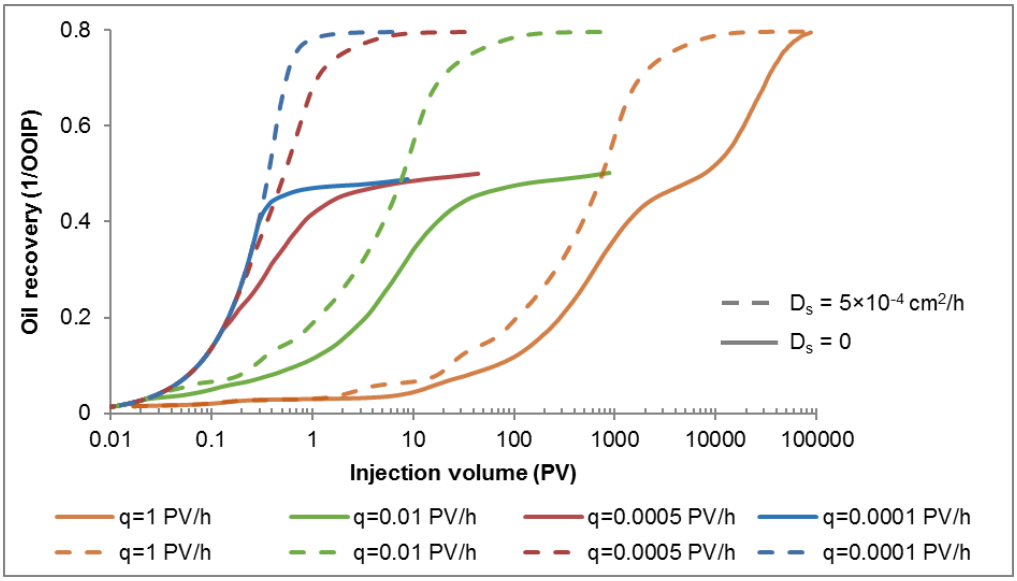

Dashed curves are oil recovery with surfactant diffusion of 5×10^{-4} cm^2/h; solid curves are oil recovery without surfactant diffusion.

Fig. 5-8—Oil recovery vs. injection volume of surfactant solution of the base case ($D_s = 5\times10^{-4}$ cm^2/h) and the contrastive case ($D_s = 0$).

5.2.2 Effect of fracture porosity

Fracture width has effect on fracture porosity and fracture permeability, which are calculated with Eq. 5.1 and Eq. 5.2, respectively. In the contrastive case, the fracture width is reduced to 0.0034 cm, so that the fracture porosity is 0.1%, and the absolute permeability is 1×10^4 mD. The properties of fracture are listed in Table 5-4. The summary of the simulation results is shown in Table 5-5.

Table 5-4—Fracture properties in the base case and contrastive case.

Case	Fracture width, b (cm)	Fracture porosity, ϕ_f (%)	Fracture permeability, K_f (mD)
Base case	0.017	0.5	2.4×10^6
Contrastive case	0.0034	0.1	1×10^4

Table 5-5—Summary of surfactant flooding with different injection rate in a fractured matrix with fracture porosity of 0.1%.

Injection rate, q		Pressure drop (atm)	Ultimate oil recovery, R_{of} (1/OOIP)
PV/h	cm^3/h		
0.00005	0.0012	0.0046	0.793
0.0001	0.0024	0.0048	0.793
0.0005	0.012	0.0061	0.79
0.001	0.024	0.0077	0.793
0.01	0.24	0.037	0.794
0.1	2.36	0.33	0.798
1	23.6	3.23	0.82

Comparing the ultimate oil recovery in two cases (Fig. 5-9), it reveals that when injection rate is smaller than 1 PV/h, the ultimate oil recovery in the base case is constant, which is about 0.796 OOIP. However, for the contrastive case with fracture porosity of 0.1%, the ultimate oil recovery is slightly smaller than the base case when injection rate is lower than 0.05 PV/h, but the ultimate oil recovery is larger when injection rate is higher than 0.05 PV/h. When injection rate is 1 PV/h, the ultimate oil recovery in the contrastive case is larger than that in the base case by 2.4% OOIP. The result indicates that the increase of injection rate is more efficient to increase the pressure difference between fracture and matrix in the system with lower fracture porosity. The pressure drop between injector and producer does not have big difference between the two cases for all the injection rates (Table 5-2 and Table 5-5), but Fig. 5-10 shows that when the fracture porosity is 0.1%, the ultimate oil recovery has obvious increase with the increase of the pressure drop when the pressure drop exceeds 0.4 atm, which demonstrates that the pressure drop between injector and producer cannot decide the pressure difference between fracture and matrix.

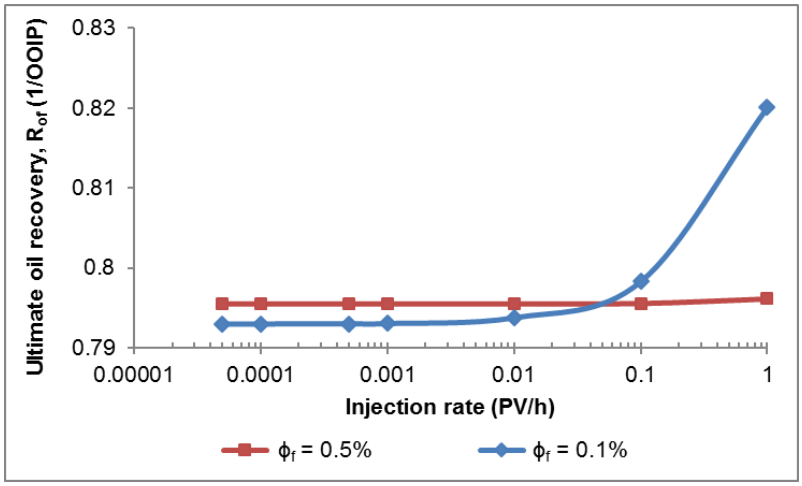

Fig. 5-9—The relationship between ultimate oil recovery and injection rate when fracture porosity is 0.5% and 0.1%.

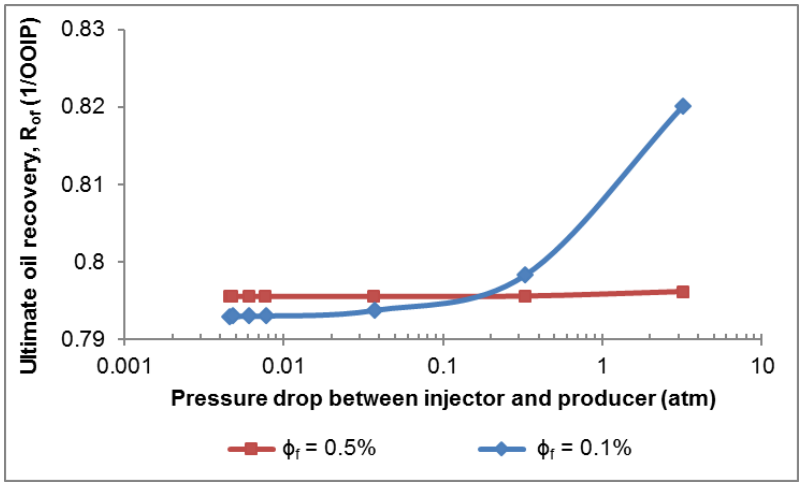

Fig. 5-10—The relationship between ultimate oil recovery and pressure drop between the injector and producer when fracture porosity is 0.5% and 0.1%.

When injection rate is higher than 0.0005 PV/h, oil recovery curves are almost the same for the base case. However, for the contrastive case, the final oil recovery time is dramatically decreasing with the increase of injection rate (Fig. 5-11). When oil recovery is 95% of ultimate oil recovery (i.e. $R_{on} = 0.95$), oil recovery time is 157 days when the injection rate is 0.01 PV/h.

And it is reduced to 64 and 9 days when the injection rate is increased to 0.1 and 1 PV/h, respectively. The results reveal that oil recovery rate is enhanced by the increase of pressure difference between fracture and matrix which results from the fracture properties and injection rate.

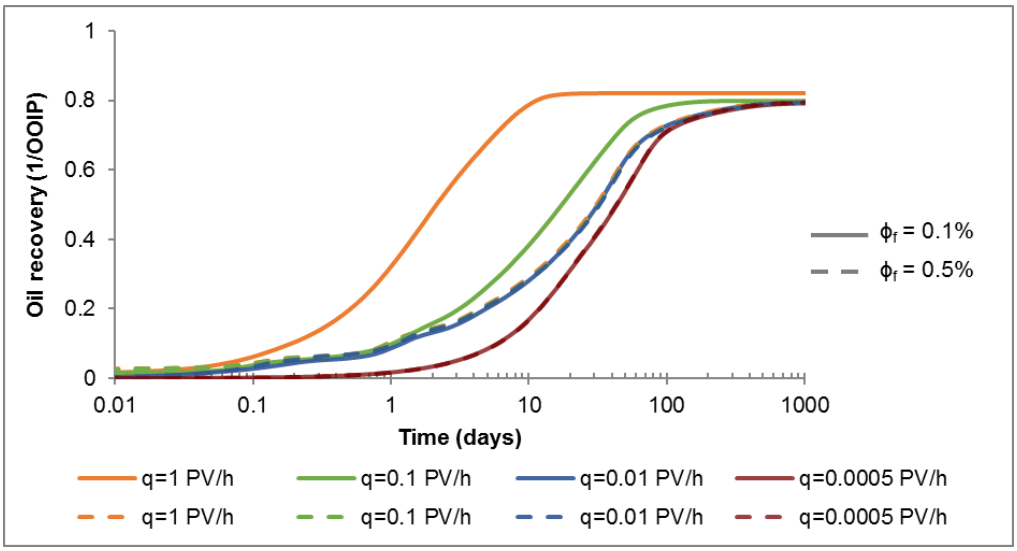

Solid curves are oil recovery of contrastive case; dashed curves are oil recovery of the base case.

Fig. 5-11—Comparison of oil recovery vs. time curves of the base case (ϕ_f = 0.5%) and the contrastive case (ϕ_f = 0.1%).

The required injection volume to obtain the ultimate oil recovery is increasing with the increase of injection rate. But when injection rate is higher than 0.1 PV/h, for the base case with higher fracture porosity (0.5%), the required injection volume is much more, and the oil recovery rate is much slower (Fig. 5-12). For the contrastive case, to recovery 95% of ultimate oil recovery, the required injection volume is increased by 46% and the surfactant injection time is decreased by 85% when the injection rate is increased from 0.1 PV/h to 1 PV/h (Table 5-6). Hence, for the contrastive case, the high injection rate (1PV/h) could be a good choice considering oil recovery rate, ultimate oil recovery, and injection volume.

When injection rate is smaller than 0.01 PV/h, the pressure difference between fracture and matrix is still too weak to accelerate oil recovery. So, the main mechanisms of surfactant oil recovery are the same for both cases, which are capillary pressure and surfactant diffusion. For

the contrastive case, when a high injection rate is applied, the brine or surfactant solution could be high-efficiently pushed into the matrix by the pressure difference, so the fluids flow faster in matrix, which increases the capillary number. Therefore, the ultimate oil recovery is increased. At the same time, because of the increased influence of pressure difference, the relative contribution of surfactant diffusion to the oil recovery becomes smaller.

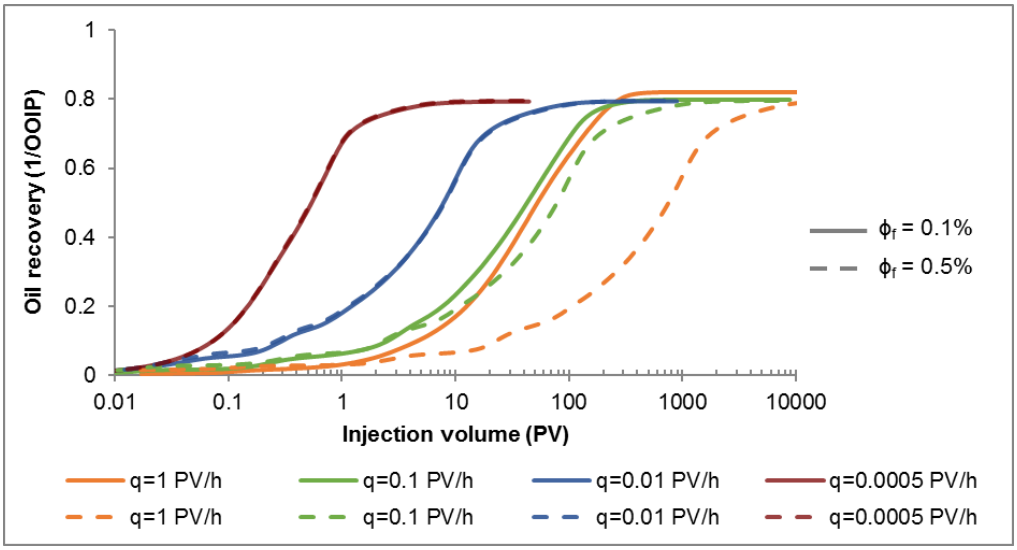

Solid curves are oil recovery of contrastive case; dashed curves are oil recovery of the base case.

Fig. 5-12—Oil recovery vs. injection volume of the base case (ϕ_f = 0.5%) and the contrastive case (ϕ_f = 0.1%).

Table 5-6—The oil recovery time and injection volume when oil recovery is 95% of ultimate oil recovery for the cases with fracture porosity of 0.5% and 0.1%.

Injection rate, q (PV/h)	Time (days)		Injection volume (PV)	
	ϕ_f = 0.5%	ϕ_f = 0.1%	ϕ_f = 0.5%	ϕ_f = 0.1%
0.00005	478	475	0.6	0.6
0.0001	288	286	0.7	0.7
0.0005	180	181	2.2	2.2
0.001	178	178	4.4	4.4
0.01	175	157	43	39
0.1	173	64	421	157
1	158	9	3844	230

5.3 Injection timing

In this section, injection timing of surfactant solution is studied to find out if surfactant should be applied in secondary or tertiary recovery stage, and whether surfactant could be used at the area swept by brine. Based on the study in section 5.2, the injection rate of 0.0005 PV/h is used. There are 8 scenarios of surfactant injection following the pre-water flooding with volume of 0.2, 0.4, 0.6, 0.8, 1, 1.5, 2, and 3 PV. The results are compared with the results of surfactant flooding and water flooding (Fig. 5-13). The ultimate oil recovery is the same, which is around 80% OOIP, for all the scenarios, which means surfactant could sweep the whole matrix for all the scenarios. Since the capillary pressure is zero after completed water flooding and the gravity is very small in this model, surfactant diffusion is the key parameter that let the surfactant go into the matrix and then change the matrix wettability and reduce the IFT, thus improve oil recovery, which is proved by the contrastive case where the surfactant diffusion is neglected ($D_s = 0$).

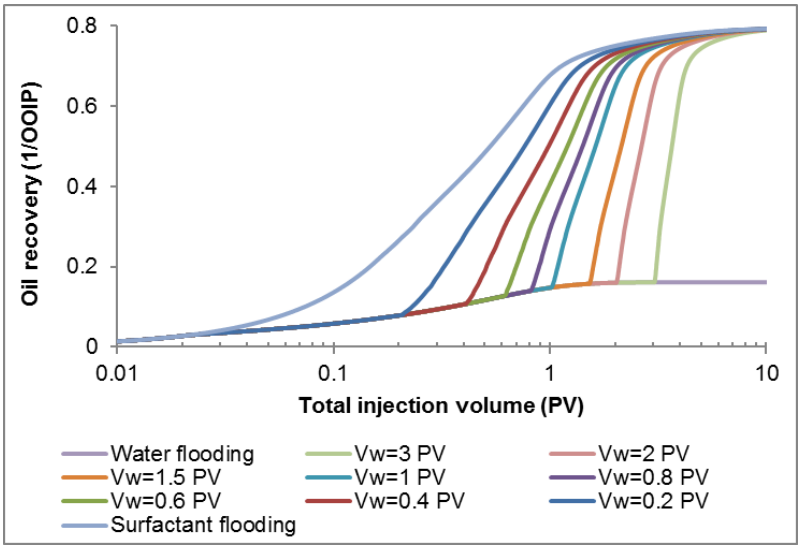

Fig. 5-13—Oil recovery of surfactant flooding following a pre-water flooding in the base case ($D_s = 5\times10^{-4}$ cm^2/h).

When the surfactant diffusion is neglected, the ultimate oil recovery is about 0.5 OOIP after injecting 10 PV surfactant solution from the beginning, and ultimate oil recovery decreases with the increase of pre-water flooding volume (Fig. 5-14). When the pre-water flooding volume is 3 PV, the oil recovery is about 0.16 OOIP, and the capillary pressure is about zero in matrix. The injected surfactant following pre-water flooding moves into matrix due to gravity and pressure difference between fracture and matrix. Because the gravity and pressure difference are very small, and the gravity will be counteracted by the negative capillary pressure, surfactant hardly moves into matrix after completed water flooding.

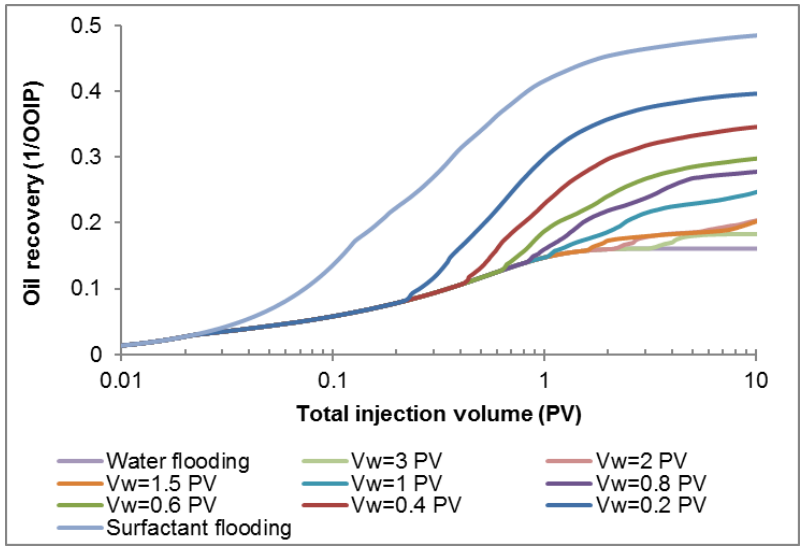

Fig. 5-14—Oil recovery of surfactant flooding following a pre-water flooding in the contrastive case ($D_s = 0$).

Fig. 5-15 shows that when surfactant diffusion coefficient is 5×10^{-4} cm^2/h, the surfactant enhanced oil recovery is almost 0.5 OOIP after injecting 1PV surfactant solution following 3 PV pre-water flooding. However, for the contrastive case without surfactant diffusion, surfactant enhanced oil recovery is dramatically decreasing with the increase of pre-water flooding volume and less than 0.04 OOIP when the pre-water flooding volume is more than 1 PV. Therefore, the surfactant with poor diffusion efficiency should not be used after completed water flooding. When the oil recovery is 95% of ultimate oil recovery, which is 0.756 OOIP, surfactant flooding could be ended considering the economics. The total injection volume of

brine and surfactant solution and the final injection volume of surfactant solution are plotted in Fig. 5-16. It shows the final surfactant volume increases with the increase of pre-water flooding volume. So even if the surfactant has high-efficient diffusion, the early surfactant application could reduce the time cost and surfactant consumption.

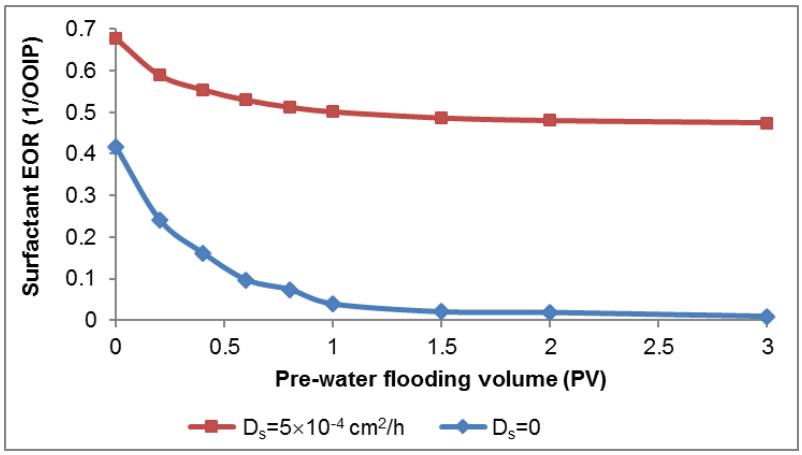

Fig. 5-15—Surfactant EOR after injecting 1 PV surfactant solution following pre-water flooding.

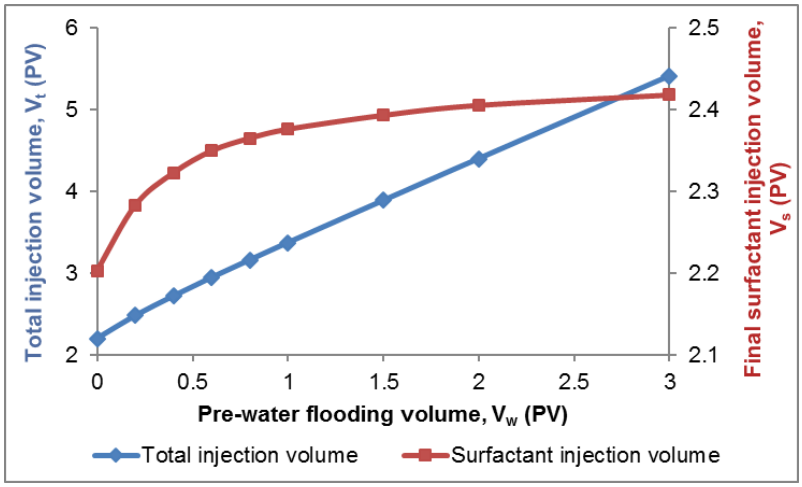

Fig. 5-16—Total injection volume of fluids and final injection volume of surfactant solution in the base case for flooding scenarios with different pre-water flooding volume.

5.4. Surfactant slug size

Surfactant assumption is an important influence factor for surfactant EOR economy. The goal of surfactant EOR is to achieve the largest oil recovery in a reasonable cost of surfactant. In sections 5.2 and 5.3, the studies indicate that the proper injection rate for the base case is 0.0005 PV/h, and surfactant should be applied before water flooding. So, in this section, surfactant is injected before water flooding with the injection rate of 0.0005 PV/h. Surfactant injection volume is varying from 0.2 PV to 3 PV. The surfactant concentration is 0.01 g/cm^3 and 0.005 g/cm^3 in the base case and the contrastive case, respectively. The summary of the surfactant flooding results of these two cases is shown in Table 5-7.

Table 5-7—Summary of surfactant flooding with different scenarios.

Surfactant slug size (PV)	Surfactant mass in matrix, Δm* (g)		Ultimate oil recovery, R_{of} (1/OOIP)	
	C_s=0.01 g/cm³	C_s=0.005 g/cm³	C_s=0.01 g/cm³	C_s=0.005 g/cm³
0	0	0	0.161	0.161
0.2	0.00717	0.00213	0.523	0.347
0.4	0.0128	0.00396	0.667	0.434
0.6	0.0156	0.00542	0.759	0.481
0.8	0.016	0.00676	0.794	0.515
1	0.016	0.00817	0.796	0.544
1.5	0.016	0.0114	0.796	0.609
2	0.016	0.0135	0.796	0.659
3	0.016	0.015	0.796	0.721

Δm* equals to the difference between injected mass of surfactant and the produced mass of surfactant.

When surfactant concentration is 0.01 g/cm^3, the maximum ultimate oil recovery (i.e. about 0.8 OOIP) is obtained by injecting 0.8 PV surfactant solution, and the maximum surfactant mass in matrix is about 0.016 g. But when the surfactant slug size is 0.8 PV, the ultimate oil recovery is about 0.52 OOIP for the contrastive case with surfactant concentration of 0.005 g/cm^3. Fig. 5-17 reveals that it requires much more surfactant solution to obtain the maximum oil recovery for the case with lower surfactant concentration. When surfactant is moving into matrix, the concentration becomes smaller and smaller with the distance into matrix due to dilution and

adsorption. For the case with small surfactant concentration, dilution and adsorption have large negative effects on the surfactant efficiency. Therefore, a lower surfactant concentration results in a smaller oil recovery using the same surfactant slug size.

The relationship between surfactant mass in matrix and the ultimate oil recovery are the same for both cases, and ultimate oil recovery has a strong positive linear function relation with surfactant mass in matrix (Fig. 5-18), which implies surfactant mass in matrix is a key parameter for the ultimate oil recovery of surfactant flooding. Fig. 5-19 reveals that when surfactant solution with lower surfactant concentration is injected, less surfactant can be imbibed into matrix, hence the surfactant efficiency is reduced, which means that more surfactant is required to inject when lower surfactant concentration is applied. Based on the previous analysis, it can be concluded that under the condition of injection safety, a relatively higher surfactant concentration is a better choice.

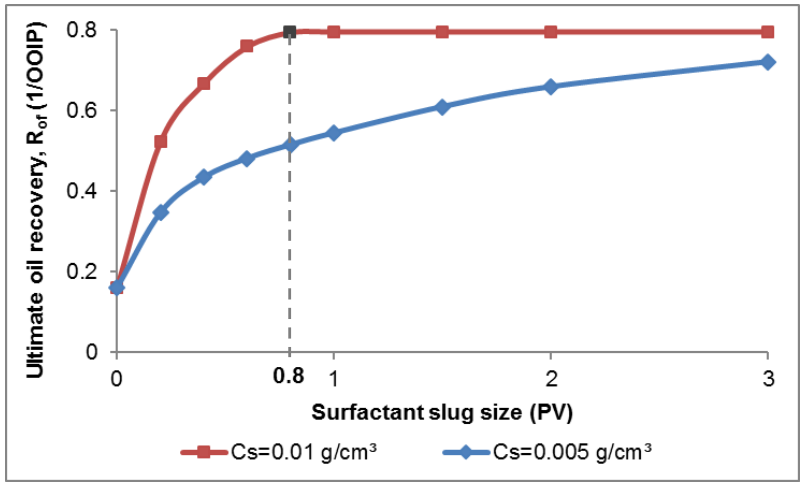

Fig. 5-17—The relationship between surfactant slug size and ultimate oil recovery obtained with different injection surfactant concentration.

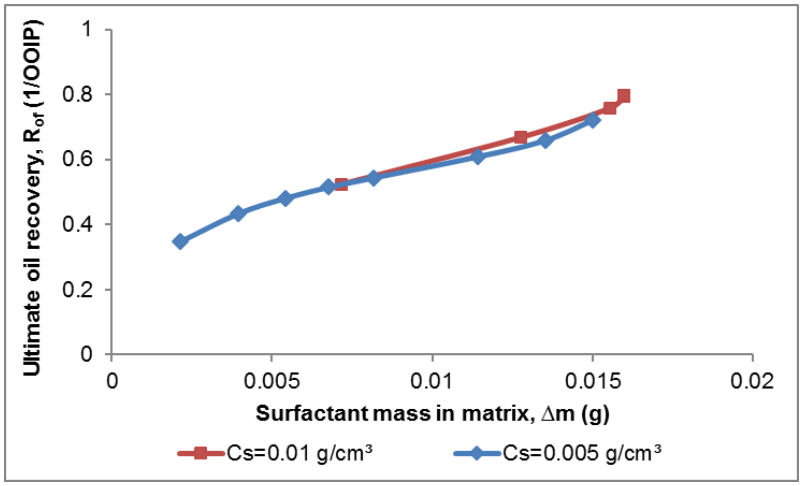

Fig. 5-18—The relationship between surfactant mass in matrix and ultimate oil recovery obtained with different injection surfactant concentration.

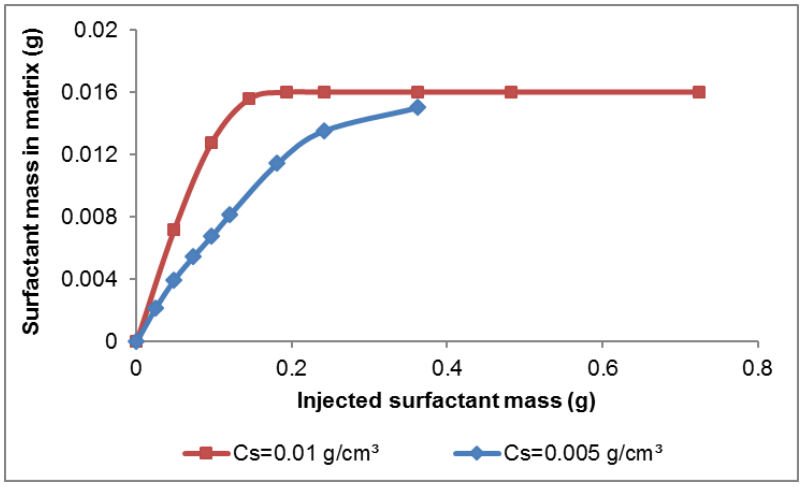

Fig. 5-19—The relationship between the injected surfactant mass and the surfactant mass in matrix.

5.5 Summary

The matrix in the model of surfactant spontaneous imbibition is cut into two parts from the middle to create a vertical fracture. The fractured matrix is used to do the simulation study in

this chapter. The injection rate, injection timing and injection surfactant slug size are studied. The main conclusions are as follows.

1. In the base case, the oil recovery rate is significantly increasing with the increase of injection rate until the injection rate is 0.0005 PV/h. After injection 1 PV surfactant solution, the oil recovery is about 70% OOIP, which is about 85% of ultimate oil recovery, when the injection rate is 0.0005 PV/h. Considering the surfactant flooding time and surfactant consumption, the injection rate of 0.0005 PV/h is the proper injection rate for the base case.
2. Comparing with the base case with surfactant diffusion coefficient of 5×10^{-4} cm^2/h, the oil recovery is dramatically decreased in the contrastive case without surfactant diffusion. Injection rate has a larger effect on oil recovery when surfactant diffusion is slower.
3. The increase of injection rate is more efficient in the system with smaller fracture porosity (0.1%) since the injection rate could increase the pressure difference between fracture and matrix, which results in an increase of oil recovery rate thus increase the capillary number. The ultimate oil recovery is improved when the injection rate is higher than 0.01 PV/h.
4. A relatively higher injection rate is a better choice for system with smaller fracture porosity. For the system with fracture porosity of 0.1%, when injection rate is increased to 1 PV/h from 0.1 PV/h, the required injection volume to obtain 95% of ultimate oil recovery is increased by 46%, at the same time, the required oil recovery time is decreased by 85%.
5. Surfactant should be applied before water flooding. Because the required injection volume of surfactant to obtain the ultimate oil recovery is increasing with the increase of pre-water flooding volume. The surfactant with low diffusion coefficient should not be used in tertiary oil recovery stage.
6. For surfactant flooding followed by post-water flooding, the maximum oil recovery is obtained after injecting 0.8 PV surfactant solution with the concentration of 0.01 g/cm^3. But when the solution with a lower surfactant concentration (e.g. 0.005 g/cm^3) is used, the oil recovery rate is much slower, and it requires to inject more surfactant solution and surfactant mass to achieve the maximum oil recovery.

6 Conclusions and recommendations for future work

6.1 Conclusions

Surfactant could change matrix wettability to more water-wet and/or reduce water/oil IFT, therefore, it could be used to improve oil recovery in mixed- or oil-wet fractured reservoirs. In this thesis, two upscaling methods are proposed, and in some cases, the methods are slightly modified based on simulation results. The individual and combined effects of surfactant mechanisms are studied, as well as the effects of surfactant and matrix properties on surfactant spontaneous imbibition and surfactant dynamic imbibition in a fractured matrix. The most frequently used existing methods, the proposed upscaling methods, and the application conditions are listed in Table 6-1. The main conclusions are as follows.

- The surfactant spontaneous imbibition model is established based on the experimental data from literature and verified by the excellent history matching of the experimental and simulation oil recovery.
- The Bond number calculation equation includes wettability alteration and IFT reduction. Then, it is used to establish two upscaling methods by combining Darcy's law, so that the new upscaling methods include the effect of wettability alteration, IFT reduction, gravity and capillary pressure.
- The proposed upscaling methods are verified by simulation results of surfactant spontaneous imbibition in three different cases: (1) $N_B \geq 1$; (2) $N_B \leq 0.1$; (3) $0.1 < N_B < 1$. The proposed upscaling method of t_{D1} is valid when $N_B > 0.1$, and the proposed upscaling method of t_{D2} is for the cases with $N_B \leq 0.1$.
- When $\sigma_{CMC} \geq 0.0154$ mN/m, the wettability alteration has significant influence on the oil recovery, but when the IFT at CMC is smaller than 0.0154 mN/m, the wettability alteration has no effect on the ultimate oil recovery.

- In general, when only matrix permeability is varying, the ultimate oil recovery of surfactant spontaneous imbibition is increasing with the increase of matrix permeability. But if the wettability is changed to strongly water-wet, the ultimate oil recovery does not change until the permeability is higher than 150 mD. The enhanced oil recovery is decreasing with the increase of bound number when $N_B < 1$, and then increasing with the increase of bound number when $N_B > 1$. The existing upscaling method for gravity imbibition can be used when $N_B \geq 1$. And the existing upscaling method for capillary imbibition is efficient to upscale the oil recovery when $N_B \leq 0.1$, but it is not valid when $0.1 < N_B < 1$. The proposed upscaling method of t_{D1} can be used to upscale the normalized oil recovery for all the cases.
- Matrix porosity has little effect on brine and surfactant spontaneous imbibition, especially when wettability is strongly water-wet.
- When only matrix porosity is varying between 0.2 and 0.6, with the increase of Bond number, the ultimate oil recovery is increasing in general, but the surfactant EOR is increasing when $N_B < 1$, and then decreasing when $N_B > 1$. The increase of ultimate oil recovery is smaller when the wettability is changed to more water-wet. And when the matrix is strongly water-wet, the ultimate oil recovery almost has no change. The proposed upscaling methods are slightly modified based on the simulation results when $N_B < 1$.
- The oil recovery rate is decreasing, but the ultimate oil recovery is increasing with the increase of matrix block size. When the wettability is changed to more water-wet, the influence of matrix block size on ultimate oil recovery is smaller. The existing upscaling method for capillary imbibition can be used when $N_B \leq 0.1$. The proposed upscaling method of t_{D1} can be used to upscale the normalized oil recovery.
- The viscosity of surfactant solution almost has no effect on surfactant spontaneous imbibition. High surfactant concentration could accelerate oil recovery. And the ultimate oil recovery is increasing with the increase of surfactant concentration when the concentration is smaller than CMC. Surfactant adsorption can lower the oil recovery rate. However, the ultimate oil recovery does not change as long as the final wettability alteration and the IFT reduction are the same. Surfactant diffusion is very important for surfactant oil recovery especially for the area with high water saturation and low capillary pressure. When surfactant diffusion is larger than 5×10^{-3} cm^2/h, surfactant

diffusion is faster than water imbibition, and when surfactant diffusion is lower than 5×10^{-3} cm^2/h, surfactant diffusion is slower than water imbibition. Two upscaling methods are proposed for the effects of surfactant concentration and adsorption.

- A model of surfactant injection in a fractured matrix in core scale is established based on the model of surfactant spontaneous imbibition.
- Considering the oil recovery rate, time and injection volume, the injection rate of 0.0005 PV/h is the optimal injection rate. The injection rate has a larger effect on the oil recovery when surfactant diffusion is low, or fracture porosity is small. High injection rate could be a good choice for the system with small fracture porosity.
- Surfactant should be applied before water flooding, and the surfactant with low diffusion coefficient should not be used in the third oil recovery stage.
- For the surfactant flooding followed by post-water flooding, surfactant solution with lower surfactant concentration has a lower efficiency because less surfactant could be imbibed into the matrix. Under the conditions of injection safety, the surfactant solution with a relatively high surfactant concentration should be applied.

Table 6-1—Summary of existing and proposed upscaling methods and the application conditions.

Cases	Conditions	Upscaling equations	
		Existing	Proposed
Gravity imbibition	$N_B \geq 1$	$t_{Dg} = \frac{K\Delta\rho}{\phi\mu_o H}t$	$t_{D1} = t\frac{K\Delta\rho gH}{\phi\mu L_c^2}\left(N_B^{-1}+1\right)$ $t_{D2} = t\frac{K\Delta\rho gH}{\phi\mu L_c^2}\left(N_B^{-0.5}+1\right)$
$0.000154 \leq \sigma_{CMC} \leq 15.4$ mN/m; $0 \leq \omega \leq 1$	$0.1 < N_B < 1$		$t_{d1} = t\left(N_B^{-1}+1\right)$ $t_{d2} = t\left(N_B^{-0.5}+1\right)$
	$N_B \leq 0.1$		$t_{d2} = t\left(N_B^{-0.5}+1\right)$
$1.5 \leq K \leq 600$ mD	$0.1 < N_B < 1$		$t_{d1} = tK\left(N_B^{-1}+1\right)$
	$N_B \leq 0.1$	$t_c = t\sqrt{K}$	$t_{d1} = tK\left(N_B^{-1}+1\right)$

Cases	Conditions	Upscaling equations	
		Existing	Proposed
$0.2 \le \phi \le 0.6$	$0.1 < N_B < 1$		$t^*_{d1} = \frac{t}{\sqrt{\phi}}\left(N_B^{-1}+1\right)$
	$N_B \le 0.1$		$t^*_{d2} = t\left(N_B^{-0.5}+1\right)$
$0.5 \le \alpha \le 10$	$0.1 < N_B < 1$		$t_{d1} = t\frac{H}{L_c^2}\left(N_B^{-1}+1\right)$
	$N_B \le 0.1$	$t_c = \frac{t}{L_c^2}$	$t_{d1} = t\frac{H}{L_c^2}\left(N_B^{-1}+1\right)$
$0.001 \le C_s \le 0.01$ g/cm^3	$\sigma_{CMC} = 0.8$ mN/m; $\omega = 0$		$t^*_{d2} = t\frac{C_s}{CMC}\left(N_B^{-0.5}+1\right)$
$3\% < \eta < 100\%$	$\sigma_{CMC} = 0.8$ mN/m; $\omega = 0$		$t^* = \frac{t}{\sqrt{\eta}}$

6.2 Recommendations for future work

Considering that no particular surfactant is used in the simulation work, and the upscaling methods are only verified by simulation results, there are some recommendations for future work.

- More experimental work is needed to select the optimal surfactants from existing commercial surfactants for different water/oil/rock systems according to the study of surfactant properties. This thesis gives a reference for surfactant screening.
- More work is needed to verify the proposed upscaling methods with experimental results.
- Some properties, like matrix heterogeneity, temperature, brine salinity, surfactant distribution in water and oil phases, hysteresis etc., should be further studied with simulation work. The reason is that in this thesis, it is assumed that the matrix is homogeneous; surfactant only exists in water phase; and the reactions between surfactant and rock and water/oil immediately occur after contact with each other. In addition, the effect of temperature and brine salinity are ignored.

References

Abbasi-Asl, Y.; Pope, G. A. and Delshad, M. 2010. Mechanistic Modeling of Chemical Transport in Naturally Fractured Oil Reservoirs. Presented at SPE Improved Oil Recovery Symposium, Tulsa, Oklahoma, USA, 24-28 April. https://doi.org/10.2118/129661-MS.

Abrams, A. 1975. The influence of fluid viscosity, interfacial tension, and flow velocity on residual oil saturation left by waterflood. *Society of Petroleum Engineers Journal* **15** (05): 437-447. https://doi.org/10.2118/5050-PA.

Adibhatia, B.; Sun, X. and Mohanty, K. 2005. Numerical Studies of Oil Production from Initially Oil-Wet Fracture Blocks by Surfactant Brine Imbibition. Presented at SPE International Improved Oil Recovery Conference in Asia Pacific, Kuala Lumpur, Malaysia, 5-6 December. https://doi.org/10.2118/97687-MS.

Adibhatla, B. and Mohanty, K. K. 2008. Oil recovery from fractured carbonates by surfactant-aided gravity drainage: laboratory experiments and mechanistic simulations. *SPE Reservoir Evaluation & Engineering* **11** (01): 119-130. https://doi.org/10.2118/99773-PA.

Ahmadall, T.; Gonzalez, M. V.; Harwell, J. H. et al. 1993. Reducing surfactant adsorption in carbonate reservoirs. *SPE reservoir engineering* **8** (02): 117-122. https://doi.org/10.2118/24105-PA.

Akbar, M.; Chakravorty, S.; Russell, S. D. et al. 2000. Unconventional Approach to Resolving Primary and Secondary Porosity in Gulf Carbonates from Conventional Logs and Borehole Images. Presented at Abu Dhabi International Petroleum Exhibition and Conference, Abu Dhabi, United Arab Emirates, 13-15 October. https://doi.org/10.2118/87297-MS.

Al-Anssari, S.; Nwidee, L. N.; Arif, M. et al. 2017. Wettability Alteration of Carbonate Rocks via Nanoparticle-Anionic Surfactant Flooding at Reservoirs Conditions. Presented at SPE Symposium: Production Enhancement and Cost Optimisation, Kuala Lumpur, Malaysia, 7-8 November. https://doi.org/10.2118/189203-MS.

Allan, J. and Sun, S. Q. 2003. Controls on Recovery Factor in Fractured Reservoirs: Lessons Learned from 100 Fractured Fields. Presented at SPE Annual Technical Conference and Exhibition, Denver, Colorado, 5-8 October. https://doi.org/10.2118/84590-MS.

Alvarez, J. O.; Neog, A.; Jais, A. et al. 2014. Impact of Surfactants for Wettability Alteration in Stimulation Fluids and the Potential for Surfactant EOR in Unconventional Liquid

Reservoirs. Presented at SPE Unconventional Resources Conference, Woodlands, Texas, 1-3 April. https://doi.org/10.2118/169001-MS.

Alvarez, J. O. and Schechter, D. S. 2016. Altering Wettability in Bakken Shale by Surfactant Additives and Potential of Improving Oil Recovery During Injection of Completion Fluids. Presented at SPE Improved Oil Recovery Conference, Tulsa, Oklahoma, 11-13 April. https://doi.org/10.2118/179688-MS.

Amirpour, M.; Shadizadeh, S. R.; Esfandyari, H. et al. 2015. Experimental investigation of wettability alteration on residual oil saturation using nonionic surfactants: Capillary pressure measurement. *Petroleum* **1** (4): 289-299. https://doi.org/10.1016/j.petlm.2015.11.003.

Amott, E. 1959. Observations Relating to the Wettability of Porous Rock. *Petroleum Transactions, AIME* **216**: 156-162.

Andersen, P. Ø.; Evje, S.; Kleppe, H. et al. 2015. A Model for Wettability Alteration in Fractured Reservoirs. *SPE Journal* **20** (06): 1261-1275. https://doi.org/10.2118/174555-PA.

Anderson, W. G. 1986a. Wettability Literature Survey- Part 1: Rock/Oil/Brine Interactions and the Effects of Core Handling on Wettability. *Journal of Petroleum Technology* **38** (10): 1125-1144. https://doi.org/10.2118/13932-PA.

Anderson, W. G. 1986b. Wettability Literature Survey- Part 2: Wettability Measurement. *Journal of Petroleum Technology* **38** (11): 1246-1262. https://doi.org/10.2118/13933-PA.

Austad, T.; Matre, B.; Milter, J. et al. 1998. Chemical flooding of oil reservoirs 8. Spontaneous oil expulsion from oil-and water-wet low permeable chalk material by imbibition of aqueous surfactant solutions. *Colloids and Surfaces A: Physicochemical and Engineering Aspects* **137** (1): 117-129.

Austad, T. and Milter, J. 1997. Spontaneous Imbibition of Water Into Low Permeable Chalk at Different Wettabilities Using Surfactants. Presented at International Symposium on Oilfield Chemistry, Houston, Texas, 18-21 February. https://doi.org/10.2118/37236-MS.

Azad, M. S. and Sultan, A. S. 2014. Extending the Applicability of Chemical EOR in High Salinity, High Temperature & Fractured Carbonate Reservoir Through Viscoelastic Surfactants. Presented at SPE Saudi Arabia Section Technical Symposium and Exhibition, Al-Khobar, Saudi Arabia, 21-21 April. http://doi.org/10.2118/172188-MS.

Babadagli, T. 1996. Temperature effect on heavy-oil recovery by imbibition in fractured reservoirs. *Journal of Petroleum Science and Engineering* **14** (3-4): 197-208. https://doi.org/10.1016/0920-4105(95)00049-6.

Babadagli, T. 2001a. Scaling of Cocurrent and Countercurrent Capillary Imbibition for Surfactant and Polymer Injection in Naturally Fractured Reservoirs. *SPE Journal* **6** (04): 465 - 478. https://doi.org/10.2118/74702-PA.

Babadagli, T. 2001b. Selection of Proper EOR Method for Efficient Matrix Recovery in Naturally Fractured Reservoirs. Presented at SPE Latin American and Caribbean Petroleum Engineering, Buenos Aires, Argentina, 25-28 March. http://doi.org/10.2118/69564-MS.

Babadagli, T. 2003. Analysis of Oil Recovery by Spontaneous Imbibition of Surfactant Solution. Presented at SPE International Improved Oil Recovery Conference in Asia Pacific, Kuala Lumpur, 20-21 October. https://doi.org/10.2118/84866-MS.

Babadagli, T. 2003a. Evaluation of EOR methods for heavy-oil recovery in naturally fractured reservoirs. *Journal of Petroleum Science and Engineering* **37** (1-2): 25-37. https://doi.org/10.1016/S0920-4105(02)00309-1.

Babadagli, T. 2003b. Selection of proper enhanced oil recovery fluid for efficient matrix recovery in fractured oil reservoirs. *Colloids and Surfaces A: Physicochemical and Engineering Aspects* **223** (1-3): 157-175. https://doi.org/10.1016/S0927-7757(03)00170-5.

Babadagli, T. 2006. Evaluation of the critical parameters in oil recovery from fractured chalks by surfactant injection. *Journal of Petroleum Science and Engineering* **54** (1-2): 43-54. https://doi.org/10.1016/j.petrol.2006.07.006.

Babadagli, T.; Al-Bemani, A. and Boukadi, F. 1999. Analysis of capillary imbibition recovery considering the simultaneous effects of gravity, low IFT, and boundary conditions. Presented at SPE Asia Pacific Improved Oil Recovery Conference, Kuala Lumpur, 25-26 October. https://doi.org/10.2118/57321-MS.

Babadagli, T.; Al-Bemani, A.; Boukadi, F. et al. 2005. A laboratory feasibility study of dilute surfactant injection for the Yibal field, Oman. *Journal of Petroleum Science and Engineering* **48** (1): 37-52. https://doi.org/10.1016/j.petrol.2005.04.005.

Bennetzen, M. V.; Mogensen, K.; Frank, S. et al. 2014. Dilute Surfactant Flooding Studies in a Low-Permeability Oil-Wet Middle East Carbonate. Presented at International Petroleum Technology Conference, Doha, Qatar, 19-22 January. https://doi.org/10.2523/IPTC-17656-MS.

Bourbiaux, B. J. 2009. Understanding the Oil Recovery Challenge of Water Drive Fractured Reservoirs. Presented at International Petroleum Technology Conference, Doha, Qatar, 7-9 December. https://doi.org/10.2523/IPTC-13909-MS.

Chabert, M.; Morvan, M. and Tabary, R. 2010. Fractured Carbonates: A Methodology to Evaluate Surfactant Performances. Presented at SPE Improved Oil Recovery Symposium, Tulsa, Oklahoma, 24-28 April. https://doi.org/10.2118/129178-MS.

Chen, H. L.; Lucas, L. R.; Nogaret, L. A. D. et al. 2000. Laboratory Monitoring of Surfactant Imbibition Using Computerized Tomography. Presented at SPE International Petroleum Conference and Exhibition in Mexico, Villahermosa, 1-3 February. https://doi.org/10.2118/59006-MS.

Chen, P. and Mohanty, K. K. 2015. Surfactant-Enhanced Oil Recovery from Fractured Oil-wet Carbonates: Effects of Low IFT and Wettability Alteration. Presented at SPE International Symposium on Oilfield Chemistry, The Woodlands, Texas, USA, 13-15 April. https://doi.org/10.2118/173797-MS.

Chilingar, G. V. and Yen, T. F. 1983. Some Notes on Wettability and Relative Permeabilities of Carbonate Reservoir Rocks, II. *Energy Sources* **7** (1): 67-75. http://dx.doi.org/10.1080/00908318308908076.

Corey, A. T. 1977. *Mechanics of heterogeneous fluids in porous media*. Fort Collins, Colorado: Water Resources Publications.

Cui, L.; Ma, K.; Abdala, A. A. et al. 2014. Adsorption of a Switchable Cationic Surfactant on Natural Carbonate Minerals. Presented at SPE Improved Oil Recovery Symposium, Tulsa, Oklahoma, 12-16 April. https://doi.org/10.2118/169040-MS.

Cuiec, L. E. 1984. Rock/Crude-Oil Interactions and Wettability: An Attempt to Understand Their Interrelation. Presented at SPE Annual Technical Conference and Exhibition, Houston, Texas, 1984/1/1/. https://doi.org/10.2118/13211-MS.

Cuiec, L. E.; Bourbiaux, B. and Kalaydjian, F. 1994. Oil recovery by imbibition in low-permeability chalk. *SPE Formation Evaluation* **9** (3): 200-208. https://doi.org/10.2118/20259-PA.

Dean, R. and Lo, L. 1988. Simulations of naturally fractured reservoirs. *SPE reservoir engineering* **3** (02): 638-648.

Delshad, M.; Bhuyan, D.; Pope, G. et al. 1986. Effect of Capillary Number on the Residual Saturation of a Three-Phase Micellar Solution. Presented at SPE Enhanced Oil Recovery Symposium, Tulsa, Oklahoma, 20-23 April. https://doi.org/10.2118/14911-MS.

Delshad, M.; Najafabadi, N. F.; Anderson, G. et al. 2009. Modeling wettability alteration by surfactants in naturally fractured reservoirs. *SPE Reservoir Evaluation & Engineering* **12** (03): 361-370. https://doi.org/10.2118/100081-PA.

Donaldson, E. C. and Thomas, R. D. 1971. Microscopic Observations of Oil Displacement in Water-Wet and Oil-Wet Systems. Presented at 46th Annual Fall Meeting of the Society of Petroleum Engineers of AIME, New Orleans, Louisiana, 3-6 October. https://doi.org/10.2118/3555-MS.

Donaldson, E. C.; Thomas, R. D. and Lorenz, P. B. 1969. Wettability Determination and Its Effect on Recovery Efficiency. *Society of Petroleum Engineers Journal* **9** (01): 13-20. https://doi.org/10.2118/2338-PA.

Dong, H. and Al Yafei, A. 2015. Optimization of Surfactant Flooding for Carbonate Reservoirs. Presented at Abu Dhabi International Petroleum Exhibition and Conference, Abu Dhabi, 9-12 November. https://doi.org/10.2118/177489-MS.

Fatt, I. and Klikoff, W. A., Jr. 1959. Effect of Fractional Wettability on Multiphase Flow Through Porous Media. *Journal of Petroleum Technology* **11** (10): 71-76. https://doi.org/10.2118/1275-G.

Figdore, P. E. 1982. Adsorption of surfactants on kaolinite: NaCl versus CaCl 2 salt effects. *Journal of Colloid and Interface Science* **87** (2): 500-517. https://doi.org/10.1016/0021-9797(82)90347-2.

Firoozabadi, A. 2000. Recovery Mechanisms in Fractured Reservoirs and Field Performance. *Journal of Canadian Petroleum Technology* **39** (11): 13-17. https://doi.org/10.2118/00-11-DAS.

Fulcher Jr., R. A.; Ertekin, T. and Stahl, C. 1985. Effect of capillary number and its constituents on two-phase relative permeability curves. *Journal of Petroleum Technology* **37** (02): 249-260. https://doi.org/10.2118/12170-PA.

Gao, B. and Sharma, M. M. 2013. A New Family of Anionic Surfactants for Enhanced-Oil-Recovery Applications. *SPE Journal* **18** (05): 829-840. https://doi.org/10.2118/159700-PA.

Garcia-Olvera, G.; Reilly, T. M.; Lehmann, T. E. et al. 2016. Analysis of Physico-Chemical Constraints on Surfactant Blends for Offshore Reservoirs. Presented at Offshore Technology Conference, Houston, Texas, 2-5 May. https://doi.org/10.4043/26929-MS.

Gatenby, W. and Marsden, S. S. 1957. Some wettability characteristics of synthetic porous media. *Producers Monthly* **22** (1): 5-12.

Golabi, E.; Seyedeyn Azad, F.; Ayatollahi, S. et al. 2012. Experimental Study of Wettability Alteration of Limestone Rock from Oil Wet to Water Wet by Applying Various Surfactants. Presented at SPE Heavy Oil Conference Canada, Calgary, Alberta, 12-14 June. https://doi.org/10.2118/157801-MS.

Goudarzi, A.; Delshad, M.; Mohanty, K. K. et al. 2012. Impact of Matrix Block Size on Oil Recovery Response Using Surfactants in Fractured Carbonates. Presented at SPE Annual Technical Conference and Exhibition, San Antonio, Texas, USA, 8-10 October. https://doi.org/10.2118/160219-MS.

Green, D. W. and Willhite, G. P. 1998. *Enhanced Oil Recovery*. Vol. 6. Henry L. Doherty Memorial Fund of AIME, Society of Petroleum Engineers Richardson, TX.

Gupta, R. and Mohanty, K. K. 2008. Wettability alteration of fractured carbonate reservoirs. Presented at SPE Symposium on Improved Oil Recovery, Tulsa, Oklahoma, 20-23 April. https://doi.org/10.2118/113407-MS.

Hagoort, J. 1980. Oil recovery by gravity drainage. *Society of Petroleum Engineers Journal* **20** (03): 139-150.

Hermansen, H.; Thomas, L. K.; Sylte, J. E. et al. 1997. Twenty Five Years of Ekofisk Reservoir Management. Presented at SPE Annual Technical Conference and Exhibition, San Antonio, Texas, 5-8 October. https://doi.org/10.2118/38927-MS.

Hjuler, M. L. and Fabricius, I. L. 2009. Engineering properties of chalk related to diagenetic variations of Upper Cretaceous onshore and offshore chalk in the North Sea area. *Journal of Petroleum Science and Engineering* **68** (3): 151-170. https://doi.org/10.1016/j.petrol.2009.06.005.

Humphry, K. J.; Suijkerbuijk, B. M. J. M.; van der Linde, H. A. et al. 2014. Impact of Wettability on Residual Oil Saturation and Capillary Desaturation Curves. *Petrophysics* **55** (04): 313 - 318.

Høgnesen, E. J.; Olsen, M. and Austad, T. 2006. Capillary and gravity dominated flow regimes in displacement of oil from an oil-wet chalk using cationic surfactant. *Energy & fuels* **20** (3): 1118-1122.

Jadhunandan, P. P. and Morrow, N. R. 1995. Effect of Wettability on Waterflood Recovery for Crude-Oil/Brine/Rock Systems. *SPE Reservoir Engineering* **10** (01): 40-46. https://doi.org/10.2118/22597-PA.

Kamath, J.; Meyer, R. F. and Nakagawa, F. M. Year. Understanding waterflood residual oil saturation of four carbonate rock types. Presented at SPE Annual Technical Conference and Exhibition, New Orleans, Louisiana, 30 September-3 October. https://doi.org/10.2118/71505-MS.

Kantzas, A.; Bryan, J. and Taheri, S. 2019. Fundamentals of Fluid Flow in Porous Media. In: PERM Tipm Laboratory, https://perminc.com/resources/fundamentals-of-fluid-flow-in-porous-media/.

Karasinghe, A. N. U.; Liyanage, P. J.; Cai, J. et al. 2016. New Surfactants and Co-Solvents Increase Oil Recovery and Reduce Cost. Presented at SPE Improved Oil Recovery Conference, Tulsa, Oklahoma, 11-13 April. https://doi.org/10.2118/179702-MS.

Karnanda, W.; Benzagouta, M.; AlQuraishi, A. et al. 2013. Effect of temperature, pressure, salinity, and surfactant concentration on IFT for surfactant flooding optimization. *Arabian Journal of Geosciences* **6** (9): 3535-3544.

Kennedy, H. T.; Burja, E. O. and Boykin, R. S. 1955. An investigation of the effects of wettability on oil recovery by water flooding. *The Journal of Physical Chemistry* **59** (9): 867-869.

Lake, L. W. 1984. A Technical Survey of Micellar Polymer Flooding. *Enhanced Oil Recovery for the Independent Producer*: 102-141.

Lake, L. W.; Johns, R. T.; Rossen, W. R. et al. 2014. *Fundamentals of Enhanced Oil Recovery*. TX, United States of America: Society of Petroleum Engineer.

Li, K. and Horne, R. N. 2001. Characterization of Spontaneous Water Imbibition into Gas-Saturated Rocks. *SPE Journal* 6 (04): 375-384. https://doi.org/10.2118/74703-PA.

Li, K. and Horne, R. N. 2002. A Scaling Method of Spontaneous Imbibition in Systems with Different Wettability. Presented at International Symposium of the Society of Core Analysts, Monterey, California, 22-25 September.

Li, K. and Horne, R. N. 2004. An Analytical Scaling Method for Spontaneous Imbibition in Gas/Water/Rock Systems. *SPE Journal* 9 (03): 322-329. https://doi.org/10.2118/88996-PA.

Li, K. and Horne, R. N. 2006. Generalized Scaling Approach for Spontaneous Imbibition: An Analytical Model. *SPE Reservoir Evaluation & Engineering* 9 (03): 251-258. https://doi.org/10.2118/77544-PA.

Lorenz, P. B.; Donaldson, E. C. and Thomas, R. D. 1974. Use of centrifugal measurements of wettability to predict oil recovery. *Rep. Invest.-US, Bur. Mines;(United States)* **7873**.

Luffel, D. L. and Randall, R. V. 1960. *Core Handling and Measurement Techniques for Obtaining Reliable Reservoir Characteristics*, Society of Petroleum Engineers (Reprint).

Ma, S.; Zhang, X. and Morrow, N. R. 1999. Influence of Fluid Viscosity on Mass Transfer Between Rock Matrix and Fractures. *Journal of Canadian Petroleum Technology* **38** (07): 6. https://doi.org/10.2118/99-07-02.

Mattax, C. C. and Kyte, J. 1962. Imbibition Oil Recovery from Fractured, Water-Drive Reservoir. *Society of Petroleum Engineers Journal* **2** (02): 177-184. https://doi.org/10.2118/187-PA.

McCaffery, F. G. and Bennion, D. W. 1974. The Effect of Wettability on Two-Phase Relative Penneabilities. *Journal of Canadian Petroleum Technology* **13** (04): 42-53. https://doi.org/10.2118/74-04-04.

Melrose, J. C. 1965. Wettability as Related to Capillary Action in Porous Media. *Society of Petroleum Engineers Journal* **5** (03): 259-271. https://doi.org/10.2118/1085-PA.

Milter, J. and Austad, T. 1996a. Chemical flooding of oil reservoirs 6. Evaluation of the mechanism for oil expulsion by spontaneous imbibition of brine with and without surfactant in water-wet, low-permeable, chalk material. *Colloids and Surfaces A: Physicochemical and Engineering Aspects* **113** (3): 269-278. https://doi.org/10.1016/0927-7757(96)03631-X.

Milter, J. and Austad, T. 1996b. Chemical flooding of oil reservoirs 7. Oil expulsion by spontaneous imbibition of brine with and without surfactant in mixed-wet, low permeability chalk material. *Colloids and Surfaces A: Physicochemical and Engineering Aspects* **117** (1-2): 109-115.

Mirzaei, M.; DiCarlo, D. A. and Pope, G. A. 2016. Visualization and Analysis of Surfactant Imbibition into Oil-Wet Fractured Cores. *SPE Journal* **21** (01): 101 - 111. https://doi.org/10.2118/166129-PA.

Morrow, N. R. 1970. Irreducible wetting-phase saturations in porous media. *Chemical Engineering Science* **25** (11): 1799-1815. https://doi.org/10.1016/0009-2509(70)80070-7.

Morrow, N. R. 1975. The Effects of Surface Roughness on Contact: Angle With Special Reference to Petroleum Recovery. *Journal of Canadian Petroleum Technology* **14** (04): 42-53. https://doi.org/10.2118/75-04-04.

Morrow, N. R. 1976. Capillary Pressure Correlations for Uniformly Wetted Porous Media. *Journal of Canadian Petroleum Technology* **15** (04): 22. https://doi.org/10.2118/76-04-05.

Morrow, N. R. 1979. Interplay of Capillary, Viscous And Buoyancy Forces In the Mobilization of Residual Oil. *Journal of Canadian Petroleum Technology* **18** (03): 35-46. https://doi.org/10.2118/79-03-03.

Morrow, N. R.; Cram, P. J. and McCaffery, F. G. 1973. Displacement Studies in Dolomite With Wettability Control by Octanoic Acid. *Society of Petroleum Engineers Journal* **13** (04): 221-232. https://doi.org/10.2118/3993-PA.

Mungan, N. 1966. Interfacial Effects in Immiscible Liquid-Liquid Displacement in Porous Media. *Society of Petroleum Engineers Journal* **6** (03): 247-253. https://doi.org/10.2118/1442-PA.

Neog, A. and Schechter, D. S. 2016. Investigation of Surfactant Induced Wettability Alteration in Wolfcamp Shale for Hydraulic Fracturing and EOR Applications. Presented at SPE Improved Oil Recovery Conference, Tulsa, Oklahoma, 11-13 April. https://doi.org/10.2118/179600-MS.

Norwegian Petroleum Directorate. Facts 2014 (No. Y-0103/15 E). Norwegain Petroleum Directorate.

Olajire, A. A. 2014. Review of ASP EOR (alkaline surfactant polymer enhanced oil recovery) technology in the petroleum industry: Prospects and challenges. *Energy* **77**: 963-982. https://doi.org/10.1016/j.energy.2014.09.005.

Owens, W. W. and Archer, D. L. 1971. The Effect of Rock Wettability on Oil-Water Relative Permeability Relationships. *Journal of Petroleum Technology* **23** (07): 873-878. https://doi.org/10.2118/3034-PA.

Parra, J. E.; Pope, G. A.; Mejia, M. et al. 2016. New Approach for Using Surfactants to Enhance Oil Recovery from Naturally Fractured Oil-Wet Carbonate Reservoirs. Presented at SPE

Annual Technical Conference and Exhibition, Dubai, 26-28 September. https://doi.org/10.2118/181713-MS.

Qi, Z.; Han, M.; Fuseni, A. et al. 2016. Laboratory Study on Surfactant Induced Spontaneous Imbibition for Carbonate Reservoir. Presented at SPE Asia Pacific Oil & Gas Conference and Exhibition, Perth, 25-27 October. https://doi.org/10.2118/182322-MS.

Rao, D. N. 1999. Wettability Effects in Thermal Recovery Operations. *SPE Reservoir Evaluation & Engineering* **2** (05): 420-430. https://doi.org/10.2118/57897-PA.

Rathmell, J. J.; Braun, P. H. and Perkins, T. K. 1973. Reservoir Waterflood Residual Oil Saturation from Laboratory Tests. *Journal of Petroleum Technology* **25** (02): 175-185. https://doi.org/10.2118/3785-PA.

Reiss, L. H. 1980. *The reservoir engineering aspects of fractured formations*. Vol. 3. Editions Technip.

Richardson, J. G.; Perkins, F. M. and Osoba, J. S. 1954. Differences in Behavior of Fresh and Aged East Texas Woodbine Cores. Presented at Fall Meeting of the Petroleum Branch of AIME, San Antonio, Texas, 17-20 October. http://doi.org/10.2118/408-G-MS.

Roehl, P. O. and Choquette, P. W. 2012. *Carbonate petroleum reservoirs*. New York: Springer Science & Business Media.

Rosen, M. J. and Kunjappu, J. T. 2012. *Surfactants and interfacial phenomena*. 4th. Hoboken, New Jersey: John Wiley & Sons, Inc.

Saidi, A. M. 1987. *Reservoir Engineering of Fractured Reservoirs (Fundamentals and Practical Aspects)*. Paris, France: Total.

Salehi, M.; Johnson, S. J. and Liang, J.-T. 2008. Mechanistic study of wettability alteration using surfactants with applications in naturally fractured reservoirs. *Langmuir* **24** (24): 14099-14107. https://doi.org/10.1021/la802464u.

Scamehorn, J.; Schechter, R. and Wade, W. 1982. Adsorption of surfactants on mineral oxide surfaces from aqueous solutions: I: Isomerically pure anionic surfactants. *Journal of Colloid and Interface Science* **85** (2): 463-478. https://doi.org/10.1016/0021-9797(82)90013-3.

Schechter, D. S.; Zhou, D. and Orr Jr, F. M. 1994. Low IFT drainage and imbibition. *Journal of Petroleum Science and Engineering* **11** (04): 283-300. https://doi.org/10.1016/0920-4105(94)90047-7.

Schwartz, A. M. 1969. Capillarity-theory and practice. *Industrial & Engineering Chemistry* **61** (1): 10-21.

Seethepalli, A.; Adibhatla, B. and Mohanty, K. 2004. Wettability Alteration During Surfactant Flooding of Carbonate Reservoirs. Presented at SPE/DOE Fourteenth Symposium on Improved Oil Recovery, Tulsa, Oklahoma, 17-21 April. https://doi.org/10.2118/89423-MS.

Sheng, J. J. 2011. *Modern Chemical Enhanced Oil Recovery: Theory and Practice*. Gulf Professional Publishing.

Shirdel, M.; Abbaszadeh, M.; Gerardo, I. G. et al. 2011. Development and Evaluation of Pseudo Capillary Pressure in Naturally Fractured Reservoirs. Presented at SPE Eastern Regional Meeting, Columbus, Ohio, USA, 17-19 August. http://doi.org/10.2118/149502-MS.

Shuler, P. J. and Tang, Y. 2010. New Chemical EOR Process for Bakken Shale. Presented at AAPG Annual Convention and Exhibition, New Orleans, LA, April 11-14.

Skjæveland, S. M.; Siqveland, O. K.; Barkved, O. L. et al. 2019. *JCR-7 Monograph North Sea Chalk*. Web version. https://jcr.ux.uis.no/.

Spinler, E. A.; Zornes, D. R.; Tobola, D. P. et al. 2000. Enhancement of Oil Recovery Using a Low Concentration of Surfactant to Improve Spontaneous and Forced Imbibition in Chalk. Presented at SPE/DOE Improved Oil Recovery Symposium, Tulsa, Oklahoma, 3-5 April. https://doi.org/10.2118/59290-MS.

Standnes, D. C. and Austad, T. 2000. Wettability alteration in chalk: 2. Mechanism for wettability alteration from oil-wet to water-wet using surfactants. *Journal of Petroleum Science and Engineering* **28** (3): 123-143. https://doi.org/10.1016/S0920-4105(00)00084-X.

Standnes, D. C.; Nogaret, L. A.; Chen, H.-L. et al. 2002. An evaluation of spontaneous imbibition of water into oil-wet carbonate reservoir cores using a nonionic and a cationic surfactant. *Energy & Fuels* **16** (6): 1557-1564.

Stoll, M.; Hofman, J.; Ligthelm, D. J. et al. 2008. Toward Field-Scale Wettability Modification—The Limitations of Diffusive Transport. *SPE Reservoir Evaluation & Engineering* **11** (03): 633-640. https://doi.org/10.2118/107095-PA.

Strand, S.; Standnes, D. C. and Austad, T. 2003. Spontaneous Imbibition of Aqueous Surfactant Solutions into Neutral to Oil-Wet Carbonate Cores: Effects of Brine Salinity and Composition. *Energy & fuels* **17** (5): 1133-1144. https://doi.org/10.1021/ef030051s.

Tabary, R.; Fornari, A.; Bazin, B. et al. 2009. Improved oil recovery with chemicals in fractured carbonate formations. Presented at SPE international symposium on oilfield chemistry, Woodlands, Texas, 20-22 April. https://doi.org/10.2118/121668-MS.

Taber, J. J. 1981. Research on Enhanced Oil Recovery: Past, Present and Future. In *Surface Phenomena in Enhanced Oil Recovery*, ed. Shah D.O., 13-52. Boston, MA, Springer.

Taber, J. J.; Martin, F. D. and Seright, R. S. 1997. EOR Screening Criteria Revisited - Part 1: Introduction to Screening Criteria and Enhanced Recovery Field Projects. *SPE Reservoir Engineering* **12** (03): 189-198. https://doi.org/10.2118/35385-PA.

Terry, R. E. 2001. Enhanced oil recovery. *Encyclopedia of physical science and technology* **18**: 503-518.

Thomas, L. K.; Dixon, T. N. and Pierson, R. G. 1983. Fractured Reservoir Simulation. *Society of Petroleum Engineers Journal* **23** (01): 42-54. http://doi.org/10.2118/9305-PA.

Treiber, L. E. and Owens, W. W. 1972. A Laboratory Evaluation of the Wettability of Fifty Oil-Producing Reservoirs. *Society of Petroleum Engineers Journal* **12** (06): 531-540. https://doi.org/10.2118/3526-PA.

van Golf-Racht, T. D. 1982. Fundamentals of fractured reservoir engineering. Vol. 12. New York: Elsevier.

Wang, D.; Zhang, J.; Butler, R. et al. 2016. Scaling Laboratory-Data Surfactant-Imbibition Rates to the Field in Fractured-Shale Formations. *SPE Reservoir Evaluation & Engineering* **19** (03): 440 - 449. https://doi.org/10.2118/178489-PA.

Wardlaw, N. C. 1980. The Effects of Pore Structure on Displacement Efficiency in Reservoir Rocks and in Glass Micromodels. Presented at SPE/DOE Enhanced Oil Recovery Symposium, Tulsa, Oklahoma, 20-23 April. https://doi.org/10.2118/8843-MS.

Wardlaw, N. C. 1982. The Effects of Geometry, Wettability, Viscosity And Interfacial Tension On Trapping In Single Pore-throat Pairs. *Journal of Canadian Petroleum Technology* **21** (03): 21-27. https://doi.org/10.2118/82-03-01.

Warren, J. and Root, P. J. 1963. The Behavior of Naturally Fractured Reservoirs. *Society of Petroleum Engineers Journal* **3** (03): 245-255.

Wissmann, W. 1963. Displacement tests with porous rock samples under reservoir conditions. Presented at 6th World Petroleum Congress, Frankfurt am Main, Germany, 19-26 June.

Xie, K.; Lu, X.; Pan, H. et al. 2018. Analysis of Dynamic Imbibition Effect of Surfactant in Microcracks of Reservoir at High Temperature and Low Permeability. *SPE Production & Operations* **Preprint** (Preprint). https://doi.org/10.2118/189970-PA.

Xie, X.; Weiss, W. W.; Tong, Z. J. et al. 2005. Improved oil recovery from carbonate reservoirs by chemical stimulation. *SPE Journal* **10** (03): 276-285.

Xu, F.; Guo, X.; Wang, W. et al. 2011. Case Study: Numerical Simulation Of Surfactant Flooding In Low Permeability Oil Filed. Presented at SPE Enhanced Oil Recovery Conference, Kuala Lumpur, 19-21 July. https://doi.org/10.2118/145036-MS.

Xu, W.; Ayirala, S. C. and Rao, D. N. 2005. Measurement of Surfactant-Induced Interfacial Interactions at Reservoir Conditions. Presented at SPE Annual Technical Conference and Exhibition, Dallas, Texas, 9-12 October. https://doi.org/10.2118/96021-MS.

Zhang, J.; Wang, D. and Olatunji, K. 2016. Surfactant Adsorption Investigation in Ultra-Lower Permeable Rocks. Presented at SPE Low Perm Symposium, Denver, Colorado, 5-6 May. https://doi.org/10.2118/180214-MS.

Appendix A: Simulation of surfactant spontaneous imbibition

```
-- SPONTANEOUS IMBIBITION _ SURFACTANT
-- CORE D:3.83 cm H:4.61cm
-----------------------------------------------------------------------------
RUNSPEC
-----------------------------------------------------------------------------

--NOSIM
CPR
/
TITLE
CASE FOR SURFACTANT SPONTANEOUS IMBIBITION

DIMENS
23 23 30 /

OIL
WATER
SURFACT
SURFACTW

TRACERS
0 1 0 1   /

LAB
UNIFIN
UNIFOUT

START
1 JAN 2016 /
```

```
WELLDIMS
0 0 0 0 /

TABDIMS
4 1 40 40 2 /

NSTACK
100 /

MESSAGES
3* 1000 5* 1000 2* /

--------------------------------------------------------------------------------
GRID
--------------------------------------------------------------------------------

INIT
OLDTRAN

DXV
1 21*0.2 1 /
DYV
1 21*0.2 1 /
DZ
1058*0.2 529*4.4 13754*0.2 529*0.6 /

PERMX
15870*1E7 /
PORO
15870*0.999 /

EQUALS
```

```
TOPS      0        1 23 1 23 1 1 /
PERMX  3        4 20 4 20 5 27 /
PORO    0.443   4 20 4 20 5 27 /
/

COPY
PERMX PERMY /
PERMX PERMZ /
/

RPTGRID
  DEPTH PERMX PERMY PERMZ PORO PORV TOPS /

---------------------------------------------------------------------------
PROPS
---------------------------------------------------------------------------

SWOF
-- Sw       Krw       Krow       Pcow
   0          0          1          0
   0.1        0.1        0.9        0
   0.2        0.2        0.8        0
   0.3        0.3        0.7        0
   0.4        0.4        0.6        0
   0.5        0.5        0.5        0
   0.6        0.6        0.4        0
   0.7        0.7        0.3        0
   0.8        0.8        0.2        0
   0.9        0.9        0.1        0
   1          1          0          0          /Amott cell

   0.277    0          0.7        0.005
   0.3        0.00013 0.59       0.0015
```

0.35	0.0023	0.406	-0.0001	
0.4	0.0085	0.266	-0.0008	
0.45	0.02	0.166	-0.0014	
0.5	0.038	0.097	-0.0025	
0.55	0.063	0.053	-0.004	
0.6	0.095	0.025	-0.01	
0.65	0.137	0.01	-0.02	
0.7	0.187	0.0033	-0.048	
0.75	0.248	0.00065	-0.09	
0.8	0.318	4.1E-05	-0.14	
0.85	0.4	0	-0.2	/matrix (oil-wet)

0.277	0	1	0.2	
0.3	5.2E-07	0.92	0.11	
0.35	5.3E-05	0.76	0.07	
0.4	4.2E-04	0.62	0.05	
0.45	0.00167	0.487	0.038	
0.5	0.00459	0.373	0.03	
0.55	0.0103	0.274	0.024	
0.6	0.0202	0.19	0.019	
0.65	0.0359	0.122	0.014	
0.7	0.0594	0.0685	0.01	
0.75	0.0929	0.03	0.006	
0.8	0.139	0.0076	0.003	
0.85	0.2	0	0	/matrix (water-wet

0	0	1	1*
0.05	0.05	0.95	1*
0.15	0.15	0.85	1*
0.25	0.25	0.75	1*
0.35	0.35	0.65	1*
0.45	0.45	0.55	1*
0.55	0.55	0.45	1*

```
  0.65    0.65      0.35     1*
  0.75    0.75      0.25     1*
  0.85    0.85      0.15     1*
  0.95    0.95      0.05     1*
  1       1         0        1*     /miscible

ROCK
1     0.0   /

PVTW
1    1.0   4.93E-5   0.8   1.10E-3    /

DENSITY
0.816   1.031    /

RSCONST
0       1    /

PVDO
 0.5    1.05      1.442
 0.75   1.0485    1.444
 1      1.0471    1.446
 1.25   1.0457    1.448
 1.5    1.0443    1.45
 /

TRACER
SUR WAT 'gm' /
/

TRDIFSUR
--tracer diffusion coefficient (cm2/h)
5E-4 /
```

```
SURFVISC
  0          0.8
  0.004      0.81
  0.01       0.86
  0.015      0.92       /

SURFADS
  0          0
  0.01       0       /
  0          0
  0.001      0
  0.002      0.00001
  0.003      0.00003
  0.004      0.000175
  0.005      0.0002
  0.015      0.0002      /
  /
  /

SURFADDW
  0              1
  0.0002         1    /
  0              1
  0.0002         0    /
  /
  /

SURFST
  0          15.4
  0.001      1.54
  0.004      0.8
  0.01       0.8
```

```
 0.048    0.8       /

SURFCAPD
 -20        0.0
 20         0.0    /
 -20        0.0
 -8         0.0
 -7         0.06
 -6         0.33
 -5         0.67
 -4         0.94
 -3         1.0
 10         1.0   /
 /
 /

SURFROCK
 2                  2.7 /
 2                  2.7 /
 2                  2.7 /
 2                  2.7 /

RPTPROPS
/

--------------------------------------------------------------------------------
REGIONS
--------------------------------------------------------------------------------

PVTNUM
15870*1 /

SATNUM
```

15870*1 /

FIPNUM
15870*1 /

SURFWNUM
15870*1 /

SURFNUM
15870*1 /

EQUALS
FIPNUM 2 4 20 4 20 5 27 /
SATNUM 2 4 20 4 20 5 27 /
SURFWNUM 3 4 20 4 20 5 27 /
SURFNUM 4 4 20 4 20 5 27 /
/

RPTREGS
/

SOLUTION

PRESSURE
15870*1 /

SWAT
15870*1.00 /

SURF
15870*0.01 /

```
EQUALS
SWAT   0.277   4 20 4 20 5 27 /
SURF    0.00     4 20 4 20 5 27 /
/

RPTSOL
ESALSUR   FIP=2 FIPRESV FIPSOL=2 FLOOIL FLOWAT
KRO KRW SOIL SURFADS SURFBLK SWAT
POIL PWAT POILD PWATD PRESSURE RECOV /

----------------------------------------------------------------------------
SUMMARY
----------------------------------------------------------------------------

ALL
FPR
FRPV
FOPV
FOE
FOEIW
FOPR
FOPT
FGOR
FGPR
FWPR
FWPT
FWIR
FWIT
FTPRSUR
FTPTSUR
FTIRSUR
FTITSUR
```

FTADSUR

RPR
/
ROE
/
ROEIW
/
ROIP
/
RWIP
/
RWIT
/
RWPR
/
RWPT
/
ROPR
/
ROPT
/
ROSAT
/
RWSAT
/
ROVIS
/
RWVIS
/
RTIPTSUR
/
RTADSUR

```
/

RUNSUM
EXCEL
SEPARATE

--------------------------------------------------------------------------------
SCHEDULE
--------------------------------------------------------------------------------

RPTSCHED
'CPU=1' 'FIP=2' 'FIPSURF=2' 'KRG' 'KRO' 'KRW' 'PRES' 'PWAT'
'RESTART=2' 'SGAS' 'SOIL' 'SWAT' 'SURFADS' 'SURFBLK' 'WELLS=1' /

RPTRST
BASIC=2 /

DRSDT
0   /

TUNING
0.1 1 0.05 0.05   /
/
100 1* 100   /

DATES
1 JAN 2016 00:01:00 /
1 JAN 2016 01:00:00 /
1 JAN 2016 06:00:00 /
1 JAN 2016 12:00:00 /
2 JAN 2016 00:00:00 /
2 JAN 2016 06:00:00 /
2 JAN 2016 12:00:00 /
```

```
3 JAN 2016 00:00:00 /
/

TSTEP
716*12   /
TSTEP
24*360   /

END
```

Appendix B: Simulation of surfactant injection in a fractured matrix

```
-- SURFACTANT DYNAMIC IMBIBITION
-- Core D:3.83 cm H:4.61cm
-- Model L:3.4 cm H:4.6 cm
-- Total volume: 53.44 ml; matrix volume: 53.176 ml
----------------------------------------------------------------------------
RUNSPEC
----------------------------------------------------------------------------

--NOSIM
CPR
/

TITLE
CASE FOR SURFACTANT DYNAMIC IMBIBITION

DIMENS
21 17 23 /

OIL
WATER
SURFACT
SURFACTW
TRACERS
0 1 0 1   /

LAB
UNIFIN
UNIFOUT
```

```
START
1 JAN 2016 /

WELLDIMS
--1 producer, 1 injector
2 30 1 2 /

TABDIMS
4 1 40 40 2 /

NUPCOL
150 /

NSTACK
100 /

MESSAGES
3* 1000 5* 1000 2* /

--------------------------------------------------------------------------------
GRID
--------------------------------------------------------------------------------

INIT
OLDTRAN

DXV
--a fracture in X axis with width 0.017 cm, ϕf = 0.5%
8*0.2   0.0762   0.0238   0.017   0.0238   0.0762   8*0.2    /

DYV
17*0.2   /
```

```
DZ
8211*0.2   /

PERMX
8211*3.0 /

PORO
8211*0.443 /

EQUALS
TOPS      0          1 21 1 17 1 1 /
PERMX  2.4E6    11 11 1 17 1 23 /
PORO    0.999     11 11 1 17 1 23 /
/

COPY
PERMX PERMY /
PERMX PERMZ /
/

RPTGRID
  DEPTH PERMX PERMY PERMZ PORO PORV TOPS /

-------------------------------------------------------------------------------
PROPS
-------------------------------------------------------------------------------

SWOF
-- Sw       Krw       Krow       Pcow
   0          0          1          0
   0.1        0.1        0.9        0
   0.2        0.2        0.8        0
   0.3        0.3        0.7        0
```

0.4	0.4	0.6	0	
0.5	0.5	0.5	0	
0.6	0.6	0.4	0	
0.7	0.7	0.3	0	
0.8	0.8	0.2	0	
0.9	0.9	0.1	0	
1	1	0	0	/Amott cell

0.277	0	0.7	0.005	
0.3	0.00013	0.59	0.0015	
0.35	0.0023	0.406	-0.0001	
0.4	0.0085	0.266	-0.0008	
0.45	0.02	0.166	-0.0014	
0.5	0.038	0.097	-0.0025	
0.55	0.063	0.053	-0.004	
0.6	0.095	0.025	-0.01	
0.65	0.137	0.01	-0.02	
0.7	0.187	0.0033	-0.048	
0.75	0.248	0.00065	-0.09	
0.8	0.318	4.1E-05	-0.14	
0.85	0.4	0	-0.2	/matrix (oil-wet)

0.277	0	1	0.2
0.3	5.2E-07	0.92	0.11
0.35	5.3E-05	0.76	0.07
0.4	4.2E-04	0.62	0.05
0.45	0.00167	0.487	0.038
0.5	0.00459	0.373	0.03
0.55	0.0103	0.274	0.024
0.6	0.0202	0.19	0.019
0.65	0.0359	0.122	0.014
0.7	0.0594	0.0685	0.01
0.75	0.0929	0.03	0.006

```
  0.8     0.139     0.0076   0.003
  0.85    0.2       0        0        /matrix (water-wet)

  0       0         1        1*
  0.05    0.05      0.95     1*
  0.15    0.15      0.85     1*
  0.25    0.25      0.75     1*
  0.35    0.35      0.65     1*
  0.45    0.45      0.55     1*
  0.55    0.55      0.45     1*
  0.65    0.65      0.35     1*
  0.75    0.75      0.25     1*
  0.85    0.85      0.15     1*
  0.95    0.95      0.05     1*
  1       1         0        1*       /miscible

ROCK
1      0.0 /

PVTW
1     1.0   4.93E-5   0.8    1.10E-3    /

DENSITY
0.816   1.031   /

RSCONST
200         250 /

PVDO

  255    1.05       1.442
  260    1.0485     1.444
  265    1.0471     1.446
```

```
 270    1.0457    1.448
 275    1.0443    1.45
 /

TRACER
SUR     WAT    'gm' /
/

TRDIFSUR
--tracer diffusion coefficient (cm2/h)
5E-4 /

SURFVISC
 0          0.8
 0.004      0.81
 0.01       0.86
 0.015      0.92       /

SURFADS
 0          0
 0.01       0       /
 0          0
 0.001      0
 0.002      0.00001
 0.003      0.00003
 0.004      0.000175
 0.005      0.0002
 0.015      0.0002      /
 /
 /

SURFADDW
 0              1
```

```
 0.0002       1    /
 0            1
 0.0002       0    /
 /
 /

SURFST
 0          15.4
 0.001      1.54
 0.004      0.8
 0.01       0.8
 0.048      0.8       /

SURFCAPD
 -20        0.0
 20         0.0    /
 -20        0.0
 -8         0.0
 -7         0.06
 -6         0.33
 -5         0.67
 -4         0.94
 -3         1.0
 10         1.0    /
 /
 /

SURFROCK
 2                2.7 /
 2                2.7 /
 2                2.7 /
 2                2.7 /
```

```
RPTPROPS
/

-------------------------------------------------------------------------------
REGIONS
-------------------------------------------------------------------------------

PVTNUM
8211*1   /

FIPNUM
8211*2   /

SATNUM
8211*2   /

SURFWNUM
8211*3   /

SURFNUM
8211*4   /

EQUALS
FIPNUM          1   11 11 1 17 1 23   /
SATNUM          1   11 11 1 17 1 23   /
SURFWNUM   1   11 11 1 17 1 23   /
SURFNUM       1   11 11 1 17 1 23   /
/

RPTREGS
/

-------------------------------------------------------------------------------
```

```
SOLUTION
--------------------------------------------------------------------------------

PRESSURE
8211*270   /

SWAT
8211*0.277
/

SURF
8211*0.0   /

EQUALS
SWAT   0.0    11 11 1 17 1 23   /
/

RPTSOL
ESALSUR   FIP=2 FIPRESV FIPSOL=2 FLOOIL FLOWAT
KRO KRW SOIL SURFADS SURFBLK SWAT
POIL PWAT POILD PWATD PRESSURE RECOV /

--------------------------------------------------------------------------------
SUMMARY
--------------------------------------------------------------------------------

ALL
FPR
FRPV
FOPV
FOE
FOEIW
FOPR
```

FOPT
FGOR
FGPR
FWPR
FWPT
FWIR
FWIT
FTPRSUR
FTPTSUR
FTIRSUR
FTITSUR
FTADSUR

WTPRSUR
PROD/
WTPTSUR
PROD/
WTIRSUR
INJE/
WTITSUR
INJE/

RPR
/
ROE
/
ROEIW
/
ROIP
/
RWIP
/
RWIT

/
RWPR
/
RWPT
/
ROPR
/
ROPT
/
ROSAT
/
RWSAT
/
ROVIS
/
RWVIS
/
RTIPTSUR
/
RTADSUR
/

RUNSUM
EXCEL
SEPARATE

SCHEDULE

RPTSCHED
'CPU=1' 'FIP=2' 'FIPSURF=2' 'KRG' 'KRO' 'KRW' 'PRES' 'PWAT'
'RESTART=2' 'SGAS' 'SOIL' 'SWAT' 'SURFADS' 'SURFBLK' 'WELLS=1' /

```
RPTRST
BASIC=2   /

DRSDT
0   /

WELSPECS
  'PROD'   G1    11   1   1*   OIL     /
  'INJE'     G1    11   1   1*   WAT   /
/

COMPDAT
  'PROD'   11   1   1   1    OPEN      1*     1 /
  'PROD'   11   2   1   1    OPEN      1*     1 /
  'PROD'   11   3   1   1    OPEN      1*     1 /
  'PROD'   11   4   1   1    OPEN      1*     1 /
  'PROD'   11   5   1   1    OPEN      1*     1 /
  'PROD'   11   6   1   1    OPEN      1*     1 /
  'PROD'   11   7   1   1    OPEN      1*     1 /
  'PROD'   11   8   1   1    OPEN      1*     1 /
  'PROD'   11   9   1   1    OPEN      1*     1 /
  'PROD'   11  10  1   1    OPEN      1*     1 /
  'PROD'   11  11  1   1    OPEN      1*     1 /
  'PROD'   11  12  1   1    OPEN      1*     1 /
  'PROD'   11  13  1   1    OPEN      1*     1 /
  'PROD'   11  14  1   1    OPEN      1*     1 /
  'PROD'   11  15  1   1    OPEN      1*     1 /
  'PROD'   11  16  1   1    OPEN      1*     1 /
  'PROD'   11  17  1   1    OPEN      1*     1 /

  'INJE'     11   1   23 23   OPEN      1*     1 /
  'INJE'     11   2   23 23   OPEN      1*     1 /
```

```
 'INJE'    11   3   23 23   OPEN      1*     1 /
 'INJE'    11   4   23 23   OPEN      1*     1 /
 'INJE'    11   5   23 23   OPEN      1*     1 /
 'INJE'    11   6   23 23   OPEN      1*     1 /
 'INJE'    11   7   23 23   OPEN      1*     1 /
 'INJE'    11   8   23 23   OPEN      1*     1 /
 'INJE'    11   9   23 23   OPEN      1*     1 /
 'INJE'    11  10  23 23   OPEN      1*     1 /
 'INJE'    11  11  23 23   OPEN      1*     1 /
 'INJE'    11  12  23 23   OPEN      1*     1 /
 'INJE'    11  13  23 23   OPEN      1*     1 /
 'INJE'    11  14  23 23   OPEN      1*     1 /
 'INJE'    11  15  23 23   OPEN      1*     1 /
 'INJE'    11  16  23 23   OPEN      1*     1 /
 'INJE'    11  17  23 23   OPEN      1*     1 /
/

WCONPROD
 PROD   OPEN    RESV    4*    0.012   265    /
/

WECON
 PROD    0     1*     1     2*      CON      YES    /
/

WCONINJE
 INJE    WATER     OPEN      RESV     1*     0.012      275     /
/

WSURFACT
 INJE   0.01    /
/
```

```
TUNING
0.1 30 0.05 0.1 /
/
100 1* 100 /

DATES
1 JAN 2016 00:10:00 /
1 JAN 2016 01:00:00 /
1 JAN 2016 06:00:00 /
1 JAN 2016 12:00:00 /
1 JAN 2016 18:00:00 /
2 JAN 2016 00:00:00 /
2 JAN 2016 12:00:00 /
3 JAN 2016 00:00:00 /
/

TSTEP
178*24   /
TSTEP
54*720   /
TSTEP
60*720   /

END
```

ISBN 978-82-326-4378-3 (printed version)
ISBN 978-82-326-4379-0 (electronic version)
ISSN 1503-8181

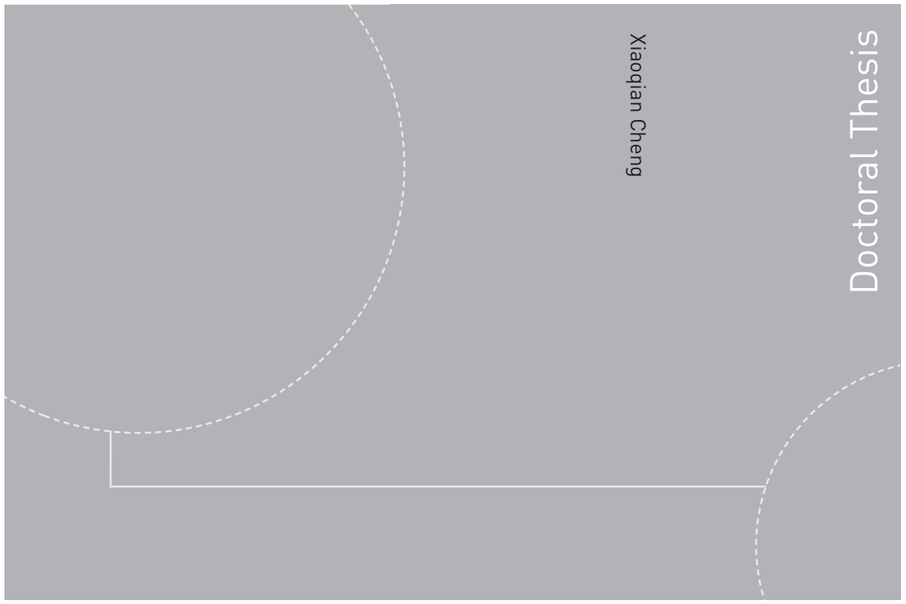

Doctoral theses at NTNU, 2019:387

Xiaoqian Cheng

Surfactant Enhanced Oil Recovery in Fractured Reservoirs

Simulation study of surfactant spontaneous and dynamic imbibition

NTNU
Norwegian University of
Science and Technology
Faculty of Engineering
Department of Geoscience and Petroleum

NTNU
Norwegian University of
Science and Technology

Doctoral theses at NTNU, 2019:387

NTNU

NTNU
Norwegian University of
Science and Technology